Methodological development and applications of cyclic cysteine-rich peptides for drug design
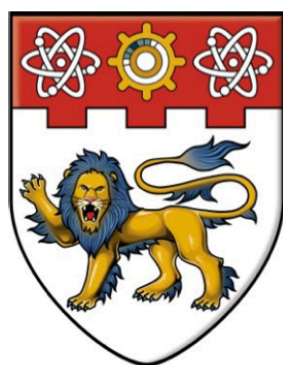
He, Muxinya

2014

He, M. (2014). Methodological development and applications of cyclic cysteine-rich peptides for drug design. Doctoral thesis, Nanyang Technological University, Singapore.

https://hdl.handle.net/10356/59522

https://doi.org/10.32657/10356/59522

METHODOLOGICAL DEVELOPMENT AND APPLICATIONS OF CYCLIC CYSTEINE-RICH PEPTIDES FOR DRUG DESIGN

HE MUXINYA

School of Biological Sciences

2014

METHODOLOGICAL DEVELOPMENT AND APPLICATIONS OF CYCLIC CYSTEINE-RICH PEPTIDES FOR DRUG DESIGN

HE MUXINYA

HE MUXINYA

School of Biological Sciences

A thesis submitted to the Nanyang Technological University in partial fulfillment of the requirement for the degree of Doctor of Philosophy

2014

Acknowledgements

I would like to express my deepest thanks to my supervisor, professor James Tam, for his constant and patient guidance, support and encouragement. Prof. Tam encouraged me to challenge new things that I might not be good at and learned from my mistakes. Under the inspiration and guidance of Prof. Tam, I got a chance to better myself and enrich my knowledge in chemistry during my PhD study.

I thank my dear colleagues, especially my seniors Dr. Nguyen Kien Truc Giang, Dr. Wong Clarence Tsun Ting, Dr. Liao Ying, Dr. Eom Khee Dong, Dr. Sui Xiaogang, my synthesis team members, Qiu Yibo and Dr. Taichi Misako, my lab mates Nguyen Quoc Thuc Phuong and How Guan Ji Adrian, who have helped and influenced me with their intelligence and passion. It is a pleasant experience to work in such friendly and helpful team.

I also want to express my sincere appreciation to my thesis advice committee Prof. Liu Chuanfa and Prof. Sze Siu Kwan for their valuable suggestions, and their lab members Dr. Yang Renliang, Dr. Zhang Xiaohong, Ms. Meng Wei for teaching me technologies of chemistry and mass spectrometry.

Last but not least, I thank my parents and my husband for their unconditional supports through out my PhD study.

Table of Contents

List of Figures

Chapter 1

Chapter 3

Chapter 4

Chapter 5

Chapter 6

List of Tables

Chapter 1

Chapter 3

Chapter 6

Abbreviations

Standard abbreviations are used for the amino acids and protecting groups [IUPAC-IUB Commission for Biochemical Nomenclature (1985) *J biol. Chem.* 260:14-42].

Acm	Acetamidomethyl
ACN	Acetonitrile
AEP	Asparaginyl-endopeptidase
AMP	Antimicrobial peptide
Boc	*tert*-butoxycarbonyl
BOP	Benzytrizol-1-yl-oxy-tris(dimethylamino)phosphonium hexafluorophosphate
BTD	*baboon* theta-defensin
CBD	Chitin-binding domain
CCK	Cyclic cystine-knot
CPP	Cell-penetrating peptide
CRP	Cysteine-rich peptide
CTX	Conotoxin
DCC	*N, N'*-dicyclohexylcarbodiimide
DCM	Dichloromethane
DIC	*N,N*-diisopropylcarbodiimide
DIEA	*N,N*-diisopropylethylamine
DMAP	4-dimethylaminopyridine
DMEM	Dulbecco/Vogt modified Eagle's (Harry Eagle) minimal essential medium
DMF	dimethylformamide
DTT	dithiothreitol
DMSO	dimethylsulfoxide
EDT	1,2-ethanedithiol;
ESI-MS	electrospray ionization mass spectrometry
EPL	expressed protein ligation
Fmoc	9H-fluroen-9-ylmethoxycarbonyl
GnHCl	guanidine hydrochloride
GSH	reduced glutathione

GSSG	oxidized glutathione
HATU	*O*-(7-azabenzotriazol-1-yl)-*N,N,N′,N′*-tetramethyluronium hexafluorophosphate
HF	Hydrofluoric acid
HOBt	N-hydroxybenzotriazole
Hyp	4-hydroxyproline
IAM	Iodoacetamide
IPTG	Isopropyl β-D-1-thiogalactopyranoside
LC-MS	Liquid chromatography mass spectrometry
MALDI	Matrix-assisted laser desorption ionization mass spectrometry
MCS	Multiple-cloning site
MeCys	*N*-methylated cysteine
MESNa	Mercaptoethanesulfonate sodium salt
MMA	Methyl mercaptoacetate
MPAA	4-mercaptophenyl acetic acid
nAChR	Nicotinic acetylcholine receptor
NEM	*N*-Ethylmaleimide
NMR	Nuclear magnetic resonance
PAGE	Polyacrylamide gel electrophoresis
PCR	Polymerase chain reaction
PDI	Protein disulfide isomerase
PyBOP	Benzotriazol-1-yloxytripyrrolidinophosphonium hexafluorophosphate
RP-HPLC	Reverse-phase high-performance liquid chromatography
rpm	Runs per minute
RPMI	Roswell Park Memorial Institute medium
RT	Retention time
r.t.	Room temperature
RTD	*Rhesus* theta-defensin
SDS	Sodium dodecyl sulfate
SS	Disulfide bond
SPPS	Solid phase peptide synthesis
TCEP	*tris*-(carboxyethyl)phosphine
TEA	Thioethylamido

TEBA	Thioethylbutylamide
TFA	Trifluoroacetic acid
TFE	Trifluoroethanol
TIS	Triisopropylsilane
TNBS	Trinitrobenzene sulfonate
TOF	Time-of-fly
VGCC	Voltage-gated calcium channel
VGNaC	Voltage-gated sodium channel

Abstract

My thesis focuses on the development of novel synthetic strategies for preparing the cyclic cysteine-rich peptides and applying the newly developed strategies for preparing bioactive cyclic cysteine-rich peptides with potential therapeutic applications. Cysteine-rich peptides are mini-proteins (2-8 kDa) with two to five intramolecular disulfide bonds. These disulfide bonds provide conformational constraints to enhance the structural stability. Cysteine-rich peptides occur ubiquitously in all organisms and they exhibit a broad range of bioactivities including antimicrobial, neurotoxic, enzyme inhibitory and hormonal functions. Interestingly, certain plant cysteine-rich peptides such as cyclotides possess an end-to-end cyclic backbone that gives an additional constraint and exceptional stability against heat and enzyme degradation. Cyclic cysteine-rich peptides have been exploited for designing and engineering orally active peptidyl therapeutics by grafting bioactive fragments into their scaffolds. A challenge in developing such engineered cyclic cysteine-rich peptides is developing an efficient and practical approach for their synthesis, and in particular, for the formation of cyclic backbones and oxidative folding of the multiple disulfide bonds.

My synthetic strategy employed Cys-thioester ligation (native chemical ligation) for preparing cyclic peptides. It involved the formation of a new peptide bond between an N-terminal cysteine and a C-terminal thioester to afford a cyclic backbone. To prepare thioesters, I developed two novel 9-fluorenylmethoxycarbonyl (Fmoc)-compatible thioester surrogates using readily available starting materials including *N*-methylated cysteine and thioethylbutylamide. These surrogates were incorporated as a C-terminal thioethylamido moiety of a peptide by solid-phase synthesis. Under acidic conditions, they transform into a thioester via an intramolecular N-S acyl shift reaction that is facilitated by the *cis*-conformation of the tertiary amide bond. In the presence of the intramolecular thiols of a cysteine-rich peptide, the C-terminal thioester is rapidly transformed into thiolactones via transthioesterification and cyclization accelerated by a thia zip mechanism. A novel oxidative folding strategy was developed in organic system to form

multiple disulfide bonds of cysteine-rich peptides within one hour. It overcame the limitations of conventional aqueous folding methods that required high dilution and long duration for completion. A combination of the newly developed cyclization and the organic folding strategy in a one-pot manner successfully afforded a shorter reaction time and an improved yield than the conventional methods. They could be used as a simple and high-throughput synthetic platform to prepare cyclic cysteine-rich peptides.

For designing cyclic peptides, I studied synthetic cyclic ω-conotoxin MVII analogs as models to demonstrate the consequence of engineering a linear peptide to form a cyclic peptide. The end-to-end cyclization of the linear created a functional neo-epitope that exhibited antimicrobial activities against bacteria and fungi. The results suggested that backbone cyclization could create new functions on a bioactive cysteine-rich peptide to expand its versatility for drug development. Collectively, my thesis works provide a new synthetic strategy for preparing and engineering cysteine-rich peptide-based biologics through backbone cyclization.

Chapter 1 Introduction

1. Cysteine-rich peptides

Cysteine-rich peptides are naturally occurring mini-proteins containing 12 to 78 residues (e.g. 12-residue "scratcher" conotoxin TxIIIC [1-3] and 78-residue NK-lysin [4]) with high content of intramolecular disulfide bonds. The occurrence of cysteine in CRPs is up to 50% (e.g. 12-residue TxIIIC contains 6 cysteine residues that form three disulfide bonds), which is remarkably higher than the average codon frequency (3.3%). These disulfide bonds provide conformational constraints, which lead to higher structural rigidity by reducing molecular flexibility and stabilizing secondary structures. Consequently, CRPs have the size of peptides but exhibit protein-like features including a stable and well-defined three-dimensional structure that usually corresponds to their biological activities.

CRPs are ubiquitously found in all organisms (**Figure 1-1**). In animals, prototypic CRPs include defensins, growth hormones and neurotoxins. In plants, the well-known CRPs include families of plant defensins, knottins, enzyme inhibitors, and cyclotides. Fungi express antibacterial defensins including plectasin [5] and eurocin [6], as well as several defensin-like CRPs with structural homology as ancient invertebrate defensins [7]. Bacterial CRPs are relatively rare, including a defensin-like anti-parasite peptide [8].
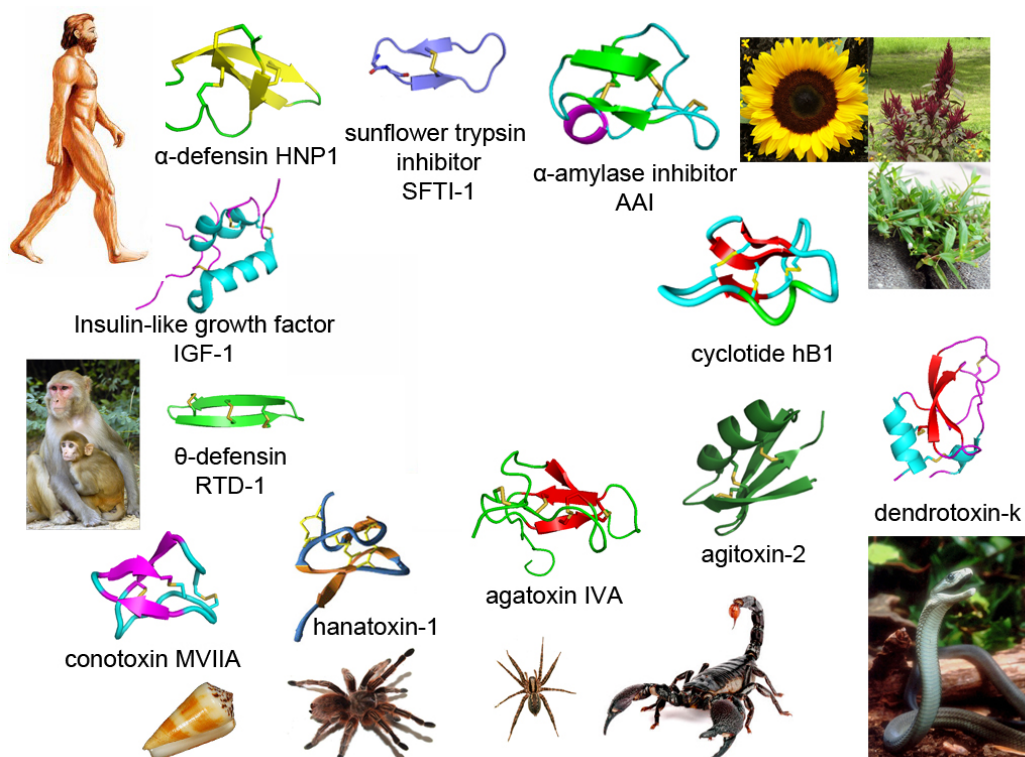
Figure 1-1. **Examples of cysteine-rich peptides from different species**. *Homo sapiens*: α-defensin HNP-1 (PDB entry: 2KHT), insulin-like growth factor IGF-1 (PDB entry: 1GZZ). *Rhesus macaque*: θ-defensin RTD-1 (PDB entry: 1HVZ). *Conus* magus: conotoxin MVIIA (PDB entry: 1OMG). *Grammostola spatulata*: hanatoxin-1 (PDB entry: 1D1H). *Agelenopsis aperta*: agatoxin IVA (PDB entry: 1OAV). *Leiurus quinquestriatus hebraeus*: agitoxin-2 (PDB entry: 1AGT). *Dendroaspis* genus: dendrotoxin-k (PDB entry: 1DTK). *Helianthus annuus*: sunflower trypsin inhibitor SFTI-1 (PDB entry: 1JBL). *Amaranthus hypochondriacus:* amylase inhibitor AAI (PDB entry: 1QFD). *Hedyotis biflora*: cyclotide hedyotide B1 (unpublished modeling structure resolved by Dr. Sui, 2010).

1.1 CRPs of animals

Defensin is one of the most intensively investigated classes of CRPs. They have been found in animals, plants, and lower organisms as an essential component of innate immune systems. In general, defensins are cationic with typically 18-50 residues and three to four disulfide bonds. They belong to the super family of anti-microbial peptides (AMP), which display a broad-spectrum of inhibitory activities against bacteria, fungi, archaea and viruses. Defensins are structurally featured by disulfide-stabilized β-sheet and are generally classified as cystine-stabilized β-strand AMPs [9, 10]. Animal defensins are classified in α-, β- and θ- defensins based on tissue distribution and disulfide framework [11]. The earliest identified human α-defensins with a disulfide framework of I-VI, II-IV and III-V were found in neutrophils. Human β-defensins with a knotted disulfide framework of I-V, II-IV and III-VI were predominantly found in leukocytes and epithelial cells. Different from α- and β-families, θ-defensins have disulfide ladder of I-VI, II-V and III-IV, and they possess a very unique end-to-end cyclic backbone, which provides additional conformational constraint [12]. The cyclic backbone of θ-defensin is formed by head-to-tail ligation of two truncated α-defensin as a homo- or heterodimer [13]. So far θ-defensins have only been identified in primate species *Rhesus macaque* (RTD) [13, 14] and *Olive baboon* (BTD) [15] . Human genome also contains an θ-defensin pseudogene which was not expressed due to a premature stop codon [16]. The artificial expression product of this pseudogene led to a "revived" θ-defensin named retrocyclin, with exciting anti-viral activities against human immunodeficiency virus (HIV-1) [17], herpes simplex virus (HSV) [18] and influenza viruses [19, 20]. Protegrins and tachyplesins are two families of θ-defensin-like linear CRPs in animals. They contain 16-18 residues with two disulfide bonds arranged in the ladder form.

The secretory neurotoxins belong to another large family of animal CRPs isolated from the venoms of cone snails, spiders, scorpions, and snakes. They modulate a wide variety of ion channels and neurotransmitter receptors such as acetylcholine (ACh), glutamate and serotonin [21]. Conotoxins are peptidyl toxins isolated from the venoms of fish-hunting marine cone snails in the genus of *Conus*. They bind and modulate ion channels and receptors with

high specificity and affinity. Conotoxins typically possess 12-30 residues with one to five intramolecular disulfide bonds. Their molecules are highly hydrophilic due to the cationic residue-rich sequences, posttranslational modification of proline to hydroxyproline, glutamate to γ-carboxyglutamate, and C-terminal amidation by glyoxylation. Injection of the conotoxin-containing venom can cause paralyzing or fatal effects on preys within a few seconds. Spider toxins (e.g. agatoxins from *Agelenopsis aperta* [22], hanatoxins from *Grammostola spatulata* tarantula [23], raventoxins from *Macrothele raveni* [24], atracotoxins from *Atrax robustus* [25]) target neurotransmitter receptors channels including glutamate-activated receptor channels, presynaptic voltage-gated Na^+ channels, voltage-gated K^+ channels and different types of Ca^{2+} channels in myocardial and neural tissues. Scorpion agitoxins contain highly organized secondary structures including three anti-parallel β-sheets and one α-helix supported by three cross-embraced disulfide bonds, which are structurally homologous to insect defensin. Agitoxins are inhibitors of voltage-gated K^+ channels expressed from *shaker (Sh)* gene of *Drosophila* and human homologous genes [26]. Snake venoms contain both neurotoxins and cytotoxins. The neurotoxins in snake venoms are potent inhibitors against ion channels and neurotransmitter receptors to immobilize and kill preys, and some snake neurotoxins can induce pain sensation [27]. The cytotoxins such as cardiotoxins and hemotoxins are not CRPs but shorter flexible peptides. They specifically attack cardiac cells and red blood cells, respectively.

The neurotoxins isolated from different animal species share many biological, chemical and structural similarities. They are highly soluble despite of the different molecular sizes and amino acid composition, which allow them to exist in the venom gland as a highly concentrated solution, and can easily diffuse in the preys' sera after injection. The classification system of peptidyl neurotoxins is tightly related with the development of electrophysiology, as the differentiation of subtypes of each ion channels were in part identified according to their responses to particular neurotoxins [28, 29]. Neurotoxins have been classified according to their specific targets, such as K^+ channel inhibitors, Na^+ channel inhibitors, and Ca^{2+} channel inhibitors.. The function of toxins in each class shows significant correlation with the cystine-stabilized structures

that conserved among species under different Phylum, which indicates a common and ancient origin of CRP toxins.

1.2 CRPs of plants

Plants expressed CRPs are diverse regarding amino acid sequences, structures and biological functions. Examples of plant CRPs are plant defensins, inhibitory knottins, cyclotides, snakins, heveins and lectin-like proteins [30]. Plant defensins are larger than animal defensins by containing more than 40 residues with three to four conserved disulfide bonds [31]. Their biological functions include anti-microbial, protein synthesis inhibitory, cytotoxic, and protease-inhibitory [32]. The lectin-like family includes *Amaranth* α-amylase inhibitor AAI [33, 34], which inhibits insect α-amylase from digesting starch [35, 36]. These inhibitors contain two disulfide bonds in one plane and the third disulfide bond penetrates through this plane to form a cystine-knot. α-amylase inhibitors share the same cysteine pattern (C-C-CC-C-C) and disulfide framework (I-IV, II-V and III-VI) and thus show similar structure as ω-conotoxins, while they exhibit completely different biochemical properties and functions.

In contrast to the only family of cyclic CRP *θ*-defensin in animals, plants produce a vanity of cyclic peptides such as cyclotides and sunflower trypsin-inhibitor (SFTI-1). Cyclotides are gene-encoded peptides that play important roles in the plant defense system. They have typically 27 to 43 amino acids and end-to-end cyclic backbone with three intramolecular disulfide bonds in the knotted arrangement of I-IV, II-V and III-VI [37-39] [40]. The cyclic cystine-knot (CCK) confers cyclotides' high metabolic stability [41-43]. Cyclotides have a diverse sequence composition and a large variety of biological functions including insecticidal, antimicrobial, immune-modulatory, enzyme-inhibitory, cytotoxic, and hemolytic. SFTI-1 is the smallest and most potent peptidyl trypsin inhibitor. It contains 14 residues that form a circle with one disulfide bond dividing it into a 7-residue trypsin-inhibition loop and a 5-residue secondary loop [44].

2. Conotoxins

2.1 Discovery and classification of conotoxins

Olivera's group have isolated the first conotoxin in *C. geographus* in late 1970s [45] and up to date over one thousand conotoxins have been sequences (refer to ConoServer). The estimated population of conotoxin is much larger since there are more than 700 species in *Conus* genus and each individual species potentially produces more than 100 different conotoxins.

Conotoxins are classified into gene-superfamilies, disulfide framework families and pharmacological families [46]. Up to date, there are 13 gene-superfamilies based on sequence similarity of ER signal peptide in the precursors, 23 cysteine framework families (named in roman number I-XXIII, the cysteine-poor conopeptides with one disulfide bond is not counted in the 23 families) **(Figure 1-2)** and 11 pharmacological families by the specific pharmacological targets (named in Greek letters).

Conotoxins under the same pharmacological family are target-specific, and in some cases tissue specific [47]. α-family conotoxins selectively inhibit nicotinic acetylcholine receptors, μ-conotoxin inhibits voltage-gated sodium channels (VGNaC), ι-conotoxin stimulates VGNaC, σ-conotoxin inhibit serotonin-gated G-protein coupled receptors (GPCR), κ-conotoxins inhibit voltage-gated potassium channels (VGKC), τ-conotoxin is recently found to inhibit somatostatin GPCR, and ω-conotoxin inhibits voltage-gated calcium channels (VGCC) (**Table 1-1**).
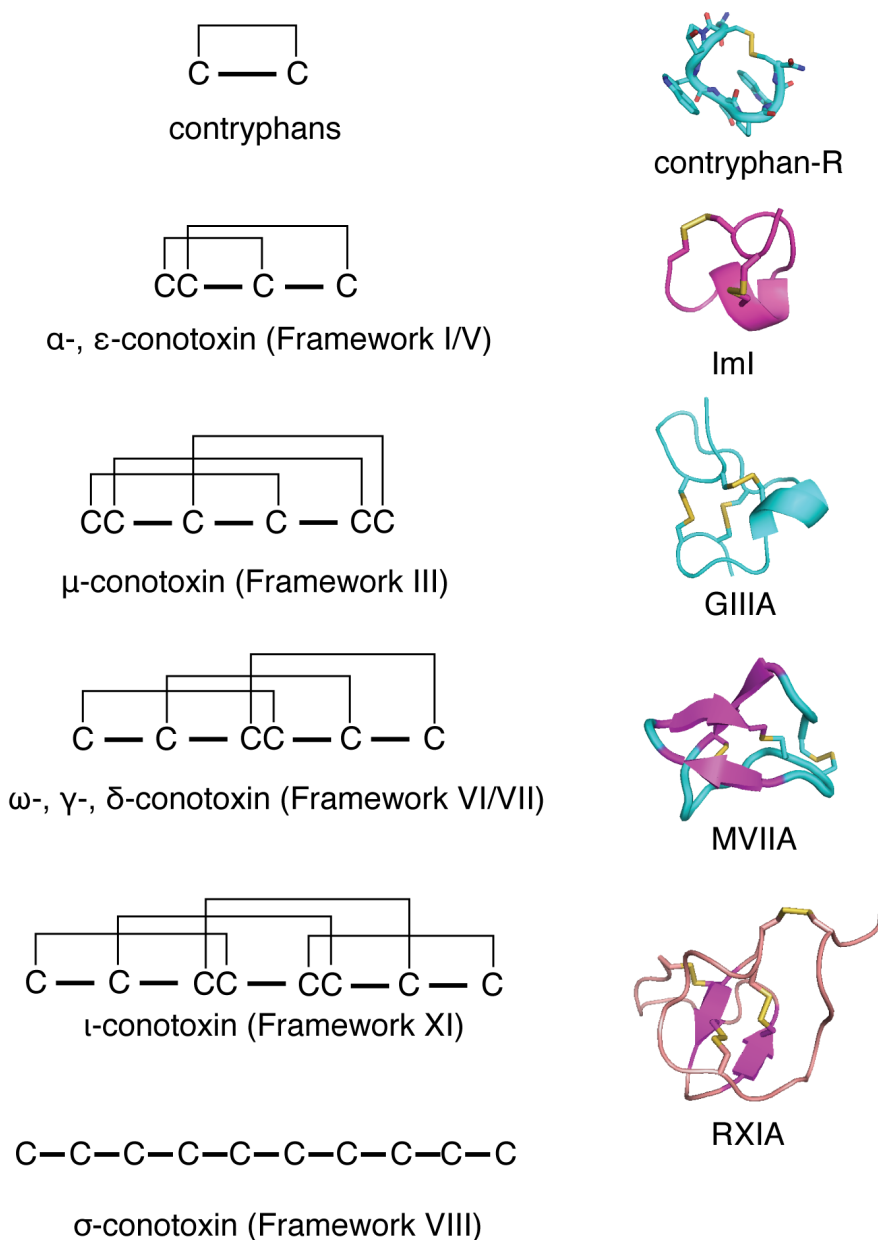
Figure 1-2. **Examples of cysteine and disulfide patterns of conotoxins**. Left lane: frameworks of cysteine-poor conopeptide contryphans (1SS), α- and ε-conotoxins (2SS), μ-, ω-, γ-, and δ-conotoxins (3*SS* but different in cysteine pattern), ι-conotoxins (4SS) and σ-conotoxins (10 cysteine residues, disulfide connectivity not reported). representitives of each framework (from top to bottom): contryphan-R (PDB entry: 1QFB), lml (PDB entry: 1IMI), GIIIA (PDB entry: 1TCG), MVIIA (PDB entry: 1OMG), RXIA (PDB entry: 2JTU).

Table 1-1. Classification of conotoxins by pharmacological activities (adapted from ConoServer).

Family	Pharmacolgcial function	Example	Ref.
α	Inhibit nAChR	ImI	[48]
γ	Activate neuronal pacemaker cation currents	TxVIIA	[49]
δ	Inhibit VGNaC, Delay inactivation of VGNaC	TxVIA	[50]
ε	Inhibit presynaptic VGCC and GPCR	TxVA	[51]
ι	Activate VGNaC	RXIA	[52]
κ	Inhibit VGKC	PVIIA	[53]
μ	Inhibit VGNaC	GIIIA	[54]
ρ	Inhibit α1-adrenoceptor	TIA	[55]
σ	Inhibit serotonin-gated ion channels	GVIIIA	[56, 57]
τ	Inhibit somatostatin receptor	CnVA	[58]
χ	Modulator of neuronal noradrenaline transporter	MrIA	[55]
ω	Antagonist of VGCC	MVIIA	[59, 60]

2.2 ω-conotoxins: voltage-gated calcium channel inhibitors
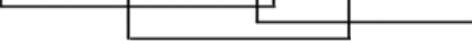
ω-conotoxins are inhibitors of presynaptic VGCCs but not blockers of calcium channels in muscle [61, 62]. They possess 24-27 residues and three knotted disulfide bonds with conserved cysteine pattern C-C-CC-C-C (**Table 1-2**). They draw a lot of interests because of their importance in the early characterization and classification of voltage-gated calcium channels and their pharmaceutical potentials.

As one of the most important ion channels in physiology, calcium channels differentiated into subtypes that play crucial roles in different signaling pathways. VGCCs are large protein complexes consist of four to five subunits. They are currently classified into Ca_v1, 2 and 3 families based on the gene of the pore-forming α1 subunit. Family Ca_v1 was earlier classified as *L*-type (L for "long-lasting") high voltage-activated calcium channels, which can be blocked by 1,4-dihydropyridine (DHP) [63]. Family Ca_v2 includes high-voltage activated $Ca_v2.1$ (*P/Q*-type, *P* for "purkinje") and $Ca_v2.2$ (*N*-type, *N* for "neuron"), and intermediate voltage-activated $Ca_v2.3$ (*R*-type, *R* for "residual"). Family Ca_v3 includes $Ca_v3.1$, $Ca_v3.2$, and $Ca_v3.3$, which are all low voltage-activated calcium channels that previously called T-type (*T* for "transient") channels.

N-type calcium channels ($Ca_v2.2$) are distributed in both peripheral and central nervous system that are rich in nociceptive neurons. Blocking of these channels at presynaptic axons causes inhibition of neurotransmitter release into the synaptic cleft, which lead to antinociceptive and neuroprotective effects (**Figure 1-3**). Therefore the specific and potent N-type calcium channel blockers such as ω-conotoxin GVIA and MVIIA are desired for development of pain-relief drugs [64-66]. These ω-conotoxins have been developed into peptidyl analgesics since 1990s [67, 68]. In 2004, FDA approved the synthetic MVIIA (SNX-111) as a non-opioid analgesic drug ziconotide (or Prialt [TM]) to be used for treatment of chronic and neuropathic pains. It is a substitute of "dirty" drugs like morphine to avoid adverse side effects. However, it's been delivered through intrathecal (IT) administration, which is unpleasant, risky and expensive.

Table 1-2. Examples of ω-conotoxins and their sequence homology, disulfide connectivity, pharmacological targets and net charges.

Species	Toxin	Sequence	Target	Net Charge
C. geographus	GVIA	CKSOGSSCSOTSYNCCR-SCNOYTKRCY-NH$_2$	N	+5
C. magus	MVIIA	CKGKGAKCSRLMYDCCTGSC-R-SGKC-NH$_2$	N	+6
C. magus	MVIIC	CKGKGAPCRKTMYDCCSGSCGRR-GKC-NH$_2$	P/Q	+6
C. consors	CnVIIA	CKGKGAOCTRLMYDCCHGSCSSSKGRC-NH$_2$	N	+5
C. catus	CVIA	CKSTGASCRRTSYDCCTGSCR--SGRC-NH$_2$	N	+5
C. catus	CVIB	CKSKGASCRKTMYDCCRGSCR--SGRC-NH$_2$	N and P/Q	+6
C. striatus	SVIB	CKSKGQSCSKLMYDCCTGSCSRR-GKC-NH$_2$	N and P/Q	+7

O: hydroxyproline. Cys residues are highlightled in yellow.

Conserved residues Y13 is highlighted in cyan.
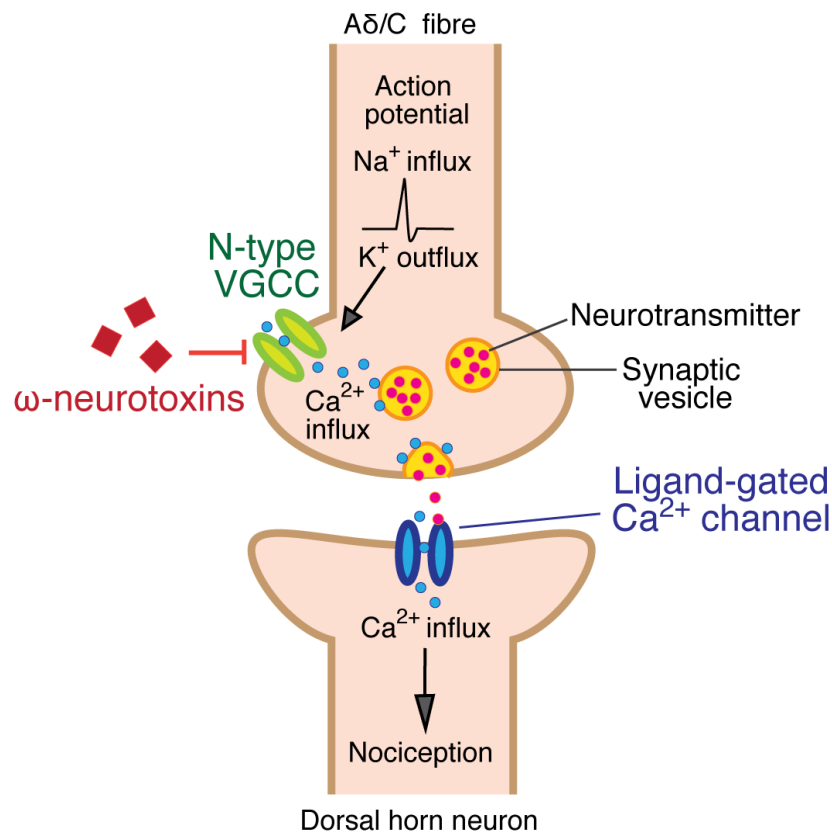
Figure 1-3. **The mechanism of N-type calcium channel inhibition by ω-neurotoxins towards analgesics.** In the axon terminal of nociceptive Aδ/C fibre, propagated action potential induces voltage-gated calcium channel open and influx of calcium ions to the presynaptic node, which triggers release of neurotransmitters from synaptic vesicles into the cleft. Binding of neurotransmitters (e.g. glutamate) to the ligand-gated receptor mediate calcium channel open at postsynaptic dorsal horn neurons, which stimulate nociception. (Adapted from [69])

3. Cyclotides

3.1 Discovery of cyclotides

The first cyclotide kalata B1 was isolated from an herbal plant *Oldenlandia affinis* [70] by a Norwegian doctor Lorents Gran during his red-cross mission at Congo. The local African women use *O. affinis* to make folk herbal tea "kalata-kalata" and drink it to facilitate childbirth. Dr. Gran isolated kalata B1, and identified it as the active ingredient with oxytocin-like activity that prolonged the smooth muscle contraction of uterus [71] (**Figure 1-4**). In the middle 1990s, the unique cyclic backbone and cystine-knot structure of kalata B1 was resolved by NMR analysis, which explained its ultra-stability in the boiled water and digestive system [38]. These plant-origin cyclic peptides with stable structures were collectively called cyclotides [72] and are abundant in plant families including Rubiaceae [73, 74], Violaceae [72, 75], Cucurbitaceae [76, 77], Fabacaea [78, 79], and Poaceae [80].

Figure 1-4. Congolese women made herbal tea kalata-kalata to facilicate child birth (left) using *Oldenlandia affinis*. (right top: whole plant. right bottom: purple flower of *O. affinis*).

3.2 Classification and sequence diversity of cyclotides

Cyclotides are classified into Möbius and Bracelet and trypsin-inhibitor subfamilies [81, 82] (**Figure 1-5**). The Möbius cyclotides such as kalata B1 are featured by a twisted backbone arranged in Möbius-ring morphology. The backbone twist is due to a conserved cis-proline in loop 5. In contrast, bracelet cyclotides do not contain this *cis*-proline and thus their cyclic backbones are like a bracelet. Trypsin-inhibitor subfamily contains several trypsin-inhibitory cyclotides including MCoTI-I and MCoTI-II isolated from *Momordica cohinchinensis* [83]. **Table 1-3** presents examples of cyclotides from Möbius, bracelet and trypsin-inhibitor subfamilies. In Möbius and bracelet cyclotides, the loop 1 is conserved as a tripeptide sequence X_1-E-X_2. Residue X_1 is a small hydrophobic amino acid like Gly, Ala or Ile. Residue X_2 is either Ser or Thr that similar by having a side-chain hydroxyl group. Bracelet cyclotides have a longer loop 3 that often forms a short helical structure. Loop 4 is the shortest loop in all three subfamilies that consist of one residue only. Loop 6 contains the cyclization site, which is typically between an N-terminal Gly and C-terminal Asn/Asp residues. This observation contains important information for resolving the biosynthesis pathway of backbone cyclization.
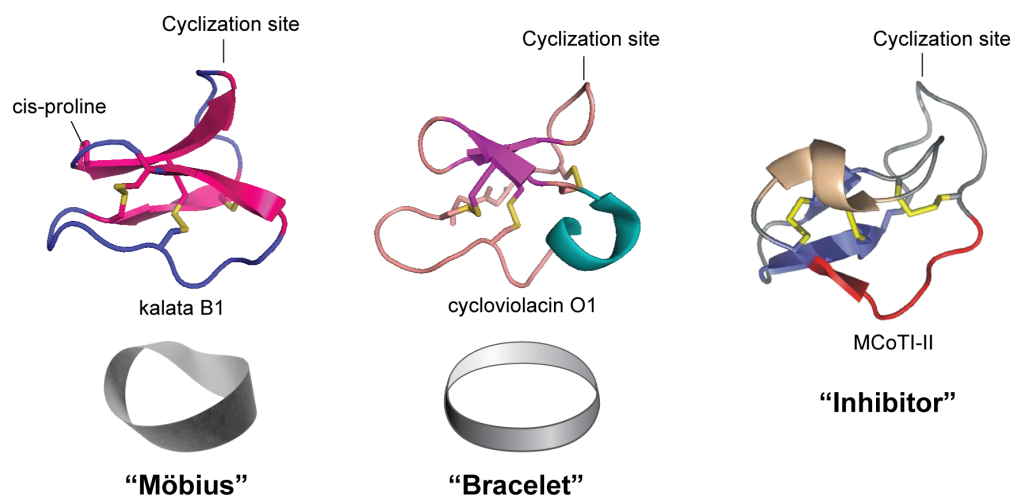
Figure 1-5. **Classification of cyclotides**. Möbius cyclotides (e.g. kalata B1, PDB entry: 1KAL) have a twisted backbone. Bracelet cyclotides (e.g. cycloviolacin O1, PDB entry: 1DF6) have bracelet-like backbone morphology. Trypsin inhibitor subfamily has the trypsin-inhibitory activities as the name indicated (e.g. MCoTI-II, PDB entry: 1HA9).

Table 1-3. Examples of cyclotides from three subfamilies

Cyclotide	Sequence	Species
Möbius		
kalata B1	CGET---CVGGT-CN-T--PGCTC-SWPVCTRNGLPV	*O. affinis*
kalata B2	CGET---CVGGT-CN-T--PGCSC-TWPICTRDGLPV	*O. affinis*
cycloviolacin H3	CGET---CFGGT-CN-T--PGCICDPWPVCTRNGLPV	*V. odorata*
cycloviolacin O16	CGET---CFTGK-CY-T--PGCTC-SWPVCTRNGLP-	*V. odorata*
varv A	CGET---CVGGT-CN-T--PGCSC-SWPVCTRNGLPV	*V. arvensis*
varv B	CGET---CFGGT-CN-T--PGCSCDPWPMCSRNGLPV	*V. arvensis*
Bracelet		
circulin A	CGES---CVWIP-C-ISAALGCSC-KNKVCYRNGIP-	*C.parvifolia*
circulin C	CGES---CVFIP-C-ITSVAGCSC-KNKVCYRNGIP-	*C.parvifolia*
cycloviolacin O1	CAES---CVYIP-CTVTALLGCSC-SNRVCY-NGIP-	*V. odorata*
cycloviolacin O2	CGES---CVYIP-C-ISSAIGCSC-KSKVCYRNGIP-	*V. odorata*
kalata B5	CGES---CVYIP-C-ISGVIGCSC-KDKVCY-NGIP-	*O. affinis*
kalata B16	CAES---CVYIP-CTITALLGCSC-KNKVCY-DGIP-	*O. affinis*
hedyotide B1	CGET---CFVLP-C-WSAKFGCYC-QKGFCYRNGTR-	*H. biflora*
Trypsin-inhibitor		
MCoTI-I	CPKILQRCRRDSDC-PGA---CICRGNGYCGSGSDGGV	*M. Cochinchinensis*
MCoTI-II	CPKILKKCRRDSDC-PGA---CICRGNGYCGSGSDGGV	*M. Cochinchinensis*

Conserved disulfide bonds and macrocyclic backbone were shown as black lines.

Cys residues were highlighted by background yellow.

Conserved *cis*-Pro residues in Möbius cyclotides were highlighted in blue.

Cyclization sites are highlighted in red.

3.3 Biosynthesis of cyclotides

The biosynthesis of cyclotide is introduced using kalata B1 as a model. As shown in **Figure 1-6**, kalata B1 gene consists of five domains: ER signal sequence, N-terminal pro-domain (NTPD), N-terminal repeating domain (NTR), cyclotide-domain and a short C-terminal domain (CTD) [84]. NTR is highly conserved within species, which is useful for discovering cyclotides form the same plant. The ER signal peptide mediates translocation of the ribosome/mRNA complex to endoplasmic reticulum (ER), where the ER signal peptide is excised followed by the synthesis of a stable intermediate NTPD-NTR-cyclotide-CTD. In the ER lumen, disulfide bond formation is catalyzed by a set of ER resident enzymes such as protein disulfide isomerase (PDI) and chaperone proteins [85]. Only one out of 15 folding isomers with the correct disulfide connectivity can be transported to Golgi. The mis-fold products are subsequently degraded by ER peptidases. The proteolytic cleavage of NTPD may occur during Golgi trafficking process to give the second intermediate NTR-cyclotide-CTR. The excision of the α-helical NTR is catalyzed by endopeptidase after a Leu-Xaa dipeptide located prior to the first residue of cyclotide domain. This dipeptide is conserved in both *Rubiaceae* and *Violaceae* families. The cleavage of cyclotide from CTR usually occurs at Asn, or less frequently at Asp. Gillon et al. suggested that the C-terminal cleavage and cyclization are mediated by the same enzyme asparaginyl endopeptidase (AEP) [86]. The short hydrophobic CTD sequence contains a conserved tripeptide motif adjacent to the cyclotide domain, which is essential for AEP recognition.
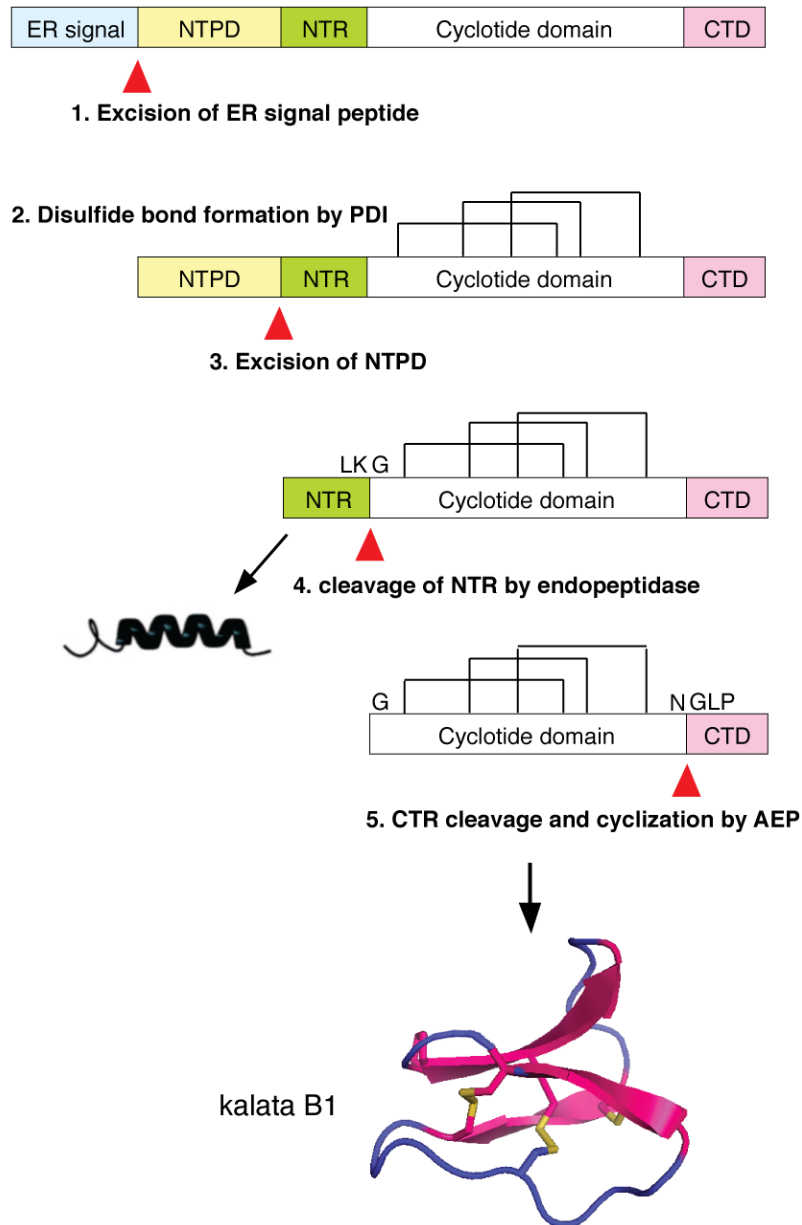
Figure 1-6. Biosynthesis processing of kalata B1 from linear precursor. The current-understood processing mechanism involves five steps: 1. Excision of ER signal peptide after translocation of translation complex. 2. Proteolytic cleavage of N-terminal pro-domain (NTPD) in ER lumen. 3. Disulfide formation catalyzed by ER enzymes like protein disulfide isomerase (PDI) and chaperone proteins. 4. Cleavage of N-terminal repeat domain (NTR) in Golgi tranffiking process. 5. Cleavage of C-terminal region (CTR) followed by end-to-end cyclization mediated by asparaginyl-endopeptidase (AEP).

The mechanism of AEP-mediated cyclization has not yet been fully revealed but transpeptidation is involved in a splicing-like process [86, 87]. Taking kalata B1 (kB1) as an example, the pro-kB1 sequence binds in the reactive pocket of AEP by a specific recognition motif TRNGLP. TRN is the C-terminal residues of cyclotide domain, which fit into substrate sites S3, S2 and S1 of AEP, respectively. GLP is the tripeptide of CTD that binds to site S1', S2' and S3'. Such multiplex binding of pro-kB1 and AEP leads to the formation of kalata B1-enzyme thioester intermediate through a nucleophilic attack on the carbonyl group of Asn by a Cys-SH of AEP (**Figure 1-7A**). Subsequently, the CTD sequence is release from reactive site of AEP, followed by binding of N-terminal residues of cyclotide domain, which possess the identical tripeptide GLP as CTD N-terminus (**Figure 1-7B**). This binding allows the amine group of the first residue Gly to locate close enough to the thioester bond of kalata B1-enzyme intermediate, which mediate a proximity-driven S-N acyl shift reaction to form the cyclic backbone of kalata B1 (**Figure 1-7C**).

Linear forms of cyclotides have been reported, designated as acyclotides or uncyclotides [88-91]. Plan, et al. suggested a degradation mechanism of linear kalata B9 and B10 during AEP-mediate cleavage between Asn-Gly, where the Asn was transformed into a succinimide intermediate [89]. Evidences at both mRNA and protein levels show that uncyclotide such as violacin A [88], psyl C [90], and chasatides C7 and C8 [92] lacked either N-terminal Gly or C-terminal Asn/Asp in the precursor sequences, which indicated that thsee two sites are essential for AEP-catalyzed backbone cyclization of cyclotides.
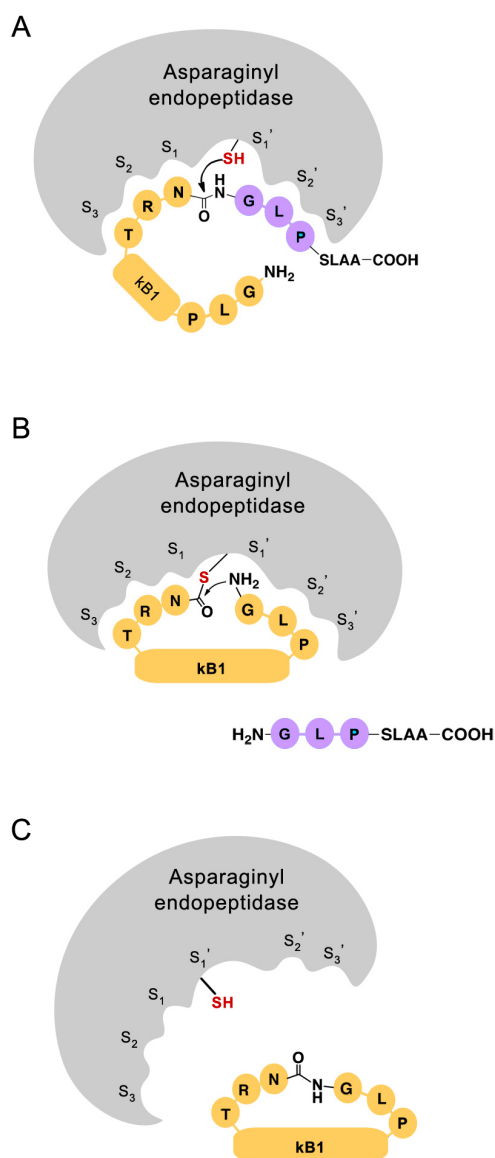
Figure 1-7. Proposed mechanism of Asparaginyl-endopeptidase (AEP)-mediated cyclization of kalata B1. (A) Asparaginyl endopeptidase (AEP, grey) recognizes the C-terminal binding motif TRN-GLP of the pro-kB1 containing cyclotide domain (orange) and CTD (purple). AEP cleaves after Asn residue to release the CTD sequence and subsequently form a kB1-enzyme thioester intermediate. (B) The N-terminal tripeptide GLP (orange) of the cyclotide domain fit into the binding pockets S_1', S_2' and S_3'. N-terminal primary amine group of Gly is located closely to the thioester bond of kB1-enzyme intermediate, which triggers a nucleophilic attack on the carbonyl group to form an amide bond. (C) The cyclized kalata B1 is released from the binding pocket of AEP (Adapted from [86, 93]).

A proteolytic enzyme other than AEP may mediate backbone cyclization. When examining the trypsin-inhibitory effect of a linear analog of SFTI-1 with one opening in the secondary loop, Marx, et al. found that trypsin could cyclize this linear SFTI-1 back to its native form [94].

3.4 Biological activities of cyclotides

During recent two decades, a wide range of biological activities of cyclotides has been identified including uterotonic, insecticidal, anti-microbial, anti-HIV, anti-cancer (cytotoxicity), hemolytic, trypsin-inhibitory, anti-neurotesin, and hormonal activities (**Table 1-4**).

Our lab firstly reported the antimicrobial activities of cyclotides [95]. Cyclotides such as kalata B1, circulin A and B, exhibit a broad range of inhibitory effects against bacteria, fungi and viruses. The antimicrobial activities are related with their membrane-binding activities. The electrophysiological experiments showed that kalata B1 could form multimeric transmembrane pores with channel-like activity that led to cellular content leakage and cell death [96]. The core region of cyclotides is filled with disulfides and thus the hydrophobic residues are externalized to form hydrophobic patches on the surface that associate with the membrane-binding activity. In Möbius cyclotides these hydrophobic patches mainly involve residues in loop 2 and 5, while in bracelet cyclotides they are distributed in loop 2 and loop 3. This difference in the location of the hydrophobic patch may explain the different binding modes of these two peptide subfamilies [97].

Table 1-4. Bioactivities of cyclotides and their representatives

Activity	Representatives	First discovery
Uterotonic	kalata B1, B2 [98]	1973
Anti-HIV	circulin A and B [73], circulin C-F [99], cycloviolin A-D [100], kalata B1 [101], kalata B8 [102]	1994
Neurotensin antagonist	cyclopsychotride A [103]	1994
Hemolytic	circulin A, B and cyclopsychotride A [95], kalata B1 [104], cycloviolacin O2, O13-15, O24 and varv A [88]	1999
Antimicrobial	circulin A, B, cyclopsychotride A and kalata B1 [95], kalata B7 [105], hedyotide B1 [106]	1999
Trypsin-inhibitory	MCoTI-I and MCoTI-II [107]	2000
Insecticidal	kalata B1 and B2 [84]	2001
Anti-cancer	cycloviolacin O2, varv A and F [108], varv E and vitri A [109], vibi E-H [110] Chassatides [92]	2002
Anti-fouling	cycloviolacin O2 [111]	2004
Cell-penetrating	McoTI-II [112]	2007
Nematocidal	kalata B1, B2, cycloviolacin O2, O3, O8 and O13-16	2008
Molluscidal	cycloviolacin O2, kalata B1 and B2 [113]	2008

4. Cyclic CRPs in drug design

Peptides are given increasing interest in drug development and design in recent years of pharmaceutical industry. The global revenues of peptide therapeutics reached 13 billion USD in 2010. In 2012, FDA approved about 40 novel drugs of which five were synthetic peptides [114].

In general, the advantage of peptides therapeutics is more specific and potent interactions upon binding with target molecules, which cause fewer side effects and toxicities as compared with small molecules. However, the intrinsic disadvantages of peptides limited the therapeutic applications regarding their poor stabilities that cause short physiological half-life and difficulty in drug delivery. This stability problem can be overcome by reducing the conformational flexibility by peptide engineering, including side chain covalent bonding such as disulfide bond formation, and backbone cyclization [115]. Backbone cyclization reduces the flexibility of two termini and it results in the intrinsic resistance against exopeptidation. The intramolecular disulfide crosslinks partition the peptide sequence into several loops and often stabilize secondary structures that significantly reduce the overall conformation flexibility. Metabolic-stable cyclic CRPs are thus given growing attentions for peptide engineering. We hypothesized that stable peptide scaffold can be prepared by cyclizing the linear backbone of a CRP. This approach avoids the conventional strategies such as introducing unnatural amino acids or building blocks to enhance the molecular stability.

There are several examples on cyclizing bioactive CRPs to give more stable analogs including cyclic α-conotoxins [116, 117], AMPs [118-120] and bradykinin antagonist [121]. α-CTX Vc1.1 is a 16-residue α-conotoxin with two disulfide bonds and one α-helix at the bioactive site. It is a potent inhibitor of neuronal α9α10 nAChR [122-124] and an agonist of $GABA_B$ receptors [125]. The channel binding properties of Vc1.1 result in anti-nociceptive activity by indirectly inhibiting the N-type calcium channels of dorsal root ganglions in the rat model via activation of $GABA_B$ receptors. A cyclic form cVc1.1 with a 6-residue linker GGAAGG (**Figure 1-8**) to fill the distance between two termini

(about 12 Å) was synthesized, which displayed enhanced binding selectivity and potency to GABA$_B$ receptors thus enhancing the inhibitory effect against *N*-type calcium channels. The cyclic analog cVc1.1 also acquired an improved metabolic stability that makes it available for oral delivery.

The cyclization of AMPs including α-defensin, protegrin (PG) and tachyplasin (TP) manipulate their biological activities and therapeutic potentials. Their backbone cyclic analogs were synthesized by ligating two termini with a peptide bond without introducing any extra residues. The resultant analogs of α-defensin maintained antimicrobial activities at high salt conditions [120]. The cyclic PG-1 and TP-1 analogs with addition of one disulfide bond displayed increasing membranolytic selectivity between microbial and erythrocyte membranes, which enlarge the therapeutic window for medication [118, 119].

A stable antagonist of bradykinin B1 receptor was prepared by grafting a linear B1-receptor antagonist including 9-residue DALK and 7-residue DAK into the stable scaffold of kalata B1. As the active ingredient in a boiled herbal tea, cyclotide kalata B1 are stable against heat, denaturing conditions such as 8 M urea or 6 M guanidine, low pH that resemble the acidity in stomach, and the peptidases in GI tract and sera [126]. The linear antagonists have limited resistance against peptidases and thus none of them have been developed into drugs for clinical use. By replacing loop 6 of kalata B1 to form cyclic product ckb-kal and ckb-kin, respectively [121], these engineered cyclic antagonists became stable and orally available (**Figure 1-9**). They are analgesics against acute pains in a writhing assay done on mice through both intraperitoneal injection and oral administration. As the negative control, kalata B1 itself shows no inhibitory activity.

CRPs provide splendid resources and useful scaffolds for developing stable peptidyl therapeutics. However only a few cyclic CRPs have been synthesized and the difficulty in backbone cyclization and disulfide folding have been reported in literatures. This problem demands us to develop an efficient and productive synthetic strategy to facilitate the application of cyclic CRPs in drug design.
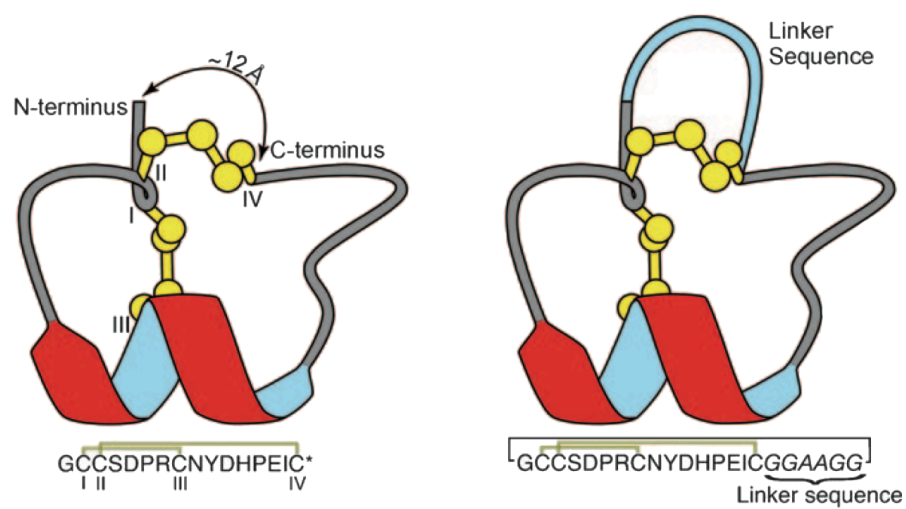
Figure 1-8. **Design of cyclic α-conotoxin Vc1.1.** Additional linker GGAAGG was added join the N- and C-termini (Cited from [*(117)*]).
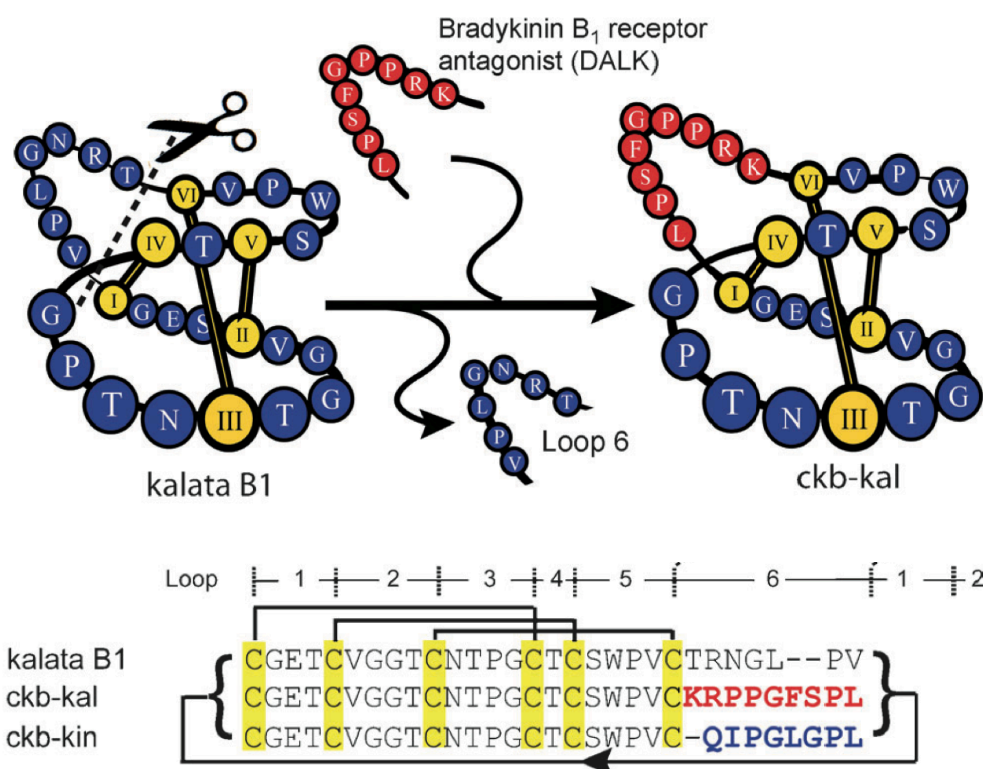
Figure 1-9. Scheme of engineered bradykinin B1 receptor antagonist ckb-kal on the cyclotide kalata B1 scaffold and their amino acid sequences (Cited from [121]).

5. Recombinant synthesis of cyclic peptides using intein-splicing

Backbone cyclization was the first challenge in preparing a stable cyclic CRP. The natural occurring cyclic backbone of cyclotides was synthesized by protease AEP through transpeptidation reactions and this phenomenon was observed on other transpeptidase such as sortase, subtiligase and intein (**Figure 1-10**). Sortase is a prokaryotic enzyme that mediate cleavage specifically after Thr residue in the sequence of LPXTG followed by transpeptidation to another N-terminal Gly-containing peptide [127]. Subtiligase was a variant of bacterial protease subtiligin that recognized C-terminal glycolated-phenylalanine-amide [128]. Peptide ligation using subtiligase was reported in 1994 [129] and subtiligase-mediated peptide cyclization was done in 1995 [130]. Intein is a protein segment that catalyzes self-excision and transpeptidation to form matured protein sequence via a protein splicing process. The revealing of intein splicing mechanism in the middle 1990s led to development of expression protein ligation strategy by Muir's group in 1998 [131]. The cyclization approaches adopting AEP, sortase or subtiligase require preparation of a specific sequence or moiety for enzyme-recognition, which restricts their application in protein synthesis. In contrast, intein can be co-expressed together with the target peptide sequence as a fusion protein, and directly mediates peptide bond breaking and reforming via intramolecular acyl shift reactions. The catalytic mechanism of intein allows an efficient and clean approach for protein ligation and cyclization.
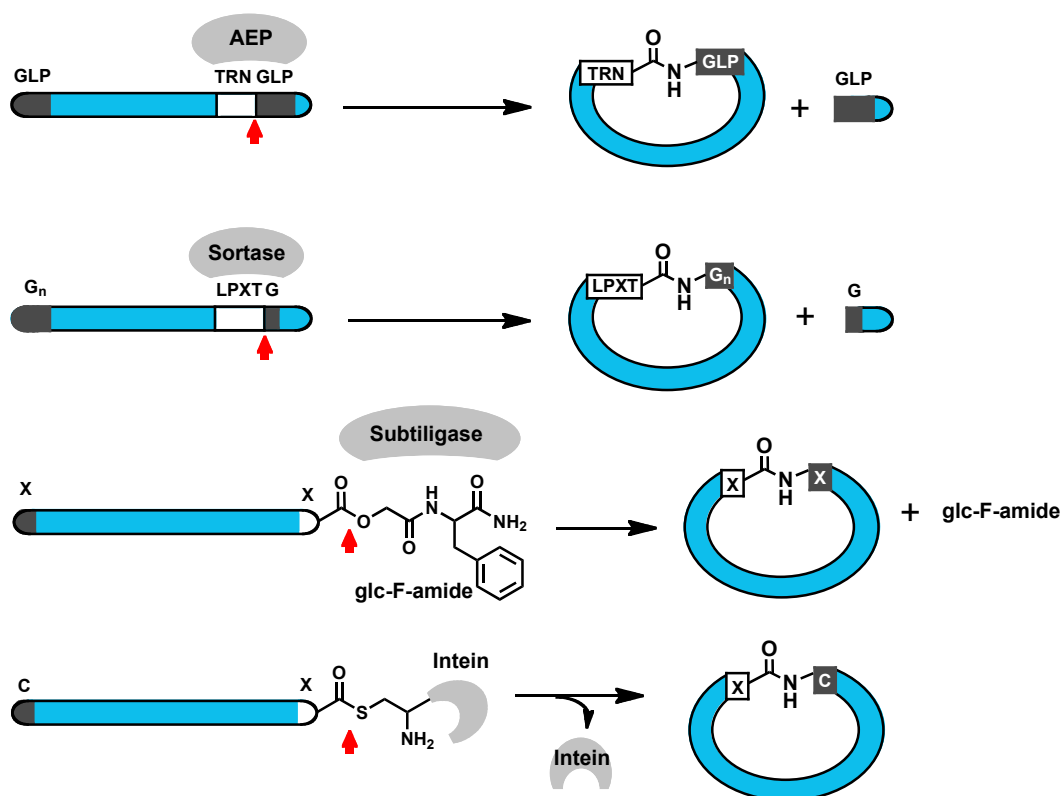
Figure 1-10. Comparison of protein cyclization mechanisms mediated by asparaginyl endopeptidase (AEP), sortase, subtiligase and intein. Red arrow indicates the cleavage and cyclization sites.

5.1 Discovery of intein

The phenomenon of protein splicing was firstly observed in 1988 in a study on yeast trifluoperazine-resistant TFP1-408 gene [132]. The open-reading frame of TFP1-408 gene encoded a >100 kDa protein with sequence homology of two ATP-dependent proton pump subunits, 69 kDa F_0F_1 ATPase subunit and 67 kDa vacuolar ATPase subunit found in *Neurospora* [133, 134]. In 1990 Hirata et al. reported the yeast vacuolar membrane ATPase VMA-1 gene, which had single open-reading frame encoding 119 kDa sequence, surprisingly produced two protein products including a 69 kDa H^+-ATPase subunit A and a 40 kDa intervening protein segment [135]. In the same year Kane reported that yeast TFP-1 gene, which produced a 69 kDa subunit of H^+-ATPase and a 50 kDa "spacer" protein Tfp1p from the ~130 kDa gene expression product [136]. The cDNA sequence of this spacer was found to be embedded inside the encoding region of the 69 kDa subunit of H^+-ATPase, indicating that the ATPase subunit was derived from protein splicing. In the following years more intervening protein sequences (IVPS) were discovered in eubacteria, archaea, and eukaryotes including *Mycobacterium tuberculosis*, *Thermococcus litoralis,* and *Candida tropicalis* [137-140]. The sequences of IVPSs were highly homologous to homing endonucleases, which explained the finding of random allocation of intein sequence in the unrelated genes. This migration and dissemination of intein sequence was referred as a "selfish" or "parasitic" genetic element [141-143].

The name "intein" (refer to "protein intron") was first used to define the enzymatic IVPS by Perler [144] in 1994, with the N-terminal and C-terminal flanking sequences named as N- and C-exteins, respectively. An intein in a newly expressed protein sequence behaves similarly as an intron in the pre-mRNA (**Figure 1-11**). Intron mediates self-cleavage and rejoins flanked RNA fragments to form matured mRNA, described as RNA splicing. Intein induces self-excision and subsequent ligation of two exteins by the formation of a native peptide bond. Up to date, there are more than three hundred inteins identified with wide occurrence in all three domains of living organisms, locating in the genes of DNA/RNA polymerases, vacuolar ATPases, metabolic enzymes, proteases and ribosomal reductases (refer to *INBase* [145]).

RNA splicing
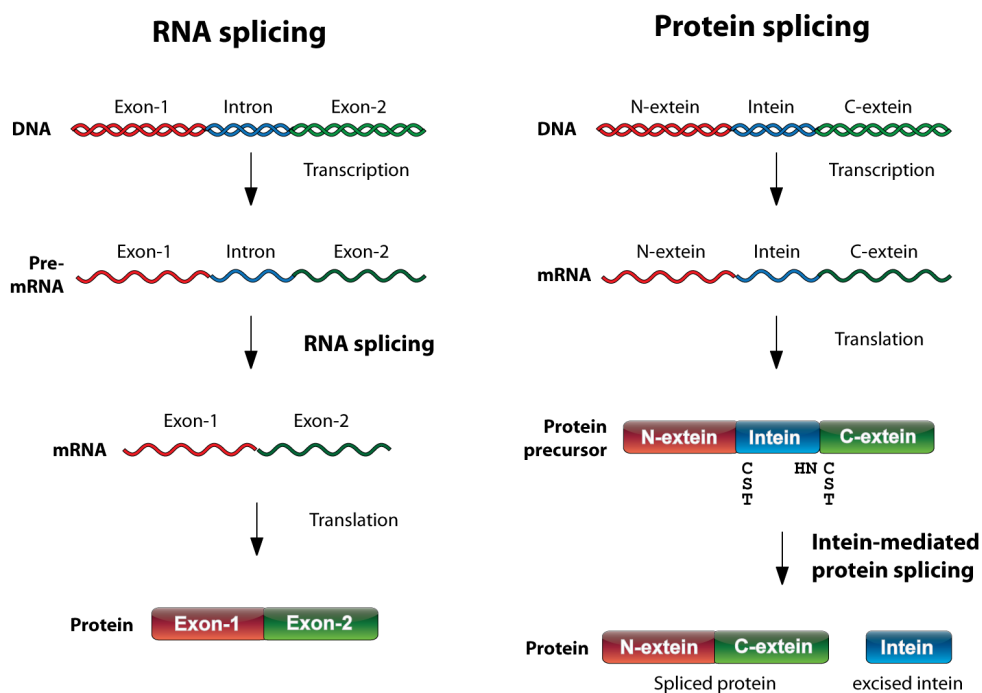
Protein splicing

Figure 1-11. **Comparison of RNA splicing and protein splicing**.

5.2 Mechanism of intein-mediated protein splicing

The alignment studies on splicing sites revealed that key residues in the splicing process included N-terminal Ser, Thr or Cys that carried nucleophilic OH/SH groups, and C-terminal Asn. The splicing activities were not relied on flanking sequences of intein. Therefore, IVPS/intein remained reactive when migrated into foreign genes in-frame [138, 139, 146]. Cooper et al. proved the formation of a new peptide bond between two spliced fragments after Tfp1p self-excision [147]. They also reported the importance of the existence of C284 and C-terminal N737 at splicing sites of Tfp1p by mutational analysis and proposed the model of intein splicing involved succinimide-mediated cleavage at N737 was followed by transpeptidation from C738 to G283 and release of spacer C284-N737.

In 1993, Xu et al. identified a very important branched intermediate with two N-terminal NH_2 groups during intein-mediated protein splicing by sequential Edman degradation analysis [148]. Later they proposed a mechanism of intein splicing as formation of an alkali-labile ester bond between N-extein and intein through N-O acyl shift followed by an O-O transesterification from intein to C-extein. The branched intein was released by C-terminal Asn succinimide cyclization and ester bond between N- and C-exteins was converted to amide bond by O-N acyl shift [149]. The mechanism of autocatalytic intein splicing was further explored by sequence alignment, mutational studies, kinetic studies and chemical modulations [143, 149-155].

The general mechanism of intein-splicing has been elaborated as four-step acyl shift reactions (**Figure 1-12**): (1) N-O/S acyl shift between N-extein and intein to afford an active ester/thioester bond at the splicing site where the amide bond is in *cisoid* conformation mediated by intein [156]. (2) Transesterification between the first residue of C-extein (Cys, Ser) and newly formed ester/thioester bond at N-splicing site, which resulted in the formation of branched intermediate. (3) N-N acyl shift at C-terminal Asn of intein to form a succinimide and spontaneously releases intein from the branched intermediate. (4) S/O-N acyl shift in proximity to afford an amide bond between N- and C-extein.
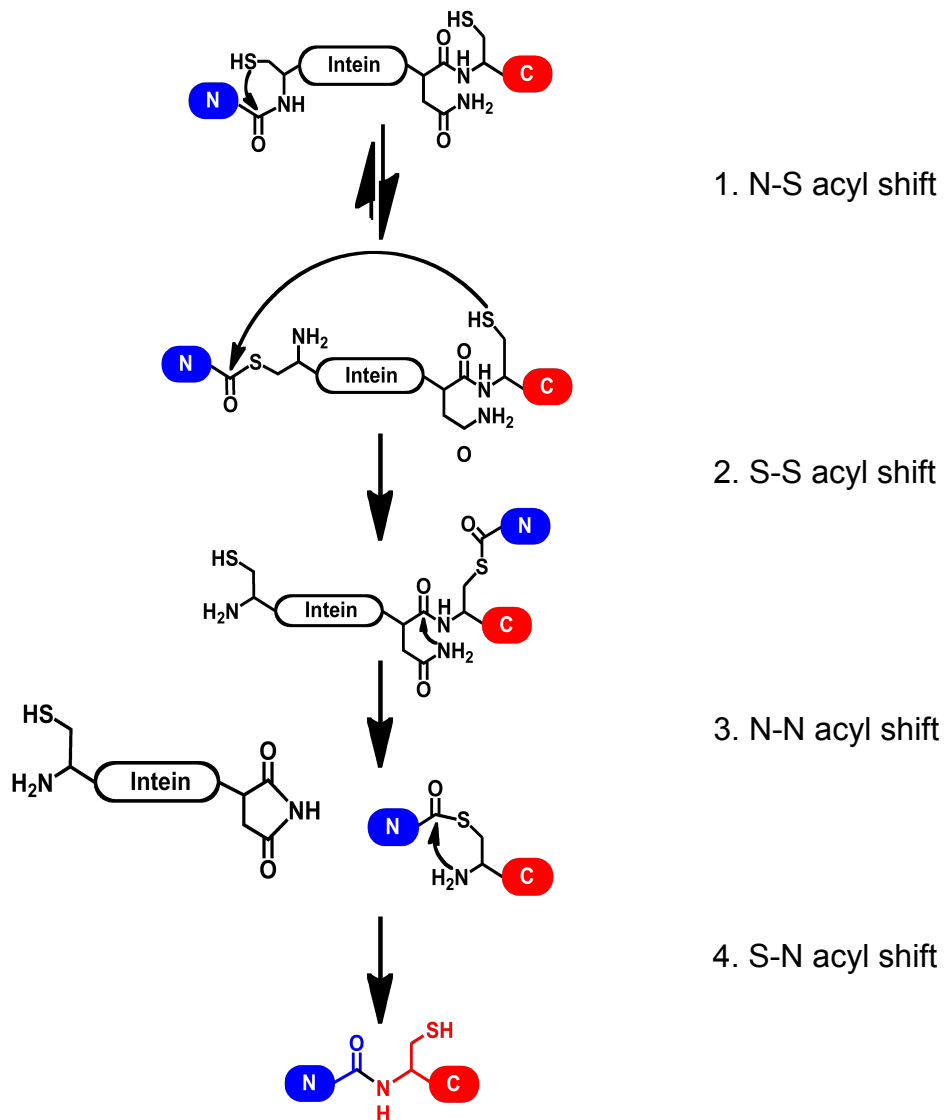
Figure 1-12. Mechanism of intein-mediated protein splicing. The N-terminal residue is Cys and occasionally Ser or Thr (N, N-extein. C, C-extein).

5.3 Development of intein-based expressed protein ligation (EPL)

The intein-mediated splicing process has been developed into various technologies in the biomedical research including protein semisynthesis, tagless purification and labeling, microarray and biosensors. In my project, I adopted intein splicing for semisynthesis of the cyclic cysteine-rich peptides.

The combination of intein splicing in recombinant expression was firstly reported as expressed protein ligation (EPL) to prepare a functional C-terminal Src kinase protein by Muir's group [131]. This kinase contained a phosphorylated Y527 residue at the C-terminal tail, thus it was not applicable for total synthesis using recombinant technology. This kinase was prepared by EPL approach involving four steps: (1) express a fusion protein containing the N-terminal fragment of the kinase, an engineered intein and an affinity tag (2) purify fusion proteins in the affinity column and conduct intein-catalyzed N-S acyl shift followed by thiol-thioester exchange reaction to release the N-terminal fragment with a C-terminal thioester, (3) synthesize the C-terminal fragment starting with a Cys residue and containing the phosphorylated Tyr (4) ligate the N-terminal fragment thioester with the C-terminal synthetic fragment to form an intact kinase protein (**Figure 1-13**). In this engineered intein, the homing endonuclease sequence was removed, which did not affect the self-cleavage activity. The C-terminal Asn of this engineered intein was mutated into Ala and attached with a chitin-binding domain (CBD) sequence in frame. The mutated intein thus only catalyzed the reactions involving the N-terminal Cys, which was N-S acyl shift to give a thioester intermediate. Under proper conditions such as excessive external thiols R-SH at pH 8, transthioesterification is actively conducted to replace intein from the thioester intermediate to release peptide-SR thioesters. This peptide thioester is ready to be "captured" by an N-terminal Cys-containing peptide to afford a ligation product via Cys-thioester ligation. This method has been converted directly into method for cyclic peptide synthesis by designing an N-terminal Cys residue on the recombinant protein [157-159] and constructing a cyclic peptide library. The stable peptide thioesters prepared from the recombinant intein fusion proteins are also accessible to nucleophilic addition of labeling tags and other non-ribosomal moieties to form a covalent linkage. Here the application of intein-mediated

protein splicing on preparing cyclic CRPs such as cyclotide hedyotide B1 is further explored and described in chapter 3.
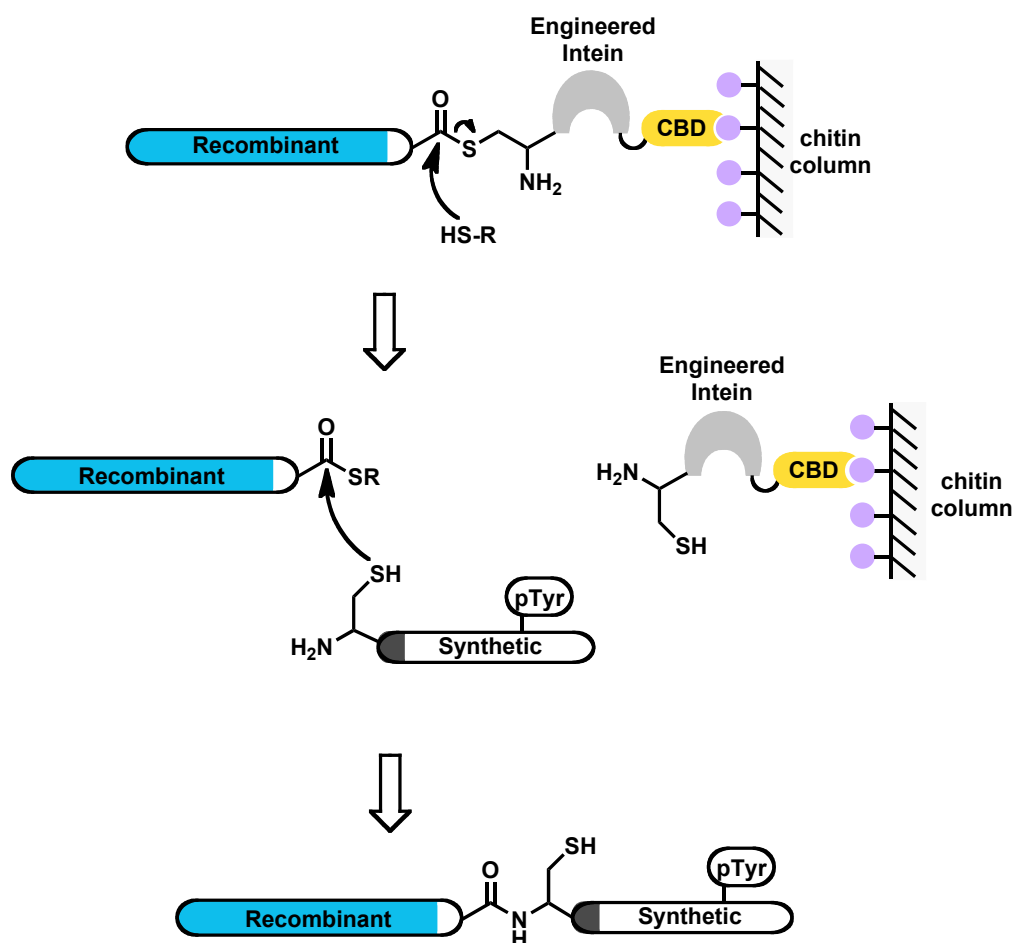
Figure 1-13. Schema of expression protein ligation (EPL). A bioactive Src kinase with a phosphorytyrosine (pTyr) tail was synthesized by this approach. The N-terminal fragment was recombinant-expressed with an engineered intein-CBD element. The fusion protein was purified in chitin column. Intein-mediated cleavage of the recombinant protein fragment resulted in a thioester intermediate in the presence of external thiols. The protein thioester was then ligated with the C-terminal synthetic fragment carrying single phopshotyrosine to afford the desired protein (Adapted from [131]).

6. Chemical synthesis of cyclic peptides

Chemical peptide synthesis is a powerful and versatile tool to prepare proteins especially when they carry unnatural amino acids, post-translational modifications such as phosphorylation and glycosylation, isotopic labeling and fluorophores. Formation of a peptide bond in chemical synthesis involves activating the α-carboxylic acid carbon of one amino acid and coupling it to the α-amine of another amino acid by a nucleophilic attack, when the α-amine of the first amino acid and side chain reactive moieties on both amino acids were protected. After the first coupling reaction, the N-terminal protection is removed by a deprotection step to release a free α-amine for the next coupling step. The reactive side-chains protecting groups are orthogonal to the N-terminal protection as they must be stable in the deprotection step, but are conveniently removable by a differential condition. The stepwise amino acid coupling is usually taken in the direction of C- to N-terminus, which is opposite to ribosomal protein synthesis.

The common coupling reagents for activation of α-carboxylic acid include carbodiimide and 1*H*-benzotriazole derivatives. Dicyclohexylcarbodiimide (DCC) is the first reported coupling reagent for peptide synthesis, which reacts with carboxylic acid to form a *O*-acylurea reactive intermediate to couple with amine [160]. Additives such as 1-hydroxy-1*H*-benzotrazole (HOBt) [161] and 1-hydroxy-7-azabenzotriazole (HOAt) [162] were introduced for the purposes of reducing epimerization and enhancing coupling efficiency. Several coupling methods were developed by associating salts (such as uranium/aminium, phosphonium, carbonium and immonium) with 1*H*-benzotriazole HOBt/HOAt [163]. For my project, phosphonium salt benzotriazol-1-yloxytri(pyrrolidino)-phosphonium hexafluorophosphate (PyBOP) [164] was used to synthesize peptide precursors by the microwave-assisted machine, and uranium salt coupling reagent *O*-(7-azabenzotriazol-1-yl)-1,1,3,3-tetra-methyluronium hexafluorophosphate (HATU) [165] was used for coupling difficult residues and coupling on secondary amines.

6.1 Solid phase peptide synthesis

The exploration on chemical synthesis of protein started in the early twentieth century. Max Bergmann successfully synthesized oligopeptides using benzyloxycarbonyl (Z) protecting group in 1932 [166]. De Vigneaud, et al reported the first synthetic bioactive peptide, a 9-residue oxytocin, by chemical synthesis in solution phase in 1953. In 1960s, Merrifield made a breakthrough by inventing solid phase peptide synthesis (SPPS) where the carboxylic acid of the C-terminal residue is protected by covalently linking to a solid support during peptide elongation (**Figure 1-14**). Ten years after Merrifield's inventions, there were already 500 solid phase synthesis in literature [167].

The solid supports used for SPPS are cross-linked resins or matrixes such as polysterene, polyacrylamide and polyethylene glycol, which are insoluble in the organic solvent but can be swelled and solvated in aprotic solvent like *N'N*-dimethylformamide (DMF) and dichloromethane (DCM). The good swelling gives a good diffusion rate of reagents to enter the resin core, which is important to the coupling efficiency. The reagents in each reaction steps can be easily washed away from the growing peptide attached to resins, and thus significantly simplify the synthesis steps.

There are two most popular SPPS methods utilizing *t*-butyloxylcarbonyl (Boc) and 9-fluorenylmethoxycarbonyl (Fmoc) chemistry. In the Boc/benzyl (Bz) chemistry, side-chain protecting groups are orthogonally stable during Boc deprotection by trifluoroacetic acid (TFA). The synthesized peptides are deprotected and cleaved from resins by super acid hydrofloric acid (HF). Fmoc group was introduced as a protecting group by Carpino in 1972 [168] and later Atherton and Sheppard developed Fmoc/tert-butyl (tBu) chemistry for SPPS [169]. In general, Fmoc can be deprotected by a mild condition such as 20% piperidine in DMF. Side-chain deprotection and cleavage of peptide from acid-labile resins are conducted in the trifluoroacetic acid (TFA) solution. Complete removal of protecting groups in both HF and TFA need addition of scavengers to prevent undesired alkylation of the protecting groups with side chain active groups.
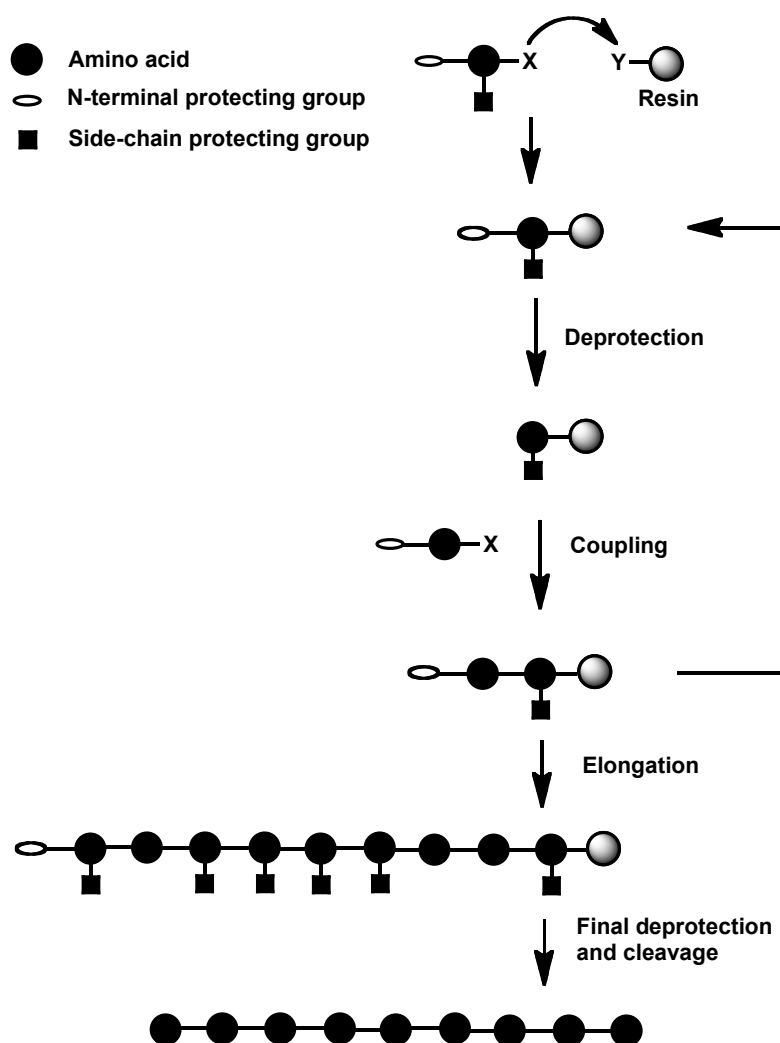
Figure 1-14. Schematic procedure of solid phase peptide synthesis.

6.2 Chemical ligation

Chemical synthesis of peptides are restricted to a limited length of amino acid sequence due to the deductive yield in each coupling step and aggregation of fully-protected peptide on resins. Ligation strategies are thus developed to fulfill the needs of preparing long peptides and proteins by joining two or more synthetic peptides, designated as convergent peptide synthesis. Kemp and co-works pioneered in developing convergent synthesis strategies based on a dibenzofuran auxiliary to conduct a prior thiol capture followed by acyl transfer to form peptide bond [170-172]. The ligation reaction does not involve any activation reagents or protecting groups. The desired N-terminal α-amine chemoselectively reacts with the carboxyl group in proximity. The dibenzofuran auxiliary could be removed subsequently by reducing the disulfide linkage to give an unprotected Cys residue at the ligation site (**Figure 1-15**).

Kemp's method was performed in organic solvent and limited by a slow reaction rate to afford long peptides and protein sequences. New methods in terms of chemoselective, native and biomimetic ligation have been developed in 1990s that were performed in aqueous conditions using unprotected peptide segments. Our group collectively called them orthogonal ligation, since these methods in general involve two unprotected peptides with two functional groups that specifically react with each other to afford a peptide bond regardless the presence of reactive side chain functionalities (**Figure 1-16**).
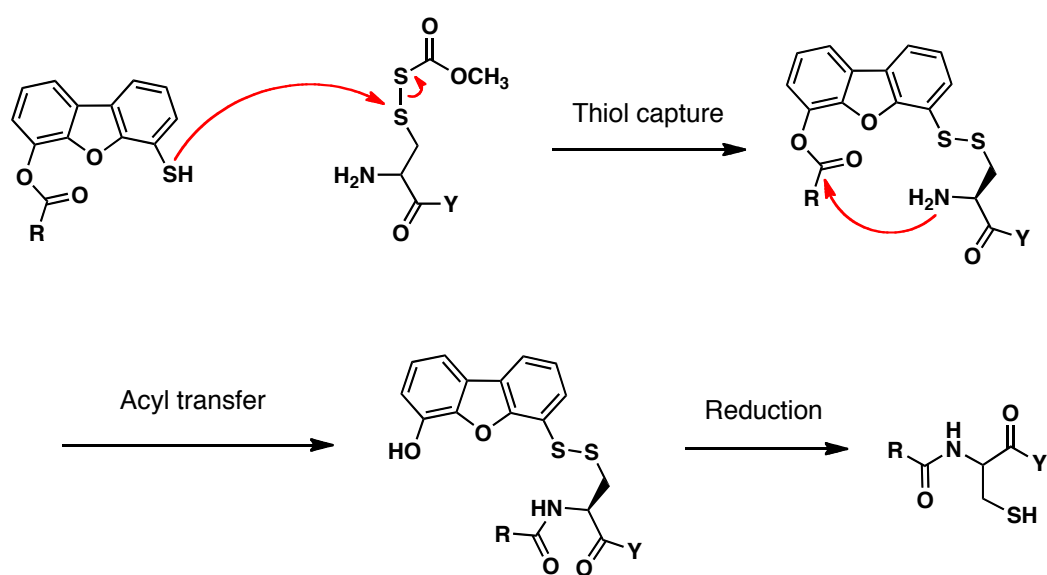
Figure 1-15. Kemp's convergent peptide synthesis. A prior thiol capture by a dibenzofuran auxiliary brought amine and carboxyl group in proximity to facilitate O-N acyl transfer to form a native peptide bond. The auxiliary group is removed by reduction to give a native peptide ligating at Cys residue.
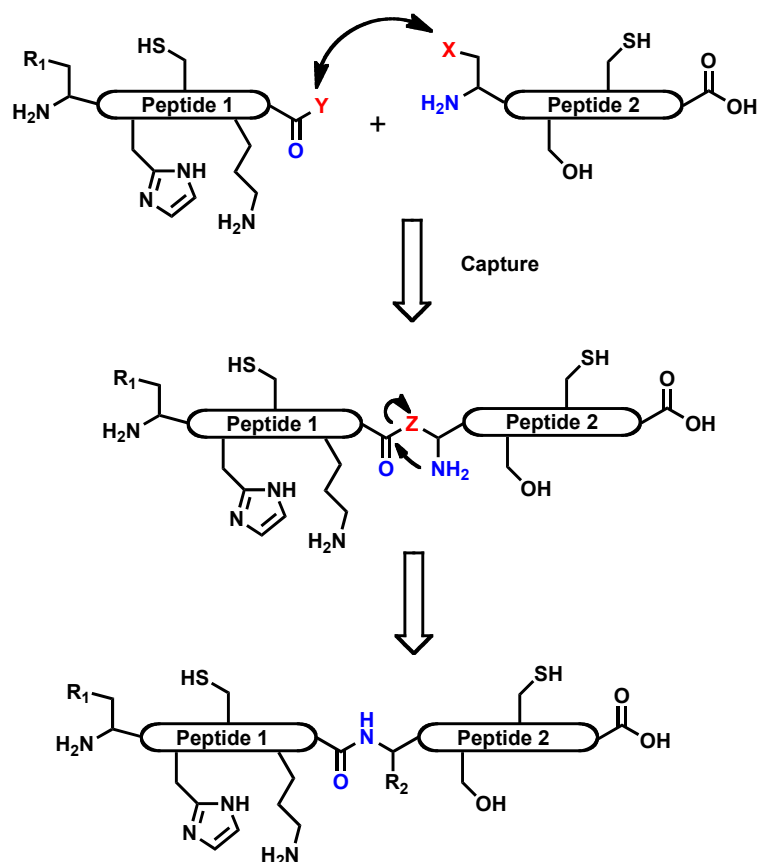
Figure 1-16. Schematic representation of orthogonal ligation. Two unprotected peptides with a pair of nucleophile (X) and electrophile (Y) are brought together by the formation of an intermediate (Z) that subsequently converted to a peptide bond.

In 1994, Tam's group reported a protecting-group-free peptide ligation method as segment condensation [173, 174]. The pair of ligation functional groups were C-terminal aldehyde of the first peptide and N-terminal residue's (Cys or Thr) α-amine and side-chain SH or OH of the second peptide. They form a thiazolidine or oxazolidine ring (Pseudo-Pro ring) to covalently link two segments together (**Figure 1-17A**). Kent's group reported another protecting-group-free ligation method named as "native chemical ligation", involving a peptide-carboxyl thioester converted from a peptide-thioacid prepared by Boc chemistry [175], and an N-terminal Cys-thiol of another peptide to form a peptide bond [176]. This concept of Cys-thioester ligation was earlier reported by Wieland in 1953 [177]. Tam group independently reported a Cys-thioester ligation approach by using a thioester resin which could be cleaved directly for the ligation raction [178]. This method was different from Kent's works, which prepared thioacid as the starting material. The current practices of chemical ligations mainly follow Tam's method using thioester resin. To distinguish this approach from other native ligation methods, I use the term "Cys-thioester ligation" in my thesis (**Figure 1-17B**). This approach has been widely applied for peptide ligation and cyclization, and as the fundament to develop more ligation methods (**Table 1-5**).

In a Cys-thioester ligation reaction, the nucleophilic attack by thiol group on the C-terminal thioester is a chemoselective transthioesterification reaction. When the N-terminal Cys of the second peptide attacks, a transient thioester bond that covalently link two peptides is formed and consequently bring N-terminal α-amino of the second peptide in close proximity to the C-terminal carboxyl group of the first peptide, where the S-N acyl shift takes place in a five-member ring transition. Notably, when N-terminal residue of the first peptide is Cys, the peptide is able to undergo end-to-end cyclization [179]. The transthioesterification reaction is the rate-determining step in the overall ligation process, and thus the reactivity of C-terminal thioester as a good leaving group upon nucleophilic attack by an N-terminal α-amine has been explored, which is correlated with the kinetics of the thiol groups. Johnson et al. reported a comparative study involving 14 alkyl or aryl thiols [180]. Their results suggested that aryl thiols with lower pKa were generally more efficient to

catalyze peptide ligation while they had poor solubility in aqueous condition that limited the effective concentration. They also recommended a thiol 4-mercaptophenyl acetic acid (MPAA) with advantages in both activity and solution.

Ligation methods at different amino acid by modified Cys-thioester ligation strategies for preparing Cys-free peptide sequences have been developed to fulfill the growing needs in peptide synthesis. Up to now the list of available ligation site residues based on thioester approach includes His [181], Met [182], Ala [183], Phe [184], Val , Lys [185], and Pro [186] (**Figure 1-18**). These ligation methods are performed in mild acidic to neutral conditions similar to Cys-thioester ligation. Most of them require additional modifications after peptide bond formation, such as methylation and desulfurization. The possible ligation sites have been further extended by other chemical approaches such as Ag+-assisted ligation at Ser/Gly/Asn [187], Staudinger ligation on azido amino acids [188, 189], and thiosugar-assisted glycopeptide ligation [190]. For our purpose of synthesizing cyclic CRPs, the Cys-thioester ligation is ideal since the CRPs sequences provide multiple choices as cyclization sites. The challenge is developing more efficient synthesis strategies to prepare peptide thioesters.
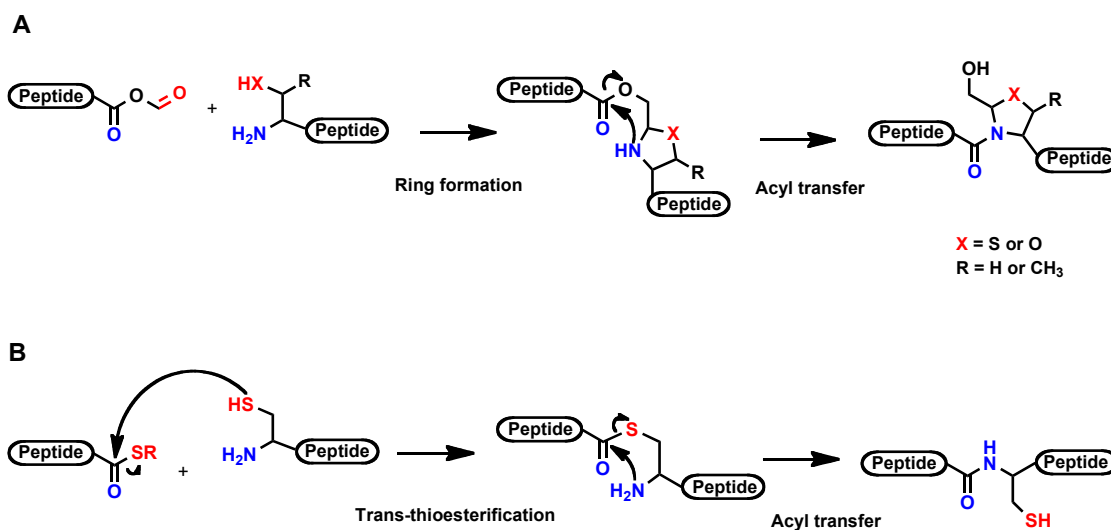
Figure 1-17. Examples of orthogonal ligation methods (A) Pseudo-Pro ligation with formation of thiazolidine or oxazolidine ring at ligation site. (B) Native chemical ligation or Cys-thioester ligation with formation of a peptide bond at ligation site.

Table 1-5. Summary of chemical ligation methods

Site-based ligation methods		Starting materials		Ref.
		N-terminal	C-terminal	
Pseudo-Pro	Thiazolidine formation	Cys/Ser/Thr	Ester aldehyde	*(173) (174)*
Cys	Native chemical ligation	Cys	Thioester	*(176) (178)*
His	Aryl disulfide-assisted ligation	His	Perthioester	*(181)*
Met	S-alkylation after ligation	Hcy	Thioester	*(182)*
Ala	Desulfurization after ligation	Cys	Thioester	*(183)*
Phe	Desulfurization after ligation	β-Mercapto-Phe	Thioester	*(184)*
Val	Desulfurization after ligation	Penicillamine	Thioester	*(191)*
Val	Desulfurization after ligation	γ-Mercapto-Val	Thioester	*(192)*
Ser/Asp	Removal of thiosugar	Thiosugar Ser/Asp	Thioester	*(190)*
Pseudo-Lys	S-alkylation after ligation	Cys	Thioester	*(193)*
Gly	Deprotection after ligation	*N*-Auxiliary Gly	Thioester	*(194)*
Lys	Desulfurization after ligation	γ-Mercapto-Lys	Thioester	*(195)*
Ser/Thr	Removal of *O*-auxiliary	Ser/Thr	Ester salicylaldehyde	*(196)*
Ser/Thr	Ag^+-assisted ligation	Ser/Thr/Asn/Gly	Thioester	*(197)*
Staudinger	Modified Staudinger reaction	Azido amino acids	Phosphanyl thioester	*(188, 198)*
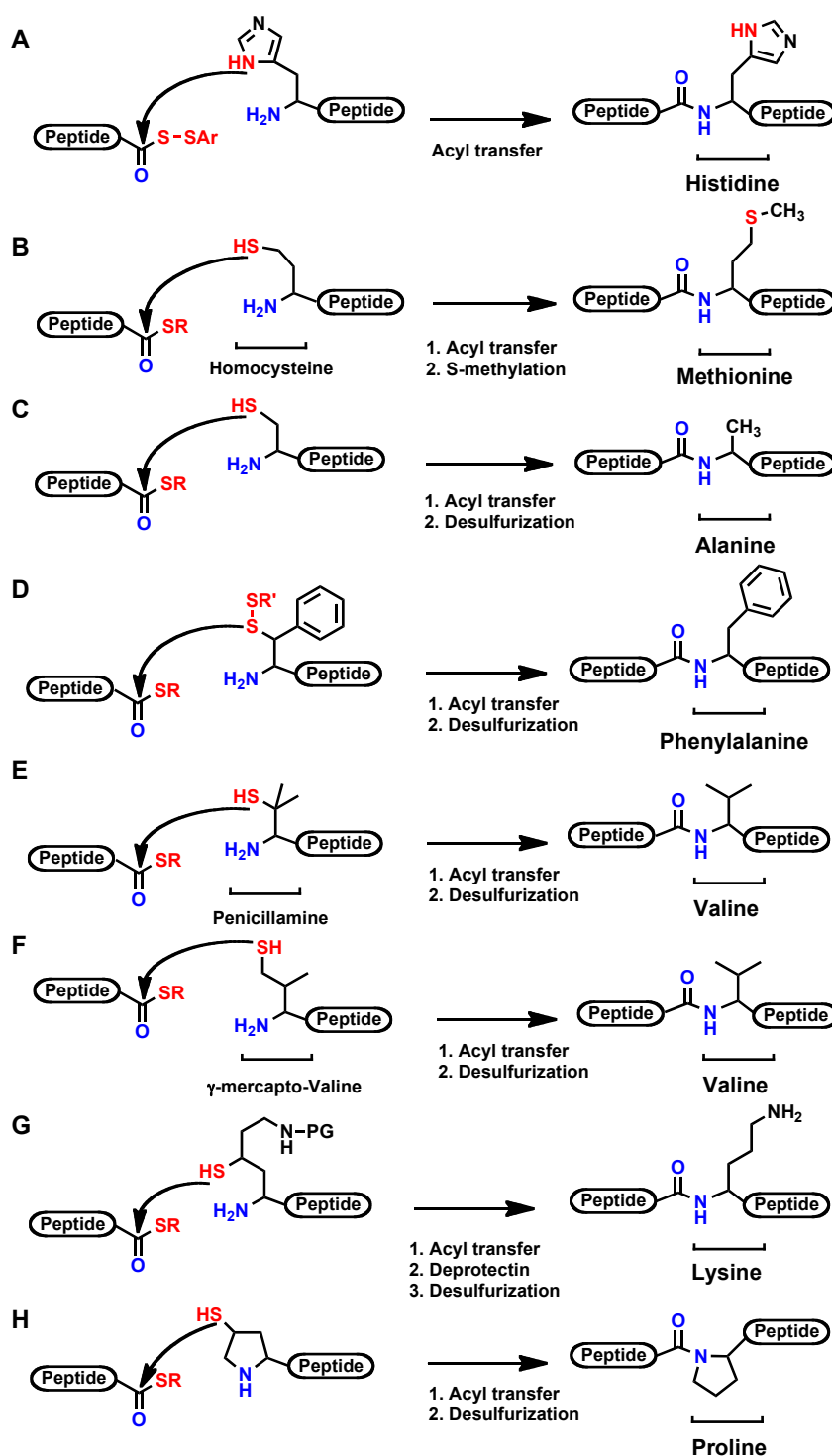
Figure 1-18. Extended thioester ligation at amino acid residues other than Cys. (A) His-ligation. (B) Met-ligation. (C) Ala-ligation. (D) Phe-ligation. (E, F) Val-ligation. (G) Lys-ligation. (H) Pro-ligation.

6.3 Preparation of thioesters for Cys-thioester ligation

Cys-thioester ligation is a common approach for synthesis of cyclic peptide and proteins from an unprotected peptide containing C-terminal thioester (for reviews: [199-201]). The key functional group thioester can be prepared directly using Boc chemistry. However, the use of HF in the final cleavage step requires safe practical and specialized apparatus, which limits the extensive application of Boc chemistry for preparing peptide thioesters. In Fmoc chemistry, thioesters are susceptible to basic conditions and intolerant to repetitive piperidine deprotections. These needs have prompted strong interests in the development of Fmoc-compatible schemes for preparing thioesters.

Fmoc-compatible methods of preparing peptide thioesters include (1) improving the deprotection step by developing mild deprotection cocktails [202, 203] or introducing base-tolerant thioester linkers [204]. (2) Introducing "safety-catch" auxiliaries, which are stable during Fmoc synthesis and later can be activated for thiolysis to give a thioester species [205-209]. (3) Attaching peptide to C-terminal amide- or ester-based surrogates that can be transformed into thioesters via an intramolecular N- or O-S acyl shift reaction, respectively, which is designated here as "safety-switch" methods.

6.3.1 "Safety-catch" thioester formation

The concept "safety-catch" was initially introduced by Kenner in 1971, which referred to a sulfonamide linker that was resistant to piperidine and thus "safe" during the deprotection steps in Fmoc chemistry [210]. After cleaving from the resin support, the sulfonamide was activated by *N*-alkylation reaction. The *N*-alkylated sulfonamide was ready to be "caught" by a thiol nucleophile and underwent intermolecular S_N2 reaction to form a thioester under basic conditions. The "safety catch" approaches also include hydrazide[211], *N*-acylurea [212], pyroglutamyl imide [208] and azide methods [209] (**Figure 1-19**). Most safety-catch auxiliaries have to be activated on the protected peptides to avoid undesired side reactions. This requirement usually results in low isolation yield of peptide thioesters. In the recent reported azide method, an Fmoc-compatible hydrazide linker is introduced that can be activated into reactive

azide followed by thioesterification. However, the activated carbonyl group is highly electrophilic, which may reduce the chemoselectivity towards thiols, as the intramolecular nucleophiles on side chains may compete with external thiols to give backbone-cyclic side products. Thus to perform this type of reactions, a large excessive and reactive external thiols are required to suppress side reactions and thus afford satisfactory yield of peptide thioesters [213].
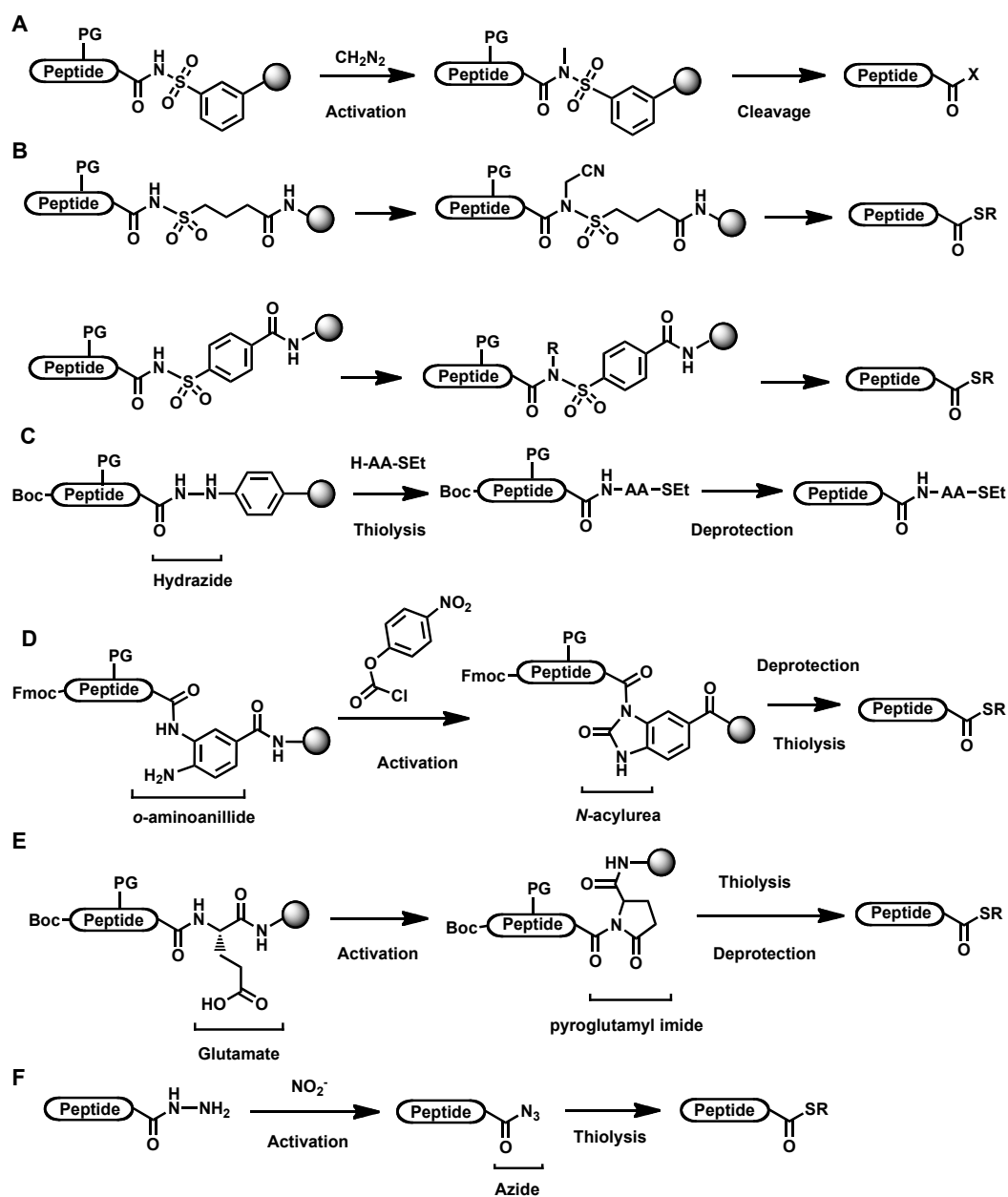
Figure 1-19. "Safety-catch" thioester formation. (A) The original Kenner's safety-catch linker. (B) Two variation based on Kenner's safety-catch linker. (C) Acyl hydrazide linker that "safe" in synthesis condition which can be activated into highly reactive acyl diazene to react with an α-amino acid alkyl thioester (H-AA-SEt). (D) o-aminoanilide linker that can be activated into *N*-acylurea for nucleophilic attack by external aryl thiols. (E) C-terminal glutamic acid that can be converted into a reactive pyroglutamyl imide. (F) A hydrazide linker that can be activated by nitrite into a reactive azide for thiolysis.

6.3.2 "Safety-switch" thioester formation

The "safety switch" strategies often incorporate an amide or an ester as a C-terminal thioester surrogate. The amide-based or ester-based thioester surrogates carry a thiol group that can undergo an intramolecular acyl shift reaction to afford a peptide thioester. The "safety switch" approach differs from the "safety catch" in two elements: formation of the first thioester is intramolecularly mediated by an N/O-S acyl shift and this reaction is generally acid-catalyzed.

A particularly appealing aspect of the amide-based thioester surrogates is that they are generally stable to both Boc- and Fmoc-chemistries in solid-phase synthesis. Examples of amide-based thioester surrogates include 2-mercaptoethanol sulfonamide [214], *N*-4,5-dimethoxy-2-mercapto-benzyl (Dmmb) [215], thio-proline [216], cysteinyl-prolyl ester (CPE) [217], *N*-alkylated Cys [218], *bis*-(sulfanylethylamino) (SEA) [219] or bis-(mercaptoethyl) amide (BMEA) [220], and thio-thiazolidine [221] (**Figure 1-20**).

The Dmmb moiety was first reported by Aimoto's group as an N-terminal amine-attached auxiliary for extended chemical ligation that could be removed by strong acid such as trifluoromethanesulfornic acid (TFMSA) [222]. The latter finding showed that an amido-Dmmb could be converted into thioester under weaker acidic conditions such as TFA solutions. Aimoto's group also developed the CPE autoactivating unit based on the diketopiperazine reaction, which was a base-induced side reaction occurring at the dipeptide stage in Fmoc deprotection step. A thiol-attached proline residue at C-terminus of the synthetic peptide sequence could mediate N-S acyl shift reaction under microwave heating at 80°C and subsequent transthioesterification with external thiols such as 3-mercaptopropionic acid (MPA). Hojo and co-workers developed a series of *N*-alkylated Cys as thioester surrogates. The N-S acyl shift reaction on *N*-alkylated Cys was accelerated by heating in the acidic 5% MPA solution. SEA or BMEA refers to the same design of thioester surrogate that has been developed by Melnyk's group and Liu's groups independently using different synthesis approach and different conditions for thioesterification and ligation. This linker contains two thiols and both of them can mediate N-S

acyl shift and hence shift the equilibrium towards thioester formation. A limitation of this design is the disulfide bond formation of two amide-linked alkyl thiols in the neutral conditions that consume reactive sites for thioesterification. Liu's group reported the condition by heating at pH 4-5 so that BMEA linker could mediate N-S acyl shift and Cys-thioester ligation in one-pot in the presence of another N-terminal Cys-containing peptide to afford a ligation product effectively. Solutions given by Melnyk's group included converting the SEA group into another thioester surrogate, amide-thiazolidine, by interacting with aldehyde [223], or performing thioesterification in a 5% aqueous solution of MPA (pH 4) to give MPA thioesters [224]. Tsuda, et al. introduced a C-terminal *N*-sulfanylethyaniline linker to prepare peptide-sulfanylethylanilide (SEAlide) for thioester formation via N-S acyl shift in acidic conditions such as 4 M HCl in DMF [225].

Recently our lab has reported a new thioester formation method using a thio-thiazolidine scaffold. Deprotection and tandem N-S, S-S acyl shift reactions were conducted by adding a trace amount of strong acid TFMSA in the TFA cleavage solution containing 5% thiocresol as scavenger and external thiol. This one-pot reaction could afford peptide-thiocresol thioester as the major product within one hour and thus it is rapid and much less laborious for thioester preparation.

A

2-mercaptoethyl
N-alkylated sulfonamide

N-S acyl shift

Direct
Cys-thioester ligation

B

Dmmb

TFA
N-S acyl shift

HSR

C

Thio-Pro

Microwave Δ, HSR

One-pot
N-S, S-S acyl shifts

D

CPE

DKP thioester

HSR

E

R = Me, Et, iBu, Bn

N-S acyl shift

HSR'

F

SEA or BMEA

N-S acyl shift

HSR

Direct
Cys-thioester ligation

G

N-sulfanylethylanilide
(SEAlide)

H
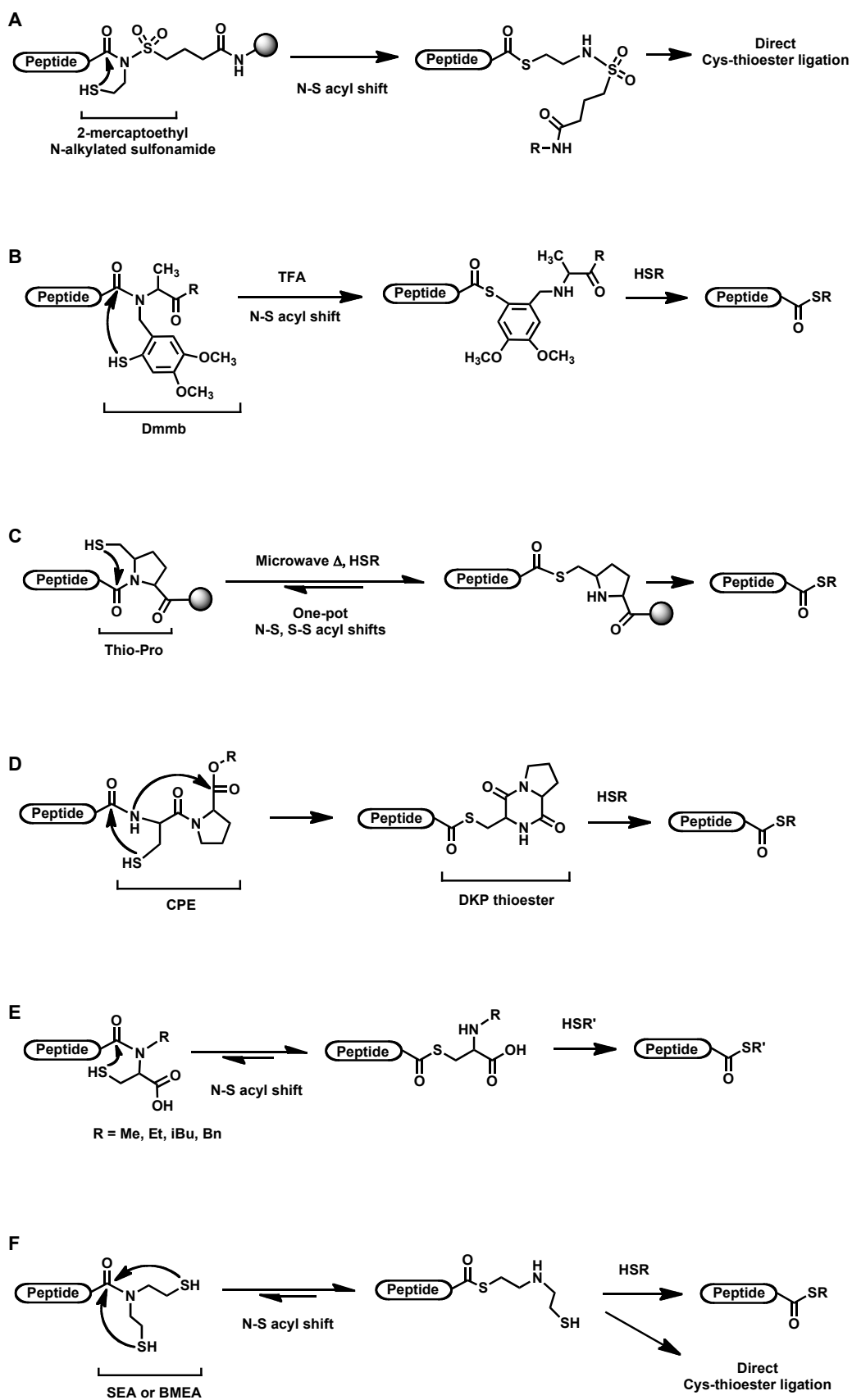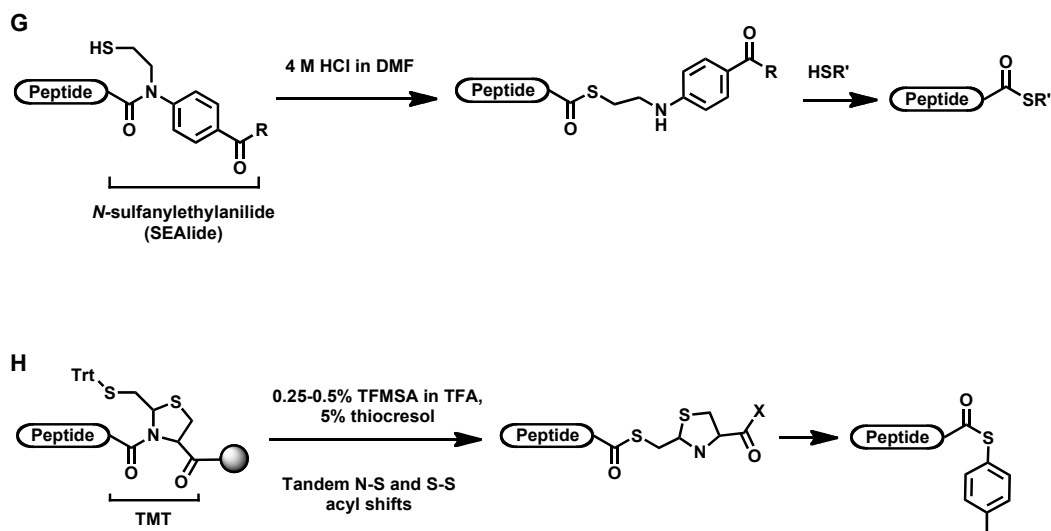
Figure 1-20. Amide-based "Safety-switch" thioester formation. (A) A modlfied Kenner's safety-catch linker: 2-mercaptoethanol N-alkylated sulfonamide. (B) N-4,5-dimethoxy-2-mercapto-benzyl (Dmmb) thioester surrogate that directly mediates N-S acyl shift to give thioester in a mild cleavage condition. (C) C-terminal thio-proline as thioester surrogate. (D) Cysteinyl-prolyl ester (CPE) autoactivating unit that undergoes N-S acyl shift to form a diketopiperazine (DKP) thioester ready for transthioesterification and Cys-thioester ligation. (E) N-alkylated Cys mediate N-S acyl shift to afford peptide thioester. Reported alkylation group R included methyl, ethyl, isobutyl, and benzyl. (F) bis-(sulfanylehtylamino) (SEA) or bis-(mercaptoethyl) amide (BMEA) can mediate N-S acyl shift by either thiol groups to form thioester. (G) A *N*-sulfanylethylanilide (SEAlide) thioester surrogate that mediates N-S acyl shift in acidic conditions. (H) A thio-thiazolidine linker thiomethylthazolidine (TMT) that mediate N-S acyl shift in one-pot with S-S acyl shift catalyzed by strong acid TFMSA in the presence of an aryl thiol thiocresol.

6.3.3 Intein-mimetic thioester surrogates

The thioethylamido moiety (TEA) is the key functional group to mediate a proximity-driven N-S acyl shift reaction in most amide-based thioester surrogates. It transforms into the desired thioester via a five-member ring transition state, which is exactly the same as the first N-S acyl shift step in intein splicing (**Figure 1-21**). Current methods in preparing amide-based thioester surrogates are fairly complicated, and a simple and practical method or a new design of TEA thioester surrogates would be desired. In intein splicing, this thermodynamically unflavored peptide bond breaking and thioester formation is catalyzed by a *cisoid* conformation. Thus a TEA thioester surrogate with tertiary amide would give an enhanced ratio of *cis* conformation and thus facilitate thioester formation and backbone cyclization via a series of acyl shifts (**Figure 1-22**).

My thesis would introduce the development of two TEA thioester surrogates with tertiary amide, *N*-methylated cysteine (MeCys) and thioethylbutylamine (TEBA), which mimic the catalytic role of intein but much smaller than an intein (> 20 kDa) (**Figure 1-23**). Both thioester surrogates can be prepared using commercially available starting materials by a sample preparation procedure. Their synthesis and applications in cyclic peptide synthesis of these TEA surrogates will be discussed in detail in chapter 4.
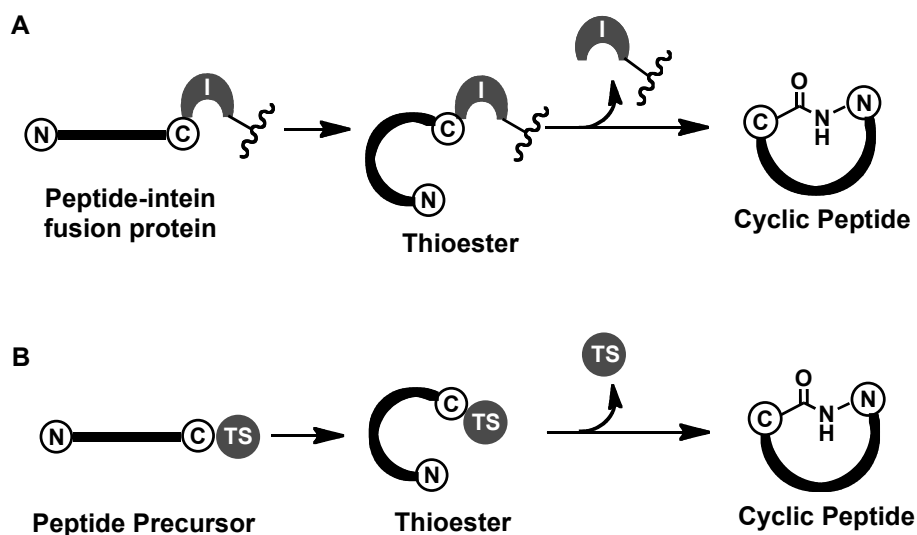
Figure 1-21. Comparison of intein-mediated cyclic peptide semisynthesis and thioester surrogate-mediated cyclic peptide chemical synthesis. (A) Target peptide is recombinant-expressed with intein as a fusion protein. Intein mediates thioester formation at the X-Cys splicing site. The newly formed thioester can be attacked by N-terminal Cys through transthioesterification and S-N acyl shift to form a cyclic peptide. (B) Target peptide is synthesized by Fmoc-SPPS with a small C-terminal thioester surrogate linker, which mediates thioester formation after cleavage. This C-terminal thioester is subsequently converted into a peptide bond also via transthioesterification and S-N acyl shift.
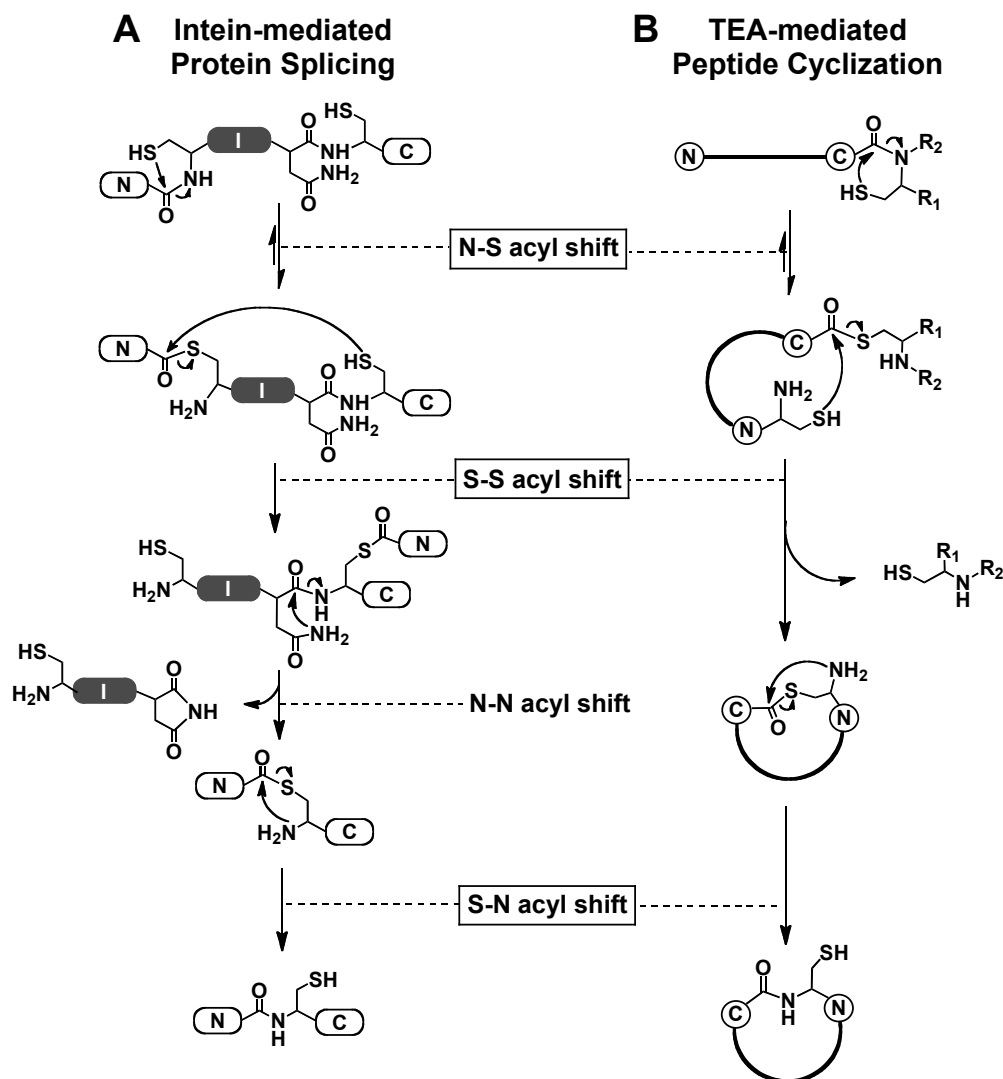
Figure 1-22. Acyl shift reactionss common to intein-meidated protein splicing and TEA-mediated peptide cyclization using thioester surrogates in chemical synthesis. (A) Four acyl shift reactions found in intein-mediated protein splicing. (I, intein. N, N-extein. C, C-extein.) (B) Three acyl shift reactions found in peptide cyclization mediated by TEA thioester-surrogate.
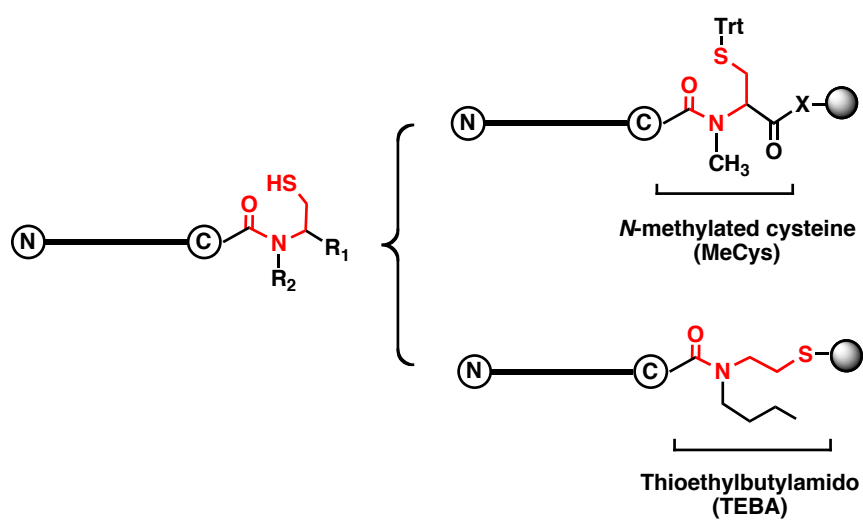
Figure 1-23. Thioethylamido (TEA) thioester surrogates MeCys and TEBA. The TEA moiety is highlighted in red. X refers to a spacer residue Gly between MeCys and resin.

6.4. Rate-accelerating thia zip cyclization

There are two aspects of advantages of using Cys-thioester ligation to prepare cyclic cysteine-rich peptides. First, CRP sequences provide multiple available cyclization sites. Second, the side-chain thiols of cysteine-rich peptides can accelerate cyclization reaction by mediating thiol-thioester exchange reactions to form a series of thiolactone intermediates from the C-terminal thioester. Expanding of the thiolactones ring via intramolecular transthioesterification reactions eventually join the N- and C-termini together by a thioester bond, followed by the subsequent S-N acyl shift reaction to afford a new peptide bond and give the end-to-end cyclic peptide. This process that specifically occurs during cyclization of cysteine-rich sequences was named as thia zip reaction to describe the zipping mechanism, which facilitate cyclization of cyclic CRPs such as cyclotides and cyclic AMPs [95, 106, 226, 227] (**Figure 1-24**).
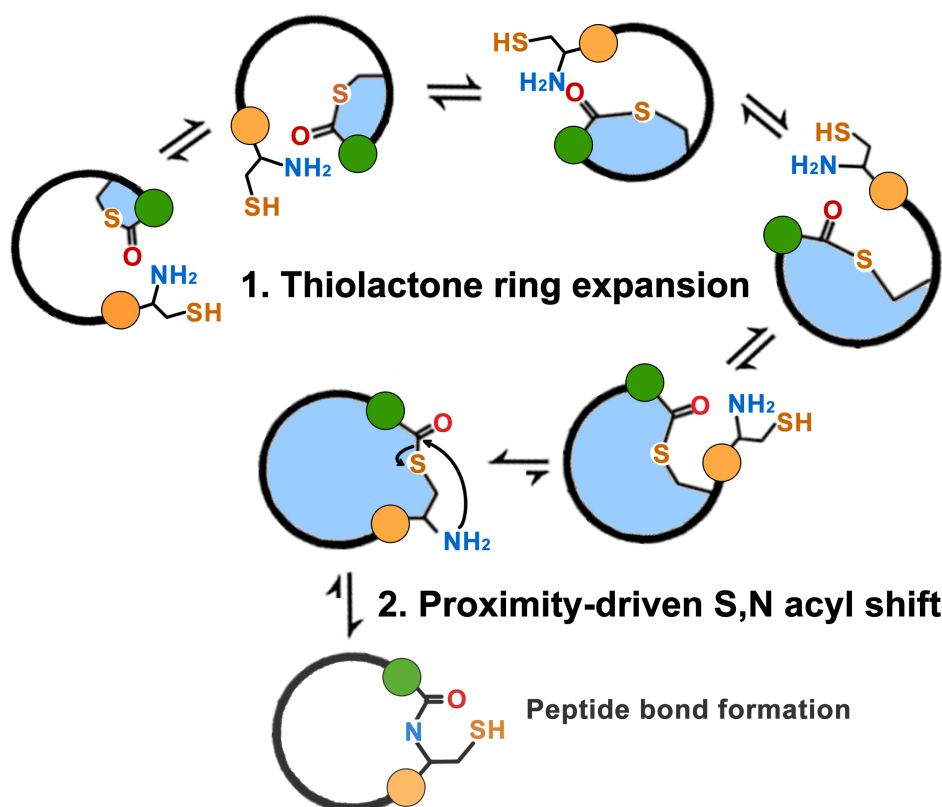
Figure 1-24. **Schematic illustration of thia zip cyclization.** Thiolactone intermediates were formed and the ring structure expanded through thiol-thiolactone exchange. Two ends of the peptide were brought together allowed end-to-end thioester formation. An proximity-driven S,N acyl shift in the local region produced peptide bond. Since the peptide bond formation was irreversible, the last expansion reaction was driven towards the product side efficiently.

7. Oxidative folding of CRPs

Protein folding is the essential maturation process that arranges a protein precursor into its functional three-dimensional conformation via a series of inter- or intramolecular interactions. Folding of CRPs is an enzyme-catalyzed process that mainly refers to the formation of native disulfide bonds and secondary motifs that are stabilized by these disulfides. For semisynthesis or chemical synthesis of CRPs, disulfide formation is the major challenge yet to be resolved.

Formation of a disulfide bond is an oxidative reaction between two cysteine residues. Sela reported disulfide formation via air oxidation in 1959, where oxygen dissolved in the solvent acted as oxidants [228]. This process was performed under slightly basic pH and it took long duration. It can be accelerated by the assistance of charcoal-surface [229]. Strong oxidative reagent $K_3Fe(CN)_6$ reagent were used in folding of one-disulfide-containing peptides oxytocin [230] and somatostatin analogs [231]. Our lab introduced the use of DMSO as a dual-function oxidative reagent since it was a good solvent for hydrophobic peptides and it could work under acidic conditions [232]. The mild oxidation by DMSO also prevented undesired oxidation of amino acids like Met and Trp. Annis introduced the use of solid-phase Ellman's reagents for disulfide bond formation in a mild oxidative condition [233].

The direct oxidization methods are not suitable for preparing cysteine-rich peptides, as the random oxidation among any two cysteine residues in the spatial proximity leads to mis-fold kinetic products rather than the native form [234]. 2*SS* CRPs can give three isomers with different disulfide connectivity. For 3*SS* CRPs, there are 15 possible disulfide isomers. To overcome this challenge, chemoselective oxidation and global oxidative folding strategies have been developed. The chemoselective strategy adopts orthogonal S-protecting groups such as Trt and Acm for different pairs of disulfide bonds. Stepwise deprotection and oxidation allow formation of correct disulfide bonds. Alternatively, global oxidative folding strategy utilizes redox reagents, i.e. a pair of reducing reagent and oxidative reagent, such as reduced and oxidized

glutathione (GSH/GSSG), to drive disulfide-reshuffling reactions. In the presence of excessive reducing reagent, mis-fold isomers can be rescued to form the correct disulfide bonds.

7.1 Chemoselective disulfide bond formation

Chemoselective approach has wide applications in the folding of multi-disulfide peptides and proteins that are prepared by chemical synthesis. It involves at least one pair of Cys residues that are protected by an S-protecting group stable during the final HF or TFA cleavage. Acetamidomethyl (Acm) is one of the these stable S-protecting groups that was firstly introduced in 1972 by Hirschmann's group [235]. This Acm protecting group can be removed by silver, thallium, mercury and iodine. The use of iodine in methanol has advantages in chemoselective oxidation since it simultaneously oxidizes the deprotected cysteine pair into a disulfide bond. Our lab has utilized chemoselective approach in the report of first synthetic cyclotide in 1997 [236]. A 2+1 strategy was developed for synthesis of cyclotides with three disulfide bonds. One pair of cysteine residues was protected by Acm group, while the other four Cys residues were protected by HF-labile 4-MeBzl. Four Cys residues were oxidized directly by DMSO after cleavage to give three isomers. The isomer containing two native disulfide bonds was isolated and underwent Acm deprotection by iodine to generate the third disulfide bond. However, iodine is a strong oxidant that may cause oxidation of Trp and Met to give undesired side products.

The other types of S-protecting groups have been introduced in the synthesis of cysteine-rich peptides. Cuthbertson and Indrevoll reported tert-butyl (*t*Bu) and 4-methylbenzyl (4-MeBn) as alternatives of Acm to prepare α-conotoxin SI [237]. *t*Bu was deprotected by TFA/DMSO/anisole solution at room temperature while 4-MeBn required heating (70°C) under this deprotection solution. This difference in temperature made them orthogonal to each other. Alewood introduced another chemoselective method in his works on α-conotoxins by replacing a pair of cysteine residues by selenocysteine. Selenium is much more reactive than sulfur, thus the diselenide bond forms almost spontaneously on resin and thus confers its selectivity over cysteine [238].

7.2 Global oxidative folding using redox reagents

The oxidative folding of an unprotected peptide precursor in redox conditions has been extensively explored for synthesis of CRPs. The redox reagents GSH/GSSG are often used by mimicking the environment of endoplasmic reticulum where the protein disulfide isomerase plays its function [239]. Chang's group suggested that the key issue in the oxidative folding process was to enhance the native-like conformation of a CRP that facilitate correct disulfide formation [240]. In the native conformation of a CRP, disulfide bonds are usually embedded in the core of the molecule and are not accessible by the reducing reagents. Therefore, the molecules with correct disulfide bonds can keep accumulating. Global oxidative folding has several advantages over chemoselective folding. It is protection-free and thus the precursor sequence can be prepared by both recombinant and chemical approaches. Chemically, the precursor sequence is easier to be prepared without usage of different S-protecting groups. The reaction is performed in one-step without repetitive purification and thus a better yield can be obtained. However, global oxidative folding cannot eliminate the possible disulfide isomers. To afford a good folding yield of the correct disulfide isomer, a number of parameters including peptide concentration, redox reagents, pH, temperature, and additional co-solvents need to be optimized.

A few CRPs have been folded successfully through global oxidative folding. Kubo et al. [241] suggest that 50% acetonitrile (ACN) in the folding buffer can improve oxidative folding yield of human defensins 1, 2, 3 and 5 from 27 to 89%. Similarly, oxidative folding of the Möbius cyclotides kalata B1 was performed in the redox buffer with 50% isopropanol [104, 242]. Addition of organic solvents as co-solvent increased the hydrophobicity of the refolding environment, which could be the explanation for the hydrophobic CRPs to fold properly. In contrast, low temperature and high salt concentration promised acceptable yield of hydrophilic ω-conotoxin MVIIC [243]. The efficiency of salts increased according to the Hofmeister series of anions and thus they suggested a salt-out effect that assisted the oxidative folding process. In the synthesis of hydrophobic δ-conotoxin, detergent was reported to be important [244]. Goldenberg et al. suggested that denaturants such as urea and GnHCl facilitates

the oxidative folding process of hydrophobic conotoxins, while the use of denaturants minimizes non-covalent interactions between hydrophobic residues [245]. Aboye *et al.* [246] reported the first successful oxidative folding of a bracelet cyclotide cycloviolacin O2 in 35% DMSO with a redox buffer containing detergent and EDTA. Gunasekera et al. reported bracelet cyclotides were more difficult to fold than the Möbius cyclotides since due to the amino acid composition difference in loop 2 and loop 6. Their result suggested that the folding conditions were sequence-related [247]. Recently, our lab reported oxidative folding of bracelet cyclotide hedyotide B1 using 70% isopropanol [106]. Similarly, oxidative folding of hydrophobic α-conotoxins such as Iml and Gl were found to be efficient in the presence of ethanol as co-solvent [248]. These results indicated the importance of conformation-enhancing co-solvents. Most conditions in the literatures adopted a low peptide concentration to avoid intermolecular disulfide crosslinking and peptide aggregation. The reshuffled thiol-disulfide exchange process usually took hours to days for the correct folding product to accumulate. Their works indicate that global oxidative folding is the method of choice for preparing CRPs but the conditions were sequence-dependent and thus needed extensive optimization. The challenge of folding CRPs efficiently still remains and I will introduce my contribution to improve the folding strategy by a novel organic folding approach in chapter 5.

8. Aims

My thesis focuses on the methodology development and applications of cyclic cysteine-rich peptides. To achieve my objective, I have two specific aims:

(1) to develop an efficient and practical synthesis strategy for cyclic CRPs that could be used for high-throughput synthesis.

(2) to apply the newly developed synthesis strategy to prepare bioactive cyclic CRPs based on two representative families of CRPs, plant CRP cyclotides and animal CRP ω-conotoxins.

- Chapter 3 describes the synthesis of cyclic CRPs using recombinant system by intein-splicing. The bracelet cyclotide hedyotide B1 was used as a model to examine the steric effect of the C-terminal amino acids on the cyclization efficiency. The findings were applied to the preparation of cyclic analogs of ω-CTX MVIIA.

- Chapter 4 describes the chemical synthesis approaches to prepare macrocyclic peptides using Cys-thioester ligation. Using the chemical principle of intein-mediated protein splicing, intein-mimetic thioethylamido (TEA) thioester surrogates are designed for synthesis of cyclic CRPs. The chemical approaches were more practical and productive than recombinant synthesis. The recent-reported "safety-catch" type of azide method was also included for comparing the synthesis efficiency, yield and side reactions.

- Chapter 5 solved the disulfide formation of CRPs through the conventional chemoselective folding, global oxidative folding, and a modified folding method using non-aqueous solvent system. The oxidative folding strategy in organic conditions can afford folded CRPs rapidly and it can be combined with azide-mediated cyclization to prepare cyclic folded CRPs efficiently in a one-pot manner.

- Chapter 6 described the application of the newly developed synthesis strategies by preparing a panel of linear and cyclic analogs of MVIIA. By incorporating the end-to-end cyclic backbone, the cyclic MVIIA analogs exhibit enhanced metabolic stability and acquired new bioactivities including antimicrobial, chemotactic and cell penetrating properties.

Chapter 2 Material and Methods

1. Synthesis of cyclic CRPs by intein-splicing

1.1 Prepare CRP clones by tandem-extension PCR

The cDNA sequence of hedyotide B1 was derived from the amino acid sequences, which had been optimized for E. *coli* expression system by correcting codon-bias based on the tRNA frequencies [249]. The precursor DNA sequences B1x (x for R, F, G, S, Y, and F) of hedyotide B1 were amplified by tandem-extension PCR. For each precursor, four primers p1f, p2f, p3r and p4r were designed and obtained commercially from 1st-Base. In one PCR reaction, 2 μl p1f/p4r (1:1, *v/v*) and 0.2 μl p2f/p3r (1:1, *v/v*) were added with 0.5 μl pfu polymerase (Invitrogen) and 2.5 μl dNTPs (Invitrogen). The first extension reaction was performed with a higher annealing temperature at 57°C for five runs where only p2f and p3r were able to anneal with their complementary sequence to give amplicon 1. The second extension reaction was performed with a lower annealing temperature at 50°C for 30 runs where primers p1f and p4r were able to anneal to amplicon 1 and extended to give amplicon 2 and 3, which were subsequently became the templates to give full-length product amplicon 4. Amplicon 4 contained all sequences carried by four primers, which was the DNA sequence of hedyotide B1 flanked with NdeI/SapI restriction sites for insertion into vector pTXB1 (NEB, IMPACT kit). Efficiency of PCR reactions was monitored by agarose-gel (2% *w/v*) electrophoresis (constant voltage 70 V, 1 h).

1.2 Construction of plasmids

PCR products obtained from each tandem-extension reactions and the vector pTXB1 were treated with NdeI/SapI double digestion (37 ˚C, 3 h). Digestion mixtures were purified (Promega, Wizard®SV Gel and PCR clean-up system) and mixed with ligation solution containing T4 DNA ligase (NEB, quickligase, 15 min) in the ratio of insertion: vector = 3:1. Ligation products were transformed into competent E. *coli* strain DH5α by 1 min heat shock at

42°C and 5min cool down on ice. Transformation mixtures were spread on pre-warmed LB-agar plate (100 mg/L ampicillin salt) for overnight incubation. Colonies were inoculated into 3 mL LB-broth and amplified overnight. Plasmids were extracted from 1 mL culture by miniprep (QIAGEN, QIAprep® spin Miniprep kit). Plasmids were screened by EcoRI/EcoRV double digestion (1h, 37°C). The clones with correct insertion displayed only single band on agarose-gel electrophoresis (1% *w/v*, constant voltage 120 V, 45 min) representing single cleavage by EcoRV. The plasmids without insertion were digested into two fragments. The plasmids passed screening were purified from agarose gel (Invitrogen, PureLink™ Quick Gel Extraction Kit) and subjected to DNA sequencing (1st base) to confirm in-frame insertion of CRPs. Correct plasmids were transformed into high-performance expression strain ER2566.

1.3 IPTG-induced Expression

One fresh-growing colony was inoculated into 3 mL pre-warm LB medium in a 15 mL culture tube and incubated for 3 h (37°C, 220 rpm). 1 ml fresh culture was added into 500ml LB in a 2 L flask and incubated in shaker incubator until A600 reached 0.7 (37°C, 180 rpm, about 4 h). Then the temperature of shaker incubator was reduced to 16°C. 0.3mM IPTG was added to induce fusion protein expression for 24 h at 150 rpm.

1.4 Fusion protein extraction

Bacterial cells from 1 litre culture were collected by ultra-centrifugation (10 min, 10000 rcf). The pellets (1 litre culture gave 2-3 g bacteria) were re-suspended in 50 mL cell lysis buffer (20 mM Tris-Cl, pH 8.5, 500 mM NaCl, 1 mM EDTA, 0.1% Triton X-100) and lysed by ultrasonication for 1 h (4 s-operation plus 10 s-pause) on ice. The cell lysate was spin in ultra-centrifugation (40 min, 8000 rcf) and the supernatant containing soluble fusion protein was filtered (pore size 0.45 nm) to obtain clarified cell extract. The precipitate containing inclusion bodies was resuspended in 50 mL lysis buffer and subject to sonication. The mixture was centrifuged again and the pellet was resuspended in 50 mL column buffer (20 mM Tris-Cl, pH 8.5, 500 mM NaCl, 1 mM EDTA) with 0.01mg/ml DNase. Repeat this step to wash the inclusion

body. Resuspend inclusion body in 10 mL recovery buffer (100 mM Tris-Cl at pH 8.0, 50 mM Glycine, 8 M urea), vortexing for 1 h and centrifuge to get the supernatant. Recover the denatured fusion protein in supernatant by rapid dilution using 90 mL 100 mM Tris-Cl, pH 8.0.

1.5 On-column cyclization

Fusion protein purification and on-column cyclization was performed in the chitin affinity column. Chitin-binding column was packed with 10 mL chitin beads and calibrated by 100 mL cold column buffer (20 mM Tris-Cl, 500 mM NaCl, 1 mM EDTA, pH 8.5) before use. 50ml Pre-chilled clarified cell extract from 1 L cell culture was loaded on column with a flow rate below 0.5ml/min. Beads were washed with 20x bead volume of column buffer at flow rate about 2ml/min to stabilize affinity binding. After wash, flash the column using 50ml column buffer to remove unspecific binding. This purification step was conducted under 4°C in the cold room.

Flash the chitin column with 20 ml cleavage buffer (20 mM Tris-Cl, 500 mM NaCl, 1 mM MESNA, pH 8.5) Stop the flow and leave the column at room temperature overnight or at 4°C for not more than 48 h. Splicing products was eluted by 10ml cold cleavage buffer. The remained portions of fusion proteins CBD-Ssp and Mxe-CBD, and partially cleavage fusion proteins were stripped from chitin-beads by 1% SDS solution. The chitin-beads were regenerated by 0.3 M NaOH and store in 20% ethanol at 4°C. The cleavage efficiency was checked by tricine SDS-PAGE.

1.6 Tricine SDS-PAGE

Tricine SDS-PAGE was designed for separating biological samples with smaller molecular weight (1-100 kDa)[250]. As compared with normal SDS-PAGE, tricine was used to substitute glycine in the running buffer. Samples for SDS-PAGE included cell pellet from 1 mL cell culture before induction, cell pellet from 0.5 mL cell culture after induction, cell debris from 50 μL crude extract, clarified extract from 50 μL crude extract, 20 μL chitin beads collected after step 4.1.2, and 20 μL chitin beads after cleavage. Six samples were resuspended/mixed with 40 μL 2x sample loading buffer (Biorad, tricine-SDS

sample buffer) and heated at 100°C for 10 min. Tricine-SDS separation gel contained 10% acrylamide/bis-acrylamide mix (29:1 stock solution), 1 M Tris-Cl/0.1% SDS (*w/v*, 3x stock solution, pH 8.5), 20% glycerol, 0.05% ammonium persulfate (APS, *w/v*, 10% stock solution), and 0.005% TEMED. Tricine-SDS stacking gel contained 4.05% acrylamide/bis-acrylamide mix (29:1 stock solution), 7.5% Tris-Cl/0.1% SDS (*w/v*, 3x stock solution, pH 8.5), 0.05% ammonium persulfate (APS, *w/v*, 10% stock solution), and 0.01% TEMED. The 5x Tricine-SDS PAGE running buffer stock was prepared by 0.5 M tricine, 0.5 M Tris-base, 0.5% SDS (*w/v*).

1.7 Reversed phase HPLC and MALDI-TOF mass spectrometry

Splicing products were analyzed by analytical RP-HPLC (Vydac Peptide C18, 218TP104, 250 x 4.6 mm) with a gradient of 1% ACN per min. For purification, eluent was adjusted to pH 2 by diluted HCl solution and peptides were reduced by 30 mM TCEP (37°C for 1 h) to un-bond any random disulfide bonds. Reduced peptides were separated by preparative RP-HPLC (Prosphere 300 C18, 300A 5u) with ACN gradient of 0.5% per min. Additional purification was performed on semi-preparative column if the purity was low. The mobile phase included buffer A (0.1% TFA, Milli-Q water) and buffer B (100% ACN, 0.085% TFA, Milli-Q water). Peaks were collected and analyzed by MALDI-TOF mass spectrometry using α-Cyano-4-hydroxycinnamic acid (CHCA) matrix (dissolved in 75% ACN, 0.1% TFA) and mass range 1000-5000 Da was scanned.

2. Solid phase peptide synthesis using Fmoc chemistry

2.1 Materials

Amino acids including Fmoc-Gly-OH, Fmoc-Ala-OH, Fmoc-Leu-OH, Fmoc-Met-OH, Fmoc-Ser(tBu)-OH, Fmoc-Thr(tBu)-OH, Fmoc-Tyr(tBu)-OH, Fmoc-Arg(Pbf)-OH, Fmoc-Cys(Trt)-OH, Fmoc-Cys(Acm)-OH, Fmoc-N-methyl-Cys(Trt)-OH Fmoc-Lys(Boc)-OH, Fmoc-Asp(OtBu)-OH, Fmoc-Glu(OtBu)-OH, Fmoc-Phe-OH, Fmoc-Pro-OH, Fmoc-Trp(Boc)-OH and Fmoc-Val-OH were purchased from NovaBioChem. Coupling reagents including DIC, HOBt, HATU, HOAt, DIEA, DMAP, and PyBOP were obtained from GLBiochem. Scavengers triisopropylsaline (TIS) and thioanisole were obtained from Sigma. Organic solvents DMF, DCM, piperidine and DMSO were obtained from Merck.

2.2 Synthesis of TIGGIR-MeCys-Gly-NH$_2$ on Rink amide resin

The Rink amide resin (1 g, 0. 34 mmol) was swollen for 10 min in DCM (10 mL) and the resin was filtered and washed with DCM (1 min x 2). The spacer amino acid Fmoc-Gly (1.36 mmol, 404 mg) was manually coupled with 4 eq. of DIC (1.36 mmol, 143 μL) and 4 eq. of HOBt (1.36 mmol, 184 mg) in DMF (10 mL) (shaking for 1 h at rt) to give Fmoc-Gly-NH-resin **1**. The resin was washed by DMF and DCM respectively followed by deprotection using 20% piperidine solution in DMF (5 min x 2). A mixture of 2 eq. Fmoc-MeCys(Trt)-OH (0.68 mmol, 408 mg), 4 eq. DIC (1.36 mmol, 143 μL) and 4 eq. HOAt (1.36 mmol, 185 mg) in DMF (10 mL) was added into resin-containing reaction vessel and shake for 2 h at room temperature (r.t.) to give Fmoc-MeCys(Trt)-Gly-amide resin **2**. The substitution of Fmoc-MeCys(Trt)-Gly-amide resin **2** (1.2 g) was about 0.32 mmol/g. Fmoc was deprotected by 20% piperidine in DMF (5 min x 2 at rt) and resin was washed (DCM x 2, DMF x 2). Fmoc-Arg(Pbf) (1.36 mmol, 881 mg) was coupled manually to the secondary amine on MeCys(Trt) of resin **2** by 4 eq. HATU (1.36 mmol, 517 mg) and 6 eq. DIEA (2.04 mmol, 341 μL) to obtain resin **3** after triple coupling. The completion of reaction was examined by acetaldehyde/chloranil test (2% acetaldehyde, 2% chloranil in DMF, 5 min at rt). The rest of the sequence TIGGI was coupled to resin **3** on a microwave-assisted peptide synthesizer

using a reagent mixture of PyBOP/DIEA/Fmoc-aa (5/10/5 eq). Thr(tBu)-Ile-Gly-Gly-Ile-Arg(Pbf)-MeCys(Trt)-Gly-NH-resin **4** was subjected to TFA/TIS/H_2O/thioanisole (89/5/5/1, *v/v*) treatment for 2 h to obtain deprotected peptide TIGGIR-MeCys-Gly-NH$_2$ **5** (calc. 788.9 Da, found 789.8 Da).

2.3 Synthesis of CG29-MeCys-Gly-NH$_2$ on MeCys resin

310 mg Fmoc-MeCys(Trt)-Gly-amide resin **2** (about 0.1 mmol) was used for synthesis of the full-length CG29 using microwave-assisted peptide synthesizer using PyBOP/DIEA (5/10 eq) to give CG29-MeCys-Gly-amide resin **14** (783 mg). A mixture of 5 ml TFA/TIS/H_2O (95/2.5/2.5, *v/v*) was added to 200 mg resin **14** to remove side chain deprotection group and cleave peptide from solid support. The reaction mixture was shaken for 2 h at room temperature and then added to chilled dimethyl ether for peptide precipitation. The precipitate was dried in vaccuo and purified by RP-HPLC to give CG29-MeCys-Gly-NH$_2$ **15** (calc. 3087.6 Da, found 3088.5 Da) (17.6 mg, 21% isolated yield).

2.4 Synthesis of TIGGIR-TEBA on 2-Cl(Trt-Cl) resin

Cl-Trt(2-Cl) resin (0.5 g, 0.6 mmol) was swollen for 30 min in DCM (10 mL) and the resin was filtered and washed with DCM (1 min x 2). (2-butylamino) ethanethiol **21** (0.3 mmol, 44 μL) in DCM (20 mL) was added, and the suspension was shaken for 1 h at room temperature. Subsequently, 3.6 mmol DIEA (3.6 mmol, 627 μL) and 1 ml MeOH was added, and the reaction mixture shaken for 10 min to quench the unreacted Cl. The resin was washed with DCM and DMF, respectively, to give TEBA resin **22**. A mixture of Fmoc-Arg(Pbf) (1.2 mmol, 778 mg), HATU (1.2 mmol, 456 mg) in DMF and DIEA (1.8 mmol, 314 μl) was added to resin **22**. The suspension was shaken for 1 h and coupling procedure was duplicated to give Fmoc-Arg(Pbf)-TEBA resin **23** (730 mg, calculated substitution 0.3 mmol/g). The rest of peptide sequence was synthesized on resin **23** (667 mg, 0.2 mmol) manually using PyBOP/DIEA to give Thr(tBu)-Ile-Gly-Gly-Ile-Arg(Pbf)-TEBA resin **24**. 5 ml TFA/TIS/H_2O (95/2.5/2.5, *v/v*) was added to resin **24** and the reaction mixture was shaken for 2 h. After dropwise addition of the reaction mixture to chilled diethyl ether for

precipitation, the precipitate was dried *in vaccuo* and purified by RP-HPLC to give TIGGIR-TEBA **25** (calc. 729.7 Da, found 730.4 Da) (27.4 mg, 17% yield).

2.5 Synthesis of conotoxin sequences on TEBA resin

Fmoc-Lys(Boc) (561 mg, 1.2 mmol), HATU (456 mg, 1.2 mmol) in DMF and DIEA (314 μl, 1.8 mmol) were added to TEBA resin **22** (300 mg, 0.1 mmol) and coupling reaction was conducted at room temperature. Coupling efficiency was monitored by chloranil/acetaldehyde test. The suspension was shaken for 1 h and coupling procedure was duplicated to give Fmoc-Lys(Boc)-TEBA resin **27**. The rest of peptide sequence was synthesized on 0.1 mmol resin **27** by microwave-assisted synthesizer to give peptide-TEBA resin **28**. A mixture of TFA/TIS/H$_2$O/thioanisole (89/5/5/1, *v/v*) was added to peptide resin **28** and the reaction mixture was shaken for 2 h. After dropwise addition of the reaction mixture to chilled diethyl ether for precipitation, the precipitate was dried *in vaccuo* and purified by RP-HPLC to give peptide-TEBA **29**. Using this protocol, linear precursors of M1B-TEBA **29a** (Cald. 2868.5 Da, found 2870.0 Da), M2B-TEBA **29b** (Cald. 2868.5 Da, found 2869.3 Da), M3B-TEBA **29c** (Cald. 2868.5 Da, found 2869.6 Da), M1B(8, 20Acm)-TEBA **48a** (calc. 3009.6 Da, found 3010.6 Da), M2B(1, 16Acm)-TEBA **48b** (calc. 3009.6 Da, found 3010.5 Da), M3B(1,16Acm)-TEBA **48c** (calc. 3009.6 Da, found 3010.6 Da), M-GS-TEBA **56** (Cald. 2904.5 Da, found 2904.8 Da), and M1B-K7biotin-TEBA **61** (Cald. 3089.5 Da, found 3090.4 Da), were prepared.

2.6 Synthesis of conotoxin sequences on hydrazine resin

2-Chlorotrityl chloride resin (1 g, 1.2 mmol/g, 100-200 mesh) was swollen for 15min in DCM. 3 eq. DIEA (627 μL) and 2 eq. hydrazine monohydrate (117.5 μL) were dissolved in DMF and added into resin suspension. Mixture was shake for 60 min at room temperature. Additional 1% Methanol was added and shaken for 10 min to disable the remaining reactive Cl on resins. After drain out coupling mixture, hydrazide resin **35** was washed with DMF (2 times) and DCM (2 times). Peptide sequence was coupled stepwisely to the hydrazine resin using the reagents PyBOP/DIEA/Fmoc-aa (4/6/4 eq) on a microwave-assisted peptide synthesizer (CEM, liberty-1) to give peptide-resin **37**. The deprotected peptide-hydrazide was obtained by

TFA/TIS/H$_2$O/thioanisole (89/5/5/1, *v/v*) cleavage and ether precipitation. Peptides obtained by this protocol included M1B-NHNH$_2$ **38a** (Cald. 2767.3 Da, found 2768.3 Da), M2B-NHNH$_2$ **38b** (Cald. 2767.3 Da, found 2768.4 Da), and M3B-NHNH$_2$ **38c** (Cald. 2767.3 Da, found 2768.3 Da).

2.7 Synthesis of linear peptides using Fmoc chemistry

The model peptide CALVIN **11** was elongated on Wang resin (0.84 mmol/g, 120 mg) using PyBOP/DIEA coupling reagents with assistance of microwave synthesizer. 208 mg dry peptide-resin **11'** was obtained after vacuum dry. The protected peptide was cleaved from resin **11'** and deprotected by 2% EDT in TFA for 2 h reaction followed by diethyl ether precipitation and RP-HPLC purification. 27 mg peptide **11** was obtained, which gave an isolated yield of 43%. Similarly, the linear conotoxin analog M-GS was synthesized on Wang resin by microwave-assisted Fmoc synthesizer using PyBOP/DIEA coupling reagents. Elongated peptide M-GS-OH **45** (Cald. 2790.3 Da, found 2790.9 Da) was cleaved and deprotected by TFA/TIS/H$_2$O/thioanisole (89/5/5/1, v/v) for 2 h.

The native sequence of conotoxin MVIIA was synthesized on Rink amide resin. 330 mg Rink amide resin (0.1 mmol) was deprotected by 20% piperidine in DMF for 5 min. Two repeated deprotection was performed followed by DMF/DCM wash (x3). The deprotected resin was mixed with Fmoc-Cys(Trt) (238 mg, 0.4 mmol), DIC (63 μl, 0.4 mmol) and HOAt (54 mg, 0.4 mmol) and coupled for 1 h to obtain Fmoc-Cys(Trt)-NH-resin **41.** The remain sequence of MVIIA was coupled to resin **41** stepwisely and elongated peptide was subsequently cleaved by TFA/TIS/H$_2$O/thioanisole (89/5/5/1, v/v) to give reduced MVIIA-NH$_2$ **42** (Cald. 2645.2 Da, found 2645.5 Da).

3. Peptide ligation and cyclization

3.1 Thioesterification of TIGGIR-MeCys-Gly-NH₂ and ligation with CALVIN

For each pH condition (pH = 0-7), TIGGIR-MeCys-Gly-NH$_2$ **5** (0.158 mg, 0.2 mmol) was dissolved in 200 μl buffers (diluted H$_2$SO$_4$ or 0.2 M sodium phosphate buffers) to give 1 mM solutions. The N-S acyl shift reaction was performed at 40°C for 24 h. Results were analyzed by RP-HPLC and MALDI-TOF. To obtain TIGGIR-MES **9** (calc. 740.3 Da, found 740.5 Da), 50 mM MESNa was added at the beginning to the reaction solutions described above. Tandem thiol switch reactions were performed also at 40°C. Reaction was monitored by RP-HPLC and MALDI-TOF. TIGGIR-MES **9** (0.24 mg, 0.3 μmol) and CALVIN **11** (0.63 mg, 1 μmol) were dissolved with 0.2 M sodium phosphate containing 20 mM TCEP, 20 mM MMA, and 6 M guanidine hydrochloride (300 μl). The ligation reaction was conducted at room temperature for 4 h. The reaction was monitored by RP-HPLC to obtain TIGGIRCALVIN **12** (calc. 1229.5 Da, found 1229.6 Da).

3.2 One-pot Cyclization of CG29-MeCys-Gly-NH₂

CG29-MeCys-Gly-NH$_2$ **15** (3.1 mg, 1 μmol) was dissolved in 5 mM H$_2$SO$_4$ solution (pH 2, 1 ml) at a concentration of 1 mM with 50 eq. MESNa (8.2 mg, 50 μmol) and incubated at 40°C for 24 h. The formation of thioester-form **16**, MES thioester **17** and thiolactones **18a-f** from **15** was monitored by RP-HPLC. TCEP (2.8 mg, 10 μmol) were added to the reaction mixture to avoid disulfide formation. The pH of reaction mixture remained about pH 2 after addition of TCEP. After adjusting pH to 7.5, thia-zip cyclization was performed at room temperature with gentle stirring for 2 h to give cyclic reduced CG29 **19** (comparative yield 73%). In the second cyclization reaction, CG29-MeCys-Gly-NH$_2$ **15** (3.1 mg, 1 μmol) was dissolved in 5 mM H$_2$SO$_4$ solution (pH 2, 1 ml) at a concentration of 1 mM without addition of MESNa. The reaction was conducted at 40°C for 36 h when **15** was not observed in HPLC monitoring. Thioester-form **16** and five out of six thiolactone **18a-f** was isolated from HPLC and identified by MALDI-TOP mass spectrometry. After adjusting pH to 7.5, thia-zip cyclization was performed at room temperature

with gentle stirring for 2 h to give cyclic reduced CG29 **19** (comparative yield 86%). To a solution of cyclic CG29 **19** (2.9 mg, 1 μmol) in 0.1 M ammonium phosphate buffer (pH 8, 100 ml) that containing 2 M ammonium sulfonate, a redox reagent including oxidized/reduced glutathione (molar ratio of peptide: GSSG: GSH = 1:10:100) was added to catalyze disulfide formation at 4°C for 72 h. Folding products were isolated by RP-HPLC and subsequently subjected to disulfide mapping.

3.3 Thioesterification of TIGGIR-TEBA

Eight conditions with pH ranged from zero to seven were tested. In each condition, TIGGIR-TEBA **25** (0.158 mg, 0.2 mmol) and MESNa (1.6 mg, 10 μmol) was dissolved in 200 μl buffers (diluted H_2SO_4 or 0.2 M sodium phosphate buffers) to give 1 mM peptide solutions with 50 mM MESNa. The N-S and S-S tandem acyl shift reaction was performed at 40°C for 24 h. Results were analyzed by RP-HPLC and MALDI-TOF.

3.4 Cyclization of conotoxins using TEBA thioester surrogates

The peptide-TEBA precursors of conotoxins **29a-c, 56, 61** were dissolved in 0.2 M sodium phosphate buffer (pH 3) with 50 equivalent MESNa and tandem thiol switch was conducted at 40-65°C. Without purifying the peptide-MES thioester or peptide thiolactones, the product mixture of thioesterification was subjected to cyclization by increasing pH to 8.0 that adjusted by 1 N NaOH. Cyclization reaction was performed at room temperature for 1-2 h. Reaction was monitored by analytical HPLC and cyclic product was purified by preparative HPLC.

3.5 Azide oxidation and cyclization

The peptide-hydrazide precursors of conotoxin **38a-c** were dissolved in Milli-Q water containing 0.1% TFA (*v/v*) to the concentration of 1 mM. 10 mM pre-chilled $NaNO_2$ stock was added into peptide solution and the reaction mixture were kept in 0°C for 30 min. 100 mM MMA was added and pH was increased quickly to 8.0 by adding 1 N NaOH solution on ice. The cyclization reaction was then performed at room temperature for 2 h. Reaction was quenched by directly subjecting to HPLC purification.

4. Disulfide formation of cyclic CRPs

4.1 Oxidative folding of cyclic CRPs in aqueous buffers

Purified hedyotide B1 (0.34 mg, 0.1 mmol) was dissolved in 10 ml deoxygenated folding buffer containing 70% iPrOH, 0.1 M Tris-Cl buffer (pH 8) and redox reagents GSSG/GSH (0.1 mM and 1 mM). Folding reaction was performed at room temperature for 48 h. Native-fold hedyotide B1 was co-eluted with natural hedyotide B1 extracted from fresh plants in analytical RP-HPLC.

The reduced conotoxin MVIIA and its analogs M-GS, CG29 and cM(1-3)B were folded in a 0.1 mM deoxygenated ammonium acetate buffer containing 2 M ammonium sulfate (pH 7.8). Peptides, redox reagents GSSG and GSH were dissolved in the folding buffer to concentration of 10 μM, 0.1 mM and 1 mM, respectively. Folding reaction was performed at 4°C for 48 h. Reaction was monitored by analytical RP-HPLC and folding mixture were purified by semi-preparative HPLC.

4.2 Chemoselective disulfide formation

Peptides with S-Trt, S-Acm and S-tBu protection groups were prepared by solid phase chemical synthesis followed by pairwise disulfide formation depending on the chemoselective properties of each protecting groups. Trt groups were removed by TFA during cleavage reaction to give one-pair of free thiols, which were oxidized by 10% DMSO in water to form the first pair of disulfide bond. The second pair of Cys residues were Acm-protected, which were removed by iodine oxidation. 1SS Peptides were dissolved in 80% acetic acid in water to the final concentration of 5 mM. HCl (15 mM) was also added into the reaction solution to prevent sulfoxide formation at methionine. An iodine solution in methanol was added into peptide solution dropwisely to reach 50 mM. This method allowed simultaneous deprotection of Acm and oxidation of thiols within 30 min at room temperature, to form the second disulfide bond. For peptides containing three disulfide bonds, the rest two Cys residues were S-tBu protected, which were deprotected and oxidized by TFA/DMSO/anisol (94.9/5/0.1 v/v) at concentration of 1 mM for 40 min at room temperature. After

each thiol oxidation reaction, RP-HPLC purification was required to remove reactive reagents and side products to prevent any undesired factors that may affect the following oxidation steps.

4.3 Oxidative folding of cyclic CRPs in organic conditions

The reduced cyclic ω-CTXs cM(1-3)B **33a-c** and hedyotide B1 were subjected to organic folding. Purified cyclic ω-CTXs **33a-c** were dissolved to a concentration of 0.1 mM in the folding solution composed by 10% DMSO, 89% pyridine and 1% morpholine in the presence of reductants MMA, cysteamine or MESNa. Folding reaction was performed at room temperature and monitored by RP-HPLC. Reaction was quenched by gradually adding equal volume of pre-chilled 20% TFA solution on ice.

The reduced hedyotide B1 was dissolved to a concentration 0.1 mM in the folding solution containing 70% iPrOH, 19% pyridine, 10% DMSO, 1% morpholine, and 10 mM reductant cysteamine. Folding reaction was performed at room temperature and analyzed by HPLC.

4.4 One-pot cyclization and oxidative folding of cyclic conotoxins

Purified peptide-TEBA precursor **29b** (10 mg) was dissolved in the pH 3 phosphate buffer at concentration of 1 mM. Thioesterification was performed at 40°C for 24 h without addition of external thiols. The completed thioesterification mixture was subjected to cyclization at pH 7.5 for 1.5 h. The cyclization mixture was diluted using organic folding solution to a final composition of 10% buffer, 10% DMSO, 79% pyridine, 1% morpholine and 10 mM MMA with peptide concentration of 0.1 mM. After incubating at room temperature for 1 h, folding reaction was quenched by adding pre-chilled 20% TFA. Pyridine was removed by rotary evaporator before HPLC purification.

Alternatively, the cyclization mixture of **33a-c** obtained from azide method was directly diluted by the folding solution to a final composition of 10% buffer, 89% pyridine, and 1% morpholine with 0.1 mM peptide. The reductant MMA (100 eq) and a mixture of oxidants (10 eq) including NO_2^-, NO^-, N_3^- existed in the cyclization mixture played the role of redox reagents in

this folding mixture. After 1 h, reaction was quenched and peptides were isolated by RP-HPLC using the procedures described above.

4.5 Global Desulfurization

Disulfide-free cM6A was obtained from desulfurizing cM-GS **57.** 1 μmol cM-GS (2.77 mg) was dissolved in 10 mL deoxygenated 0.1 M phosphate buffer (pH 6.5) containing phosphine source TCEP (143 mg, 0.5 mmol), glutathione (306 mg, 1 mmol), 2,2'-azobis(2-(2-imidazolin-2-yl)propane) dihydrochloride (VA-044) (3.12 mg, 10 μmol). The desulfurization reaction was performed for 3 h at 40°C.

5. Characterization of disulfide connectivity

5.1 Isolation of native hedyotide B1 from plants for comparison

Native hedyotide B1 was extracted from the aerobic portion of fresh plants. 0.1 kg of fresh leaves and stems of *Hedyotis biflora* was frozen at -80 ˚C and blended with 50% methanol to prepare 1 L of extracts. Chlorophylls, membranes and large proteins were separated by repeating DCM partitions until the DCM layer became light brown. The clear aqueous layer was collected and concentrated by rotary evaporator. Concentrated clear extract was fractionated by preparative C18 column in RP-HPLC in a gradient of 10-60% buffer B, 100 min. All fractions were subjected to MALDI-TOF mass analysis and the fractions containing MS peak corresponding to hedyotide B1 were collected for further purification to obtain pure peptide product. The sequence and disulfide connectivity were identified through partial acid hydrolysis and LC-MS/MS [106].

5.2 Disulfide bond determination by partial reduction and S-alkylation

Cyclic conotoxins analogs with two disulfide bonds were subjected to partial reduction and S-alkylation to characterize their disulfide connectivity. peptides were dissolved in 5 mM TCEP solution (pH ~2) to prepare 1 mM reduction mixture. Immediately after 5 min incubation at room temperature, excessive NEM (> 20 mM) was added in to the solution and incubated for additional 60 min to quench the reduction and alkylated to the reduced free SH groups. The mixture of alkylated peptides were separated by RP-HPLC using high-pressure analytical column (Aeris Peptide 3.6u XB-C18, 250 x 4.6 mm) in a gradient of 5-25% buffer B, 60 min. Products that with 2SS, 1SS+ 2S-NEM and 4S-NEM were collected and characterized by MS. The 1SS+2S-NEM alkylated isomers were digested by chymotrypsin (30 min, rt) and reduced again by TCEP. The linear reduced peptides were analyzed by MS/MS to match the original disulfide connectivity.

5.3 1D proton NMR

cM2B isomers **54b-i/ii** and MVIIA were dissolved in water solution composed by 20% TFE-d3, 5% D_2O and 75% H_2O. One-dimensional H^+ NMR

79

was performed on a Brucker 600 mHz NMR spectrometer that equipped with cryo-probe at 298 K. The spectra were processed and analyzed using Topspin software.

6. Bioassays

6.1 Stability tests

The metabolic stability of synthetic peptides was test by heating, acid hydrolysis and trypsin digestion. Heating stability of cyclic peptides were examined at 100°C by performing a constant heating on a water solution of peptides (0.1 mM) for 1-24 h. The resultant peptide and degraded products were analyzed on a reverse-phase analytical-grade HPLC. Acid hydrolysis test was performed in a 200 mM HCl solution with peptide concentration of 0.1 mM. The resultant peptide and hydrolysis products were analyzed on a reverse-phase analytical-grade HPLC. The trypsin digestion reactions were perform in citrate buffer (0.2 M) with molar ratio of enzyme: peptide = 1: 200. Reaction was performed at 37°C for 10 min to 2 h. The resultant peptide and digested products were analyzed on a reverse-phase analytical-grade HPLC.

6.2 Radial diffusion assay

The radial diffusion assay of Leher et al. [251] was used for testing the antimicrobial activity of omega-conotoxin and its cyclic analogs. Bacteria *E. coli, S. aureus, and Fungus C. tropicalis* were tested. Single colony of each strains was cultured in TSB broth overnight (37°C, 220 rpm) and 1 ml culture was subculture in 3 ml full-strength TSB broth for another 3 h. Culture was diluted using 10 mM phosphate butter and cell density was measured by OD600. Diluted cells containing 4×10^6 CFU were mixed with 10 mL agarose gel with minimal nutrient (30mg TSB/mL, 10 mM phosphate buffer) and pour on petri dish to form underlay gel. Equal size wells (2 mm diameter) were punched in the solidified underlay gel by 1 mL pipette tip connected to a vacuum pump. An aliquot (3 μL) of peptide samples with stack of dilution from 0.1 mM to 3.125 μM was loaded into each well. The peptide and the underlay gel with bacteria were incubated at 37 °C for 3 h with gel-side up. A nutrient-rich overlay gel (6 mg TSB/mL) was added on top of underlay gel, and the bacteria were allowed to grow overnight. The minimal inhibitory concentration (MIC) was calculated by measuring the diameter of the clear zone against different peptide concentrations.

6.3 Hemolytic assay

Hemolytic activities were determined by the lysis of human fresh erythrocyte. EC_{50} referred to the peptide concentration causing 50% hemolysis were derived from the dose-response curves. Membranolytic activity index was calculated as the ratio of hemolytic activity (EC50) to the antimicrobial activity (MIC) of the peptide against a type of organism. (Eur. J. Biochem. 267:3289, 2000)

6.4 Chemotaxis assay

The chemotaxis assays was performed in cell migration boyden chamber as described in previous research paper [252]. Peptides MVIIA, cM1B, cM2B, cM3B, cM6A, CG30(M12A), and M3B-GS were examined as peptidyl chemoattractants of THP-1 cells (human monocyte cell line). The 96-well cell migration plate (CytoSelect™, CBA-105, Cell Biolabs, inc.) contains a cover, a 96-well membrane chamber, and a 96-well feeder tray. The polycarbonate membrane with 5 μm pore size allows THP-1 cells to migrate from membrane chamber towards the concentration gradient of chemoattractant that loaded in the feeder tray. Series dilutions (0.1 nM to 0.1 mM) of peptides MVIIA and cM(1-3B) in RPMI medium (1% penicillin and streptomycin) were loaded to the feeder tray as 150 μl per well and two wells for each concentration. The THP-1 monocyte cells were cultured in RPMI medium (7% FBS, 1% P/S) at 37°C with 5% CO_2. After starving in serum-free RPMI medium overnight, cells were collected by centrifugation (700 rpm, 10 min) and washed with PBS twice. The rinsed cell pellet was re-suspended in RPMI medium to 1 x 10^6 cells/ml. In each well of membrane chamber, 100 μl cell suspension was loaded (about 10^5 cells) and the membrane chamber was placed gently on top of feeder tray that membrane was attached to the medium layer without any bubbles under the membrane. The assembled plate was incubated at 37°C for 6 h. Membrane chamber was transfer into 96-well harvest tray containing 150 μl detaching buffer in each well and incubated at 37°C for 30 min. 75 μl cell-containing detaching solution and 75 μl medium in the feeder tray was transfer to a new 96-well plate. In each well, 50 μl lysis buffer containing CyQuant GR dye wasadded and cells were lysed for 20 min at room temperature. The CyQuant

GR dye bind with released DNA, which was excited at 480 nm and gave fluorescent readout at 520 nm. The fluorescent unit against cell number was plotted as reference to calculate the chemotactic activity of each peptide.

6.5 Membrane-permeability assay (Immuno-fluorescence test)

Human lung carcinoma cell line NCI-H1299 cell culture in one T25 flask (25 cm^2) was detached by trypsin and resuspended in 15 ml RPMI medium (with glutamine) containing 7% FBS and 1% penicillin/streptomycin. 0.3 ml cell suspension was transferred to the each well of a 4-well µ-slide and incubated overnight at 37°C to reach 70-80% confluency. Biotinated peptide cM1B(K7-biotin) solution with concentration of 10 µM was prepared by dissolving 148 µg peptide (0.05 µmol) in 1 mL RPMI medium (with 1% antibiotics). After rinse the cells with phosphate buffered saline (PBS) solution for three times, 200 µl peptide solution was added into each chamber and incubated for 30 min. After three times PBS washing, the cells were fixed with 4% paraformaldehyde (PFA, solution in PBS, sigma) for 45 min at room temperature. After removing PFA and washing cells using PBS, 200 µl 0.2% Triton X-100 in PBS was added to permeabilize the cells for additional 10 min, followed by three times PBS washing. The cells were then incubated with the FITC-conjugated avidin (Nutravidin^{TM}, Sigma) (200x dilution in 5% FBS in PBS) avoiding-light for 1 h at 4°C. After three washes with PBS, Alexa Fluor-594 conjugated phalloidin was applied to stain actin by 1 h incubation in dark room at 4°C. cells were mounted with glass coverslips using mounting medium containing DAPI and 15 mM NaN$_3$ (Dako). The µ-slide with fixed cells and fluorescent dyes were observed under confocal microscope (LMS510, Zeiss) at 405 nm (DAPI), 488 nm (TIFC-conjugated avidin) and 594 nm (Alexa Fluor-594 conjugated phalloidin).

For co-localization assay, Golgi was probed by Golgin 97 human monoclonal antibody (mouse IgG$^+$) followed by marking with anti-mouse IgG secondary antibody (Alexa Fluor® 680 donkey, Invitrogen), which gave pink color at 680 nm. The endoplasmic reticulum was stained with ER-Tracker ^{TM} Blue-White DPX (Invitrogen) that exhibit emission between 430-640 nm.

Chapter 3 Biosynthesis of cyclic CRPs using intein-splicing

1. Introduction

In Singapore, a plant genus called *Hedyotis* is widely distributed with most species in this genus is recognized as herbal medicines in traditional Chinese medicine and Indian medicine. *Hedyotis biflora* (**Figure 3-1A**) was one species of this genus containing anti-infective and anti-inflammatory ingredients. Cyclotide isolation and characterization studies show that this plant produces more than 30 cyclotides with wide range of antimicrobial activities [106]. The first isolated cyclotide discovered by our lab was designated hedyotide B1. Cyclotide hedyotide B1 contains 30 amino acid residues with net-charge of +3 (**Figure 3-1B**). It is a typical bracelet cyclotide, as the amino acid sequence does not contain the *cis* proline at loop 5 in Mobius cyclotides (**Figure 3-1C**). Using hedyotide B1 as a model, I aim to develop the recombinant synthesis method of preparing CRPs using intein-splicing tool.

The amino acid sequence of hedyotide B1 contains six Cys residues, which can serve as six different cyclization sites. To understand the relationship between cyclization efficiency and cyclization site residues, I designed six precursors B1x (x for a C-terminal residue R, F, G, S, Y, or F) for the recombinant synthesis of cyclic hedyotide B1 (**Table 3-1**).
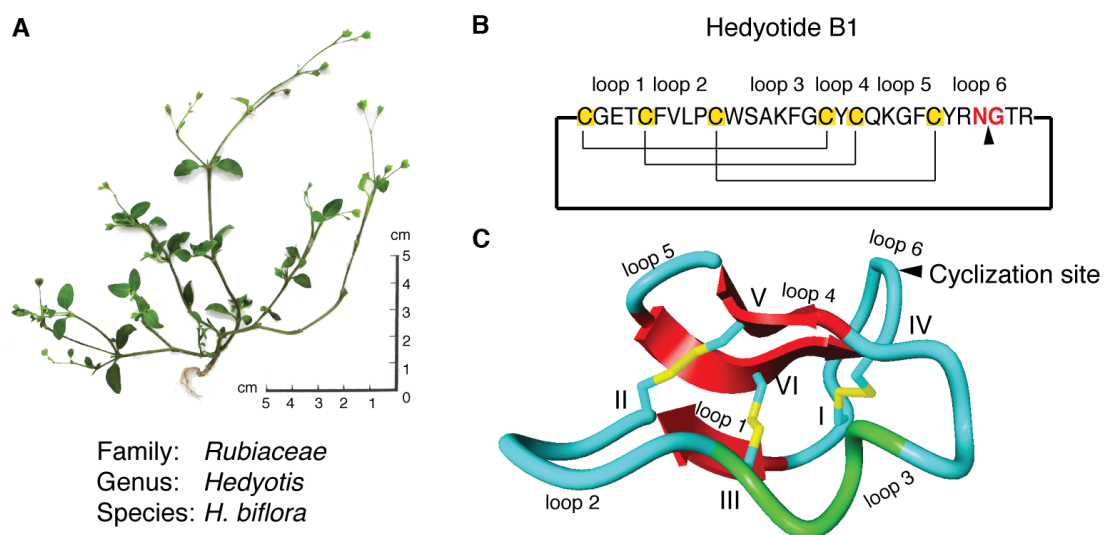
Figure 3-1. Cyclotide-producing plant *Hedyotis biflora* and the first isolated cyclotide hedyotide B1. (A) Plant morphology and classification of *H. biflora.* (B) Amino acid sequence, disulfide bonds and end-to-end cyclic backbone of hedyotide B1. (C) Computer modeling structure of hedyotide B1.

Table 3-1. **Six hedyotide B1 precursors B1x (x: R, T, P, G, Y, F) with different ligation site residues**.

Peptides	Amino acid sequences
hedyotide B1	I II III IV V VI GTR**C**GET**C**FVLP**C**WSAKFG**C**Y**C**QKGF**C**YRN
B1R	**C**GET**C**FVLP**C**WSAKFG**C**Y**C**QKGF**C**YRNGT**R**
B1T	**C**FVLP**C**WSAKFG**C**Y**C**QKGF**C**YRNGTR**C**GE**T**
B1P	**C**WSAKFG**C**Y**C**QKGF**C**YRNGTR**C**GET**C**FVL**P**
B1G	**C**Y**C**QKGF**C**YRNGTR**C**GET**C**FVLP**C**WSAKF**G**
B1Y	**C**QKGF**C**YRNGTR**C**GET**C**FVLP**C**WSAKFG**C**Y
B1F	**C**YRNGTR**C**GET**C**FVLP**C**WSAKFG**C**Y**C**QKG**F**

Cysteine residues (in yellow) were aligned with the native sequence.

C-terminal residues were highlighted in red.

Each B1x was co-expressed with an engineered intein *Mxe* in *E. coli*. This engineered intein *Mxe* was derived from *Mxe* GyrA intein from *Mycobacterium xenopi* [253], of which the C-terminal Asn was modified into Ala and linked with a chitin-binding domain (CBD) sequence. Formation of a cyclic B1x from the fusion protein B1x-*Mxe*-CBD was a combinatory process of enzyme catalysis and chemical reactions as shown in **Figure 3-2**. The N-terminal Cys residue was the key site to mediate thioester bond formation. The peptide-intein thioester was cleaved from column bond intein-CBD by thiolysis. The following thia zip cyclization reaction was no longer enzyme-driven. It was a chemoselective process involving thiolactone ring expansion by S-S acyl shift reactions and a final S-N acyl shift reaction occurred in a five-member transition state.
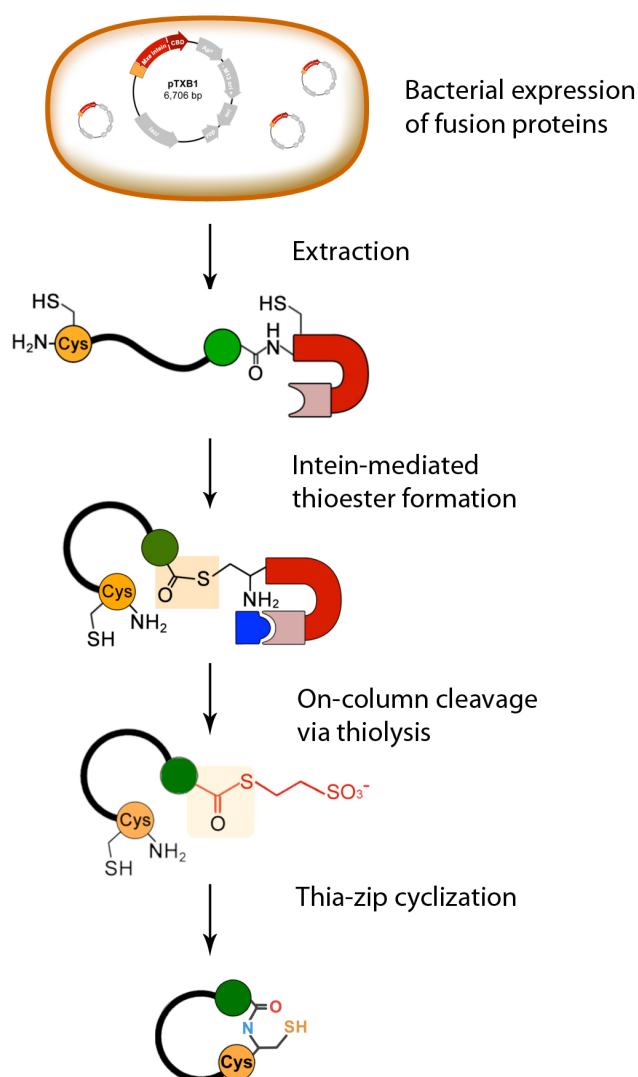
Figure 3-2. **Schematic illustration of cyclic CRP recombinant biosynthesis using intein-splicing tool**. Peptides (highlighted N-terminal cysteine in orange and C-terminal residues in green) were co-expressed with intein (red) and chitin-binding domain (brown) as fusion proteins. After binding to chitin beads (blue), intein mediated N,S acyl shift that resulted in formation of peptide-thioester. The peptides were cleaved from fusion protein through thiolysis by addition of thiol MESNA and formation of MES-peptide thioester. At pH 7-8, thia-zip cyclization occurs and results in end-to-end cyclic CRP peptides.

2. Design and construction of plasmids

2.1 Codon-bias correction

The cDNA sequence of hedyotide B1 (GenBank: JN542706.1) has been reported in previous studies [254]. Notably, the native nucleic sequence was not ideal for expression using prokaryotic system due to the difference in tRNA frequency. The encoding sequence of hedyotide B1 used in this study was optimized for E. *coli* expression system by correcting codon-bias according to the Relative Synonymous Codon Usage (RSCU) value [249] (**Table 3-2**).

Table 3-2. Amino acid sequence, cDNA Sequence and codon-bias corrected sequence of hedyotide B1. cDNA sequences (cB1) and corrected sequences (cB1-r) were aligned with the amino acid sequence of hedyotide B1 (1-letter code). Codon bias was corrected based on tRNA frequencies in *E. coli* (highlighted in red and underlined). Higher tRNA frequencies were indicated by larger RSCU values.

hedyotide B1	1- G T R C G E T C F V L P C W S -15
cB1	GGA ACT CGA TGC GGT GAG ACT TGC TTC GTT TTA CCA TGC TGG TCC
cB1-r	GGC ACT CGC TGC GGT GAG ACT TGC TTC GTT TTA CCG TGC TGG TCC

hedyotide B1	16- A K F G C Y C Q K G F C Y R N -30
cB1	GCC AAG TTC GGC TGC TAC TGC CAA AAG GGT TTT TGT TAC AGA AAC
cB1-r	GCC AAG TTC GGC TGC TAC TGC CAA AAG GGT TTT TGT TAC CGC AAC

RSCU		
	Arginine	CGA/AGA 0.017 → CGC 1.561, AGG 0.008 → CGT 4.380
	Glycine	GGA 0.022 → GGC 1.652
	Cysteine	TGT 0.667 → TGC 1.333
	Leucine	CTT 0.225 → CTG 5.326
	Lysine	AAG 0.404 → AAA 1.596
	Proline	CCA 0.441 → CCG 3.288
	Serine	TCA 0.198 → TCC 1.921
	Tyrosine	TAT 0.386 → TAC 1.614

2.2 Primer design and tandem-extension PCR

The DNA sequences containing restriction sites were prepared by tandem-extension PCR reactions (**Figure 3-3**). The tandem extension PCR reaction mixture contained four primers p1f, p2f, p3r and p4r, pfu polymerase and dNTPs without presence of a template sequence. Two forward primers p1f, p2f and two reversed primers p3r, p4r overlapped one by one to cover the full length CRP and two terminal primers p1f and p4r carried restriction sites NdeI/SapI for insertion into vector pTXB1 (NEB, IMPACT kit). In the first extension reaction, primers p2f and p3r were annealed first at a higher annealing temperature (57.6-59.1°C) and amplified for 5 cycles to provide amplicon 1. The higher annealing temperature suppressed random binding and interactions by p1f or p4r although they existed in large amounts in the reaction mixture. The amplicon 1 was then used as the template for the second extension involving p1f and p4r with a lower annealing temperature (51.3-53.8°C). This extension reaction produced full-length DNA sequences in the following 30 cycles. The sequences of primers were listed in **Table 3-3**. PCR products from multiple reactions were summed up and purified together by silica columns. The final concentration of PCR products was determined by UV spectrometry.
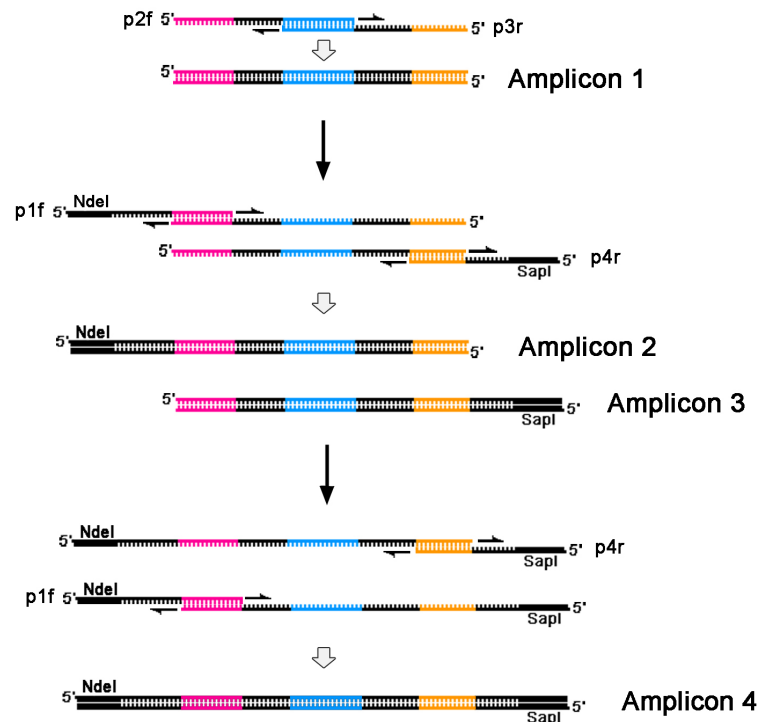
Figure 3-3. **Schema illustration of tandem-extension PCR**. Forward primer p1f carried NdeI restriction site and 5'-end of CRP cDNA. Forward primer p2f contained 14-17bp overlapping sequence that complementary to p1f (red) and 15-21bp overlapping sequence that complementary to p3r (blue). Reversed primer p3r overlapped with p2f (blue) and p4r (orange). Reversed primer p4r overlapped with p3r (orgnge) and carried SapI restriction site on its 3'-end. In the first chain reaction with higher annealing temperature (56-58°C), only p2f and p3r participated in the polymerization to generate amplicon 1 for 5 runs. In the second chain reaction, p1f and p4r annealed with amplicon 1 at lower annealing temperature (51-53°C) to produce amplicon 2 and 3. In the following runs, all four primers participated in extension reactions to produce amplicon 4, the expected product that possessed the full length of CRP cDNA sequences flanked by NdeI/SapI restriction sites.

2.3 Construction of recombinant plasmids

PCR products obtained from each tandem-extension reactions and the vector pTXB1 were digested by NdeI/SapI (37 ˚C, 3 h). The digested products were ligated upstream of intein-CBD encoding region in the pTXB1 vector by T4 DNA ligase (**Figure 3-4**). Ligation products were transformed into competent *E. coli* strain DH5α and colonies grew on pre-warmed Amp$^+$ LB-agar plate overnight.

EcoRI/EcoRV double digestive screening was performed to examine the plasmids with insertions. The only EcoRI restriction site located in the MCS region and EcoRV site located about 2 kbp upstream of EcoRI site. Thus, the plasmids with correct insertion was only digested by EcoRV and displayed a single band of 6 kbp in the agarose electrophoresis. The empty vectors without insertion were digested into two fragments at 2 kbp and 4 kbp by both RcoRI and EcoRV (**Figure 3-5**). Plasmids with insertion were subjected to DNA sequencing.
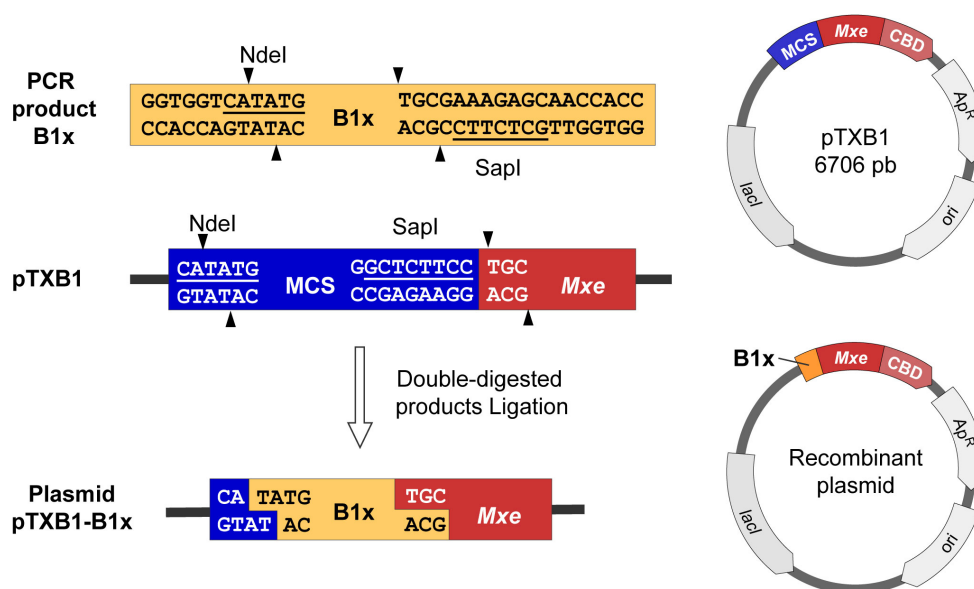
Figure 3-4. **Preparation of recombinant plasmid pTXB1-B1x**. The PCR products B1x that flanked with enzyme binding sites (orange) and pTXB1 vector (MCS in blue, *Mxe* intein in red) were subjected to NdeI/SapI double digestion. Ligation of the digested products gave a recombinant plasmid with the in-frame insertion of B1x sequence upstream of *Mxe* intein.
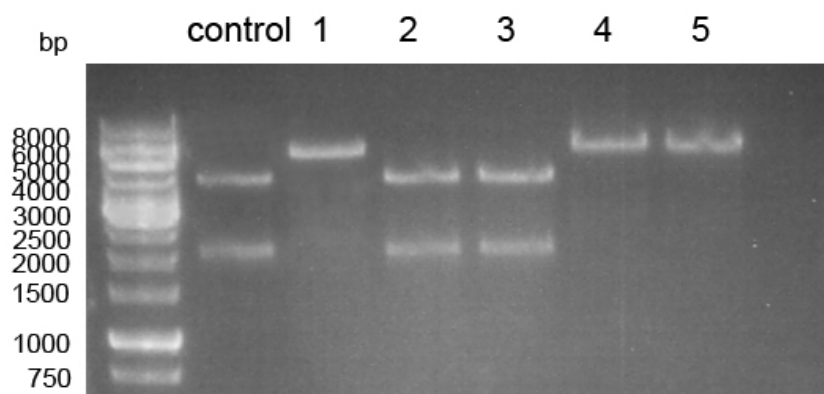
Figure 3-5. EcoRI/EcoRV double digestion screening of plasmids with PCR product insertion. Vector pTXB1 was used as negative control, which was digested into two fragments. Five colonies were picked for overnight culture. Plasmids extracted by mini-prep were subject to double digestion and agarose gel electrophoresis. Plasmids 1, 4 and 5 were suggested to contain PCR product insertion, which replaced MCS region containing EcoRI restriction site. Plasmids 2 and 3 were empty vectors.

3. Recombinant expression of CRP-intein fusion proteins

Six pTXB1-B1x plasmids with the encoding sequence of fusion proteins B1x-*Mxe*-CBD were transformed into competent *E. coli* strain ER2566. The expression of fusion proteins was induced by the inducer of *lac* operon isopropyl β-D-1-thiogalactopyranoside (IPTG). I found that under the general expression condition using 1 mM IPTG and incubating at 37°C overnight, the expressed fusion proteins were unexpectedly aggregated in the inclusion bodies, which were difficult to be extracted due to the poor solubility.

To increase the expression level and solubility of fusion proteins, IPTG concentration, temperature and incubation periods were optimized. In a batch of small-scale experiments using 3 ml culture, the transformed bacteria were incubated with different IPTG concentrations from 0.1 to 1 mM at 37°C for overnight expression. The amount of fusion protein produced was increased in the presence of higher concentration of IPTG. However, fast accumulation of expressed fusion protein induced by high concentration of IPTG also leaded to higher level of protein aggregation. By considering both rate and prevention of aggregation, the final IPTG concentration was determined at 0.3 mM.

Reduce the incubation temperature led to a decreased expression rate and prolonged period but less protein aggregation. After adding 0.3 mM IPTG, expression was performed at 37°C or 16°C. Protein expression at 16°C overnight resulted in less expression level than that at 37°C. However, the soluble protein in 16°C reaction was about two folds more than that at 37°C. Incubation at low temperature also suppressed intein-mediated B1x peptide cleavage before the extreaction process.

Collectively, the optimized condition for fusion protein expression was given with IPTG concentration of 0.3 mM, at temperature of 16°C and prolonged incubation for 24 h (**Figure 3-6A**). Cells were collected by centrifugation and the cells pellets were resuspended in lysis buffer followed by ultrasonication. About 50% fusion proteins were able to dissolve in the lysis buffer and be extracted for purification (**Figure 3-6B**). Fusion proteins in the inclusion bodies were recovered used denaturing buffer containing 8 M urea in

the extensive sonication. The ratio of solubilized proteins from inclusion bodies was very low and the fusion proteins treated by urea lost the intein catalyzing activity. Overall, 20-30 mg B1x-*Mxe*-CBD fusion proteins were obtained from 1 L bacterial culture.
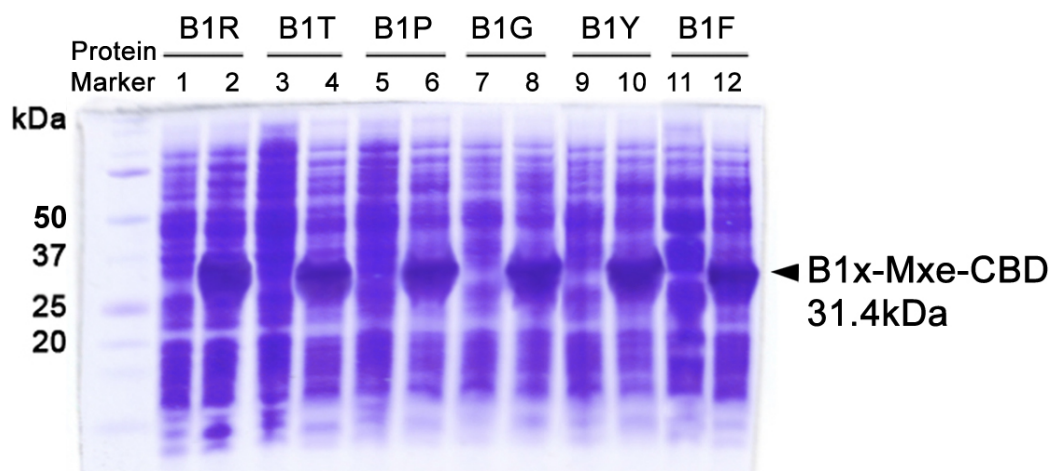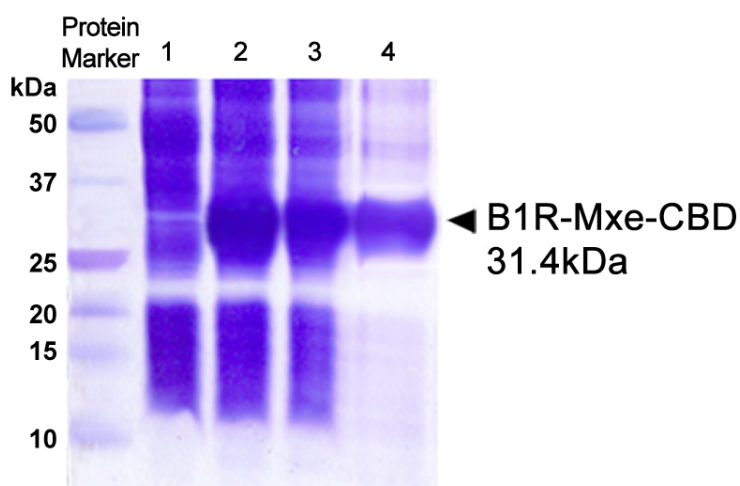
Figure 3-6. **Expression and extraction of fusion protein B1x-Mxe-CBD**. (A) The overall expression level of fusion proteins (x for R, T, P, G, Y or F). Lanes in odd number: cell lysate before IPTG induction. Lanes in even number: cell lysate after IPTG induction (B) The solubility of single-intein fusion protein B1-R-Mxe CBD. Lane 1: cell lysate before induction. Lane 2: cell lysate after induction. Lane 3: insoluble cell pellet containing inclusion bodies. Lane 4: clarified cell extraction.

4. Intein-mediated on-column cleavage of B1-thioesters

Intein-mediated peptide thioester formation readily occurred after the functional intein was expressed. During expression and extraction procedures, low incubation temperature, chilled buffer for lysis, extraction and washing provided effective control on the un-expected cleavage of target peptides from fusion proteins before loading on chitin-columns. The clarified extract was loaded into chitin column slowly with flow rate 0.5 ml/min at 4°C. Fusion proteins were retained on the chitin beads by the affinity binding. Chitin beads were rinsed by 10x volume washing buffer at a flow rate of 2 ml/min to remove unspecific binding.

After washing, the column was perfused by cleavage buffer containing external thiols MESNa (50 mM) and incubated at 4°C for the peptide cleavage reactions to occur. Addition of excessive external thiols induced cleavage via thiol-thioester exchange reactions by attacking the B1x-S-*Mxe* thioester bond, which resulted in B1x-MES thioesters that separated from column-bound *Mxe*-CBD. The secondary role of MESNa was to maintain the reduced form of side-chain thiols of Cys residues on B1x. The reduced intramolecular thiols led to intramolecular S-S acyl shift reactions to give thiolactones in the eluent, and only the reduced N-terminal Cys could mediate S-N acyl shift to afford peptide bond formation.

The efficiency of on-column cleavage was monitored by SDS-PAGE after incubating beads in the MESNa-containing cleavage buffer for 12 h and 24 h. Since the cyclized hedyotide B1 (3.4 kDa) were barely observed in the tricine SDS-PAGE gel by Coomassie-blue staining, bands for B1x-*Mxe*-CD and *Mxe*-CBD were compared to examine the cleavage rate (**Figure 3-7A**).

As shown in **Figure 3-7B**, six precursors B1x-Mxe-CBD had different cleavage rate. After 12 h reaction, B1G was completely cleaved from the fusion protein. B1R, B1T, B1Y and B1F reached about 50% cleavage. Only 10% B1P was cleaved. After 24 h incubation, B1R, B1Y and B1F were cleaved by more than 80%. The cleavage ratios of B1T and B1P were about 70% and 60%, respectively. We envisioned that the efficiency of the thiol-mediated cleavage

was determined by the accessibility of the cleavage site by a nucleophile, which was affected by the steric hindrance of the C-terminal residues. The first N-S acyl shift reaction was catalyzed by intein, while the following S-S acyl shift reactions were enzyme-free and dependent on the chemoselective force of thiol to substitute sulfur atom in the thioester bond. These thiol-thioester exchange reactions were affected by the side-chain steric hindrance adjacent to the thioester bond. B1G had the highest cleavage efficiency due to no steric hindrance at the C-terminal Gly residue. While B1P gave the lowest cleavage efficiency due to the backbone pyrrolidine ring tha blocked the α-carbonyl by from nucleophilic substitution.

A
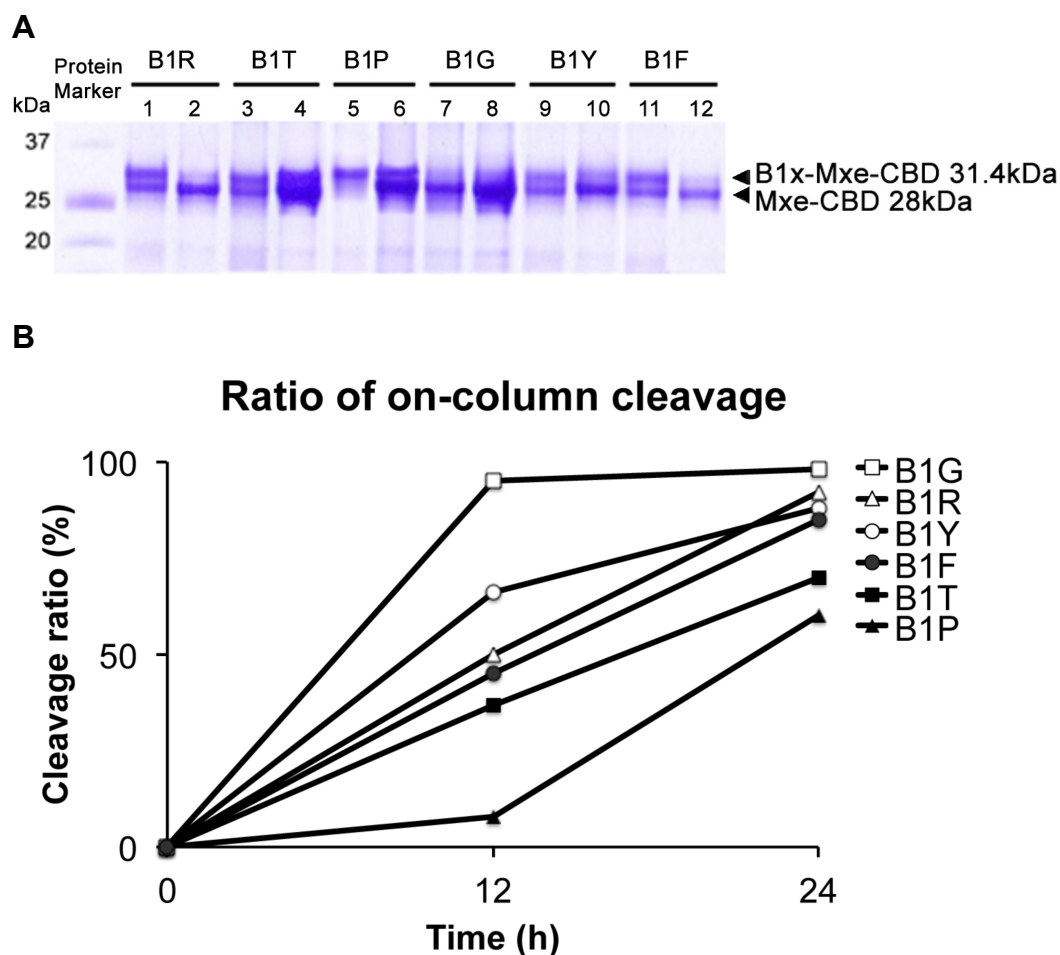
Figure 3-7. **Comparative results of six B1x-*Mxe*-CBD fusion proteins on-column cleavage after 12 h and 24 h incubation**. (A) SDS-PAGE results of proteins remained on chitin column. Protein samples were prepared by dissolving 30 µl chitin beads in 15 µl 2x loading buffer and heating at 100°C for 1 min. The odd-number lane of each clone shows cleavage ratio after 12 h incubation in column buffer containing MESNA and the even-number lane shows the cleavage ration after 24 h incubation. (B) Comparison of cleavage efficiency of six B1x-*Mxe*-CBD fusion proteins.

5. Thia-zip cyclization

The on-column cleavage by thiolysis was conducted in the cleavage buffer with a neutral to basic pH. Subsequently, the mixture of cleavage products including thioester and thiolactones were converted into cyclized hedyotide B1. The cyclization process involved transthioesterification and S-N acyl shift reaction to give the new N-to-C peptide bond formation. The transthioesterification led to thiolactone ring expansion, which accelerate cyclization by bringing N- and C-termini together through a "zipping" mechanism. After 24 h cleavage and cyclization, the eluents were analyzed by RP-HPLC (**Figure 3-8**). Six precursors of hedyotide B1 resulted in different product profiles. The cyclized hedyotide B1 was the major products in all six precursors except B1P, which resulted in hydrolyzed hedyotide B1 and B1P-MES thioester as the major products. The yield of hedyotide B1 from the on-column cleavage and cyclization reactions derived from each B1x-*Mxe*-CBD precursors were summarized in **Table 3-4**. The yield of cyclized hedyotide B1 from B1G was more than 95% and B1R, Y and F was more than 90%. The cyclization yield of hedyotide B1 from B1T was only 65% and one third of peptides were hydrolyzed. The cyclization yield of hedyotide B1 from B1P dropped drastically to less than 10%. Notably, in the cleavage mixture of B1P fusion proteins, about 30% remained as B1P-MES thioester, which indicated a slow substitution rate on the thioester bond, affected by the pyrrolidine ring of C-terminal proline.
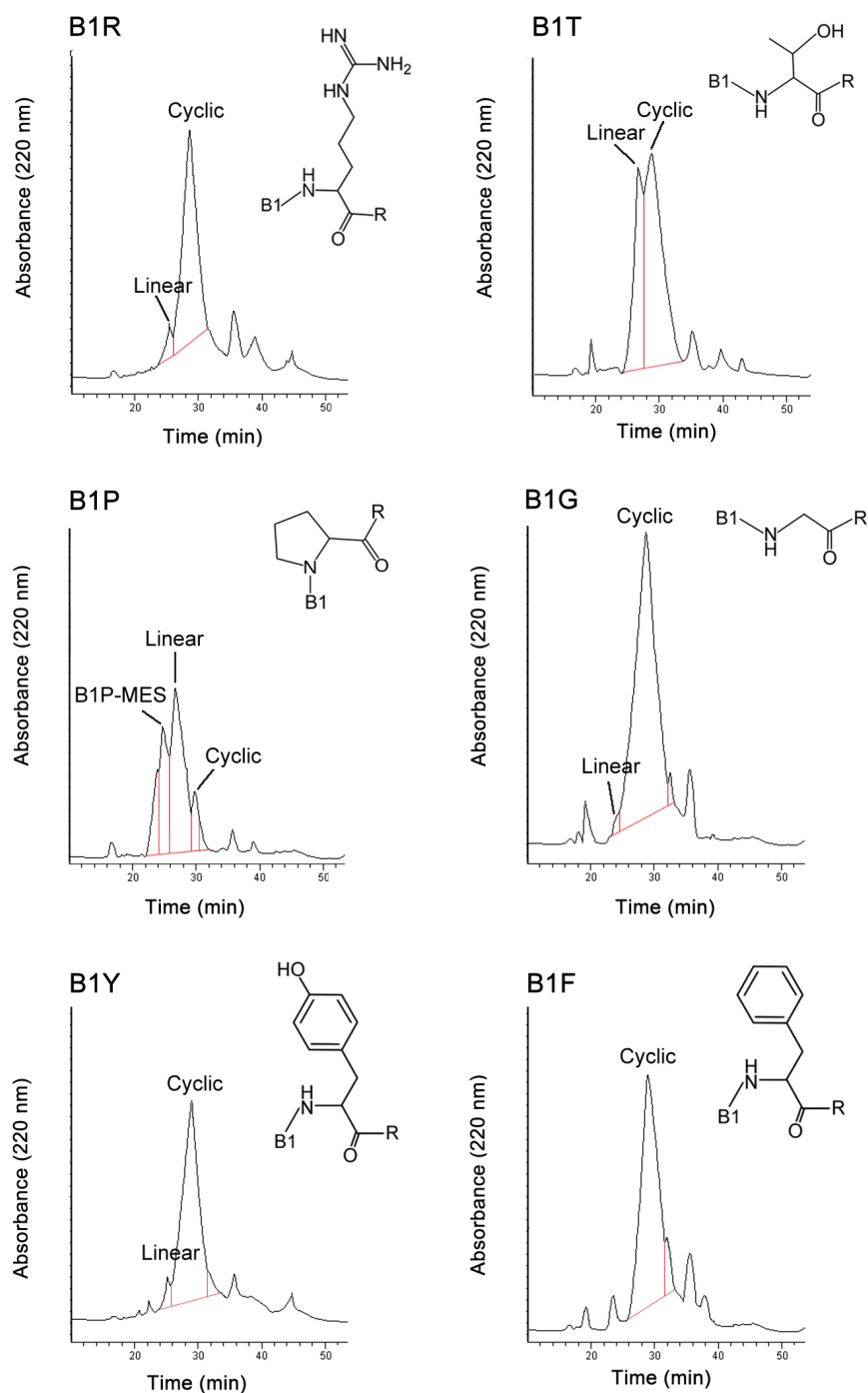
Figure 3-8. **HPLC profiles of hedyotide B1 cyclization from six peptide precursors after 24 h on-column cleavage**. Cyclic hedyotide B1 (RT = 28.8 min), linear hedyotide B1 (RT = 27.5 min) and B1P-MES (RT = 25.4 min) were identified by MALDI-TOF MS and the mass readouts were 3410.3, 3428.1, and 3553.1, respectively. Impurity peaks eluted from the chitin column were not labeled. (HPLC condition: C18 column, 5 u, 4.6x250 mm, gradient of 10-50% ACN for 40 min, 1 ml/min.)

Table 3-4. **Cyclization yield of hedyotide B1 after on-column cleavage**.

Peptide precursors	N-terminal residues	C-terminal residues	Cyclized product (%)*	Hydrolyzed product (%)	MES thioester (%)
B1G	C20 (IV)	G19	97.7	2.3	-
B1Y	C22 (V)	Y21	94.6	5.4	-
B1F	C27 (VI)	F26	93.8	6.2	-
B1R	C4 (I)	R3	91.3	8.7	-
B1T	C8 (II)	T7	65.9	34.1	-
B1P	C13 (III)	P12	9.1	60.2	30.7

* Percentages were calculated based on the ratio of peak areas summed from three isolated products.

6. Oxidative folding of hedyotide B1

Hedyotide B1 was a typical bracelet cyclotide with very hydrophobic amino acid sequence. Wong, et al. reported that the global oxidative folding of hedyotide B1 was efficient in the presence of high level of alcohols such as 70% isopropanol, which provided a hydrophobic solvent system that promote solubility and conformation that favored native disulfide bond formation [106]. The oxidative folding reaction was conducted in the 0.1 M Tris-Cl buffer (pH 8.5) with 10 μM peptide and the redox reagents reduced/oxidized glutathione in the molar ratio of peptide: GSSG: GSH = 1: 10: 100. Reaction was performed at room temperature up to 48 h and monitored by HPLC (**Figure 3-9**). In the RP-HPLC purification, the native-fold hedyotide B1 was more hydrophobic, which was eluted later than the reduced cyclic hedyotide B1 or the mis-fold isomers. This native-fold product N was characterized by co-elution with extracted hedyotide B1 from fresh plant tissue of *H. biflora*.
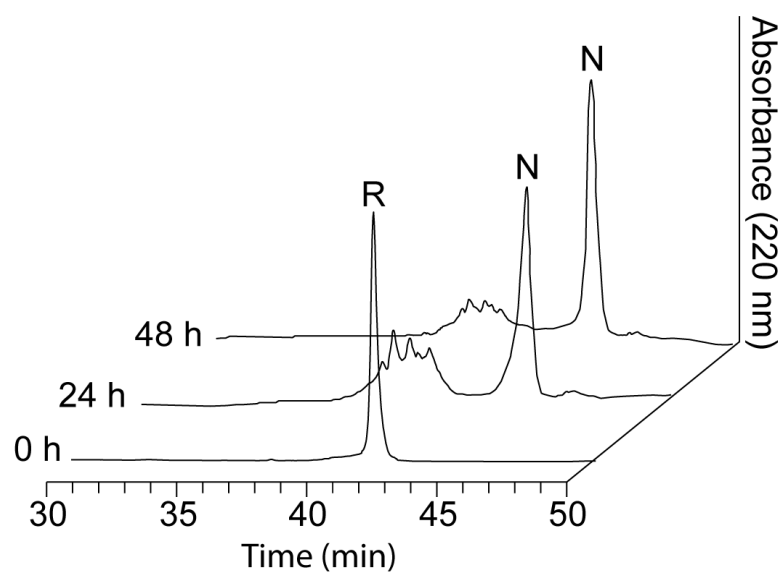
Figure 3-9. Oxidative folding of hedyotide B1. Reduced hedyotide B1 (R) was eluted at 42 min. Native-fold hedyotide B1 (N) was eluted at 43.8 min. (HPLC condition: Jupiter C18 column, 5 u, 4.6x250 mm, gradient of 10-50% ACN for 40 min, 1 mL/min.)

7 Discussion

7.1 Recombinant expression

Intein has been introduced into recombinant protein synthesis as an efficient tool to mediate peptide ligation. It provides complementary approaches in protein engineering to synthesize long peptides or proteins with post translational modifications that are not affordable by chemical synthesis. For preparation of cyclic CRPs, using bacterial system has both advantages and disadvantages. As an alternative to plant enzyme AEP and chemical synthesis, bacterial expression system adopts intein-splicing tool to prepare peptide-thioester as the reactive intermediate that is ready for peptide ligation and cyclization. Inteins are bacterial-origin, thus they are fully functional after bacterial ribosomal translation. The canonical intein-splicing mediates ligation of two extein peptides flanking on both side of intein through the standard four-step acyl shift reactions (**Figure 1-16**). For preparing macrocyclic peptides, target peptide replaced N-extein and engineered intein with dysfunctional C-terminus was adopted (**Figure 1-17**). The disadvantage of bacterial expression system is that *E. coli* tends to trigger the charge-rich recombinant fusion proteins aggregation into inclusion bodies when the translated protein that not in correct-fold, or be recognized "toxin" to the host bacteria. The attempt on recovery of fusion proteins from inclusion bodies was unsatisfied.

The efficiency of recombinant expression was determined by the overall expression level and solubility of the fusion proteins. By using low temperature, low inducer concentration and prolonged incubation time, about 50% expressed fusion proteins were kept in soluble form. The six precursors of hedyotide B1 did not result in significant difference in expression level or solubility when they were expressed under the same condition.

7.2 Side-chain steric effects on cyclization

In the comparative study of six precursors of hedyotide B1, we found that the rate of tandem acyl shift reactions was affected by the steric hindrance provided by side chains of C-terminal residue. The overall cyclization yield of

B1G is more than 90% since C-terminal Gly provide minimal steric hindrance to the cyclization site in the intein-mediated thioester formation (N-S acyl shift), peptide release (S-S acyl shift) and thia zip cyclization (S-S, S-N acyl shifts) steps. Precursors B1Y, B1F and B1R can provide about 90% yields in both steps although the reactions were slower than that of B1G, since their C-terminal residues with flexible side chains produced limited steric effects in cyclization. For B1T, the β-branched side chain of C-terminal Thr hindered the nucleophiles to attack the α-carbonyl, which resulted in less than 70% peptide cleavage and only two third of cleaved peptide-thioesters transformed into cyclized product. For B1P, the bulky backbone ring of C-terminal proline resulted in the lowest cleavage efficiency (~60%) and the lowest thia zip cyclization yield (<10%) and accumulation of the hydrolyzed product.

Considering both peptide release efficiency and thia zip cyclization ratio, the different cyclization sites resulted in about 20-fold difference in cyclization yield in a ranking of Gly > Arg/Tyr/Phe > Thr >>> Pro. This result could help the design of a proper precursor of a cyclic CRP using in the recombinant and chemical synthesis. Small amino acid residues could also be used for the Cys-thioester cyclization for a sequence lacking a Cys-Gly site.

The prototypic cyclotide kalata B1, only provided three types of Xaa-Cys sites including three Thr-Cys, two Val-Cys and one Gly-Cys sites. In Kimura's work to prepare kB1 by recombinant synthesis [157], he demonstreated that the second last residue also affect cyclization efficiency, as (Gly-Thr)-Cys and (Pro-Gly)-Cys resulted in equally high yield of cyclized product, while the (Glu-Thr)-Cys was worse than (Gly-Thr)-Cys, and (Cys-Thr)-Cys resulted lowstest cyclization yield among six precursors. This second residue steric effects can be oberseved in hedyotide B1 precursors. Both B1Y and B1F had aromatic rings on the C-terminal side chains, but they contribute to similar cyclization yields as B1R, which had a linear side chain. The second last residue involved in B1Y, B1F and B1R were (Cys-Tyr)-Cys, (Gly-Phe)-Cys and (Thr-Arg)-Cys, respectively. The explanation could be that the second last Thr residue of B1R also contributed to C-terminal hindrance.

Overall, the cyclized hedyotide B1 obtained by recombinant biosynthesis was about 1-2 mg per litre bacteria culture. The yield was affected by expression level, solubility of fusion protein, multiple purification, and steric effect at the cyclization site. To obtain sufficient peptide for oxidative folding to afford native hedyotide B1, labor-intensive large-scale expression, extraction and purification has to be performed. Therefore, it is necessary to develop chemical synthesis method for developing a high-throughput synthesis platform to prepare cyclic CRPs.

7.3 Oxidative folding

The disulfide bond formation of cyclotides has been reported on several prototypic models including Möbius cyclotide kalata B1 and bracelet cyclotide cycloviacin O2. Kalata B1 could easily fold in an ammonium bicarbonate buffer (pH 8.5) in the presence of redox reagents. Addition of isopropanol would further enhance the folding efficiency of kalata B1 to above 90% [255]. In contrast, Leta Aboye reported oxidative folding of bracelet cyclotide cycloviolacin O2 with isopropanol, Brij35, DMSO and redox GSH/cystamine at 3°C and the final folding yield was about 50% [256]. They speculated the hydrophobic loop3 formed a surface patch that could be stabilized by DMSO and Brij 35. Together with the results about oxidative folding of hedyotide B1, we conclude that these additional factors such as alcohols, detergents and organic solvents were conformation-promoting agents. For the very hydrophobic sequence of hedyotide B1, 70% iPrOH played important role in externalize the hydrophobic side chains, which maintained the intrinsic conformation of cyclotides, of which the internal core was filled with cystine and the side chains, either hydrophilic or hydrophobic, were force to protrude outside. The free space of the internal core also facilitated disulfide exchange reactions and thus accelerates the folding process.

Chapter 4. Chemical Synthesis of Cyclic CRPs

1. Introduction

Macrocyclic peptides can be synthesized by both the recombinant system using intein-splicing tool and chemical synthesis using ligation strategies. Each method has its merits over the others. Compared with recombinant synthesis, chemical synthesis has advantages in preparing peptides with unnatural amino acids, building blocks, tags or cargos, and site-specific modifications and particularly the C-terminal thioester functionality for Cys-thioester ligation. In addition, the cyclic CRPs of interest are about 30-residues, which can be more efficiently prepared by solid phase synthesis.

As introduced in chapter 1, Fmoc-compatible methods for thioester preparation are generally categorized into "safety-catch" linkers and "safety-switch" thioester surrogates. The existing approaches require complicated synthesis steps and hence there are still strong needs on more simple and practical methods for thioester preparation. I envisioned that a simple thioethylamido (TEA) moiety could fulfill the catalytic role of intein to mediate a series of N-S, S-S and S-N acyl shift reactions to ligate a thioester with a N-terminal Cys residue. Based on this hypothesis, I developed two novel TEA-based thioester surrogates MeCys and TEBA. The synthesis approach, mechanism, kinetic studies, applications on cyclic peptide preparations and limitations of these two new surrogates was studied and described in the sections below. For comparison, the recently reported "safety-catch" method using active azide was also applied to the preparation of cyclic CRPs.

ω-CTX MVIIA was chosen as a model for chemical synthesis of cyclic CRPs. Since both termini of MVIIA were Cys that constrained by disulfide linkages, additional linker peptides were added to join both ends together to afford a macrocyclic backbone. These linker peptides were designed based on computer modeling.

2. Preparation of cyclic CRPs using *N*-methylated cysteine (MeCys) thioester surrogate

2.1 Synthesis of MeCys-peptide on solid supports by Fmoc chemistry

The preparation of MeCys-resin commenced with coupling of a "spacer" residue Fmoc-Gly to Rink amide resins using DIC/HOBt reagents (**Figure 4-1**). Fmoc-MeCys(Trt) was coupled to deprotected α-amine of Gly by DIC/HOAt to give Fmoc-MeCys(Trt)-Gly-Rink amide resins **2**. A 6-residue peptide sequence Thr-Ile-Gly-Gly-Ile-Arg (TIGGIR) was coupled to the MeCys resin **2** and used as a model to study the optimal conditions of MeCys-mediated thioester formation. The C-terminal residue Fmoc-Arg(Pbf) was coupled manually using HATU/DIEA by double or triple coupling. This coupling reaction was monitored by acetaldehyde/chloranil that reacted with a secondary amine to give a green-blue color. The rest of peptide TIGGI was synthesized using PyBOP/HOBt. The completely synthesized peptide Thr(tBu)-Ile-Gly-Gly-Ile-Arg(Pbf)-MeCys(Trt)-Gly was then cleaved from the resin support by a TFA solution containing scavenger mixture of TFA/triisopropylsaline (TIS)/H_2O/thioanisole (88/5/5/2, *v/v*). Unprotected peptide products were precipitated in cold diethyl ether followed by purification through HPLC. Purified TIGGIR-MeCys-Gly-NH_2 **5** (cald. 788.9 Da, found 789.8 Da) was obtained with 56% isolated yield.
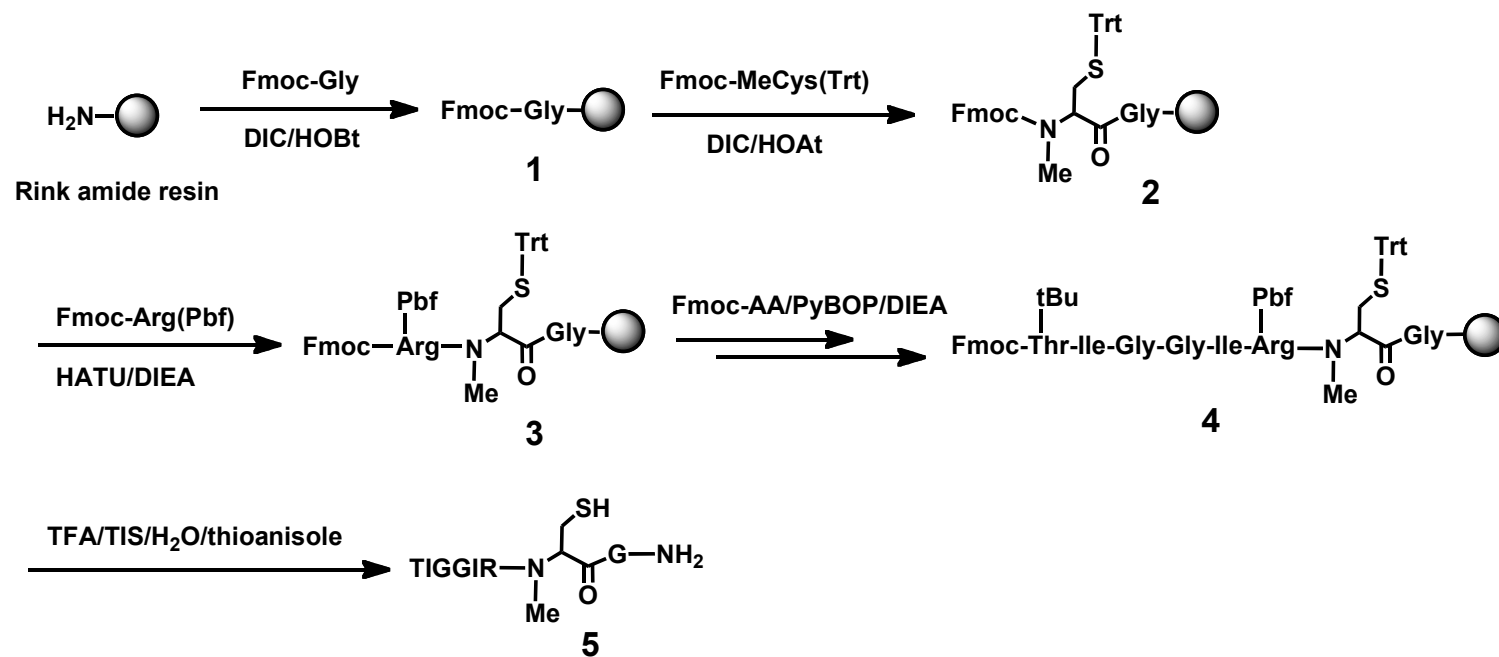
Figure 4-1. Scheme of TIGGIG-MeCys-Gly-NH₂ synthesis on Rink amide resins.

In the previous trial experiments, I found that Wang resins were not suitable for the MeCys thioester surrogate, since *N*-alkylated residue at C-terminus was known to cause a base-induced diketopiperazine (DKP) formation that resulted in deletion of dipeptide from the benzyl ester-type of peptide-resin linkage [257, 258]. When synthesizing TIGGIR-MeCys sequence directly on the Rink amide resin without a spacer Gly, another unexpected +51 Da side product was obtained that confirmed by tandem MS/MS as TIGGIR-MeAla(pip). This side reaction was previously reported by Lukszo, *et al* [259] as a base-catalyzed β-elimination on a C-terminal Cys(Trt) or Cys(Acm) followed by a Michael addition of piperidine to form 3-(1-piperidinyl)alanine. MeCys(Trt) was also susceptible to this side reaction and the side product was accumulated during each piperidine deprotection step in Fmoc solid-phase synthesis (**Figure 4-2**). Thus we initiated another trial experiment on peptide **5**. HPLC analysis showed that addition of a Gly spacer reduced the MeAla(Pip) side products from 30% to traceless (**Figure 4-3**). Therefore, we kept on using resin **2** for synthesis of MeCys peptides.
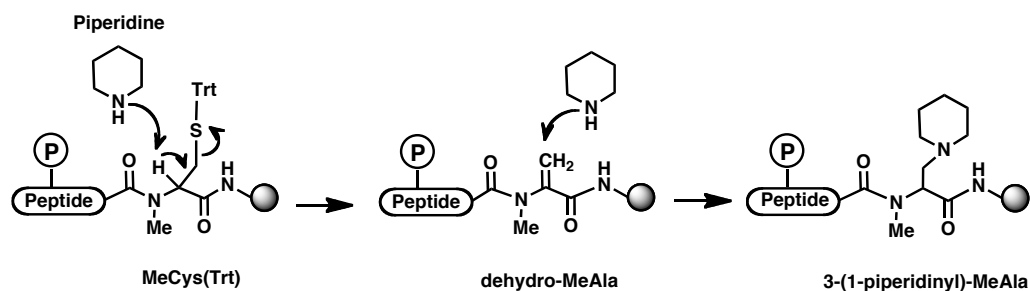
Figure 4-2. Schema of MeCys(Trt) β-elimination and piperidine addition to give a MeAla(Pip) side product.
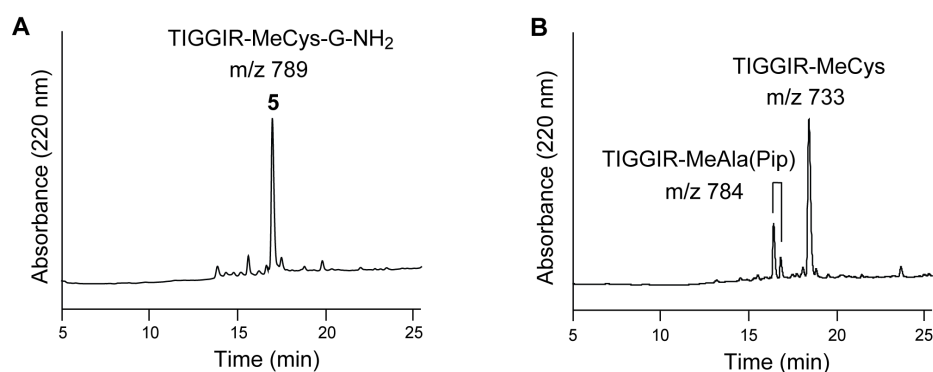
Figure 4-3. **Comparison of synthesis of MeCys peptides TIGGIR-MeCys-Gly-NH$_2$ and TIGGIR-MeCYs by analytical RP-HPLC**. (A) Synthesis check of TIGGIR-MeCys-Gly-NH$_2$ **5** (molecular weight 789 Da). (B) Synthesis check of TIGGIR-MeCys. Side products TIGGIR-MeAla(Pip) and its racemization product was about 30%. (HPLC condition: Aries column 4.6x250 mm, 3.6 u, gradient of 0-60% ACN (0.1% TFA) for 30 min, 1 ml/min).

2.2 MeCys-mediated N-S acyl shift and thioester formation

The N-S acyl shift reactions catalyzed by MeCys thioester surrogate was examined with 1 mM TIGGIR-MeCys-Gly-NH$_2$ **5** solution that prepared by a series of aqueous buffers with pH ranged from 0-7 (diluted HCl for pH 0-1, 0.1 M sodium phosphate buffer adjusted with 3 N HCl for pH 2-4, and 1 N NaOH for pH 5-7). Reaction was accelerated by heating at 40°C. The transformation of peptide amide (N-form) resulted in a TIGGIR-S-MeCys-Gly-NH$_2$ thioester **6** (S-form) (**Figure 4-4A**). Besides the acyl transfer reaction, deamidation product TIGGIR-S-MeCys-Gly-OH **7** (+1 Da) was observed in the acidic solutions (pH 0-1) (**Figure 4-4B**). The disulfide-homodimer **8** of peptide **5** (1576 Da) was accumulated in the neutral solution (pH 7) (**Figure 4-4C**).

The reversible MeCys-mediated N-S acyl shift reactions were monitored by RP-HPLC and all intermediates were characterized by MALDI-TOF. The HPLC traces taken at 24 h reflected the equilibrium state of N-form **5** and S-form **6** (**Figure 4-5A**). At acidic conditions (pH 0-2), the direction of N → S was favored and thus S-form was dominant. The deamidation side product **7** was observed at pH 0 and 1. This peptide was found to be the deamidated S-form TIGGIR-S-MeCys-Gly-OH, since it had strong UV absorbance at 260 nm that was contributed by a thioester bond. Therefore, both thioesters **6** and **7** were counted together to reflect the nucleophilic activity of MeCys thiol groups. At pH 3-6, the peptides remained in N-form. The plot in **Figure 4-5B** displayed a pH-dependent linear trend of MeCys-mediated N-S acyl shift. When the pH increased from 2 to 6, the ratio of thioesters over total peptide amount dropped from 60% to less than 1%. At pH 7, no S-form was observed and disulfide-homodimer **8** was accumulated. This part of results was not added into the plot, since disulfide formation block the thiols to act as nucleophiles in the acyl transfer reactions.
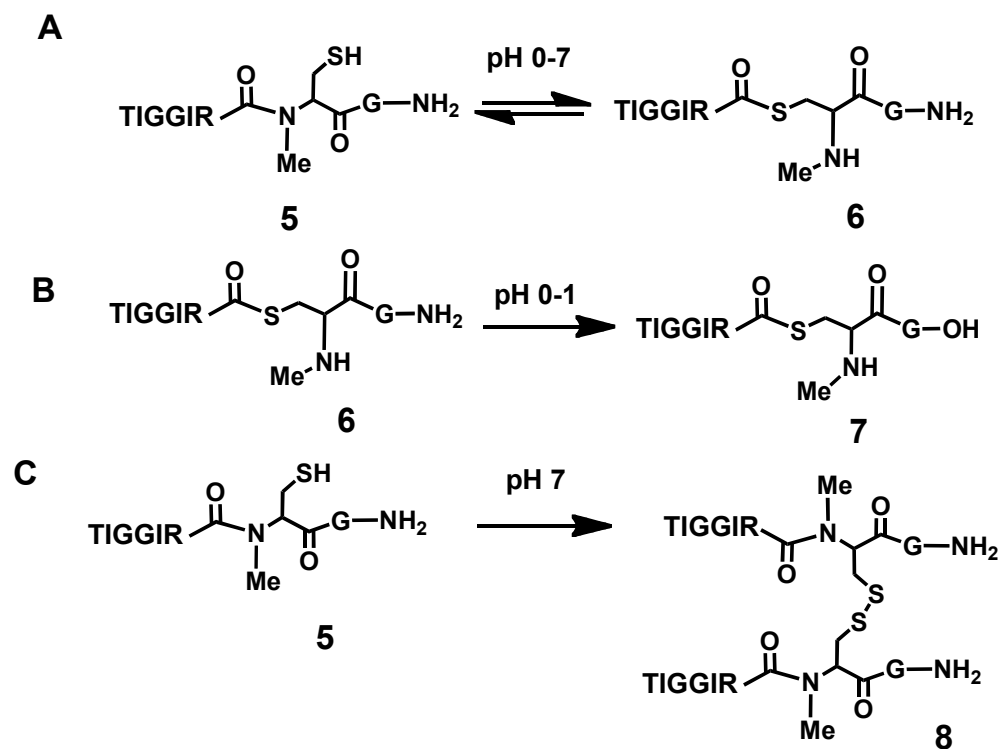
Figure 4-4. **Schemes of MeCys-mediated N-S acyl shift in pH 0-7 and side reactions.** (A) The reversible N-S acyl shift reaction converted TIGGIR-MeCys-Gly-NH₂ **5** to thioester (S-form) TIGGIR-S-MeCys-Gly-NH₂ **6**. (B) Deamidation of peptide **6** into **7** with C-terminal caroboxylic acid at pH 0-1. (C) Disulfide bond formation of two **5** at pH 8 resulted in homodimer **8**.
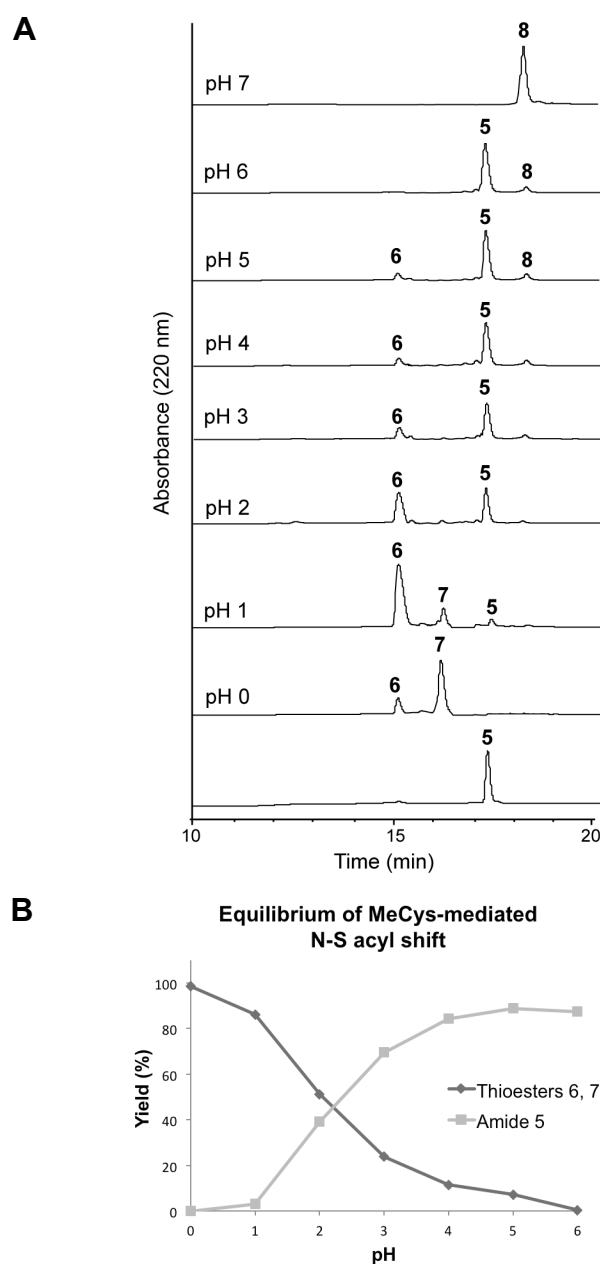
Figure 4-5. Equilibrium of MeCys-mediated N-S acyl shift of TIGGIR-MeCys-Gly-NH$_2$ 5 at 24 h. (A) HPLC traces of product distribution at equilibrium state for non-treated peptide **5** and under each pH condition. The bottom trace was purified peptide **5** (RT = 17.3 min). The S-form **6** result from N-S aycl shift was eluted earlier at 15.2 min. At pH 0-1, deamidated thioester **7** from S-form **6** was obserserved with retension time 16.3 min. At pH 5-7, peptide **5** homodimer by disulfide bond formation appeared that eluted at 18.1 min. (HPLC condition: C-18 column 4.6x250 mm, 3.6 u, gradient of 0-60% ACN (with 0.1% TFA) for 30 min, flow rate 1 ml/min). (B) Yield of N-form **5** and S-form **6, 7** at pH 0-6.

To trap the reversible S-form, external thiols sodium mercaptoethanesulfonate (MESNa, 50 equivalent) was added to the solution at the beginning of thioesterification, which reacted with S-form via S-S acyl shifts (i.e. transthioesterification) to give another TIGGIR-MES thioester **9** that was not able to go back to N-form (**Figure 4-6**). Thus, the equilibrium of N-S acyl shift reaction was shifted towards thioester formation by the addition of excessive external thiols. Reactions were examined at pH 1-7 at 40°C and monitored by analytical HPLC at different time course (**Figure 4-7A**). At low pH, N-S acyl shift was favored while S-S shift was slow. When pH increased, the rate of S-S acyl shift also increase, which rapidly converted S-form into stable thioester TIGGIR-MES **9** (calc. 740.3 Da, found 740.5 Da), while the N-S acyl shift was not favored. At pH 7, the disulfide-homodimer **8** was not observed due to the presence of excessive MESNa that had moderate reducing activity. However, thioesters were not stable at this pH and they gradually hydrolyzed to give side product TIGGIR-OH **10**. Taken together, the MeCys-mediated thioester formation via the tandem N-S, S-S acyl shifts against pH gave a bell-shape curve with the acme at pH 2 (**Figure 4-7B**). The plot of thioester formation against time showed that the MeCys-mediated thioester formation could be performed at a broad pH range (pH 2-5) with >80 % completion after 24 h (**Figure 4-7C**).
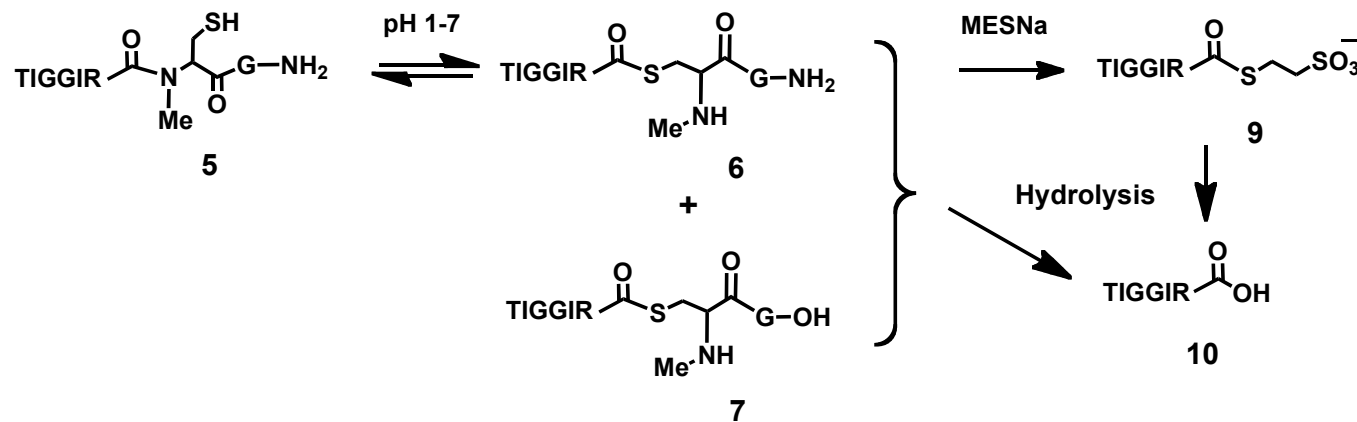
Figure 4-6. **Scheme of tandem N-S, S-S acyl transfer to prepare stable thioester TIGGIR-MES 9.** A side product TIGGIR-OH **10** was resulted from thioester hydrolysis.
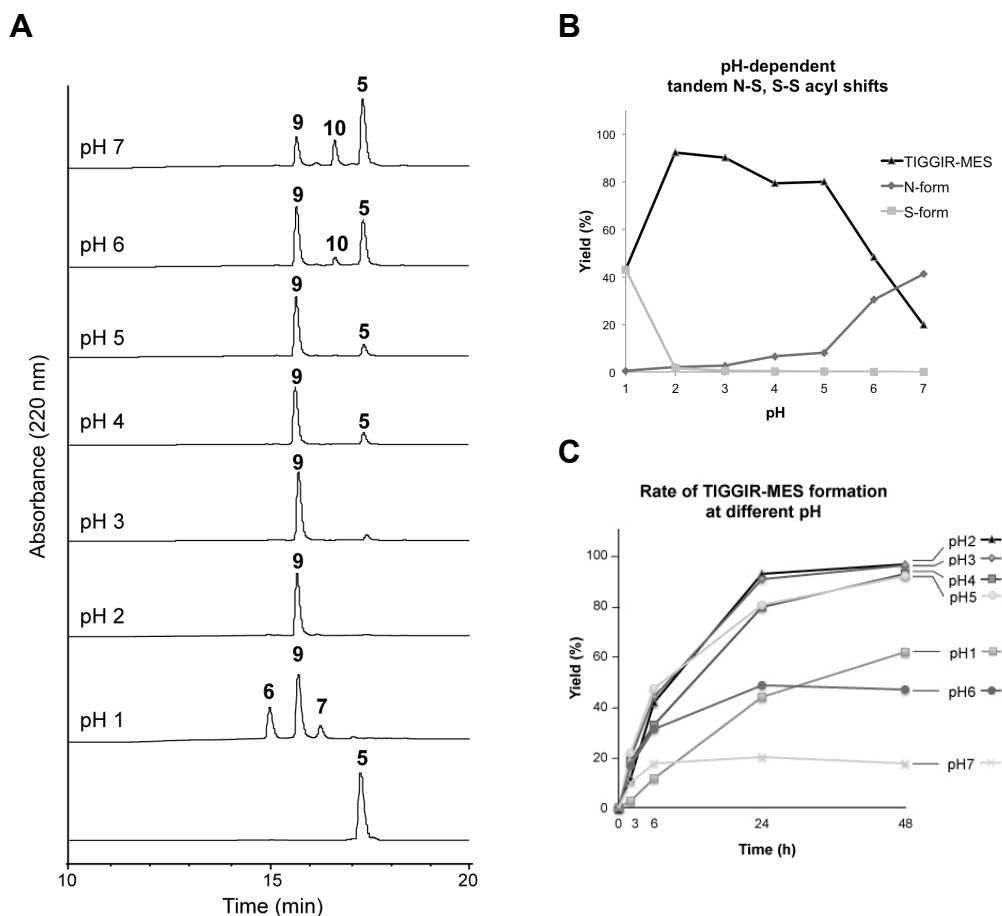
Figure 4-7. **Formation of TIGGIR-MES thioester 9 by Tandem N-S, S-S acyl shift of TIGGIR-MeCys-Gly-NH₂ 5 at different pH.** (A) HPLC traces of product distribution at 24 h for non-treated peptide **5** and under each pH condition. The bottom trace was purified peptide **5** (RT = 17.1 min). The desired stable thioester **9** was eluted at 15.8 min. At pH 1, S-form **6**, deamidated thioester **7** and MES thioester **9** were obtained. At pH 6 and 7, hydolysis product TIGGIR-OH **10** was observed with RT = 16.8 min (HPLC condition: C-18 column 4.6x250 mm, 3.6 u, gradient of 0-60% ACN (with 0.1% TFA) for 30 min, flow rate 1 ml/min). (B) Ratio of starting material **5**, S-form **6** and TIGGIR-MES thioester **9,** at different pH after 24 h reaction. (C) Rate of TIGGIR-MES thioester **9** formation at pH 1-7. The yield of TIGGIR-MES was recorded at 3 h, 6 h, 24 h and 48 h.

2.3 Cys-thioester ligation mediated by MeCys thioester surrogate

The stable thioester TIGGIR-MES **9** was subjected to Cys-thioester ligation with another model peptide Cys-Ala-Leu-Val-Ile-Asn **11** (CALVIN) prepared on Wang resin using Fmoc chemistry (**Figure 4-8A**). The ligation reaction was performed with 1 mM **9** and 2 mM **11** at 40°C in a sodium phosphate buffer (0.1 M, pH 7.6) with 6 M guanidine-HCl, 50 mM external thiol methyl mercaptoacetate (MMA) and 10 mM TCEP (**Figure 4-8B**). HPLC profiles showed that in the presence of excessive MMA, TIGGIR-MES **9** was rapidly converted into TIGGIR-MMA thioester **9'** by S-S exchange. Both **9** and **9'** thioesters participated in ligation reaction with **11** to give a stable ligation product TIGGIR-CALVIN **12**. The ligation reaction was completed after 4 h at room temperature (**Figure 4-8C**).
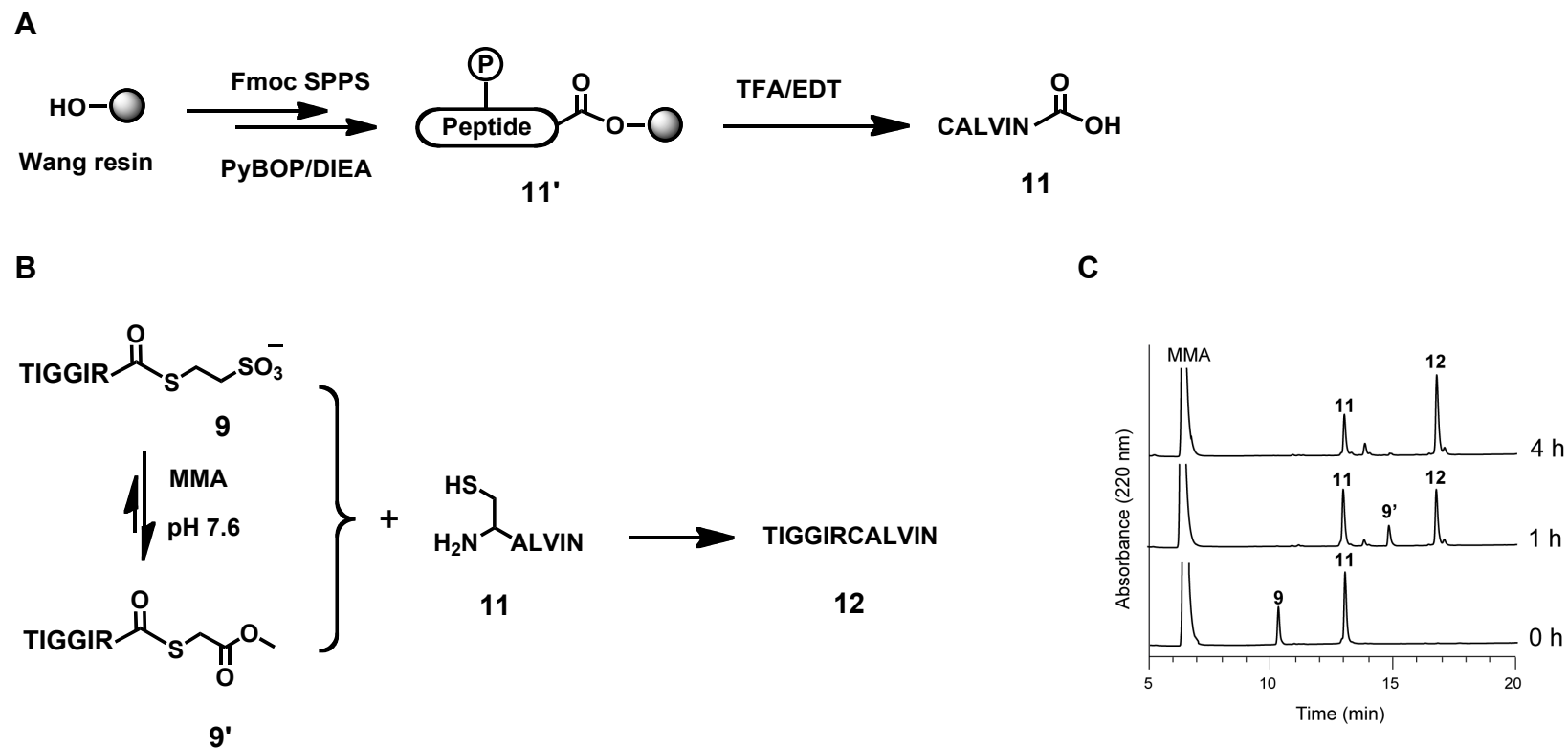
Figure 4-8. **Cys-thioester ligation of TIGGIR-MES 9 and CALVIN 11 to form TIGGIRCALVIN 12.** (A) Synthesis scheme of model peptide CALVIN. (B) Scheme of the Cys-thioester ligation reaction. (C) HPLC traces at starting, 1 h and 4 h. (HPLC condition: C-18 column 4.6x250 mm, 3.6 u, gradient of 10-80% ACN (with 0.1% TFA) for 35 min, flow rate 1 ml/min).

2.4 Preparation of cyclic *ω*-conotoxin using MeCys thioester surrogate

Based on computer modeling, a 4-residue spacer was able to incorporate into the N- and C-terminus of *ω*-CTX MVIIA to confer a macrocyclic backbone. Thus we designed a cyclic analog of MVIIA, cyclic MVIIA-GGPG (cCG29) by adding a flexible 4-residue-linker GGPG at the C-terminus. The choice of a Gly-rich linker as a spacer facilitated its end-to-end cyclization at Gly. The proline ring enhanced backbone turning (**Figure 4-9**). The unprotected linear CG29 precursor with a C-terminal MeCys thioester surrogate (CKGKGAKCSRLMYDCCTGSCRSGKCGGPG-MeC-G-NH$_2$) was prepared using Fmoc chemistry (**Figure 4-10**). The C-terminal Gly of CG29 sequence was coupled to the hindered secondary amine of MeCys(Trt) on resin **2** using coupling reagent HATU/DIEA with repeated couplings to afford Fmoc-Gly-MeCys(Trt)-Gly-Rink amide resin **13**. The remaining sequence of CG29 was coupled to resin **13** by a stepwise Fmoc solid-phase synthesis using PyBOP/DIEA in a microwave-assisted peptide synthesizer to give CG29-MeCys(Trt)-Gly-Rink amide resin **14**. The unprotected peptide CG29-MeCys-Gly-NH$_2$ **15** (calc. 3087.6 Da, found 3088.5 Da) was removed from resin **14** by treating with TFA/TIS/H$_2$O (95/2.5/2.5, *v/v*) for 2 h to give 21% isolated yield after HPLC purification and lyophilization.
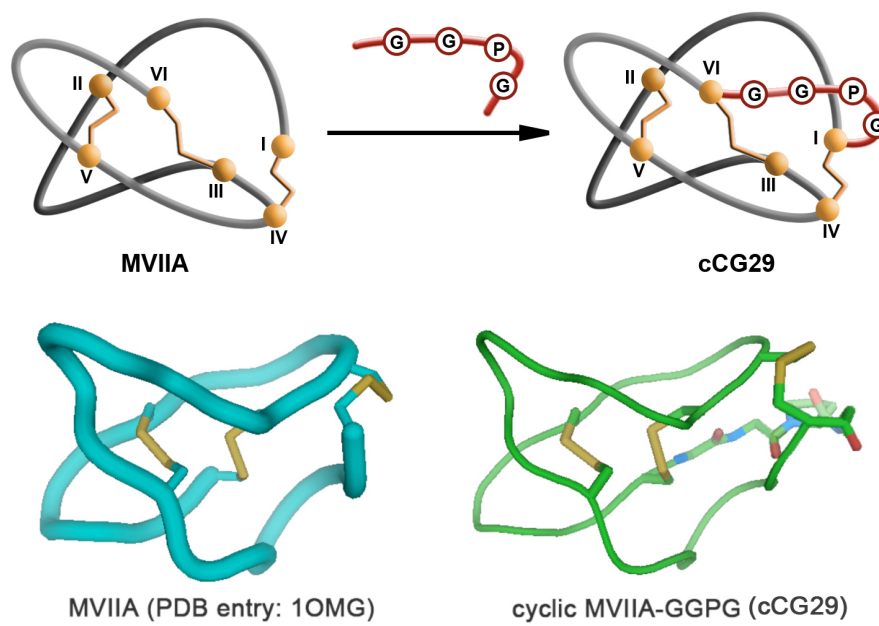
Figure 4-9. Dynamic modeling structure of cCG29 based on the NMR structure of MVIIA.
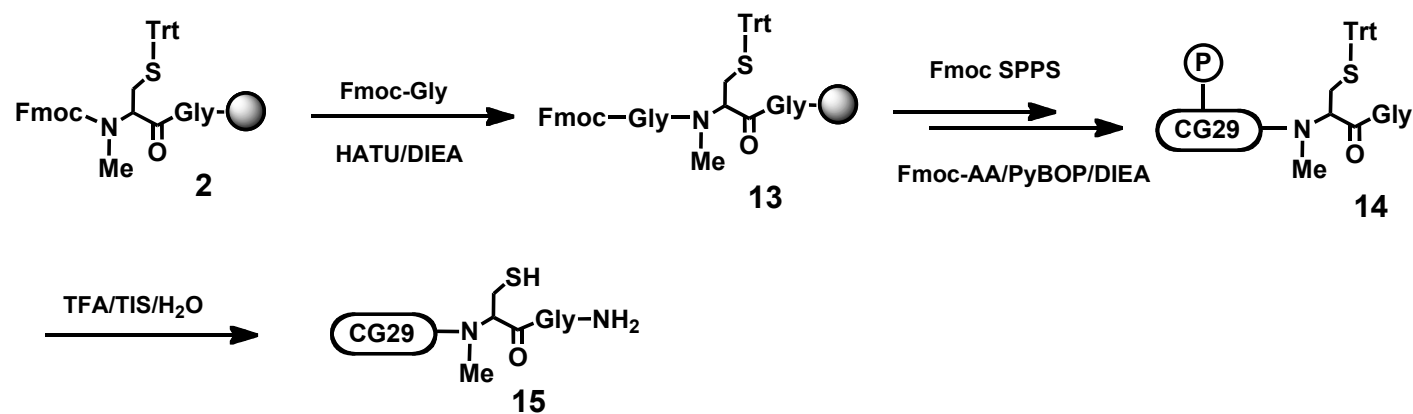
Figure 4-10. **Scheme of CG29-MeCys-Gly-NH$_2$ 15 on Fmoc-MeCys-Gly-Rink amide resin 2.**

The acid-catalyzed N-S acyl shift of CG29-MeCys-Gly-NH$_2$ **15** to give its thioester intermediate **16** was performed in an aqueous solution at pH 2 (**Figure 4-11 A**). In the absence of an external thiol, we found that the internal thiols of CG29 spontaneously underwent a series of S-S acyl shift reactions to form CG29 thiolactones **18 (i-vi)**. For example, after treating CG29-MeCys-Gly-NH$_2$ **15** in a pH 2 solution at 40°C for 24 h, we isolated five out of six expected thiolactone isomers **18 (i-vi)** by RP-HPLC (**Figure 4-11C**). The thiolactones **18 (i-vi)** gave m/z 2896.4 in MALDI-TOF mass spectrometry and have the same molecular weight of cyclic cCG29 **19**. These thiolactones could be distinguished from the cyclic peptide **19** by monitoring at wavelength 260 nm in HPLC traces due to the strong absorbance at 260 nm of thioesters and thiolactones. Observation of thiolactone formation as a result of S-S acyl shift reactions indicated that side-chain thiols actively participated in transthioesterification. Thus we expected that cysteine-rich peptides, such as CG29 containing six cysteines, were able to cyclize without addition of external thiols. The series of thiolactones **18 (i-vi)** with different ring sizes were exchangeable and collectively act as the starting materials for the subsequent end-to-end backbone cyclization reaction. This cyclization reaction was performed at pH 7.5 buffered by 0.1 M phosphate buffer for 2 h at room temperature in 86% yield. The S-S exchange reactions were favored under pH 7.5 to permit the expansion of thiolactone rings as an end-to-end thiolactone formed by the N- and C-termini, and which led to a proximity-driven S-N acyl shift to form a backbone amide of the desired macrocycle.

In the presence of an external thiol, a stable thioester was obtained from the peptide precursor CG29-MeCys-Gly-NH$_2$ **15**. The reaction was performed in a pH 2 solution at 40°C using an excessive amount of an external thiol (50 eq. MESNa). HPLC profile after 24 h treatment showed two thioesters CG29-MES **17** (76%), MeCys thioester **16** (5%) and one thiolactone CG29 **18-vi** (4%) (**Figure 4-11D**). Compared with the N-S, S-S acyl shift reactions performed without an external thiol, the HPLC traces were simplified by the addition of excessive MESNa to give CG29-MES **17** as the most abundant thioester product. The thiolactone **18-vi** with the retention time (RT) at 43.6 min was closest to the RT of cyclic CG29 **19** at 43.9 min and we speculated that it could

be the end-to-end thiolactone, which was conformationally similar with the end-to-end cyclic CG29. The thia-zip cyclization was performed at pH 7.5 for 2 h at room temperature. The cyclic CG29 **19** was transformed from **16**, **17** and **18-vi** via S-S and S-N tandem acyl shift reactions to the desired cyclic CG29 **19** (**Figure 4-11E**). Increasing the reaction temperature could accelerate the thioesterification of CG29. In the trial experiments, thioesterification of CG29 completed within 16 h at 50°C, and this time was shortened to 8 h at 65°C. However, the rate of side reaction was also increased. More than 10% thioester/thiolactone intermediates were hydrolyzed at 65°C.

From synthetic peptide precursor with thioester surrogate to end-to-end cyclized peptide product, the MeCys-mediated cyclization of cysteine-rich peptide resembled the mechanism of intein-mediated protein splicing. And only single purification step by RP-HPLC was required after completion of cyclization. Thus this method could afford a good yield in preparation of circular proteins such as cCG29.

The oxidative folding of cyclic CG29 **19** was conducted based on folding condition of MVIIA, by using a highly diluted peptide solution (10 μM) in 0.1 M ammonium phosphate buffer (pH 7.8) containing 2 M ammonium sulfonate and oxidized/reduced glutathione (GSSG/GSH = 10/100 eq) at 4°C for 72 h. Unfortunately, the correctly folded cCG29 **20** ([M+H] = 2891 Da) gave a very low yield as shown in **Figure 4-11F**. The isolated yield of 3*SS* cCG29 was <1% (0.35 mg lyophilized cCG29 from 123 mg crude CG29-MeCys-Gly-NH$_2$ precipitant after TFA cleavage).
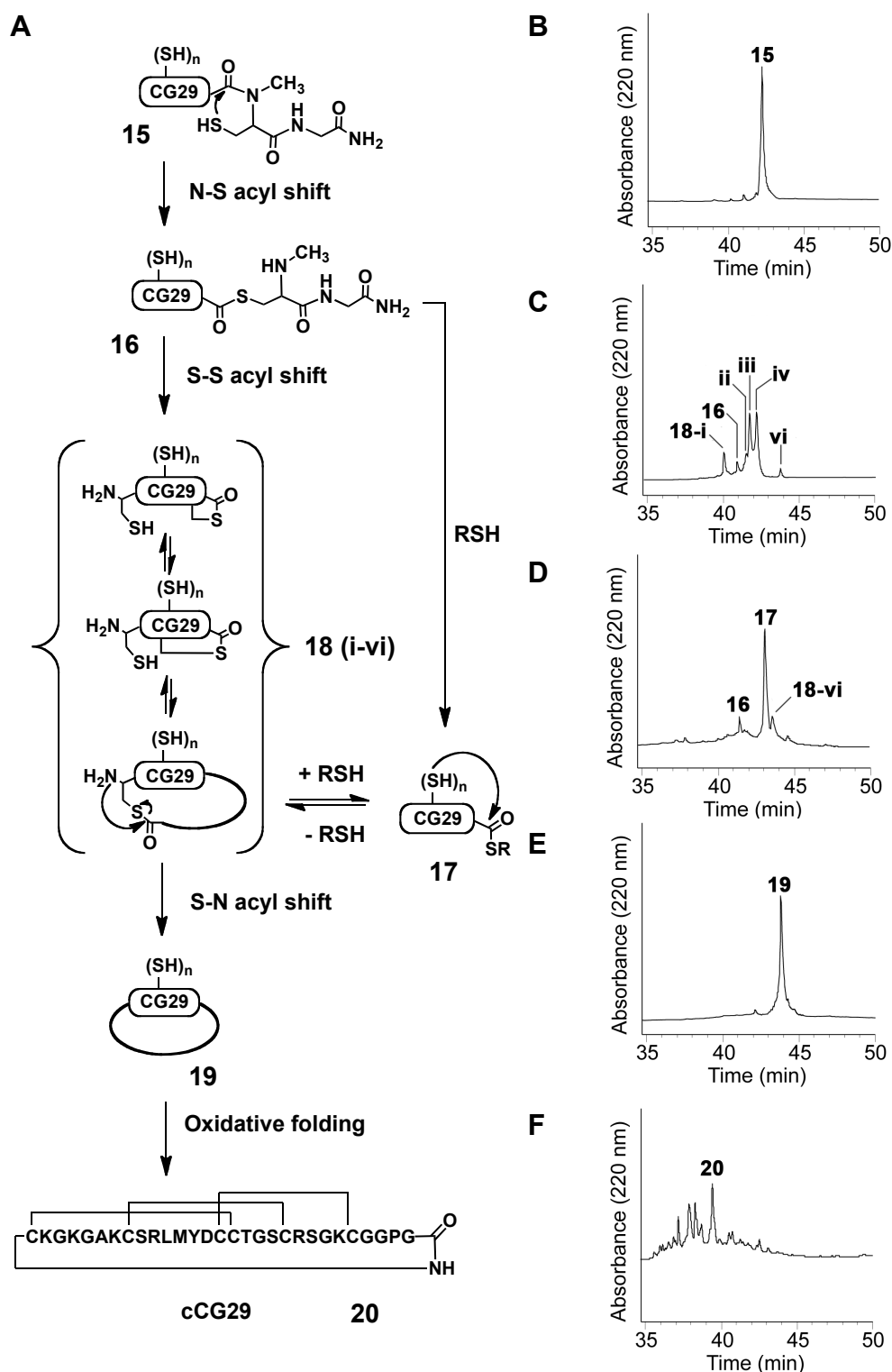
Figure 4-11. **Schema and HPLC analysis of CG29-MeCys-Gly-NH$_2$ 15 cyclization**. (A) Scheme of CG29-MeCys-Gly-NH$_2$ cyclization via tandem thiol switch reactions mediated by intramolecular thiols or external thiols. (B) HPLC trace of **15** (RT = 42.4 min). (C) The first N-S acyl shift of CG29-MeCys-Gly-NH$_2$ **15** in pH 2 solution resulted in thioester **16** that was trapped by internal thiols to give intramolecular thiolactones **18 (i-vi)** after 36 h. (D) In the presence of external thiol MESNa, **16** and

18 (i-vi) underwent transthioesterification into thioester CG29-MES **17** for 24 h reaction at 40°C. (E) Thia zip cyclization was performed at pH 7.5 at room temperature for 2 h to give cyclic CG29 **19.** (F) Oxidative folding of purified cyclic CG29 **19** to give a folding mixture containing native folded cCG29 **20** (RT = 39.3 min). (HPLC condition: C-18 column 4.6x250 mm, 3.6 u, gradient of 0-40% ACN (with 0.1% TFA) for 80 min, flow rate 1 mL/min).

The disulfide connectivity was determined by partial reduction and S-alkylation, followed by enzyme digestion and MS analysis. Purified cCG29 **20** (0.2 mg) was reduced by 10 mM TCEP for 30 min at room temperature followed and 40 mM *N*-ethylmaleimide (NEM) was added into the solution to alkylate the reduced Cys for another 1 h. The alkylated product mixture was isolated by RP-HPLC (**Figure 4-12A**). The 2SS+2NEM species **P1**, **P2** ([M+H] = 3140 Da) were subjected to a complete reduction by 10 mM DTT for 1 h followed by completed alkylation using 50 mM iodoacetamide (IAM) to give two 2NEM+4IAM species **S1**, **S2** ([M+H] = 3372 Da). After HPLC purification, these two 2NEM+4IAM species were subjected to trypsin and chymotrypsin digestion, to give fragments LMYDCCTGSCR (1NEM+2IAM, [M+H] = 1492 Da) and DCCTGSCRSGKCGGPGCKGKGAKCSRLMY (2NEM+4IAM, [M+H] = 3390 Da) with corresponding S-alkylation groups, respectively. MS/MS analysis showed that the trypsin-digestion fragment of S1 contained C15(IAM), C16(IAM) and C20(NEM) and the chymotrypsin-digestion fragment of S1 contained C25(IAM), C1(IAM) and C8(NEM), which confirmed the first disulfide bond C8-C20 (**Figure 4-12B**). The enzyme digestion fragments of S2 showed C15(IAM), C16(NEM), C20(IAM), C25(IAM), C1(NEM) and C8(IAM), which confirmed the disulfide bond C1-C16 (**Figure 4-12C**). Thus the rest 2*SS* species P3 would be C15-C25 reduced and NEM-alkylated and native disulfide connection of cCG29 **20** was confirmed. The ratio of P1/P2/P3 reductant products also indicated that disulfide bond C1-C16 had the highest accessibility by reducing reagents (such as TCEP) among three disulfide bonds and C15-C16 was the least accessible one.

A
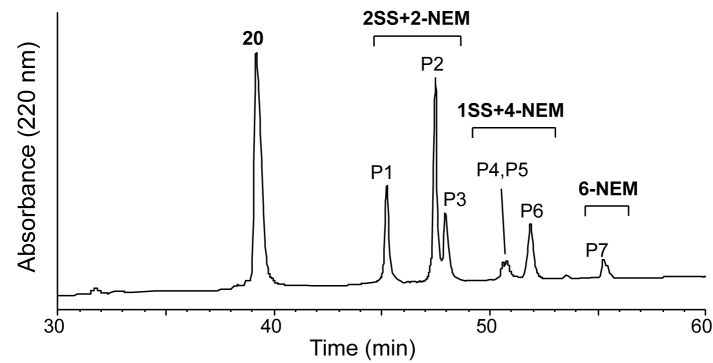
B

S1 trypsin digestion fragment (1492 Da)

S1 chymotrypsin digestion fragment (3390 Da)
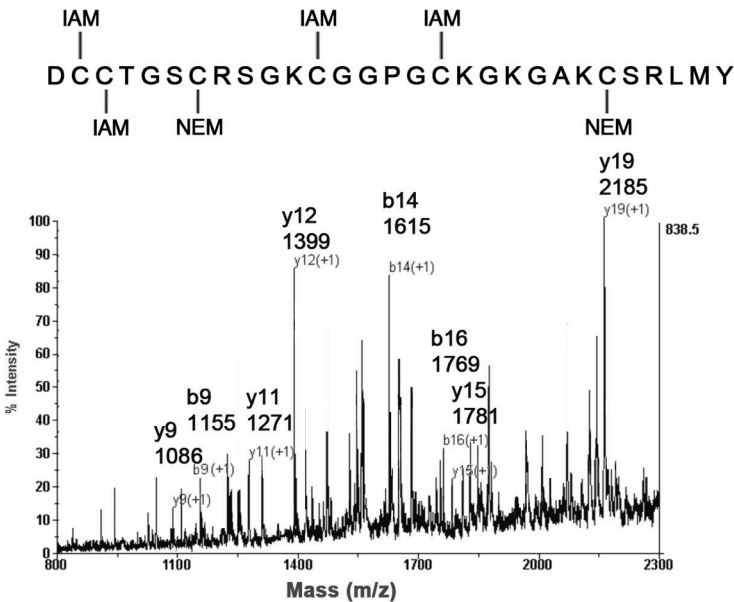
C

S2 trypsin digestion fragment (1492 Da)

IAM
|
L M Y D C C T G S C R
| |
NEM   IAM

y1 175
y2 335
y3 422
b4 523
b5 701
y7 970
y8 1084
y9 1248

4.3E+4

% Intensity

Mass (m/z)

S2 chymotrypsin digestion fragment (3390 Da)

IAM   IAM   IAM
| | |
D C C T G S C R S G K C G G P G C K G K G A K C S R L M Y
| | |
NEM IAM   NEM

b9 1155
y11 1271
y12 1332
y13 1560
b14 1615
y15 1782
b16 1769
y18 2057
y19 2185

995.6

% Intensity

Mass (m/z)
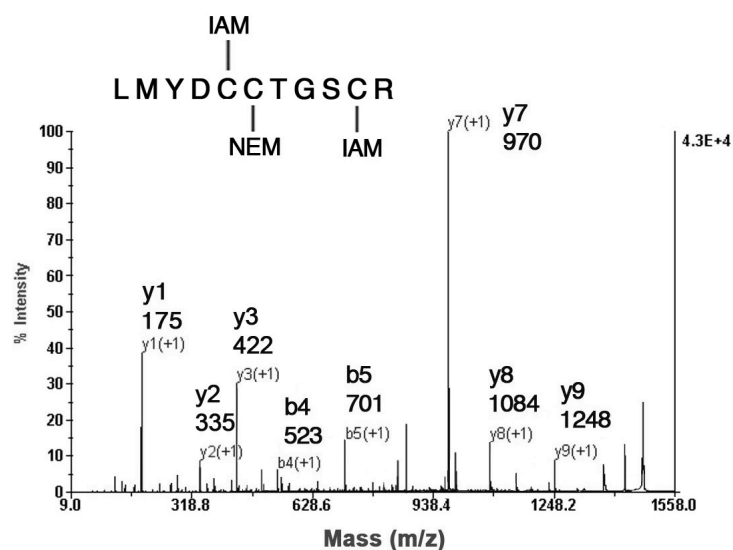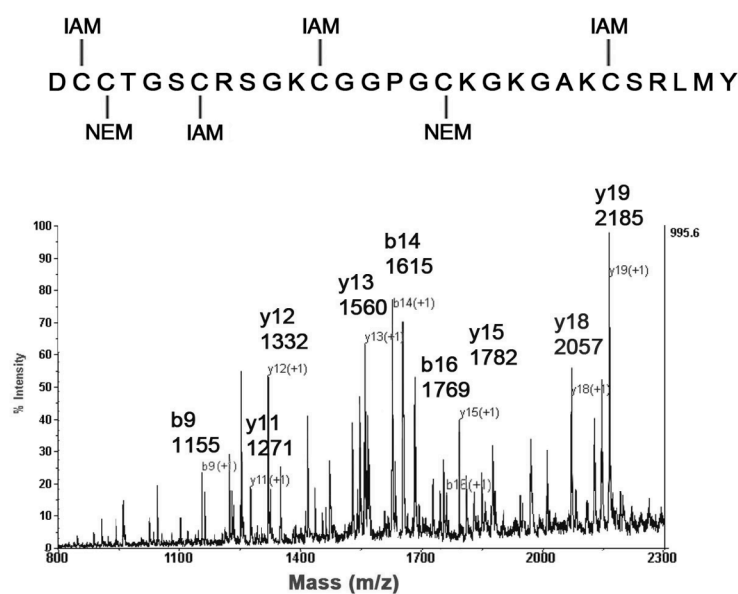
Figure 4-12. **Disulfide connectivity determination of cCG29 20 by partial reduction and S-alkylation.** (A) HPLC traces of partially reduced cCG29 with NEM alkylation. The 2SS+2NEM species P1, P2 were labeled. (B) Enzyme digestion and MS/MS analysis of alkylated peptide S1 confirmed C8-C20 disulfide bond. (C) Enzyme digestion and MS/MS analysis of alkylated peptide S1 confirmed C1-C16 disulfide bond.

3. Preparation of cyclic CRPs using thioethylbutylamido (TEBA) thioester surrogate

3.1 Synthesis of peptide-TEBA on solid supports by Fmoc chemistry

Compared with MeCys surrogate and TMT surrogate, The TEXA thioester surrogates (X stands for the *N*-alkylation group) were simplified by removing the C-terminal carboxylic acid (**Figure 4-13**). This modification prevented side reactions such as β-elimination of MeCys followed by piperidine addition to give a MeAla(Pip). The synthesis of TEXA resin was simple and practical by attaching a commercial-available starting material 2-butylamino(ethanethiol) to Cl-Trt(2-Cl) resins to give TEBA-Trt resin. During peptide elongation, the S-Trt-resin linkage protected the thiol on the TEBA group.

The TEBA linker was attached to Cl-Trt(2-Cl) resins efficiently in solvent dichloromethane (DCM). To improve the coupling efficiency of amino acids on the TEBA resins, the Cl-Trt(2-Cl) resin with high-substitution 1.14 mmol/g was converted into TEBA-Trt resin **22** with moderate substitution 0.3-0.4 mmol/g. This step was achieved by adding only 0.8 mmol TEBA to 1 g Cl-Trt(2-Cl) resin that swelled in DCM. The substitution reaction was quenched after 30 min shaking at room temperature. The reactive Cl remained on the resin were rapidly removed by methanol and excess of DIEA, where the Cl-Trt(2-Cl) was transformed into corresponding methyl ether [260].

A model peptide TIGGIR-TEBA **25** was synthesized using TEBA-resin **22** (**Figure 4-14**). After coupling of C-terminal Fmoc-Arg(Pbf) to resin **22** using HATU/DIEA coupling reagents, the accurate substitution was calculated by the increment of dry weight from resin **22** to resin **23.** The remained peptide sequence was coupled to Fmoc-deprotected resin **23** stepwisely using PyBOP/DIEA. Final product TIGGIR-TEBA **25** (calc. 729.7 Da, found 730.4 Da) was cleaved from peptide-resin **24** using TFA/TIS/H$_2$O (90/5/5, *v/v*) for 2 h.

TEA-mediated thioester formation

Figure 4-13. Mechanism of thioethylamido(TEA)-mediated thioester formation and examples of TEA thioester surrogates MeCys, TMT and TEXA. TEA moiety was highlighted in red.
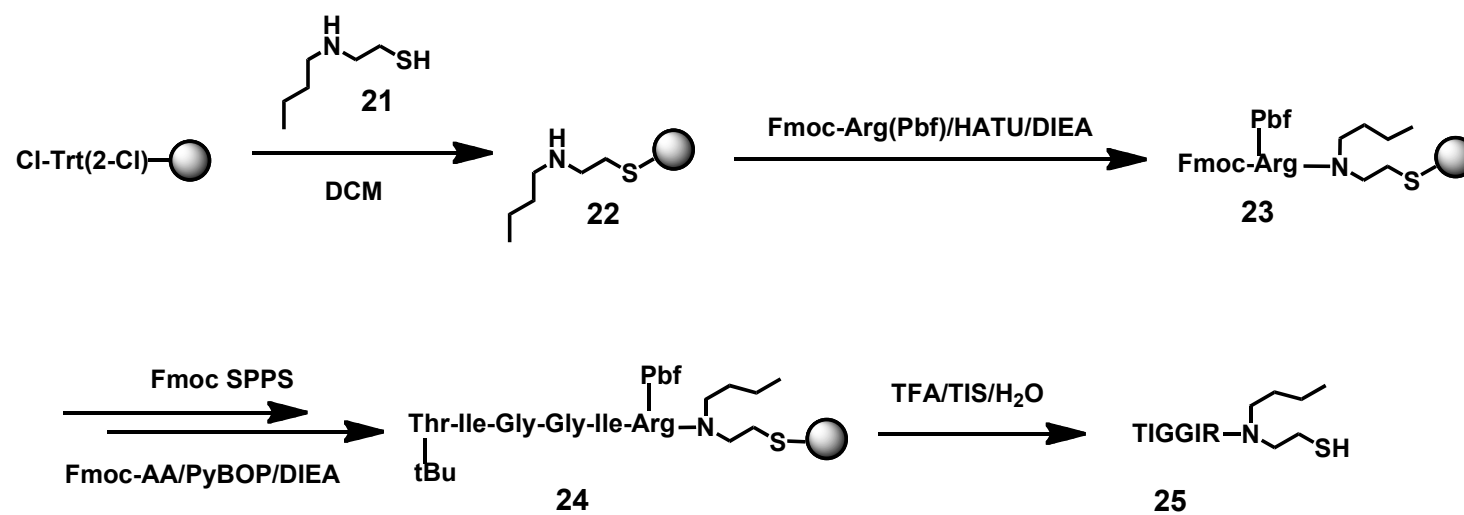
Figure 4-14. **Synthesis scheme of TIGGIR-TEBA 25 on Cl-Trt(2-Cl) resins**.

3.2 TEBA-mediated N-S acyl shift and thioester formation

During TFA cleavage and purification using RP-HPLC with acidic mobile phase, TIGGIR-TEBA **25** was gradually converted into TIGGIR-S-TEBA **26** by TEBA-mediated N-S acyl shift. Therefore, the optimized condition for TEBA-mediated N-S acyl shift reaction followed by a transthioesterification reaction to prepare stable thioesters was studied in different pH buffers using a mixture of **25** and **26** (7:3) as the starting material. The stable TIGGIR-MES thioester **9** was obtained from tandem acyl transfer with 50 equivalent MESNa (**Figure 4-15A**). The reaction was performed at 40°C for up to 48 h. HPLC monitoring was performed at various time points. TEBA-mediated tandem thiol shifts were performed in seven conditions with pH ranged from 1 to 7 (**Figure 4-15B**). Similar as MeCys, the equilibrium of TEBA-mediated N-S acyl shift reaction was pH-dependent. The optimal condition of TEBA-mediated tandem thiol shifts was at pH 3 (**Figure 4-15C**). The reaction could be performed in the pH ranged from 2 to 5 (**Figure 4-15D**).

Overall, both TEBA and MeCys thioester surrogates mediated tandem thiol switch reaction by the same mechanism with a similar pH-dependent trend (**Figure 4-16A**). TEBA thioester surrogate was more reactive than MeCys in the tandem acyl shift, as in their optimal conditions, the conversion of TIGGIR-TEBA to thioester TIGGIR-MES **9** was completed within 18.5 h, which was faster than MeCys-mediated tandem reactions that took 24 h to complete (**Figure 4-16B**).
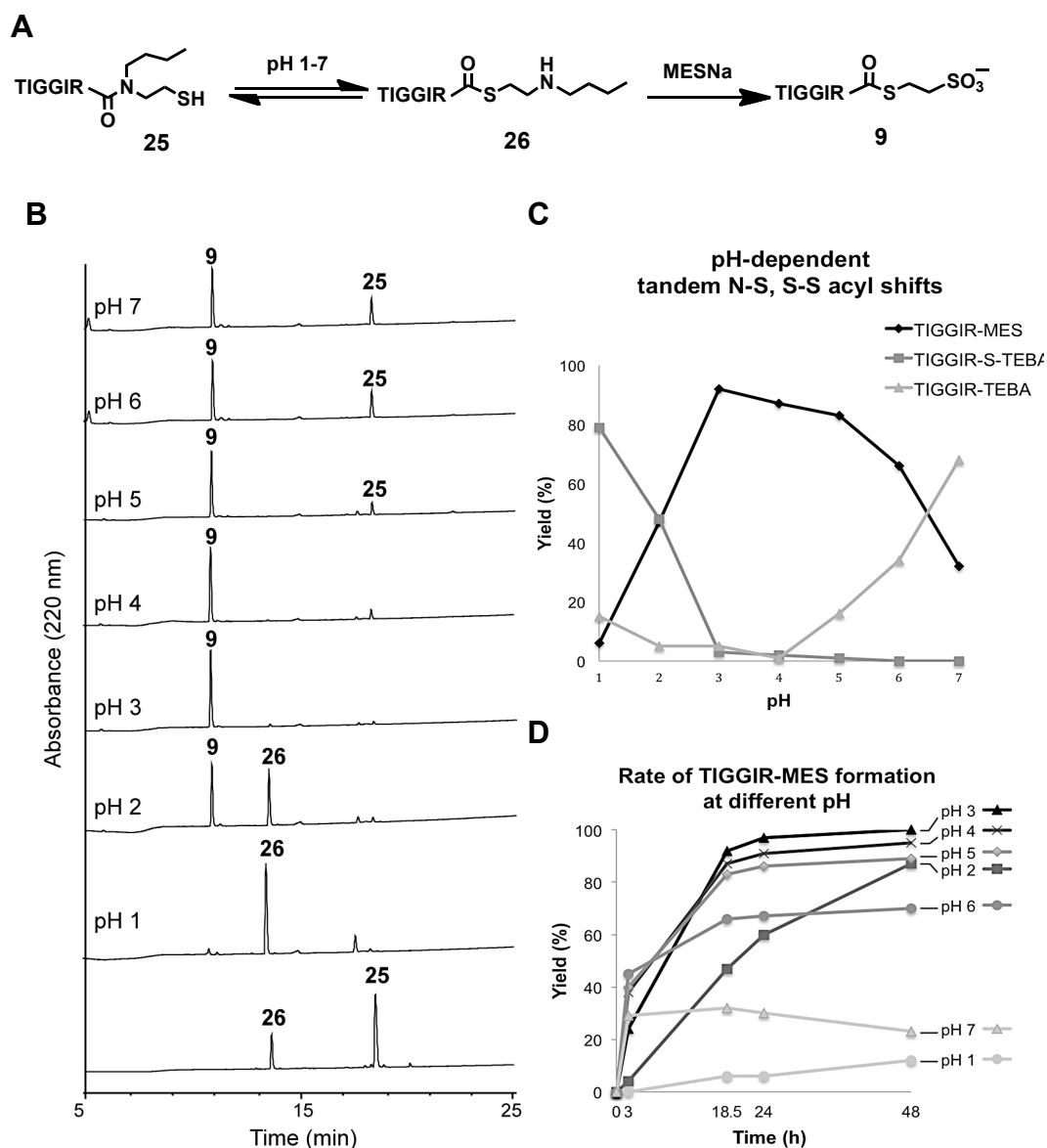
Figure 4-15. Formation of TIGGIR-MES thioester 9 by Tandem N-S, S-S acyl shift of TIGGIR-TEBA 25 at different pH. (A) Scheme of tandem N-S, S-S acyl shift reactions to prepare thioester TIGGIR-MES **9** from TIGGIR-TEBA **25**. (B) HPLC traces of product distribution at 18.5 h for non-treated peptide **25/26** and under each pH condition. The bottom trace was purified TIGGIR-TEBA **25** (RT = 18.3 min) with its S-form **26** (RT = 13.5 min). The desired product TIGGIR-MES **9** was eluted at 10.6 min. (HPLC condition: C-18 column 4.6x250 mm, 3.6 u, gradient of 0-60% ACN (with 0.1% TFA) for 30 min, flow rate 1 ml/min, 60°C column heating). (C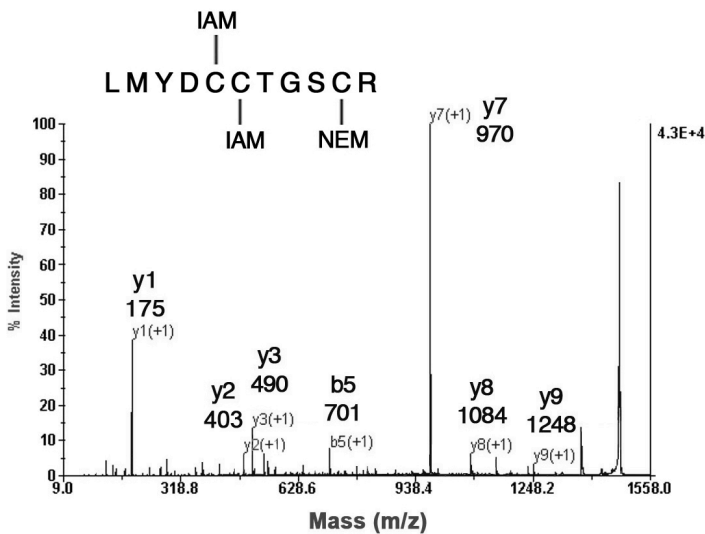) Ratio of starting material **5**, S-form **6** and TIGGIR-MES thioester **9,** at different pH after 24 h reaction. (D) Rate of of TIGGIR-MES thioester **9** formation at pH 1-7. The yield of TIGGIR-MES was recorded at 3 h, 18.5 h, 24 h and 48 h.

A
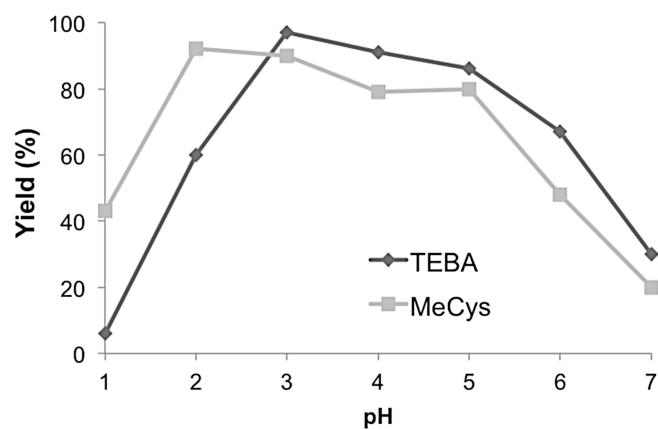
B
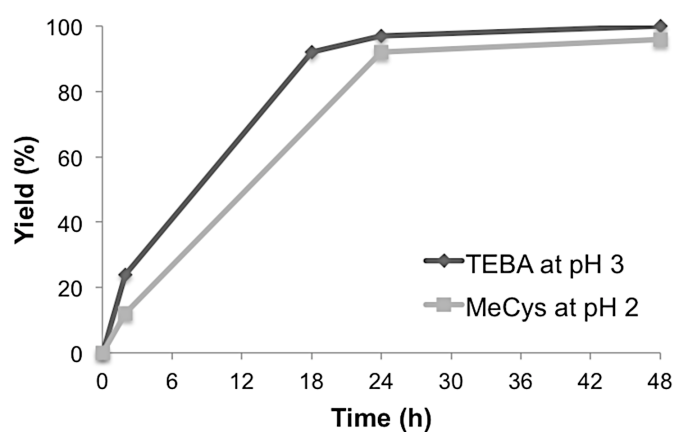
Figure 4-16. Comparison of TEBA and MeCys thioester surrogates. (A) The pH-dependent tandem thiol shift reactions mediated by two TEA-type thioester surrogates. (B) Comparison of reaction rate of TEBA at its optimal pH 3 and MeCys at its optimal pH 2.

3.3 Preparation of Cyclic *ω*-Conotoxin using TEBA thioester surrogate

Based on computer modeling, three cyclic MVIIA analogs with two disulfide bonds were designed. The linker between two termini was a simple dipeptide Gly-Ser. These 2*SS* cyclic MVIIA analogs were named as cM1B (C8-C20, C15-C25), cM2B (C1-C16, C15-C25) and cM3B (C1-C16, C8-C20), of which two native disulfide bonds were retained and the third pair of cysteine residues was replaced by aminobutyric acid (Abu, B) (**Figure 4-17**).

The linear precursors of these three cyclic analogs were synthesized on TEBA-resin **22** using Fmoc chemistry (**Figure 4-18**). M1B-TEBA (CGS<u>B</u>KGK GAKCSRLMYDCBTGSCRSGK-TEBA) and M2B-TEBA (CGS<u>C</u>KGKGAKB SRLMYDCCTGSBRSGK-TEBA) were started with K24 as the C-terminal residue and C25 as the N-terminus. M3B-TEBA (CSRLMYDBCTGSCRSGK BGS<u>C</u>KGKGAK-TEBA) was started with K7 as the C-terminus and ended with C8. The resin substitution of Fmoc-Lys(Boc)-TEBA resins **27** was calculated by dry weight to give a substitution of 0.33 mmol/g. Started with 0.1 mmol resins **27** (300 mg), linear peptide sequences were coupled using microwave-assisted SPPS machine by PyBOP/DIEA. After synthesis, peptides were deprotected and cleaved form resin supports using TFA/TIS/H_2O/ thioanisole (88/5/5/2, *v/v*) cleavage solution for 2 h followed by diethyl ether precipitation. For linear peptide precursor M1B-TEBA **29a** (calc. 2868.5 Da, found 2870.0 Da), M2B-TEBA **29b** (calc. 2868.5 Da, found 2869.3 Da), M3B-TEBA **29c** (calc. 2868.5 Da, found 2869.6 Da), the crude precipitants were 194 mg, 188 mg and 207 mg, respectively. The HPLC-purified peptide-TEBA precursors (**29a-c)** were obtained with 16-22% isolated yield.
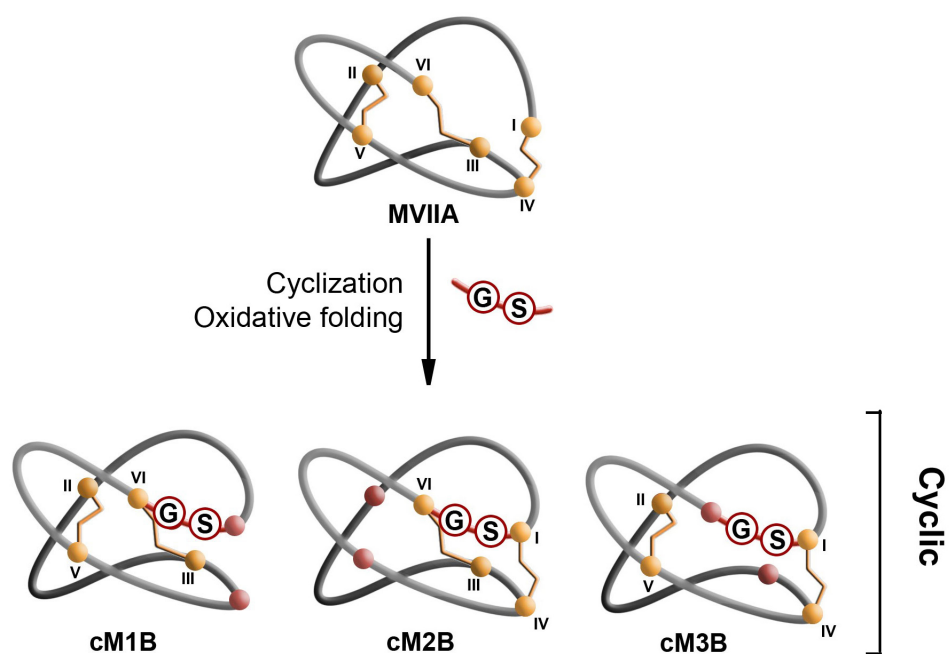
Figure 4-17. **Scheme of two-disulfide cyclic analogs of ω-conotoxin MVIIA cM(1-3)B**. For each cyclic analog, the N- and C-termini were joined using a Gly-Ser linker and two pairs of Cys residues (orange spheres) formed native-like disulfide bonds. The rest one pair of Cys residues was substituted by aminobutyric acid (Abu, B, red sphere).
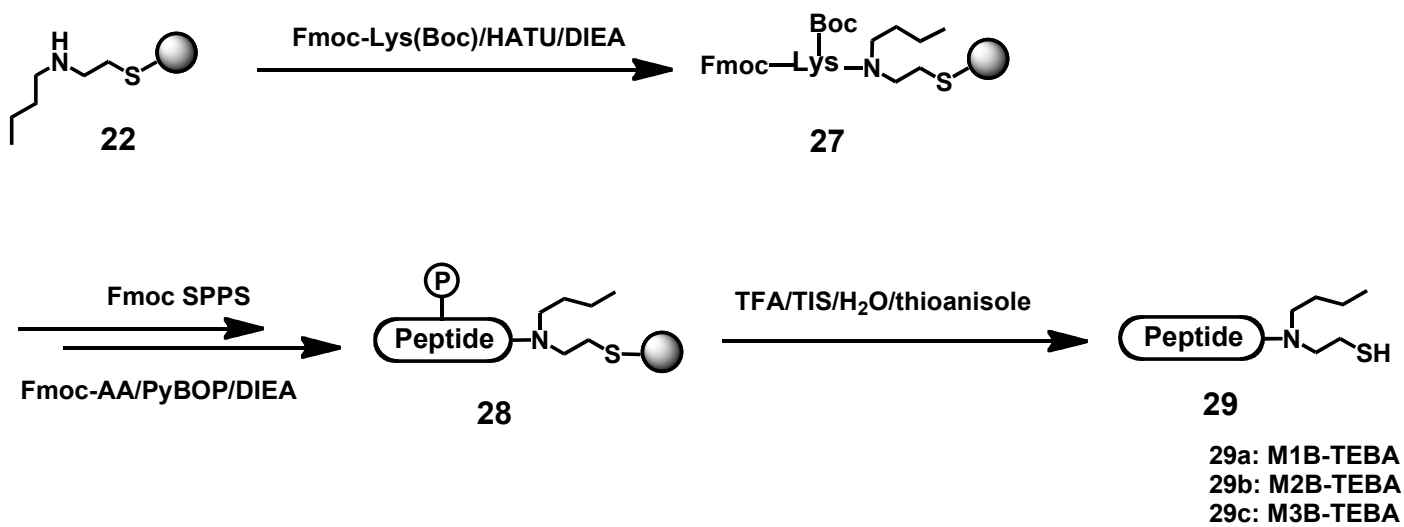
Figure 4-18. Scheme of synthesizing precursors of MVIIA analogs on TEBA resins.

The optimized condition for TEBA thioesterification was applied to the cyclization of **29a-c** (**Figure 4-19A**). Taking cM1B as the example for illustration, the M1B-TEBA **29a** ([M+H] = 2870 Da) was partially converted into S-form **30a** in HPLC mobile phase condition (**Figure 4-19B**). After dissolving the lyophilized powder mixture of **29a/30a** in sodium phosphate buffer (0.1 M, pH 3) to a final concentration of 1 mM, tandem thiol switch initiated immediately as TEBA mediated N-S acyl shift and the intramolecular thiols started to convert S-form **30a** into thiolactones **32 (i-iv)** ([M+H] = 2736 Da). By adding 50 mM MESNa, thioesterification was further facilitated towards formation of the stable M1B-MES thioesters **31a**. ([M+H] = 2878 Da) The tandem N-S, S-S acyl shift reactions were performed at 40°C and subjected to HPLC monitoring. Consequently, thioesterification reactions of M1B-TEBA after 16 h resulted in a mixture of MES thioester **30a** and one major intramolecular thiolactones **32a-iv** (**Figure 4-19C**). Thiolactone **32a-iv** had same mass as cM1B and same RT in HPLC. It was differentiated from cM1B by UV absorbance at 260 nm. The thia zip cyclization reaction commenced by increasing pH to 7.5-8.0. One hour cyclization reaction at room temperature completely converted all thioester and thiolactone species into macrocyclic cM1B **33a** with >80% yield (**Figure 4-19D**). The oxidative folding of engineered cM(1-3)B peptides were not efficient in aqueous conditions. A novel folding method using non-aqueous reagents will be introduced in section 4.5 to fold the two-disulfide cyclic MVIIA analogs rapidly with high yield.
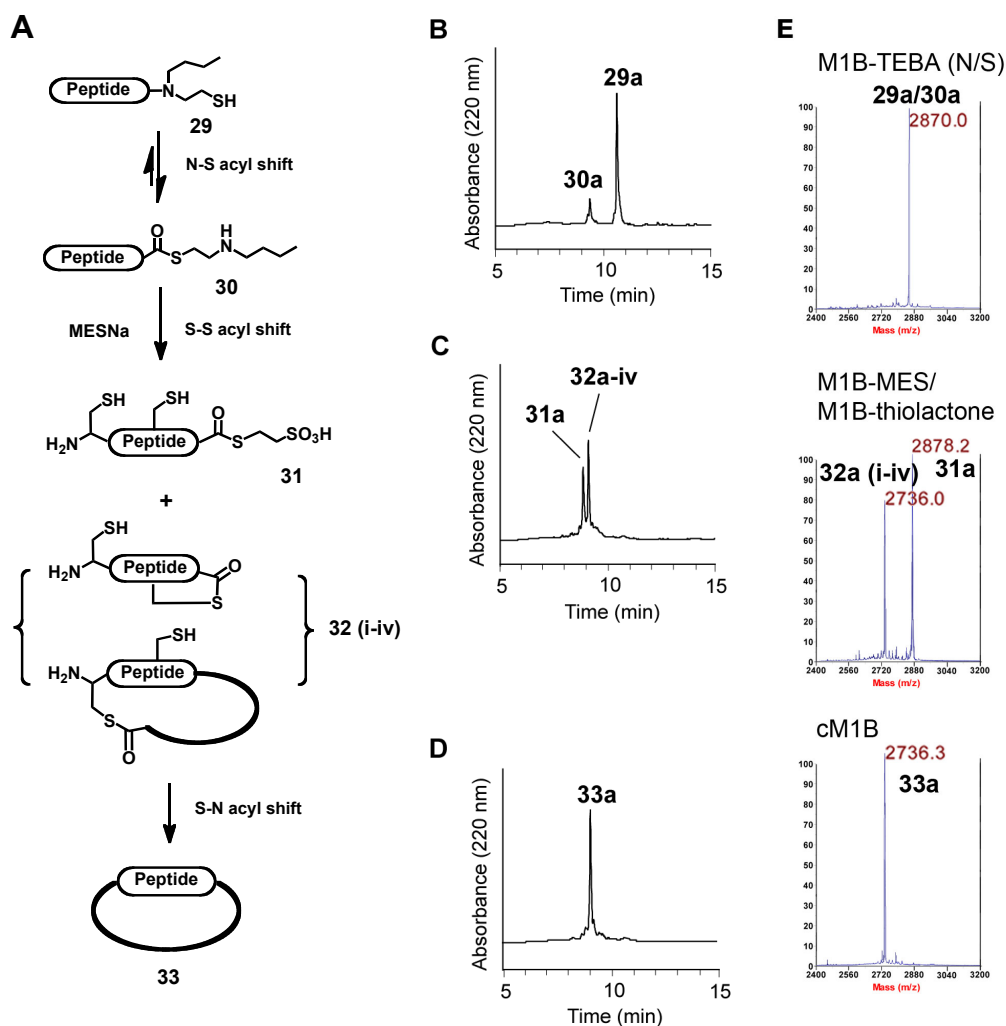
Figure 4-19. **Preparation of reduced cM(1-3)B using TEBA thioester surrogate**. (A) Synthesis scheme. (B) HPLC trace of M1B-TEBA **29a** (RT = 10.7 min) with small amount of M1B-S-TEBA **30a** (RT = 9.4 min). (C) HPLC profile of tandem thiol switch reaction after 16 h, which resulted in M1B-MES thioester **31a** (RT = 8.9 min) and one thiolactone **32a-iv** (RT = 9.1 min). (D) HPLC profile of cyclization reaction after 1 h, which resulted in one dominant peak cM1B **33a** (RT = 9.1 min). (HPLC condition: C-18 column 4.6x150 mm, 3.6 u, gradient of 0-50% ACN (with 0.1% TFA) for 15 min, flow rate 1.5 ml/min, 60°C column heating). (E) MS spectra of M1B-TEBA, M1B-MES thioester, M1B-thiolactones and cM1B.

4. Preparation of cyclic CRPs by azide method

The acyl azide was introduced by Curtius as one of the earliest α-carbonyl group activation method in 1900s [261, 262], almost at the same time as Fischer's acid chloride for peptide bond formation [263, 264]. Activation of α-carbonyl by acyl azide is moderate, and the soft electron shell of azide shields the carbonyl atom, which reduce the tendency of oxazolone-formation through a nucleophilic attack by oxygen atom thus less racemization occurred [265]. Azide method was then envisioned to be a useful and "racemization-free" method to prepare large peptide and proteins via segment condensations, by preparing peptide fragments with the C-terminal hydrazide directly from acyl esters via hydrazinolysis and subsequently converting into peptide azides by nitrous acid [266]. Wang and Merrifield also developed hydrazide resins for solid-phase synthesis [267-269]. Azide coupling method has a major side reaction by forming isocyanate via Curtius rearrangement [270]. By conducting peptide bond formation reaction below 0°C, this side reaction can be largely reduced. Low temperature, as well as increased acidity (e.g. pH 2 by HCl), also reduces the amide formation side reaction during hydrazide oxidation to give desired azide compounds [271].

Liu Lei's group has recently reported a safety-switch method based on the reactive acyl azide for thioester formation and subsequent peptide cyclization [209]. The peptide azide was derived from the peptide-hydrazide by sodium nitrite. The acyl azide was transformed into thioester in the presence of excess of thiols, which could be performed in aqueous conditions and ready for Cys-thioester ligation. Herein, this azide approach has been applied for the synthesis of cyclic CRPs to compare with TEA-type of thioester surrogates.

4.1 Synthesis of peptide-hydrazide by Fmoc chemistry

As shown in **Figure 4-20**, the hydrazide resins were synthesized by attaching the commercially available hydrazine monohydrate **34** (2 eq.) to Cl-Trt(2-Cl) resins (1.2 mmol/g, 1 eq.) in DMF in the presence of excessive DIEA (3 eq.). After 1 h, the reaction was stopped and remained reactive Cl groups on Cl-Trt(2-Cl) resins were removed by treating with methanol. After coupling of C-terminal Fmoc-Ser(tBu) on H_2NHN-Trt resin **35**, the resultant Fmoc-Ser(tBu)-hydrazide resin **36** had a reduced substitution of about 0.5 mmol/g. Stepwise elongation of the peptide sequences was performed on resin **36** followed by TFA deprotection and cleavage to give the linear precursors of cyclic MVIIA analogs M1B-NHNH$_2$ **38a** (calc. 2767.3 Da, found 2768.3 Da), M2B-NHNH$_2$ **38b** (calc. 2767.3 Da, found 2768.4 Da), and M3B-NHNH$_2$ **38c** (calc. 2767.3 Da, found 2768.3 Da) with isolated yields 24-31%.
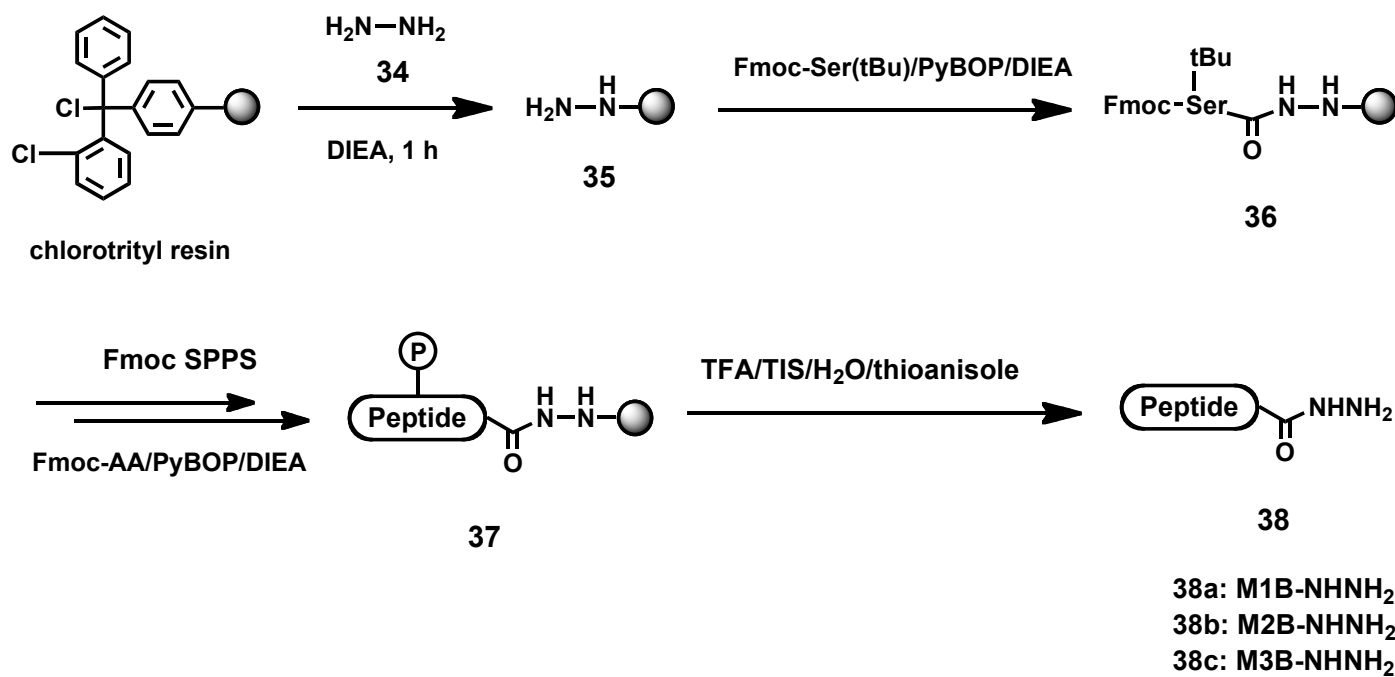
Figure 4-20. **Preparation of the linear peptide precursors of cyclic MVIIA analogs on hydrazide resins**.

4.2 Azide formation and one-pot cyclization

Unlike peptide-MeCys or peptide-TEBA, the peptides with C-terminal hydrazide linkers were not reactive to give thioesters in acidic solutions. The acyl hydrazide needed be nitrite-oxidized into active azide to facilitate nucleophilic substitution by external thiols to afford peptide thioester and subsequent cyclization (**Figure 4-21A**). Purified and lyophilized peptide-hydrazide **38a-c** ([M+H] = 2768 Da) was dissolved in a sodium acetate buffer (0.1 M, adjusted by 3 N HCl to pH 2.0) to give 1 mM peptide solutions. Addition of 6 M guanidine-HCl into the reaction buffer was required to obtain good solubility and product yield for hydrophobic peptides such as cyclotide hedyotide B1. The high concentration of denaturing reagents also prevent buffer frozen when conducted the reaction below 0°C.

Before adding the fresh-prepared sodium nitrite solution, the peptide solution must be chilled on ice to reach 0°C. The nitrite catalyzed azide **39** formation was monitored by analytical HPLC, which usually indicated a completed consumption of peptide hydrazide within 30 min at 0°C. MALDI-TOF MS analysis of azide intermediated resulted in a des-N_2 mass as [M+H-N_2] = 2750 Da since high-energy laser would break azide N=N double bond to give one nitrogen gas molecule and a CO-N^+ ion. 100 equivalent of MMA (0.1 M, = 1% *v/v*) was added into oxidation mixture to trap the active acyl azide **39**. The thioester formation was performed at room temperature at pH to 7.5 (adjusted by 1 N NaOH). Both peptide-MMA thioester intermediate **40** ([M+H] = 2842 Da) and peptide-thiolactones **33 (i-iv)** ([M+H] = 2736 Da) were detected by MALDI-TOF mass spectrometry immediately after pH change, which suggested a rapid and efficient nucleophilic substitution of azide by thiols. Under the neutral to basic condition, thiol-thioester exchange reactions were facilitated, which led to formation of end-to-end thiolactone **33-iv** formation and subsequent S-N acyl shift reactions on the end-to-end thiolactones to afford cyclization products **33a-c**. The HPLC monitoring of macrocyclization of cM2B was shown in **Figure 4-21(B-D)** as example. The one-pot thioester formation and cyclization from M2B-N_3 **39b** to cM2B **33b** took less than 2 h to complete with a HPLC yield >80%.

My results showed that the azide-catalyzed thioester formation and one-pot cyclization was fast and efficient for preparing cyclic CRPs. But this method required careful handling to govern a satisfied yield. There were several factors that often caused unsuccessful experiments. First, the azide formation step must be performed at or below 0°C to prevent irreversible Curtius rearrangement to occur. Second, large excess of thiols was required for thioesterification. Since the acyl azide was a good leaving group by activating the α-carbonyl for nucleophilic attack, the intramolecular nucleophiles such as side chain -OH and -NH_2 may also substitute azide to give lactones and lactams side products in their deprotonated conditions. Excessive thiols would compete over other nucleophiles to trap the acyl azide to give desired thioesters. Moreover, unlike TEA-thioester surrogates that mediated thioesterification under acidic conditions when the intramolecular thiols were in reduced forms, the nitrite used for azide formation also oxidized SH of Cys into S-NO, which was promptly reactive with other thiols to form disulfide bonds. Third, the pH increment from pH 2 to pH 7.5 for thioesterification must be performed after the addition and well mixing of external thiols. The handling needed to be quick and accurate on ice to prevent the formation of lactone/lactam side products.
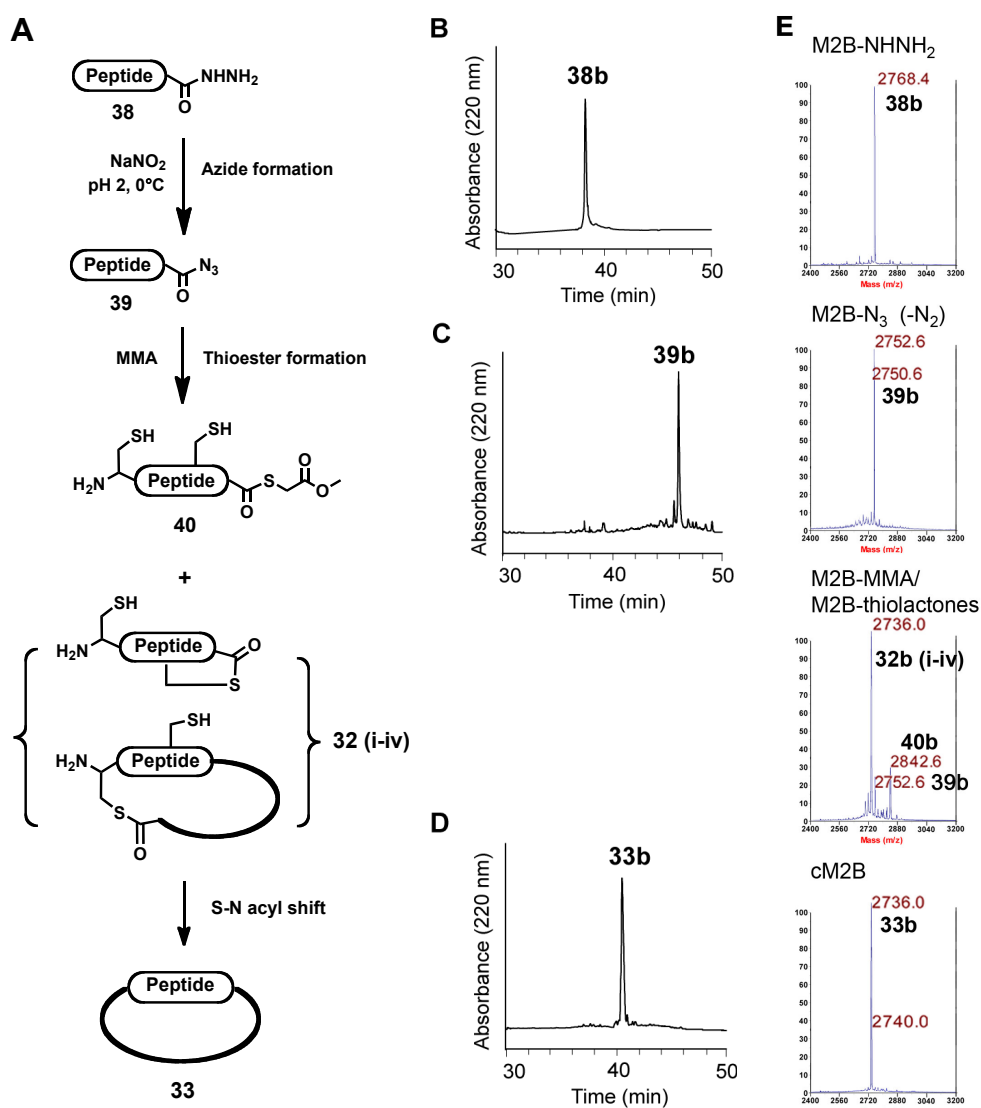
Figure. 4-21. **Prepare cyclic MVIIA analogs via azide-mediated thioester formation and one-pot thia zip cyclization**. (A) Scheme of one-pot cyclization from peptide hydrazide **38** to macrocyclic conotoxins **33.** (B) HPLC profile of purified M2B-NHNH₂ **38b** (RT = 38 min). (C) HPLC profile of M2B-N₃ **39b** (RT = 46.2 min) (C) HPLC analysis of one-pot cyclization reaction after 2 h that resulted in a dominant cyclization product cM2B **33b** (RT = 40.5 min). (HPLC condition: C-18 column 4.6x250 mm, 3.6 u, gradient of 0-40% ACN (with 0.1% TFA) for 80 min, flow rate 1 ml/min). (E) MS spectra of hydrazide, azide intermediate, thioester/thiolactone intermediates and cyclization product of M2B species.

5. Discussion

The design of TEA-based thioester surrogates was inspired by the neat intein splicing reaction. Intein catalyzes the N-S acyl shift reaction on the thioethylamido group of its N-terminal Cys. Without the assistance of other residues in the reactive pocket, Cys residue along had limited activity to undergo N-S acyl shift to give a thioester. This N-S acyl shift occurred at Cys was early discovered by Sakakibara in 1967 during HF cleavage of a cysteine-containing peptide [272]. Aimoto's group observed Cys-mediated N-S acyl shift in TFA on a 4-residue synthetic peptide [273, 274]. The reaction was slow (>910 h) and reversible as monitored by ^{13}C NMR and RP-HPLC. Macmillan's group reported a sequence-dependent Cys-catalyzed peptide bond breaking that restricted in the sequence GC, CC and HC [275]. With large excessive thiols and 80°C heating, thioesterification took place at the cleavage site to afford peptide thioesters. Hojo et al found that *N*-alkylated Cys were more reactive self-catalysts for N-S acyl shift than Cys [218]. Our design and studies on intein-mimetic MeCys linker explained the improved activity, as alkylation at α-amine enhanced the *cis* conformation of TEA moiety, which promoted the nucleophilic substitutions.

In the numerous strategies for preparing macrocyclic peptides by chemical synthesis, the Fmoc-compatible, simple and practical thioethylamido (TEA) thioester surrogate indeed was one of the most promising ways to producing thioesters for Cys-thioester ligation to afford end-to-end cyclized peptide products. The TEA linkers can be attached to a Rink amide resin or chlorotrityl resin in one step. Peptide sequence can be added on to these linkers using common coupling reagents. The cleaved peptide-TEA was readily reactive to give a thioester via intramolecular acyl shift reaction in a pH-dependent manner.

The TEA-mediated N-S acyl shift preferentially occurred at lower pH whereas the subsequent S-S thioester exchange reaction preferred in neutral to basic conditions. Thus the tandem N-S, S-S acyl shift reactions in the presence of internal or external thiols can afford a broad range of reaction conditions

from pH 2 to 5 with the optimal condition at pH 2-3. In these mild aqueous conditions, the chemoselective acyl shift reactions were almost side-reaction free. Heating could accelerate the tandem thiol switch reaction. However, higher temperature caused more side reaction, such as hydrolysis, to take place.

The Cys-thioester ligation reaction was particularly useful for synthesis of cyclic CRPs due to the existence of multiple intramolecular thiols on Cys side-chains that could accelerate cyclization via a thia zip mechanism. The intramolecular thiols could participate in thioesterification that usually act faster than intermolecular reactions to afford thiolactones with increased ring sizes, which efficiently leads to a N- and C-terminal covalent linkage by a thioester bond followed by a S-N acyl shift in a five-member transmission state to form a peptide bond.

During the study of MeCys and its application for preparing cyclic CRPs, we found that the synthesis of peptide precursors with a C-terminal MeCys thioester surrogate using Fmoc chemistry has several limitations. First, coupling of amino acid on the secondary amine of MeCys(Trt) was slow, especially when the following residue was bulky such as Fmoc-Arg(pbf). In the synthesis of CG29 when the next residue after MeCys was Fmoc-Gly, performing a double coupling using strong reagents such as HATU/DIEA could compromise this difficulty. Hojo *et al.* reported a method to circumvent the difficulty of the coupling problem of the *N*-alkylated Cys on resin by a solution-phase preparation of different dipeptide units, which can be easily introduced on resin to give MeCys(R)-containing peptides [276, 277]. The second drawback of the MeCys(R) surrogate group was the formation of a MeAla(Pip) side product (+51 Da) during Fmoc-synthesis of a peptide containing a C-terminal MeCys(Trt) on resin that previously reported by Lukszo *et al.* [259] as a base-catalyzed β-elimination on a C-terminal Cys(Trt) or Cys(Acm) followed by a Michael addition of piperidine to form 3-(1-piperidinyl)alanine. MeCys(Trt) was also susceptible to this side reaction and the side product was accumulated during each piperidine deprotection step in Fmoc solid-phase synthesis. This synthetic problem was not fully resolved by addition of a spacer residue Gly between MeCys(Trt) and the resin support. In the microwave-assisted peptide

synthesis of CG29-MeCys(Trt)-Gly-NH$_2$, the side product CG29-MeAla(Pip)-Gly-NH$_2$ accumulated to 10% at the completion of the synthesis, suggesting that an average of 0.3% side reaction per deprotection cycle. The third drawback of using MeCys(Trt) was that it was an expensive reagent. Preparation of an *N*-methylated Cys building block by methyl nitrobenzenesulfonate alkylation followed by nitrobenzenesulfonate reduction has been reported by Erlich, *et al.* [278], which provided a cheaper but more laborious alternative. The other side reaction was reported by Urban *et al.* in 1996 as C$^\alpha$-cleavage on *N*-methylated amino acid due to oxazolone formation in TFA, which resulted in cleavage of residues after the *N*-methylated residues [279]. This side reaction product was not identified from HPLC traces in the synthesis of peptide-MeCys-Gly precursors of cyclic conotoxins but this problem could not be negligible.

To completely avoid the β-elimination and C$^\alpha$-cleavage side reactions, it would be desirable to remove the electron withdrawing α-carbonyl moiety of a MeCys(R) and the α-CH susceptible to abstraction by piperidine during the deprotection cycles. To achieve this objective, we have developed a novel family of TEA-thioester surrogates, which we designated as the TEXA thioester surrogates. Without the carboxylic group, the TEXA design could decrease the steric hindrance during the coupling reaction and eliminate the side reaction of β-elimination and the piperidine addition product. TEXA has an advantage of using the resin support as a S- protecting group for the thioethyl moiety. Such a strategy further simplifies the synthesis of functionalization of the TEA thioester. TEBA (where X=butyl) was described intensively here as an example of TEXA thioester surrogate. In the synthesis of peptide-TEBA precursors, the β-elimination problem was completely resolved.

The synthesis of peptide precursors also affected by the TFA cleavage regarding the proper usage of scavengers in the cleavage cocktail. The multiple S-Trt protecting groups were completely removed by 5% (*v/v*) scavengers TIS. The deprotected Cys residues were susceptible to alkylation. Thus the *O*-tBu ion cleaved from Ser/Thr/Tyr required thiol scavengers such as 2% (*v/v*) thioanisol to remove.

The TEBA-mediated N-S acyl shift was found to be more efficient than MeCys. The N-S acyl shift occurred during HPLC purification, which resulted in about 10-30% S-form. Formation of stable thioester from peptide-TEBA via tandem N-S, S-S acyl shift was completed in a shorter period. The difference in reactivity might be due to the butylation of α-amine that promoted higher level of *cis* conformation than methyl in MeCys. A single HPLC isolation step was only performed after cyclization reaction to obtain purified cyclic peptides.

The new "safety-catch" azide method was applied to the preparation of cyclic MVIIA analogs with a good yield in a short preparation period. This method could afford thioesterification and ligation at most amino acids even at hindered Pro or β-branched Thr, Val and Ile, by extending the reaction time [209]. However the reactive azide required excessive external thiols and careful handling of pH and temperature to confer the thioester formation, otherwise side reactions occurred, such as nucleophilic side chain groups in the unprotected peptide would interact with azide to give lactones or lactams. In contrast, thioester formation by TEA-type thioester surrogates through intramolecular N-S acyl shift reaction preferentially involved thiols as the major nucleophiles to confer the dominance of thioesterification. It was a safe and chemoselective reaction with a broad adaptation to acidity (pH 2-5), which conferred peak-to-peak conversion of peptide precursor to peptide thioester and subsequent Cys-thioester reaction to give the expected ligation or cyclization product.

Chapter 5. Oxidative folding of ω-conotoxins

1. Introduction

The disulfide bonds are important for stabilizing the biological-active structures of CRPs. The calcium-channel-inhibiting ω-CTXs contain three disulfide bonds and the disulfide formation places a challenge for the development of efficient synthetic strategy to prepare them. Chemoselective disulfide formation has been ultilized as a promising approach for the synthesis of CRPs, but global oxidative folding would be a better choice to avoid peptide loss during the multiple purification steps that are necessary for chemoselective folding. The global oxidative folding approaches generally require long reaction time and high dilution of peptides. To overcome these problems, I aimed to develop new folding approach using organic system. I hypothesized that the disulfide reshuffling reactions would be much faster in an organic solvent system, when the solvation effect of water was avoided. Thus the folding process could be facilitated with shorter reaction time and higher product yield. To prove this point, MVIIA and its analogs were recruited as models for the comparative study using different folding approaches including the conventional oxidative folding in aqueous conditions, chemoselective folding, and the novel organic folding approach. The roles of basicity, temperature, and redox reagents were explored for optimizing this novel organic approach to confer a rapid and efficient folding method that could be performed in one-pot with the newly developed cyclization strategy to prepare cyclic ω-CTXs.

2. Oxidative folding of cyclic *ω*-conotoxins in aqueous conditions

The folding efficiency of MVIIA, a linear analog M-GS and three 2SS cyclic analog cM(1-3)B were examined using the conventional folding method in aqueous conditions. For each peptide, a diluted folding solution (20 μM peptide) was prepared in 0.1 M ammonium acetate buffer (pH 7.8) with or without 2 M ammonium sulfate. The redox reagents were reduced and oxidized glutathione in the ratio of peptide: GSSG: GSH = 1:10:100. The folding reaction was performed at 4°C and monitored by HPLC every 24 h.

Linear precursor of MVIIA **42** (calc. 2645.2 Da, found 2645.5 Da) was prepared by Fmoc solid-phase synthesis on Rink amide resins with 13.6% isolated yield (0.1 mmol scale synthesis resulted in 87 mg ether precipitant and finally gave 36 mg purified peptide) (**Figure 5-1A**). Its linear analog M-GS-OH **45** (calc. 2790.3 Da, found 2790.9 Da) with a C-terminal Gly-Ser tail was synthesized on Wang resin with 20% isolated yield (0.1 mmol scale synthesis resulted in 119 mg ether precipitant and finally gave 55 mg purified peptide) (**Figure 5-1B**).

Oxidative folding of MVIIA in the presence of 2 M ammonium sulfate achieved 63 % yield of 3*SS* MVIIA **43** after 24 h and 81% after 48 h. In contrast, the folding yield was barely 10% without addition of salts (**Figure 5-2A**). The oxidative folding of linear M-GS in the presence of 2 M ammonium sulfate resulted in 84% yield of 3*SS* M-GS **46** ([M+H] 2784.8 Da) after 48 h (**Figure 5-2B**). The C-terminal GS-tail might enhance folding process like the Gly-tail in MVIIA-Gly precursor. In contrast, the oxidative folding of cyclic reduced cM(1-3)B **33a-c** were not efficient in aqueous conditions. Less than 20% cyclized peptides form the native-like disulfide bonds (peak N in Figure **5-2C**) in the HPLC analysis. These yields were similar as the oxidative folding of cCG29 **20,** which suggested that the aqueous folding method was not efficient for preparing the cyclic analogs of MVIIA.
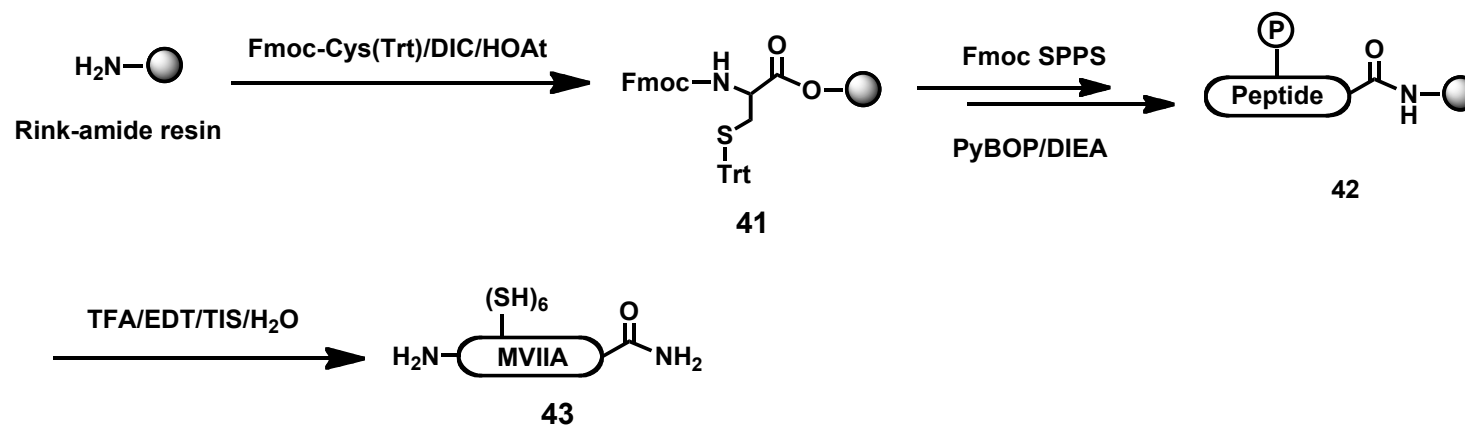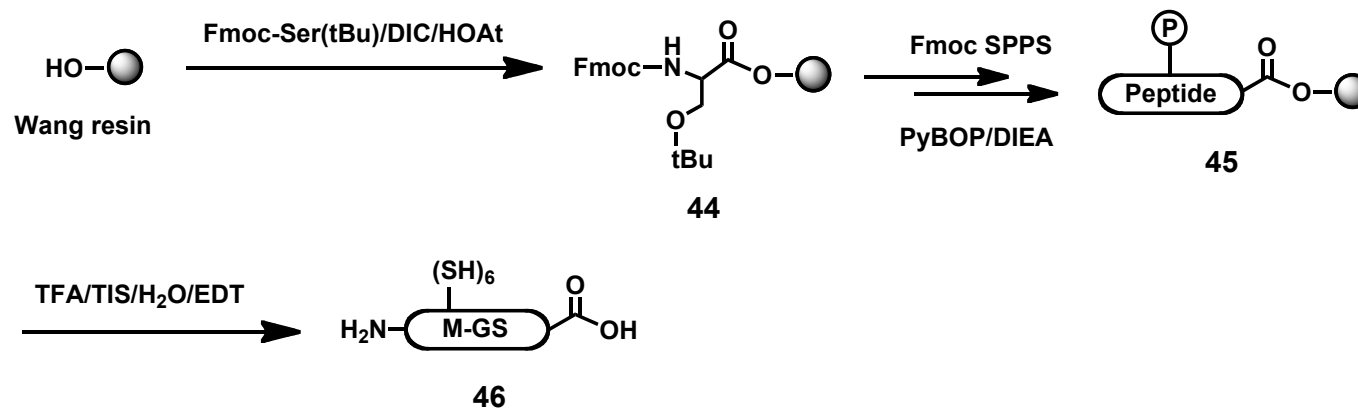
Figure 5-1. **Synthesis scheme of MVIIA 43 and its linear analog M-GS 46.** (A) MVIIA precursor **43** synthesis on Rink amide resin using Fmoc chemistry. (B) M-GS-OH **46** synthesis on Wang resin using Fmoc chemistry.
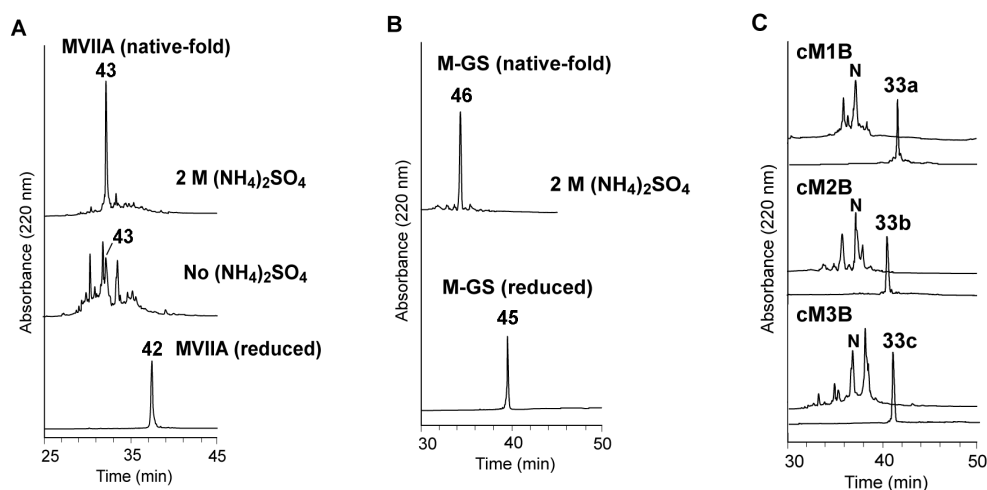
Figure 5-2. Oxidative folding of reduced MVIIA 42, M-GS 45 and reduced cM(1-3)B 33a-c in aqueous conditions. (A) HPLC analysis of MVIIA folding mixture after 48 h in the presence or absence of 2 M ammonium sulfate after 48 h reaction at $4°C$. The reduced MVIIA **42** was eluted at 37 min and native-fold MVIIA **43** was eluted at 32 min. (B) HPLC analysis of M-GS folding mixture in the presence of 2 M ammonium sulfate after 48 h reaction at $4°C$. The reduced M-GS **45** was eluted at 39.6 min and native-fold M-GS **46** was eluted at 34.5 min. (C) HPLC analysis of oxidative folding of reduced cM(1-3)B **33a-c** in the presence of 2 M ammonium sulfate after 48 h reaction at $4°C$. The reduced cyclic starting materials gave clear peaks at 40-41 min. HPLC traces of folding mixtures showed completed oxidation of starting materials. The native-fold peak was labeled by N. (HPLC condition: C-18 column 4.6x250 mm, 3.6 u, gradient of 0-40% ACN (with 0.1% TFA) for 80 min, flow rate 1 ml/min).

3. Chemoselective folding of cyclic *ω*-conotoxins

I performed chemoselective folding to prepare the 2*SS* cyclic MVIIA analogs with native-like disulfide bonds. Chemoselective folding confirmed the correct disulfide connectivity and thus the folding products were used as standard for characterizing the folding products obtained from global oxidative folding by coelution. In this approach, the precursors cM(1-3)B(Acm)-TEBA **48a-c** with one pair of Cys residues protected by Acm were synthesized on Fmoc-Lys(Boc)-TEBA resin **27** (**Figure 5-3**). Sequence of M1B(8, 20Acm)-TEBA **48a** (CGS<u>B</u>KGKGAKC_{Acm}SRLMYDCCTGS C_{Acm}RSGK-TEBA) and M2B(1, 16Acm)-TEBA **48b** (CGS<u>C</u>_{Acm}KGKGAKBSRLMYDCC_{Acm}TGSBRS GK-TEBA) were started at C25 and ended at K24. Sequence of M3B(1, 16Acm)-TEBA **48c** (CSRLMYDBC_{Acm}TGSCRSGKBGS<u>C</u>_{Acm}KGKGAK-TEBA) was started at C8 and ended at K7. The Fmoc synthesis on 0.1 mmol resins **27** resulted in about 80 mg purified M1B(8, 20Acm)-TEBA **48a** (calc. 3009.6 Da, found 3010.6 Da), M2B(1, 16Acm)-TEBA **48b** (calc. 3009.6 Da, found 3010.5 Da), and M3B(1,16Acm)-TEBA **48c** (calc. 3009.6 Da, found 3010.6 Da).
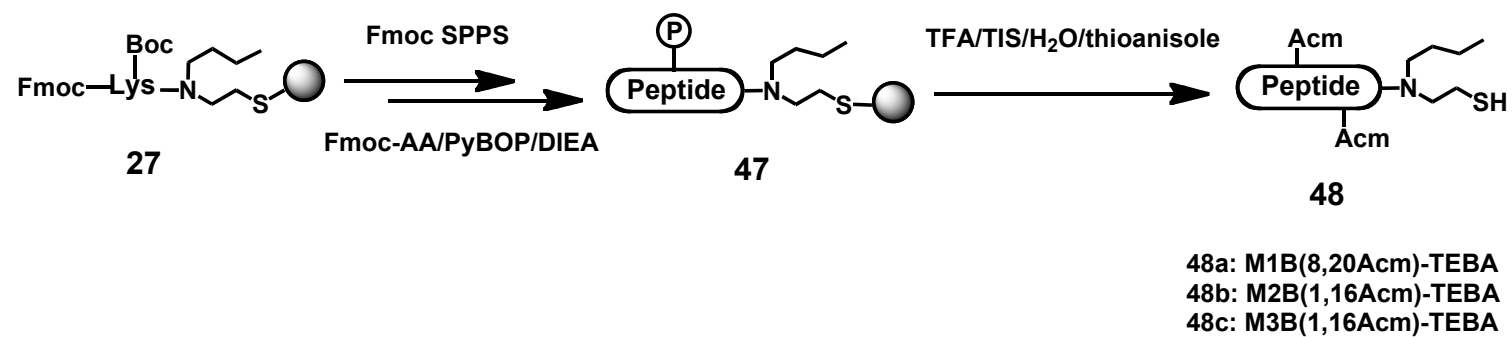
Figure 5-3. Synthesis scheme of Acm-protected peptide precursors M1B(8, 20Acm)-TEBA, M2B(1, 16Acm)-TEBA and M3B(1, 16Acm)-TEBA 48a-c.

Thioesterification of M(1-3)B(Acm)-TEBA **48a-c** was performed with a 1 mM solution in the sodium phosphate buffer (pH 3) containing 10 mM MESNa for 18 h at 40°C followed by thia zip cyclization at pH 8.0 for 1 h to give cM(1-3)B(Acm) **52a-c** ([M+H] = 2877 Da) (**Figure 5-4A**). After purification by preparative HPLC, about 30-35 mg lyophilized **52a-c** were obtained from 80 mg M(1-3)B(Acm)-TEBA **48a-c**.

The cyclic and reduced cM(1-3)B(Acm) **52a-c** were then subjected to DMSO oxidation by adding 10% DMSO (*v/v*) to the cyclization mixture and reacted overnight at room temperature. Oxidation of the two Cys residues into a disulfide bond was monitored by analytical HPLC and MALDI-TF MS. After DMSO oxidation, cM(1-3)B(1*SS*, Acm) **53a-c** ([M+H] = 2875 Da) were purified by preparative-HPLC to give 15-20 mg lyophilized **53a-c**.

Removal of S-Acm protecting group and simultaneous formation of disulfide bond was conducted by iodine oxidation in a reaction mixture containing 5 mM peptide (**53a-c**), 50 mM iodine and 12 mM HCl that dissolved in 80% Acetic acid, 10% methanol and 10% H_2O. The oxidation reaction was completed within 1 h at room temperature, as monitored by analytical RP-HPLC. HPLC and MS analysis showed that chemoselective folding of cM1B (2SS) **54a** and cM3B (2SS) **54c** were efficient with > 90% separation yield. After purification and lyophilization, 6-8 mg **54a** and **54c** were obtained. The overall yield of cyclic folded analogs was less than 10%, which indicated that loss of peptides by multiple purification steps of chemoselective disulfide formation was a major problem for preparing cyclic CRPs containing multiple disulfide bonds.
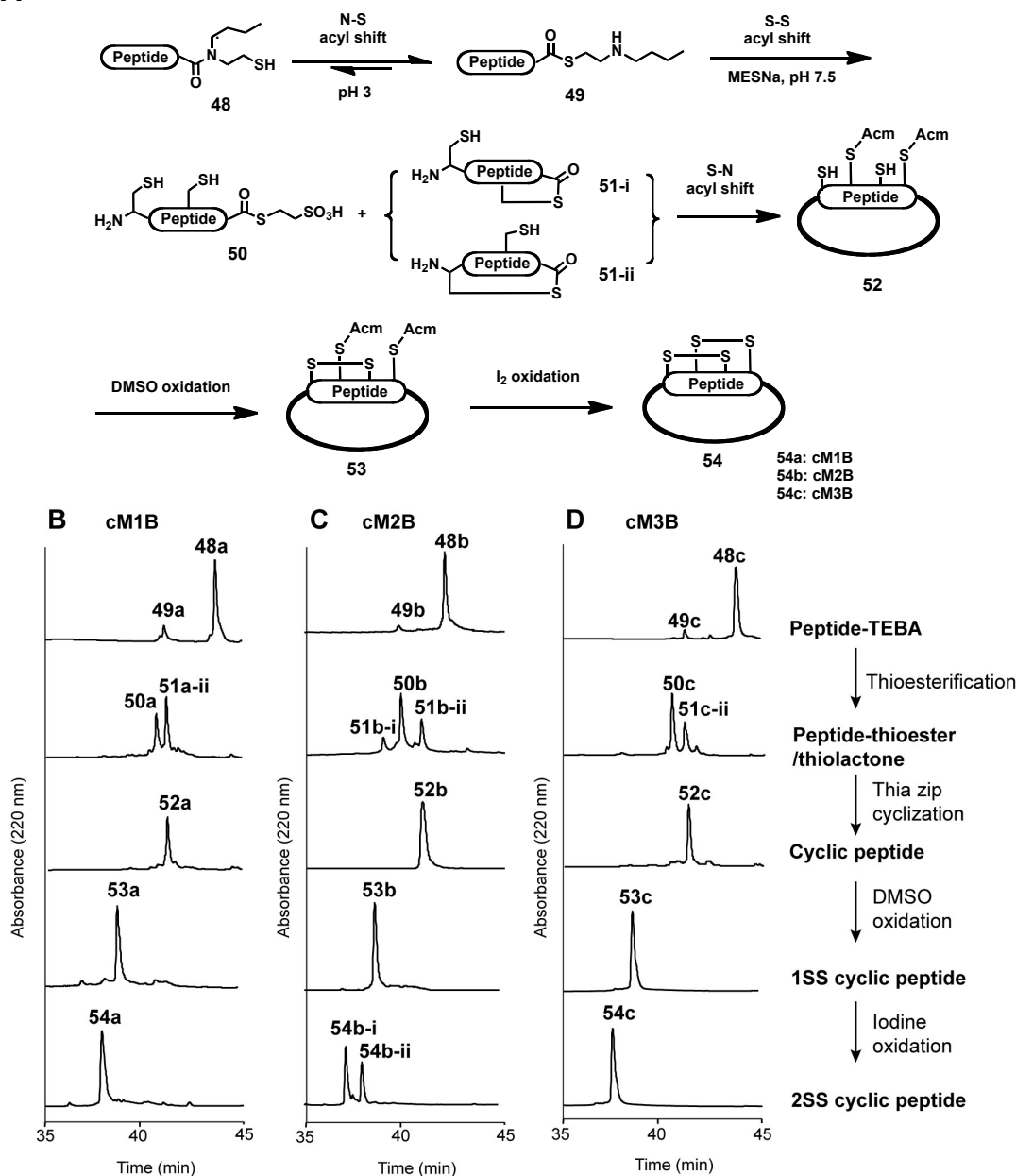
Figure 5-4. **Synthesis of 2*SS* cM(1-3)B 54a-c through TEBA-mediated cyclization and chemoselective disulfide formation**. (A) Synthesis scheme for cyclization and disulfide formation to prepare cyclic MVIIA analogs with two native disulfide bonds. (B) HPLC analysis of each reaction from M1B(8,20Acm)-TEBA **48a** to cM1B (C8-C20, C15-C25) **54a**. (C) HPLC analysis of each reaction from M2B(1,16Acm)-TEBA **48b** to two isomers of cM2B (C1-C16, C15-C25) **54b-i/ii**. (D) HPLC analysis of each reaction from M3B(1,16Acm)-TEBA **48a** to cM3B (C1-C16, C8-C20) **54c**. (HPLC condition: C-18 column 4.6x250 mm, 3.6 u, gradient of 0-40% ACN (with 0.1% TFA) for 80 min, flow rate 1 ml/min).

Exceptionally, iodine oxidation resulted two cM2B (2SS) isomers **54b-i/ii**. These two isomers were subjected to disulfide characterization using partial reduction and S-NEM alkylation. Purified peptides **54b-i/ii** (0.1 mg/ml in 0.2 M citrate buffer, pH 3.0) were reduced by 10 mM TCEP for 15 min followed by addition of 50 mM NEM to alkylate the reduced pair of Cys residues. Partially reduced and NEM-alkylated species were purified by HPLC (**Figure 5-5A**). Isolated peak P3 (1SS+2NEM, [M+H] = 3003 Da) was completely reduced by DTT and digested by trypsin or Chymotrypsin. The digested peptide fragments were analyzed by MSMS, which showed that **54b-i** possessed disulfide bonds C1-16 and C15-25. Similarly, purified **54b-ii** was partially reduced by 10 mM TCEP for 20 min followed by NEM alkylation (**Figure 5-5B**). The isolated peak P3 (1SS+2NEM, [M+H] = 3003 Da) was subjected to the same analysis procedure. The MSMS profiles of enzyme digestion fragments gave very similar spectra as **54b-i** P3. Assignment of charged fragments showed that both isomers possess the same disulfide connections C1-C16 and C15-25. In both isomers, the disulfide bond C15-C25 was more accessible by reductant than C1-C16. The 1D proton NMR of two isomers and the synthesized MVIIA was performed in 20% TFE-D3 in H_2O with 5% D_2O. The spectra reflected very different structure of these three peptides (**Figure 5-5C**). Formation of two isomers suggested that removal of C8-C20 disulfide bond reduced the molecular rigidity. **54b-i** and **54b-ii** might be different in 3D conformation due to the non-covalent interactions occurred on the flexible loops K2-D14 and T17-K24, despite of their identical disulfide connectivity.

A

54b-i P3 trypsin digestion fragment (1358 Da)

L M Y D C C T G S B R
|
NEM

54b-i P3 Chymotrypsin digestion fragment (3003 Da)

D C C T G S B R S G K C G S C K G K G A K B S R L M Y
| |
NEM   NEM

B

54b-ii P3 trypsin digestion fragment (1358 Da)

L M Y D C C T G S B R
|
NEM

54b-ii P3 Chymotrypsin digestion fragment (3003 Da)

D C C T G S B R S G K C G S C K G K G A K B S R L M Y
| |
NEM   NEM
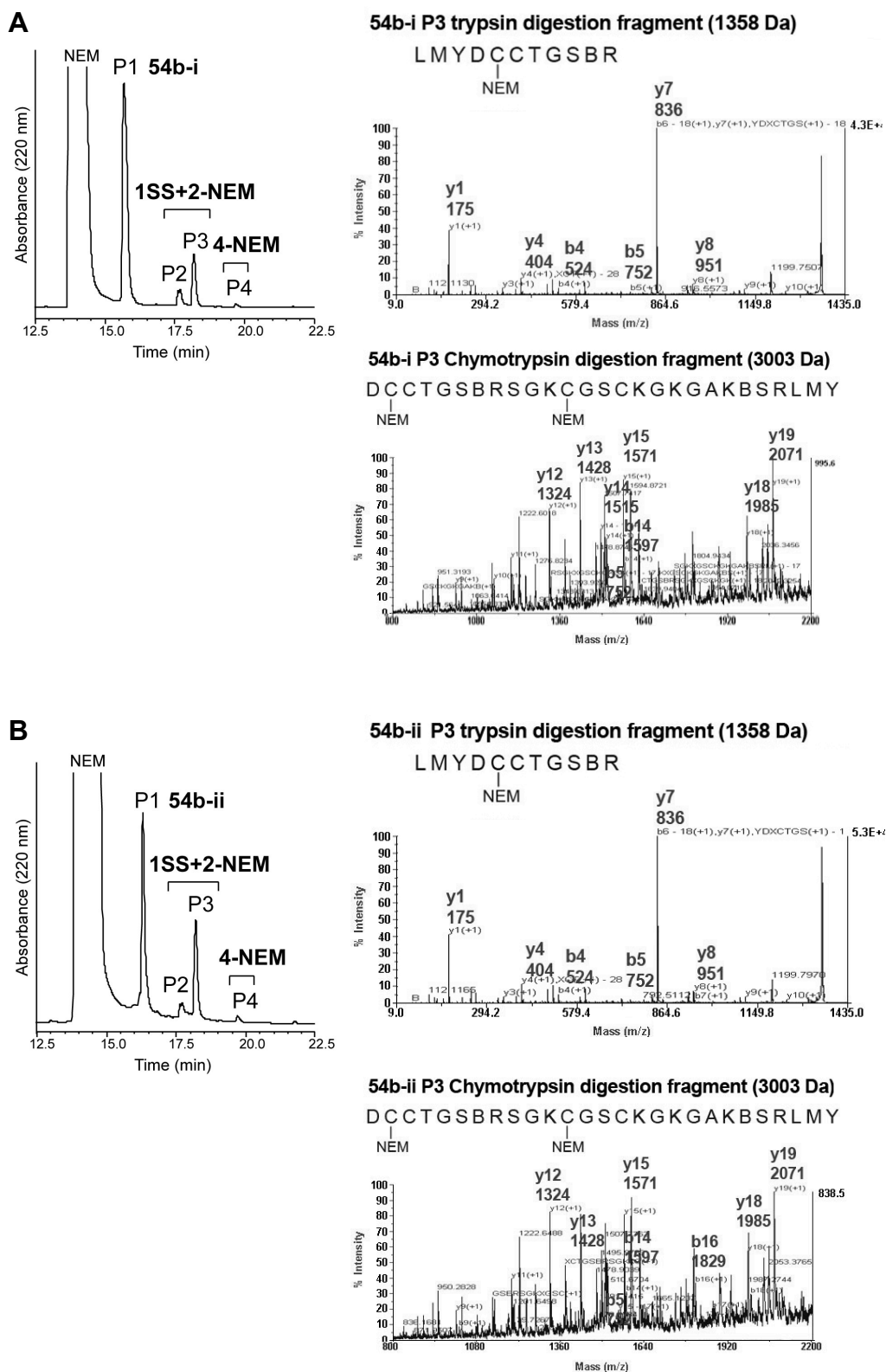
C
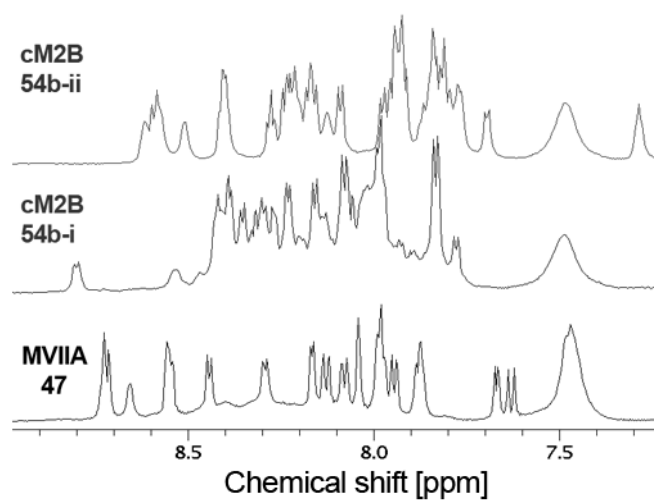
Figure 5-5. Characterization of cM2B isomers 54b-i/ii by disulfide mapping and ^{1}H NMR. Disulfide mapping was conducted by partial reduction and alkylation. (A) and (B) HPLC trace of alkylation products and MSMS analysis of enzyme digestion products for **54b-i** and **54b-ii**, respectively. (C) Comparison of ^{1}H NMR spectra (the amide region) of synthetic MVIIA and two cM2B isomers.

4. Oxidative folding of cyclic *ω*-conotoxins in organic conditions

The conventional oxidative folding reaction is conducted by redox-assisted disulfide reshuffling. This process could be largely accelerated in organic conditions when the solvation effect of water was eliminated to allow more intensive S_N2 interactions between sulfurs on peptide and reductants. In addition, the organic solvent prevented peptide aggregation and thus could tolerant more concentrated peptide solution than the conventional aqueous folding method. Here I introduced novel oxidative folding approach using organic system for prepare cyclic MVIIA analogs cM(1-3)B and cyclotide hedyotide B1. Solvent system, pH, temperature and redox reagents were examined for optimizing this new method. In general, the organic solvent pyridine was used to substitute water. Small amount of organic base morpholine was added to adjust the basicity. DMSO was given as both the organic oxidant and co-solvent. Organic-soluble thiols methyl mercaptoacetate (MMA), cysteamine and mercaptoethanesulfonate (MES) were tested as reductant.

4.1 Role of basicity in disulfide formation

Reduced cM2B **33b** was used as a model to investigate the optimal condition. By keeping a constant condition of 0.1 mM peptide, 100 eq. MMA (10 mM) and 10% DMSO in pyridine, the effect of basicity was examined. Thiol disulfide exchange was favored at basic condition above pH 8.0 when more Cys side-chain thiols were deprotonated and thus become stronger nucleophiles. Pyridine itself was an organic base (pKa of the conjugated acid, 5.25) but not strong enough to give a basicity that favored thiol-disulfide exchange. Adding small amount of morpholine (pKa of the conjugated acid, 8.36) increased the basicity, which effectively increased the oxidative folding rate. As shown in **Figure 5-6**, the reaction mixture with 0.1% morpholine resulted <5% native-fold cM2B (peak labeled as "N") after 1 h reaction. When the ratio of morpholine increased to 1%, resultant product N was increased to 66% yield. Further increase of morpholine content from 1% to 2% accelerate the thiol-disulfide exchange rate by shorten the reaction time from 1 h to 30 min. However, the folding yield did not increase. At too basic condition like

2% morpholine, accumulation of MMA disulfide homodimer that eluted near the folding products was observed, which caused a lump on the baseline in HPLC isolation profile.
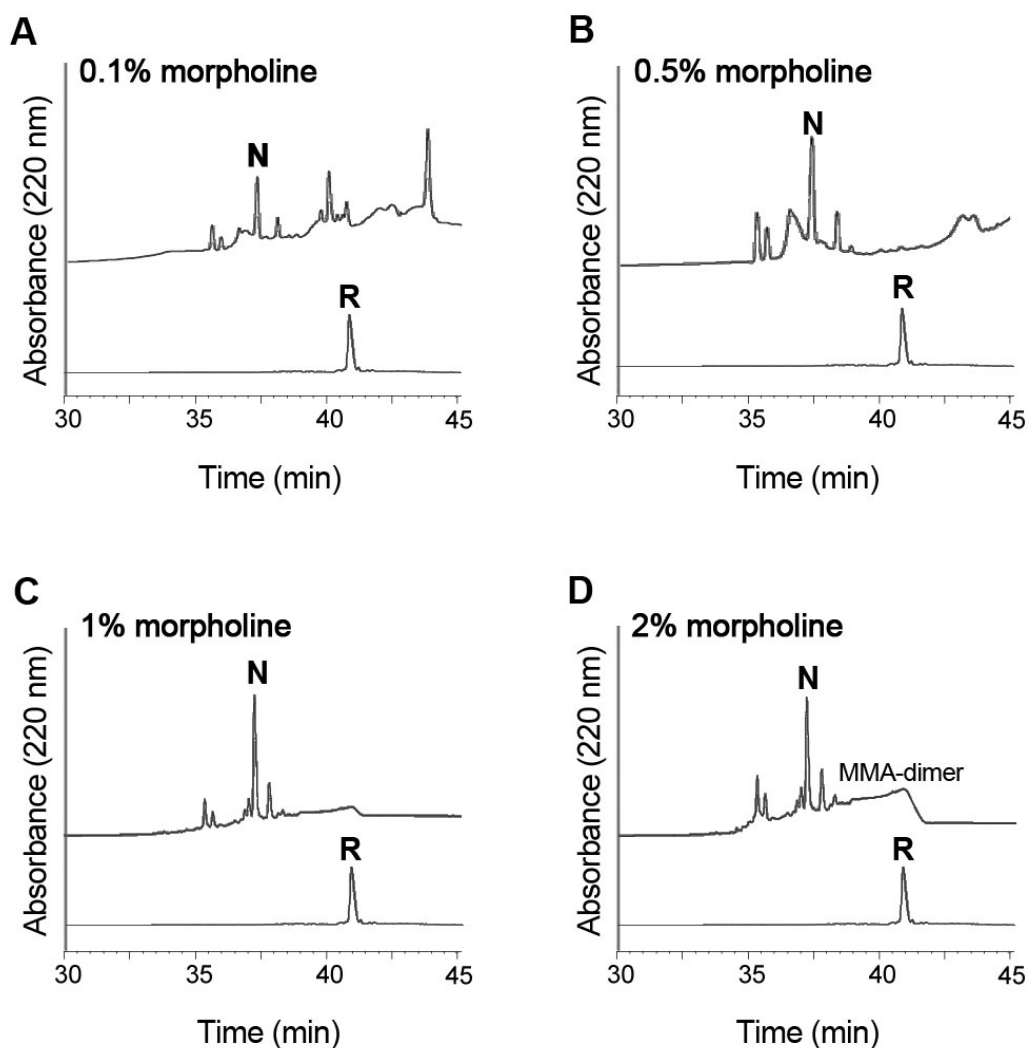
Figure 5-6. **Oxidative folding of cM2B in organic conditions with 0.1-2% morpholine**. Reaction was performed in pyridine with 10% DMSO and 10 mM MMA at room temperature and analyzed by RP-HPLC. The HPLC profiles of folding mixture with 0.1%, 0.5%, 1% or 2% morpholine was shown in block (A)-(D) respectively. For condition (A-C) reaction was quenched at 1 h while for condition (D) reaction was quenched at 30 min. The HPLC trace of reduced cM2B **33b** (peak **R**) (RT = 41 min) was shown in (A) for comparison. The RT of native-fold cM2B (peak **N**) was 37 min that same as **54b-i**. (HPLC condition: C-18 column 4.6x250 mm, 3.6 u, gradient of 0-40% ACN (with 0.1% TFA) for 80 min, flow rate 1 ml/min).

4.2 Effect of temperature

According to Kubo and others' results [243, 280-282], the oxidative folding of ω-CTX was facilitated by a low reaction temperature, which enhanced the native conformation of conotoxins in the folding buffer. Two folding reactions were performed in parallel at 25°C and 4°C with gentle stirring (about 2 rpm). Both reactions resulted in about 50% yield with similar HPLC profiles as shown in **Figure 5-5C**, while the latter reaction that conducted at lower temperature was much slower with a completion of oxidation after 6 h. This result suggested that the reaction rate in organic solvents with higher viscosity that water were more sensitive to temperature changes. Since the conformation-promoting effect of low temperature was not apparent in organic conditions, folding reaction at room temperature that completed more rapidly would be the better choice.

4.3 Role of thiols

With constant 1% (*v/v*) morpholine and 10% (*v/v*) DMSO, four conditions using different reductants were tested. 100 eq. MMA ($pK_{a\,SH}$ 8.22), 100 eq. cysteamine ($pK_{a\,SH}$ 8.6) 50 eq. MMA + 50 eq. cysteamine and 50 eq. MES ($pK_{a\,SH}$ 9.2), respectively. MMA and MES were the thiols used in thioesterification and cyclization. They were tested here for the purpose of developing a one-pot cyclization and folding method. Cysteamine was expected to be the ideal thiol for catalyzing thiol-disulfide exchange due to its structural similarity with cysteine. As shown in **Figure 5-7**, only condition 1 with 100 eq. MMA gave the best folding efficiency among four conditions, which resulted in near 70% yield of native-fold cM2B. In condition 2 and condition 3, cysteamine were found to have the tendency to form mix-disulfide species with peptides (+75 Da for each addition of cysteamine), which resulted in a cluster of undesired side products. Adding equal amount of MMA (50 eq.) and cysteamine (50 eq.) resulted in a similar profile as the condition with MMA alone, while mix-disulfide products still exist. For the condition using 50 eq. MES, more than 60% starting material remained in the reduced form after 1 h oxidation. Thus in this case, 50 eq. MES was considered too reducing to pair with 10% DMSO as a suitable redox reagents.
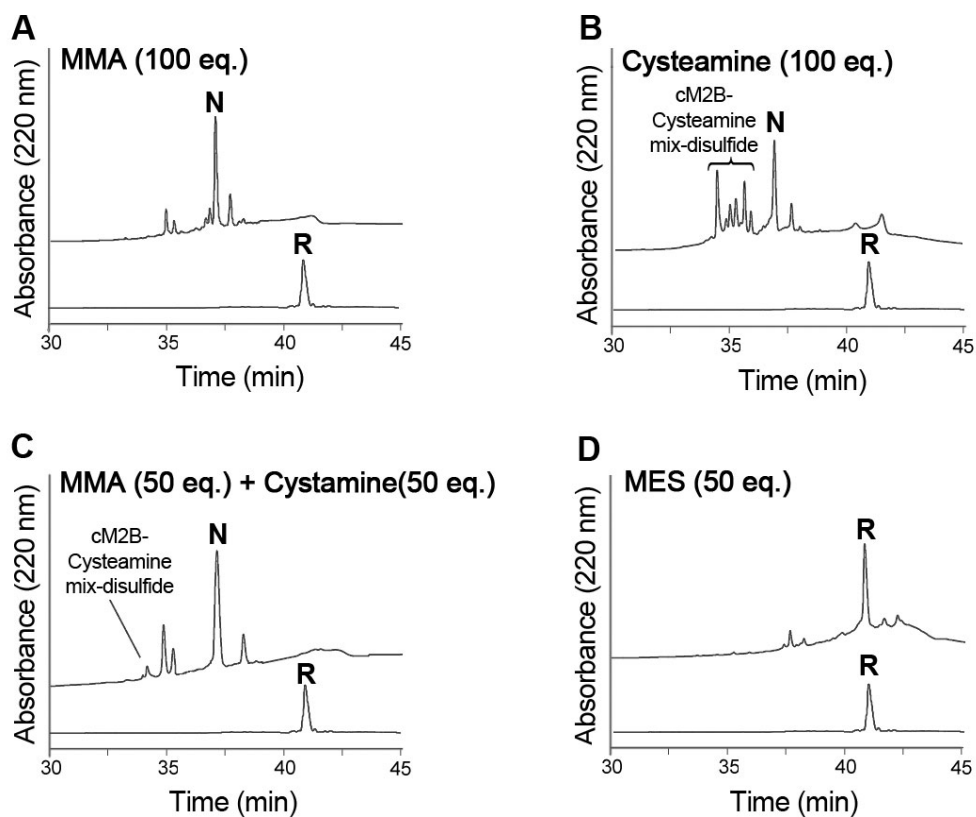
Figure 5-7. **Oxidative folding of cM2B in organic conditions with different thiols**. Reaction was performed in pyridine with 10% DMSO and 1% morpholine at room temperature and analyzed by RP-HPLC after 1 h. (A) 100 eq. MMA, (B) 50 eq. MMA and 50 eq. cysteamine, (C) 100 eq. cysteamine and (D) 50 eq. MEA. (HPLC condition: C-18 column 4.6x250 mm, 3.6 u, gradient of 0-40% ACN (with 0.1% TFA) for 80 min, flow rate 1 ml/min).

4.4 Role of oxidants

The success of MMA as the reducing reagent for oxidative folding in organic solvent inspired us to incorporate azide-mediated cyclization with the oxidative folding in non-aqueous condition to develop a one-pot synthesis procedure. The cyclization mixture containing 1 mM peptide mixture including reduced cM2B **33b,** and reagents including 100 mM MMA, 10 mM nitrous species (NO_2^-, NO^+, N_3^-). The nitrous species were known to be oxidant. Therefore we envisioned that the oxidative folding could proceed in the presence of cyclization reagents without additional redox reagents.

To compare the oxidative effect of $NaNO_2$ with DMSO, the trial experiments started with a purified sample of cM2B **33b**. The peptide stock solution (1 mM in water) was diluted with pyridine to give a 0.1 mM final concentration. DMSO and $NaNO_2$ were added to prepare three different fractions containing either 10% DMSO, 10% DMSO plus 10 eq. $NaNO_2$, or $NaNO_2$ alone without DMSO. After adding 1% morpholine and 100 eq. MMA, the folding reaction was performed as described before. After 1 h reaction, the folding mixtures were subjected to HPLC analysis (**Figure 5-8**). The HPLC profiles of three conditions revealed that NO_2^- could serve as an organic oxidant, which resulted in the same level of folding efficiency as DMSO.
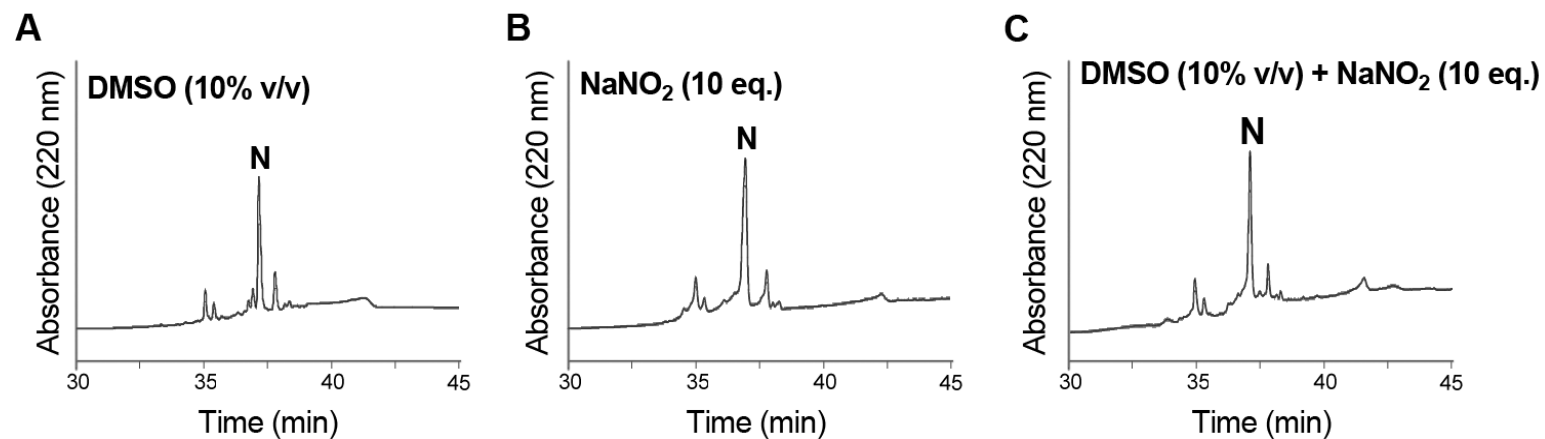
Figure 5-8. **Oxidative folding of cM2B in organic conditions with different oxidants**. Reaction was performed in pyridine with 1% morpholine and 100 eq. MMA at room temperature and analyzed by RP-HPLC after 1 h. (A) 10% (v/v) DMSO, (B) 10 eq. NaNO$_2$, (C) 10% DMSO and 10 eq. NaNO$_2$. (HPLC condition: C-18 column 4.6x250 mm, 3.6 u, gradient of 0-40% ACN (with 0.1% TFA) for 80 min, flow rate 1 ml/min).

5. One-pot cyclization and oxidative folding of cyclic conotoxins

A cyclization mixture of cM2B **33b** prepared from TEBA precursors **29b** without addition of any external thiols was directly used for oxidative folding. A 10-time dilution of the cyclization mixture using organic solvents and reagents resulted in a folding mixture containing 0.1 mM cyclic products, 10 mM MMA, 10% DMSO, 1% morpholine, and 89% pyridine. Oxidative folding was conducted at r.t. for 1 h and was quenched by adding pre-chilled 20% TFA water solution into the ice-cold reaction mixture. Pyridine was removed by rotary evaporation. The remained solution was subjected to a single step of HPLC purification. This one-pot folding reaction resulted in the same folding product profile in analytical HPLC as shown in **Figure 5-8A**, which showed that a small amount of aqueous buffer (e.g. 10% *v/v*) did not obviously influence the rate-accelerating effect of organic solvents in this folding condition. 1.3 mg cM2B was obtained from 10 mg linear precursor.

Alternatively, the one-pot synthesis was performed as a combination of azide method and organic folding. Started with a cyclization mixture that initially contained 1 mM peptide-hydrazide precursors of cM(1-3)B, 9-time volume of pyridine and 0.1-time volume of morpholine were added to make a final folding mixture with 0.1 mM peptide, 1 mM nitrous oxidants, 10 mM MMA, and 1% morpholine. The folding reaction was performed for 1 h at room temperature, which resulted in 27%, 52%, and 44% native-fold cM1B **54a**, cM2B **54b-i** and cM3B **54c**, respectively (**Figure 5-9**). For the scaled-up one-pot experiment using 10 mg peptide-hydrazide **38a-c**, reaction proceeded without any purification steps until the folding reaction completed. The resultant purified cM(1-3)B were 0.6-1.1 mg, giving 6-11% isolated yield.
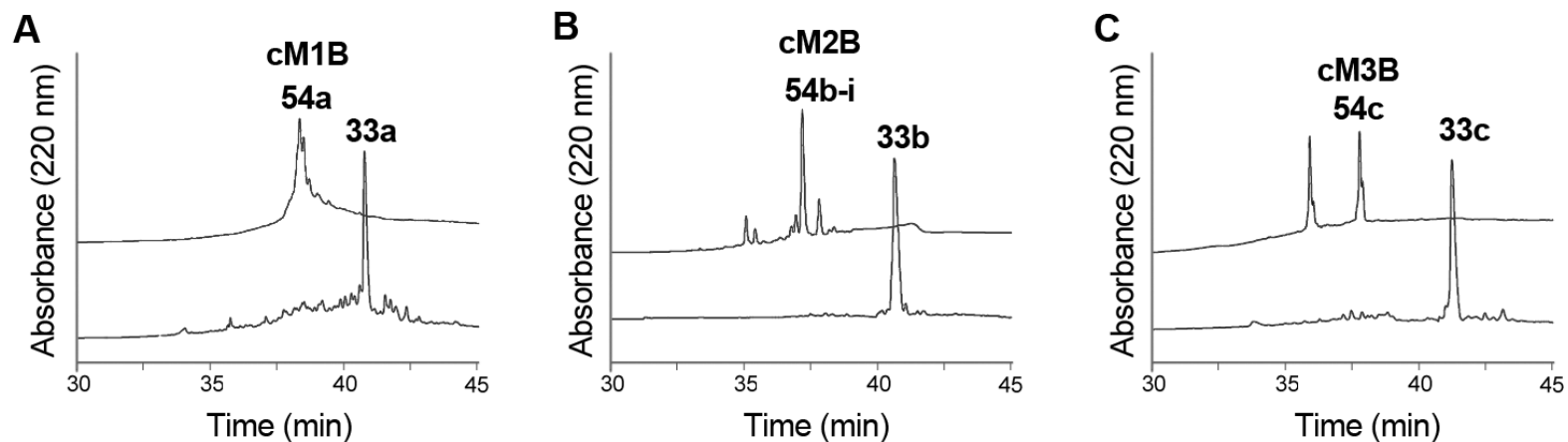
Figure 5-9. **One-pot cyclization and oxidative folding of cM(1-3)B in organic conditions**. Folding reaction was conducted by diluting cyclization mixture using pyridine with 1% morpholine at room temperature and analyzed by RP-HPLC after 1 h. HPLC traces for both cyclization mixture and folding mixture were shown for (A) cM1B, (B) cM2B and (C) cM3B. (HPLC condition: C-18 column 4.6x250 mm, 3.6 u, gradient of 0-40% ACN (with 0.1% TFA) for 80 min, flow rate 1 mL/min).

6. Folding of hedyotide B1 in organic condition

Cyclic reduced hedyotide B1 peptide was subjected to organic folding in a 0.1 mM concentration solution with 70% iPrOH, 10% DMSO, 1% morpholine 19% pyridine, and 100 eq. cysteamine (10 mM). Similar as oxidative folding in buffer described in chapter 3, 70% iPrOH was also a necessary co-solvent in the organic condition. The reaction resulted in 28% yield of native hedyotide B1 within 1 h folding reaction (**Figure 5-10**).
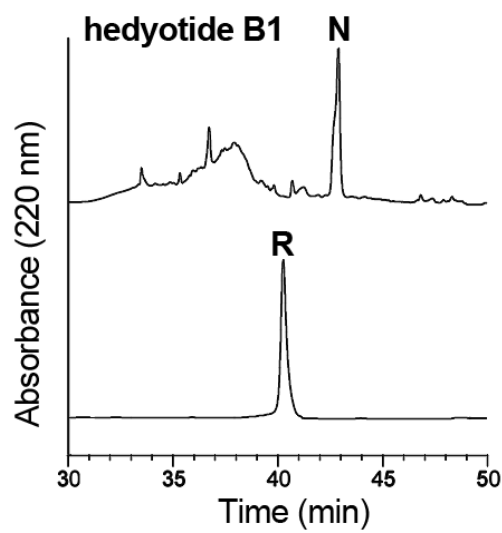
Figure 5-10. **Oxidative folding of hedyotide B1 in the organic condition**. Reaction was performed at room temperature for 1 h. The folded hedyotide B1 was eluted later than its reduced form and mis-fold isomers at 42.5 min. (HPLC condition: C-18 column 4.6x250 mm, 3.6 u, gradient of 0-60% ACN (with 0.1% TFA) for 60 min, flow rate 1 ml/min).

7. Discussion

This chapter describes the development of a new oxidative folding approach using organic system for preparing the disulfide bonds of synthetic cyclic CRPs. This approach performed effectively on two types of model CRPs, hydrophilic cyclic ω-CTXs and hydrophobic cyclotide hedyotide B1. In this novel folding system, several parameters including basicity, temperature, redox reagents and co-solvent were examined to afford an optimized folding yield. In general, pyridine, an organic base with the pKa of 5.2 was used as the major solvent instead of water. Morpholine (pKa 8.4) was used to adjust the basicity that favored the thiol-disulfide exchange. Organic-compatible redox reagents (DMSO, nitrite, MMA, cysteamine and MESNa) were used to facilitate disulfide reshuffling. Various co-solvents were added to enhance the solubility and native conformations of CRPs.

The first improvement of the novel folding approach is shortening the folding reaction time of cyclic ω-CTXs and hedyotide B1 from more than 48 h in the aqueous folding conditions to less than 1 h in the organic conditions. This improvement could be explained by the acceleration of disulfide exchange rate in the organic solvent pyridine. Singh and Whitesides reported the solvent effects on thiol-disulfide exchange reactions [283]. Disulfide reshuffling was S_N2 substitution reactions involving the inter- and intra-molecular nucleophilic thiols. In the aqueous environment, two effects reduced this S_N2 reaction rate, including the solvation of thiols by water and the intramolecular hydrogen bonding of thiols. The use of organic solvent such as DMSO and DMF could avoid both effects and thus accelerate the exchange reaction by 1000-fold. This drastic rate difference varied according to the ratio of water and polar organic solvents as increasing the proportion of water in a mixed solution led to gradual decrease of exchange rate. In my experiments, large increment of the oxidative folding rate as the consequence of the solvent effect was also observed. Even in the presence of 10% water in the one-pot total synthesis of cyclic ω-CTXs and the 70% protic solvent iPrOH as the conformation-promoting co-solvent in the folding of hedyotide B1, the rate of oxidative folding in the organic system were at least 48-fold faster than that in the aqueous conditions. The use of

organic system to confer a fast and efficient folding strategy is therefore a breakthrough in the aspect of disulfide formation.

The other factors, basicity, temperature and redox reagents also influence the reaction rate. In the tested conditions, 1% morpholine provide sufficient basicity to deprotonate thiols into reactive thiolates. Further increase of basicity to 5% could accelerate the reaction by shortening the duration from 1 h to less than 30 min but high basicity might trigger undesired side reactions that lower the folding yield. The aqueous folding of MVIIA performed at low temperature (e.g. 4°C) could afford a better yield than the reaction conduced at room temperature. In the organic folding conditions, this temperature-related effect was not shown. Reactions performed at both temperatures resulted in similar folding profiles.

Three thiols cysteamine (pKa 8.35), MESNa (pKa 9.2), and MMA (pKa 8.08) were examined here. In the presence of mild oxidant DMSO, we expected that these thiols will be oxidized into disulfide dimers and act together with their reduced forms as redox pairs. My results showed that MMA could mediate oxidative folding of the ω-CTXs more efficiently than cysteamine (**Figure 5-7**). MESNa had higher reducing potential than the other two thiols and resulted in more peptides remained in the reduced-form or 1*SS* intermediate states. The difference in the thiol-disulfide exchange mediated by these thiols could be explained by their difference in acidity. Freter *et al*. reported this significant relationship between disulfide exchange rate and the acidity of thiols [284]. After forming the thiol-Cys mix-disulfide species, the substitution of thiolate by another thiol in the solvent depended on their nucleophilicity: the more acidic thiolate was released and the less acid one was retained to yield a new disulfide bond. Therefore, a thiol of Cys (pKa 8.3) could attack the MMA-Cys mix-disulfide species to release MMA and form an intramolecular disulfide bond, while the exchange of cysteine thiol group with cysteamine-Cys only resulted in about 50% chance to give a desired disulfide bond. In the folding of hedyotide B1, cysteamine worked efficiently due to a different reason. The organic environment and high alcohol content enhanced the conformation of hedyotide B1 by externalize the hydrophobic side chains to the surface and

gave space to disulfide exchange in the core region. Thus the intramolecular disulfide exchange occurred in proximity, which brought the reaction towards formation of native disulfide bonds.

The second improvement of the organic folding is increasing the peptide concentration in the folding reactions. For both MVIIA and hedyotide B1, the peptide concentration used in the aqueous folding reaction was 10 μM. The reason for using such diluted solutions in the aqueous conditions is to prevent intermolecular disulfide crosslinking that often result in peptide aggregation and precipitation. However, the high dilution results in a large volume of folding mixture that often causes more peptide loss by sticking to the container surface and during the extensive purification. In the organic folding conditions, the use of pyridine increased peptide solubility and suppressed intermolecular interactions, thus allowed oxidative folding to perform in more concentrated peptide solutions (e.g. 0.1 mM). After folding, pyridine could be easily removed from the folding mixture by *in vacuo* evaporation.

Co-solvents including detergents, denaturants, salts, or alcohols are often used to prevent peptide aggregation by suppressing intermolecular non-covalent interactions and act as conformation-promoting reagents. The organic environment was ideal for the hydrophobic hedyotide B1 and addition of 70% iPrOH would further facilitate its folding by promoting the native conformation of hedyotide B1. In contrast, the conventional additive in the oxidative folding of hydrophilic CRPs are salts or charged amino acids (e.g. Arg for negatively-charged CRPs) [285-288]. Surprisingly, the optimized conditions for MVIIA folding in the 0.1 M ammonium acetate buffer with 2 M ammonium sulfate did not promise the folding of the cyclic analogs of MVIIA, which suggested that the folding condition was already changed on these cyclic engineered analogs. A similar report by Price-Cartier *et al*. described the oxidative folding of 2*SS* linear analogs of MVIIA (one-pair of disulfide bond Cys residues substituted by Ala) [289]. In the aqueous folding conditions, these *2*SS linear analogs tended to form disulfide isomers in an equilibrium state rather than accumulated in the native-fold form. In the organic conditions, we found that high salt condition is not necessary for the folding of cyclic ω-CTXs. The 10% DMSO served as both

oxidant and solvent in the folding mixture [232]. The hydrophilic sequences of cyclic ω-CTXs did not dissolve well in 100% pyridine and thus needed to be dissolved in the DMSO/thiols mixture first followed by addition of pyridine. In the one-pot reaction, small proportion of water solved the solubility problem of hydrophilic cyclic ω-CTXs. The fast exchange rate in the 90% organic solvent condition allowed accumulation of folding products in a short reaction time.

The third advantage of the organic folding approach was the establishment of a one-pot total synthesis scheme incorporating the newly developed TEA-mediated cyclization approach. A cyclization mixture of cyclic ω-CTXs (without MESNa during thioesterification and cyclization) could be diluted 10 times with pyridine/morpholine/DMSO solution and started the organic folding reaction after addition of external thiols. This approach resulted in similar HPLC profile as the reaction using purified cyclic peptides, but the overall yield of folded cyclic product was more than two times better than the two step reaction. More excitingly, I found that t-butyl-nitrite could be used as the oxidant to pair with MMA as redox reagents, which gave the similar folding yield as DMSO/MMA pair. Nitrite was the key compound used in azide formation, thus the cyclization mixture of azide method already contained the redox for the organic folding. In the one-pot system incorporating azide-mediated cyclization and organic folding, cyclic ω-CTXs were able to be prepared within 3 h with a slightly lower yield than the combination of TEBA-mediated cyclization and organic folding.

The chemoselective folding used to be considered as a promising approach for preparing cysteine-rich peptides but limited by the complicated procedures and peptide loss during the intensive purification steps. Moreover, I found that the chemoselective disulfide formation of cM2B resulted in two products **54b-i/ii**. These two isomers had identical disulfide connectivity but they might be different in the orientation of loops K2-D14 and T17-K24 (**Figure 5-11**). After removal of organic solvents, non-covalent interactions might occur to stabilize these two conformations. This unexpected finding suggested that the chemoselective disulfide formation was not "100% promising" for preparing CRPs containing flexible loops. Such phenomenon

has been observed previously in the folding of human uroguanylin, a CRP with 16 residues and two disulfide bonds, using chemoselective approach [277]. Chino *et al*. reported the formation of two topological isomers of uroguanylin, with identical disulfide connectivity but different in bioactivity, optical rotation or 2D NMR. The ratio of these two isomers obtained from iodine oxidation was found to be depended on the order of disulfide-bond-formation.

Collectively, the novel oxidative folding strategy using organic system accelerated the folding rate of cyclic ω-CTXs and hedyotide B1 by more than 48-fold as compared with the conventional aqueous folding conditions. The peptide concentration could be brought up to 0.1 mM without formation of precipitants. The neat and efficient organic folding reaction could be performed in one-pot with the TEA-mediated or azide-mediated cyclization reactions. The shortened reaction time, tolerance of higher peptide concentration and one-pot reaction established a rapid and high-throughput one-pot synthesis scheme for the preparation of cyclic CRPs including cyclic conotoxins and cyclotides.
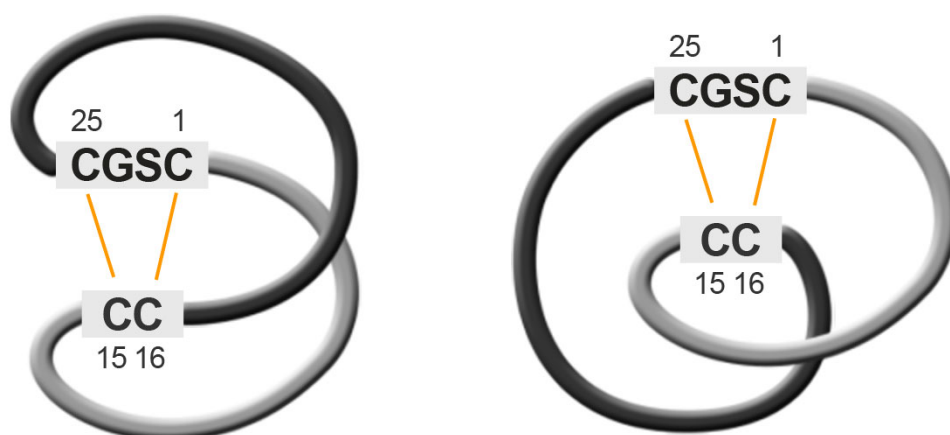
Figure 5-11. A putative model to illustrate the conformational difference between two cM2B isomers 54b-i/ii. Two cM2B isomers prepared by chemoselective folding reactions possess the same disulfide bonds C1-C16 and C15-C25. The orientation of loops K2-D14 and T17-K24 may be different, which lead to different conformations of these two folding products.

Chapter 6. Design and Synthesis of cyclic conotoxins with new bioactive functions

1. Introduction

Cationic and cysteine-rich sequences are the common characters observed in host-defense antimicrobial peptides (AMP). The membrane-associated mechanism of AMPs can effectively prevent development of drug resistance. The works herein describe for the first time that a ω-conotoxin MVIIA has been converted into AMP by backbone cyclization. Although MVIIA possesses the cationic and cysteine-rich characters that related to AMPs, it only exhibits weak inhibitory effect against fungi and it is not toxic to common bacteria strains. The antimicrobial activity was evoked after joining the N- and C-termini together by a short Gly-Ser linker to form a neo-epitope on the three cyclic 2*SS* analogs cM(1-3)B. This neo-epitope contains five out of six positive residues of the whole sequence (**Figure 6-1**). Therefore I hypothesize that the backbone cyclization not only increases the molecular rigidity and also stabilizes the neo-epitope with an enhanced microbial membrane-recognition activity. The increased hydrophobicity due to Cys→Abu substitution can also enhance the membrane disruption activity upon interaction of the neo-epitope with microbial membrane.
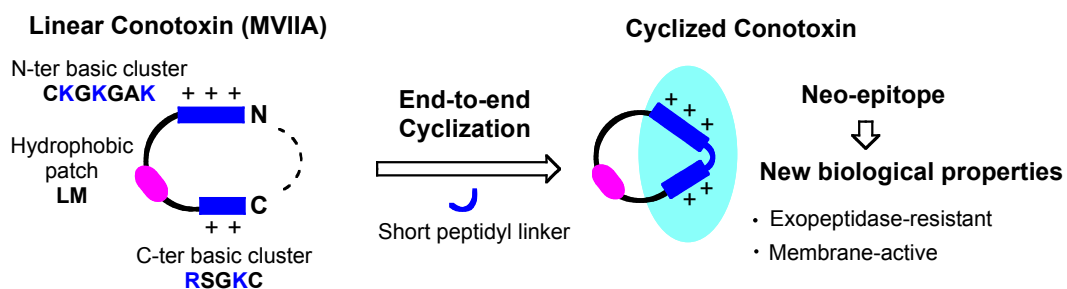
Figure 6-1. **Schematic representation of engineering cyclic ω-conotoxin MVIIA by backbone cyclization**. It creates a neo-epitope as a contiguous cationic segment in the cyclic form that exhibits new biological functions. The topological changes of positively charged residues and hydrophobic amino acids are highlighted in blue and pink, respectively.

The list of synthetic conotoxins derived from MVIIA and their synthesis strategies were summarized in **Figure 6-2** and **Table 6-1**. I prepared synthetic MVIIA **47**, a 3*SS* linear analog M-GS **48**, three 2*SS* cyclic analogs cM(1-3)B **54a-c**, six (1SS+2Acm) cyclic analogs **53a-c (i/ii)** obtained by DMSO oxidation, and a cysteine-free cyclic analog cM6A **59** prepared by global desulfurization of which all Cys residues were converted into Ala.

These cyclic and linear synthetic conotoxin analogs were subjected to a series of biological assays to characterize their AMP-like properties, which included anti-microbial assays against gram-positive bacteria, gram-negative bacteria and fungi, hemolytic assay against human erythrocytes, chemotaxis assay using human monocytic THP-1 cells and cell penetration assay using lung carcinoma H1299 cells. The effects of backbone cyclization and modified disulfide linkages to the structure and functions have been explored. The intrinsic calcium channel binding activities of conotoxins was not examined here on these 0-2*SS* cyclic ω-CTXs, since the potency of MVIIA on blocking *N*-type calcium channels has been proved to be largely affected by removing any disulfide bond from the cystine-knot [289].
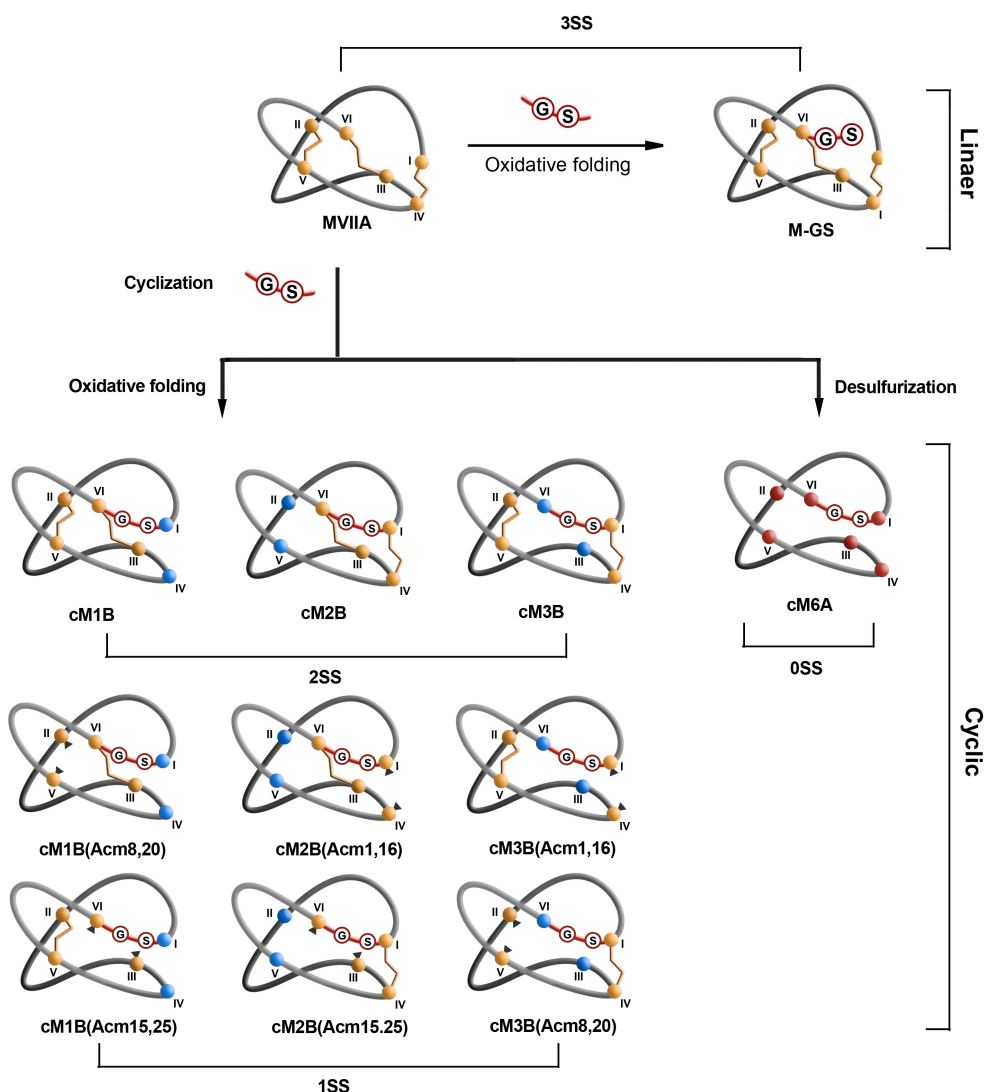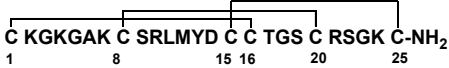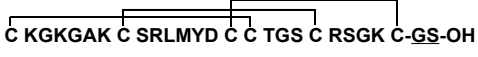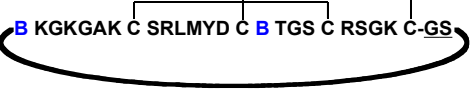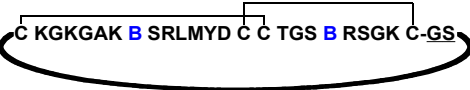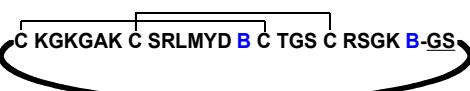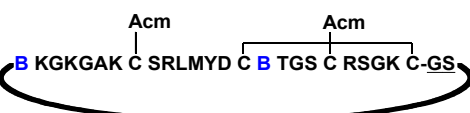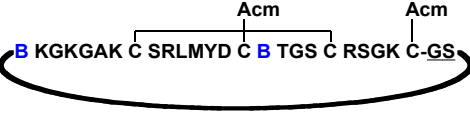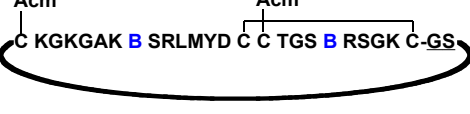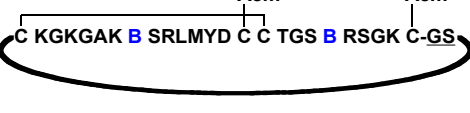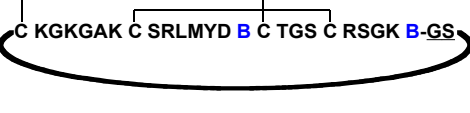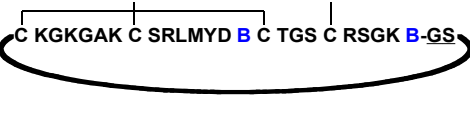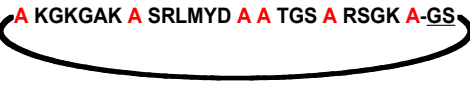
Figure 6-2. **Schematic illustration and synthetic strategies of linear and cyclic analogs of ω-conotoxin MVIIA**. All ten possible cyclic analogs with zero to two disulfide bonds were synthesized. One linear analog with GS-tail and three disulfide bonds was prepared for comparison. (Color theme: GS linker - single letter code in the red circle; Cys - orange solid sphere; Abu - blue solid sphere; Ala - red solid sphere disulfide bonds - yellow sticks, Acm - black triangles).

Table 6-1. **List of synthetic conotoxin peptides used in antimicrobial assays.**

Peptides	Sequence and disulfide bonds	Synthesis steps
MVIIA **43**	C KGKGAK C SRLMYD C C TGS C RSGK C-NH$_2$ (positions 1, 8, 15 16, 20, 25)	Fmoc-SPPS, Oxidative folding (aqueous)
M-GS **46**	C KGKGAK C SRLMYD C C TGS C RSGK C-GS-OH	Fmoc-SPPS, Oxidative folding (aqueous)
cM1B **54a**	**B** KGKGAK C SRLMYD C **B** TGS C RSGK C-GS (cyclic)	Fmoc-SPPS, Cyclization, Oxidative folding (organic)
cM2B **54b**	C KGKGAK **B** SRLMYD C C TGS **B** RSGK C-GS (cyclic)	Fmoc-SPPS, Cyclization, Oxidative folding (organic)
cM3B **54c**	C KGKGAK C SRLMYD **B** C TGS C RSGK **B**-GS (cyclic)	Fmoc-SPPS, Cyclization, Oxidative folding (organic)
cM1B (Acm8, 20) **53a-i**	**B** KGKGAK C SRLMYD C **B** TGS C RSGK C-GS (cyclic, Acm, Acm)	Fmoc-SPPS, Cyclization, DMSO oxidation
cM1B (Acm15,25) **53a-ii**	**B** KGKGAK C SRLMYD C **B** TGS C RSGK C-GS (cyclic, Acm, Acm)	Fmoc-SPPS, Cyclization, DMSO oxidation
cM2B (Acm1,16) **53b-i**	C KGKGAK **B** SRLMYD C C TGS **B** RSGK C-GS (cyclic, Acm, Acm)	Fmoc-SPPS, Cyclization, DMSO oxidation
cM2B (Acm15,25) **53b-ii**	C KGKGAK **B** SRLMYD C C TGS **B** RSGK C-GS (cyclic, Acm, Acm)	Fmoc-SPPS, Cyclization, DMSO oxidation
cM3B (Acm1,16) **53c-i**	C KGKGAK C SRLMYD **B** C TGS C RSGK **B**-GS (cyclic, Acm, Acm)	Fmoc-SPPS, Cyclization, DMSO oxidation
cM3B (Acm8,20) **53c-ii**	C KGKGAK C SRLMYD **B** C TGS C RSGK **B**-GS (cyclic, Acm, Acm)	Fmoc-SPPS, Cyclization, DMSO oxidation
cM6A **59**	**A** KGKGAK **A** SRLMYD **A** **A** TGS **A** RSGK **A**-GS (cyclic)	Fmoc-SPPS, Cyclization, Desulfurization

Color theme followed Fig. 5-2 as Abu (blue) and Ala (red).

2. Synthesis of cyclic and linear conotoxins

Preparation of MVIIA, linear analog M-GS, and cyclic analogs with one or two disulfide bonds has been reported in chapter 4 and 5. The synthetic MVIIA was prepared on Rink amide resins using the Fmoc synthetic scheme shown in **Figure 5-1A** to give reduced MVIIA-NH$_2$ **42**. The linear conotoxin analog M-GS was synthesized on Wang resins using the scheme described in **Figure 5-2B** to give M-GS-OH **45**. These two linear precursors were subjected to oxidative folding to afford 3*SS* MVIIA **43** and M-GS **46**. The cyclic analogs cM(1-3)B **54a-c** with two disulfide bonds were prepared using both TEBA-linker and azide method followed by oxidative folding in organic conditions. The (1*SS*+2Acm) cyclic analogs **53a-c(i/ii)** were prepared by TEBA-mediated cyclization and DMSO oxidation as shown in **Figure 5-4**. The disulfide-free cM6A **59** was obtained by global desulfurization of cM-GS (Fig. 6-3A). The cyclic reduced precursor cM-GS **57** ([M+H] = 2772 Da) was synthesized using TEBA method with isolated yield of 17.8% (0.05 mmol synthesis scale resulted in 63 mg crude precipitant and 23 mg purified cM-GS), and then it was subjected to global desulfurization mediated by free radicals as introduced by Wan and Danishefsky [290]. Purified cM-GS **57** (0.1 mM) was mixed with a water-soluble radical initiator VA-044 (10 eq.), a phosphine source TCEP (500 eq.), a proton donor glutathione (1000 eq.) in a phosphate buffer (pH 6.5). The reaction mixture was treated at 40°C with gentle stirring for 3 h to afford a cysteine-free cyclic analog cM6A **59** (calc. 2579.9 Da, found 2580.7 Da) (**Figure 6-3B**). VA-044 is a thermal initiator, therefore without acceleration by heating, the desulfurization reaction was slow.

A

B

C
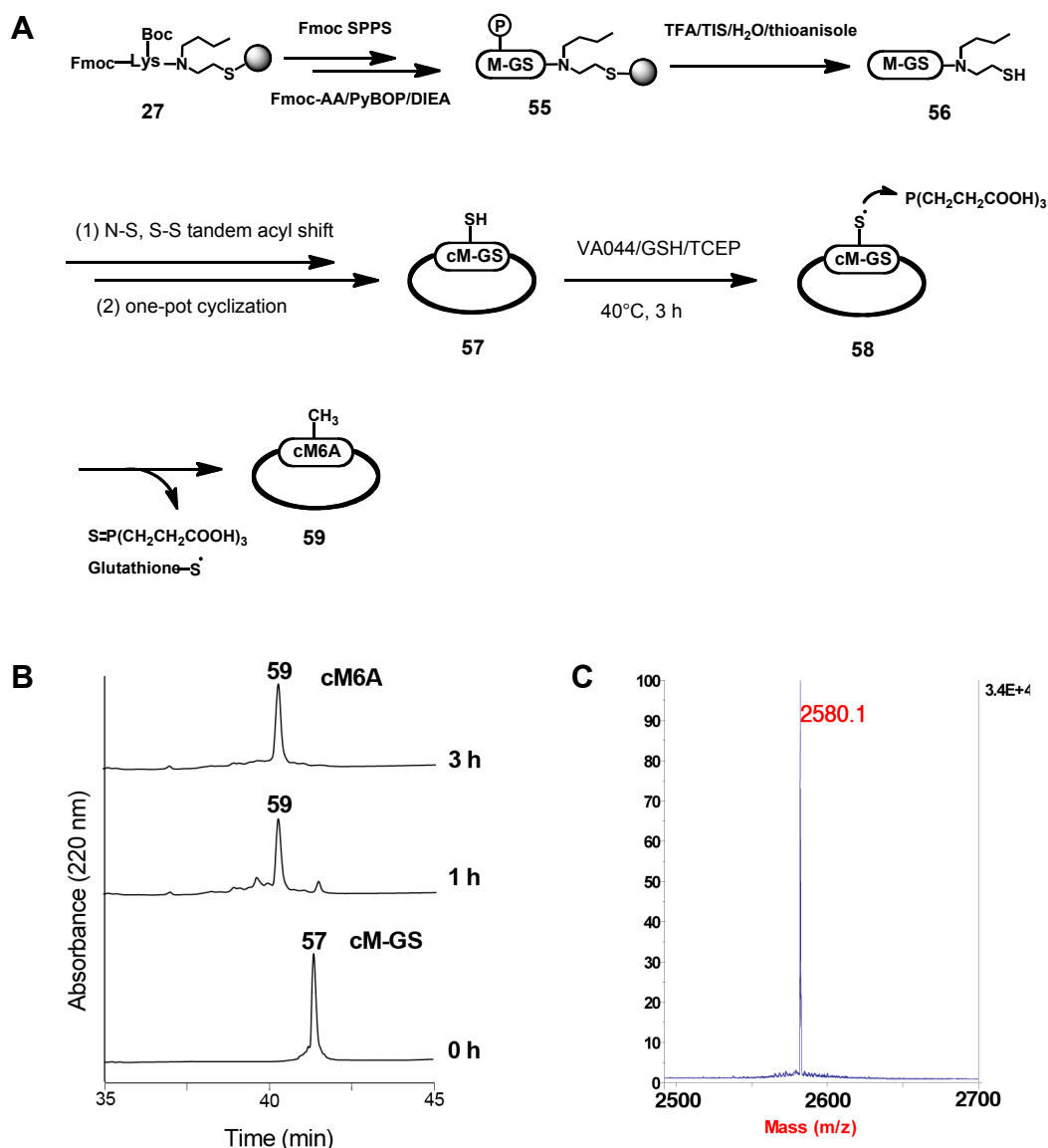
Figure 6-3. **Synthesis of cystine-free cyclic MVIIA analog cM6A 59 from precursor peptide cM-GS 58.** (A) Synthesis scheme of cM6A **59** by TEBA-mediated one-pot cyclization followed by radical-mediated desulfurization that converted Cys residues into Ala. (B) HPLC profile of the radical-catalyzed global desulfurization to prepare cM6A **59** from its precursor cM-GS **57.** (HPLC condition: C-18 column 4.6x250 mm, 3.6 u, gradient of 0-40% ACN (with 0.1% TFA) for 80 min, flow rate 1 ml/min). (C) Characterization of cM6A by MALDI-TOF MS.

3. Stability of cyclic conotoxins

To investigate the roles of cyclic backbone and disulfide bonds on molecular stability, MVIIA and analogs M-GS, cM(1-3B) and cM6A were subjected to stability tests including heating, acid hydrolysis and trypsin digestion.

The heating stability assay was conducted by dissolving peptides (0.1 mM) in deoxygenated water (prepared by 15 min N_2 bubbling) and boiling at constant 100°C (utilizing PCR machine with heat cap). The integrity of peptides was monitored by analytical HPLC at several time points as shown in **Figure 6-4**. After 3 h heating, 48% MVIIA were hydrolyzed. The linear analog M-GS with additional C-terminal tail to the pseudo-cyclic backbone produced 55% hydrolysis. The cysteine-free cyclic analog cM6A showed low heat stability of which only 30% remained after 3 h heating. The 2*SS* cyclic conotoxins cM1B, cM2B and cM3B showed better heating stability as 67.1%, 86.6% and 61.2% of the respective starting peptides remained intact after 3 h heating. A few degradation products with mass ranged from 1 kDa to 2kDa were formed due to two or more hydrolysis. Trace amount of products with mass same as the starting 2*SS* cyclic conotoxins were detected by MALDI-TOF MS with different RT as the start material, which suggested formation of thermal-induced conformers or disulfide-reshuffled products.

The stability tests against acid hydrolysis were performed at 37°C in the acidic condition of 0.25 M HCl that simulated the acidity of stomach. The hydrolysis progresses were monitored by analytical HPLC (**Figure 6-5**). Consequently, majority (>85%) of MVIIA, M-GS and 2*SS* cyclic conotoxins remained intact after 6 h treatment. Cysteine-free cM6A was exceptionally not acid stable as about 50% peptides were hydrolyzed. The results suggested that disulfide bonds played a major role in stabilizing MVIIA and its cyclic analogs against acid hydrolysis.
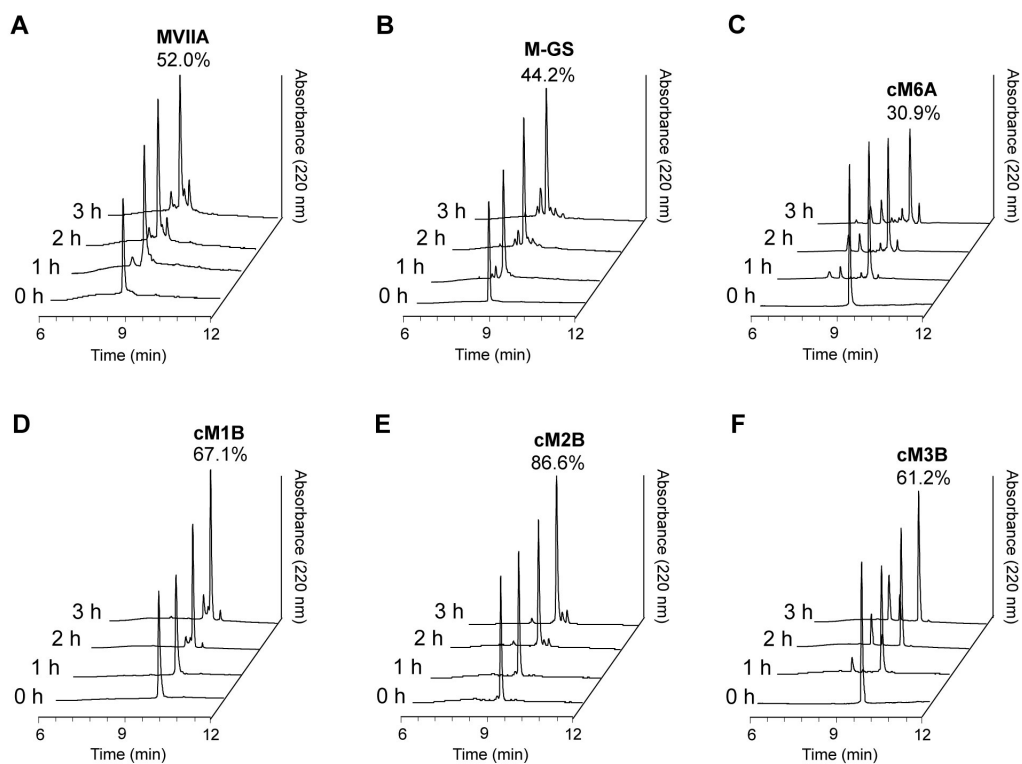
Figure 6-4. **HPLC analysis of synthetic conotoxins against boiling at 100°C. (A) MVIIA, (B) M-GS, (C) cM6A, (D) cM1B, (E) cM2B, (F) cM3B**. (HPLC condition: C-18 column 4.6x150 mm, 3.6 u, gradient of 0-50% ACN (with 0.1% TFA) for 15 min, flow rate 1 ml/min, column-oven at 60°C).
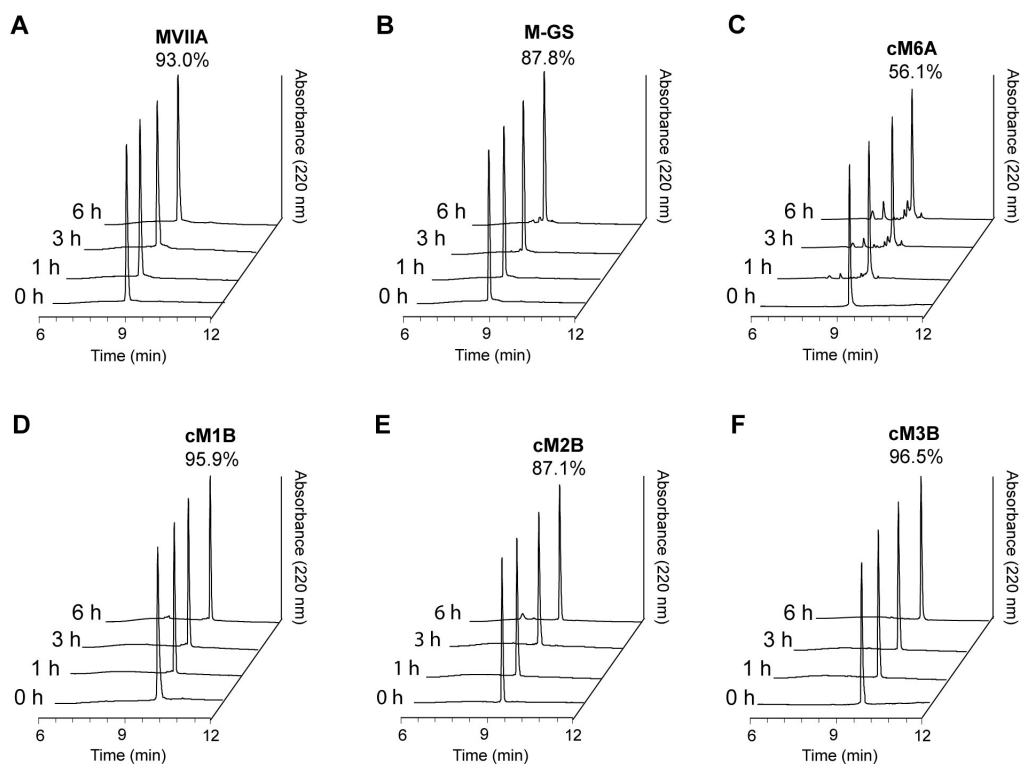
Figure 6-5. **HPLC analysis of synthetic conotoxins under acid hydrolysis in 0.25 M HCl at 37°C.** (A) MVIIA, (B) M-GS, (C) cM6A, (D) cM1B, (E) cM2B, (F) cM3B. (HPLC condition: C-18 column 4.6x150 mm, 3.6 u, gradient of 0-50% ACN (with 0.1% TFA) for 15 min, flow rate 1 ml/min, column-oven at 60°C.)

As shown in the summary chart of heating and acid stability assays (**Figure 6-6**), in the heating stability assays, all three 2*SS* cyclic ω-CTXs were more stable than their 3*SS* linear counterparts, MVIIA and M-GS, due to backbone cyclization. In the acid hydrolysis assays, the cyclic backbone partially restored the function of cystine-knot motif, which provided the 2*SS* cyclic ω-CTXs comparable stability as MVIIA. In contrast, the disulfide-free cM6A possessed the lowest stability in both assays. Collectively, both cyclic backbone and cystine-knot motif played important roles on protecting the molecules from peptide bond hydrolysis. The reduced conformational rigidity due to deletion of single disulfide bond could be partially rescued by backbone cyclization.
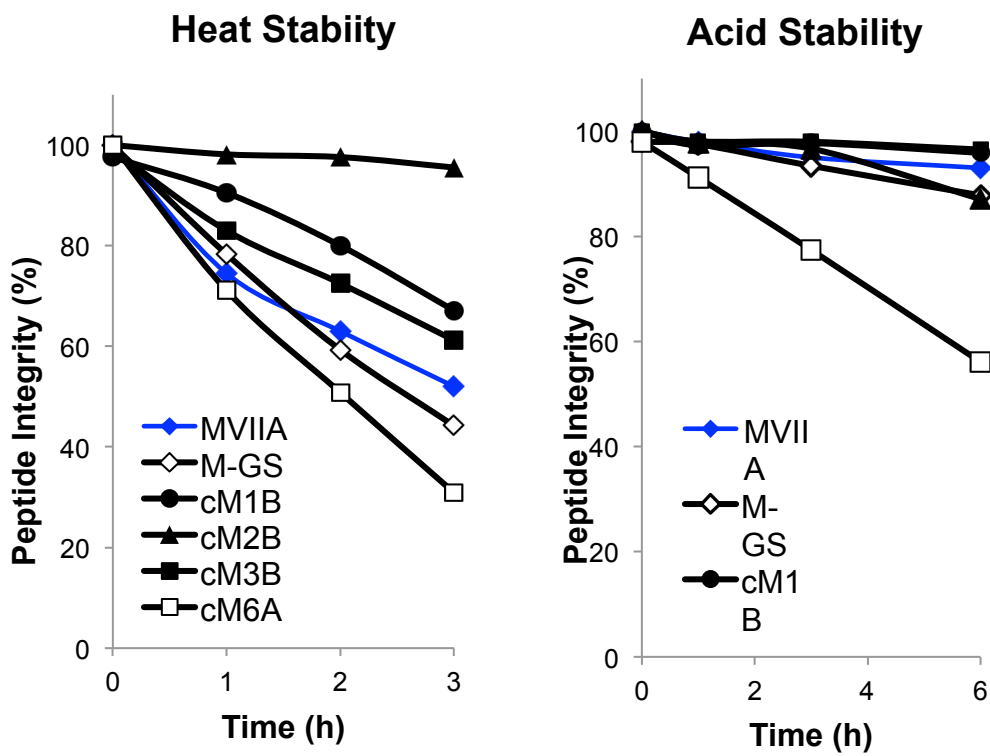
Figure 6-6. **Comparison of stabilities against heating and acid hydrolysis.**

To evaluate the metabolic stability of synthetic cyclic conotoxins, the tryptic digestion reaction was performed using a peptide: trypsin = 50:1 (*w/w*) ratio at pH 7 at 37°C. Digestive products were analyzed by analytical HPLC and MALDI-TOF MS. As shown in **Figure 6-7**, all four peptides were completely digested by trypsin at Arg/Lys residues after 30 min to give digestive fragments that linked by disulfide bonds. In a short time course of 5 min digestion, HPLC monitoring showed that more 3*SS* MVIIA was remained intact than the 2*SS* cyclic *ω*-CTXs. These data showed that linear conotoxin with cystine-knot motif had better trypsin-resistance than the 2*SS* cyclic analogs. The primary structure of MVIIA possessed six Arg/Lys residues and thus highly trypsin-susceptible. My results indicated that the structure-stabilizing effect of macrocyclic backbone was not sufficient to protect the trypsin-susceptible sites on 2*SS* cyclic analogs. For CRPs that resistant against proteolytic degradation, their cystine-knot structure may be the most important factor that prevents them to be digested by proteases.
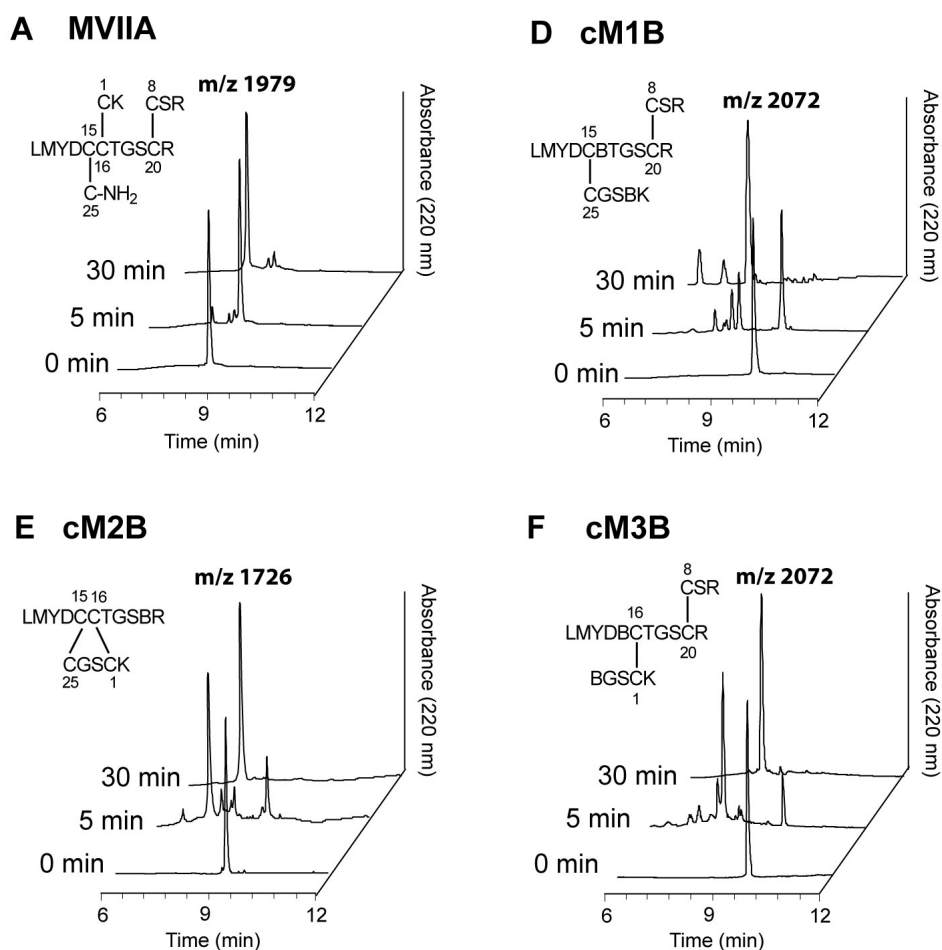
Figure 6-7. **The HPLC analysis of tryptic digestion of synthetic conotoxins**. Reaction mixture was directly injected into analytic column after 30 min reaction. (A) MVIIA and its largest tryptic digestion product LMYDCCTGSCR-C-CK-CSR ([M+H] = 1979 Da). (B) cM1B and its largest tryptic digestion product LMYDCBTGSCR-CGSBK-CSR ([M+H] = 2072) (C) cM2B and its largest tryptic digestion product LMYDCCTGSBR-CGSCK ([M+H] = 1726) (D) cM3B and its largest tryptic digestion product LMYDBCTGSCR-BGSCK-CSR ([M+H] = 2072). (HPLC condition: C-18 column 4.6x150 mm, 3.6 u, gradient of 0-50% ACN (with 0.1% TFA) for 15 min, flow rate 1 ml/min, column-oven at 60°C).

196

4. Antimicrobial activity

The antimicrobial assays of linear and cyclic conotoxins were performed on Gram negative strain *E. coli*, Gram positive strain *S. aureus* and fungus *C. tropicalis* using radial-diffusion assay as described by Steinberg and Lehrel [291] (Table 5-2). An underlay gel containing 0.3 mg/mL tryptic soy broth (TSB) powder and overlay gel containing double-strength nutrient of 60 mg/mL TSB powder were prepared using 10 mM sodium phosphate and 1% agarose. In the assays under high-salt condition, additional 100 mM NaCl was added into underlay gel. The series dilution of synthetic conotoxin analogs was prepared using 0.1% AcOH containing 1% bovine serum albumin (BSA) culture medium. The microbial inhibitory effect was reflected by the size of clear zone on the culture gel. The diameter of each clear zone was measured and plotted against corresponding peptide concentration, which gave a linear regression when the x-axis (peptide concentration) was in logarithmic scale. The minimal inhibitory concentration (MIC) of the antimicrobial reagent was obtained from the x-intercept directly from the plot.

The native MVIIA and its linear analog M-GS were inactive at concentrations up to 500 μM against both Gram-negative *E. coli* and Gram-positive *S. aureus* whereas its cyclic MVIIA analogs were active with MICs at μM level (**Table 6-2**). The MICs of 2*SS* cyclic analogs against both strains were below 9 μM. The MICs of 1*SS* cyclic conotoxins against the tested strains varied from 3.3 to 78.2 μM. The cystine-free cM6A displayed antibacterial activity with MICs below 10 μM and a larger zone outside the clear inhibition zone, which had about 50% less colony density (**Figure 6-8**). This phenomenon indicated that cM6A might possess a concentration-dependent bimodal activity, as at sub-μM concentration, it was bacteriostatic. The MVIIA exhibited moderate anti-fungal activity against *C. tropicalis*, with MIC 38 μM, and its 2*SS* cyclic cM(1-3)B analogs showed a 3- to 18-fold improvement with MICs ranging from 2 to 13 μM. The inhibitory effects of most 1*SS* cyclic analogs against fungus were improved to MIC < 20 μM, except cM1B(Acm15, 25) with MIC at 42.2 μM.

Similar to human defensins and cyclotides, the effect of end-to-end cyclization did not expand the range of antimicrobial activities in a serum-like high-salt condition. All cyclic analogs showed no inhibition against microbial strains up to 0.5 mM peptide concentration in the presence of 100 mM NaCl.

Comparing the linear and cyclic MVIIA analogs, only the cyclic MVIIA analogs exhibited antimicrobial activity against bacteria. In contrast, the linear derivative M-GS with a C-terminal Gly-Ser dipeptide was inactive against bacteria. This result suggested that the GS linker had no effect in promoting the antimicrobial activity, while backbone cyclization played a key role on creating the antimicrobial neo-epitope. From this set of data, I observed that the antimicrobial activity was not correlated with the number of disulfide bonds, which suggested that this membrane-active property was more relied on the primary sequence rather than disulfide-stabilized structures. Similar phenomenon has been reported in disulfide-containing β-defensin HBD-3, as the completed reduction did not abolish its antimicrobial activity [292].

Table 6-2. **Antimicrobial activities of synthetic conotoxins.**

Peptide	SS	Backbone	*E. coli* (Gram-) MIC (μM)	*S. aureus* (Gram+) MIC (μM)	*C. tropicalis* MIC (μM)
MVIIA	3	Linear	> 500	> 500	39.8
M-GS	3	Linear	> 500	> 500	ND
cM1B	2	Cyclic	8.9	7.9	11.2
cM2B	2	Cyclic	8.4	8.0	2.0
cM3B	2	Cyclic	8.6	4.2	2.3
cM1B(Acm8,20)	1	Cyclic	12.6	30.2	6.74
CM1B(Acm15,25)	1	Cyclic	3.32	78.2	42.2
cM2B(Acm1,16)	1	Cyclic	11.4	21.2	15.6
cM2B(Acm15,25)	1	Cyclic	39.4	18.8	4.88
cM3B(Acm1,16)	1	Cyclic	7.94	18.2	7.90
cM3B(Acm8,20)	1	Cyclic	4.12	7.42	6.92
cM6A	0	Cyclic	7.4	8.9	ND

MIC: minimal inhibitory concentration
ND: not determined

cM1B (100 µM)   cM6A (100 µM)

10 mm
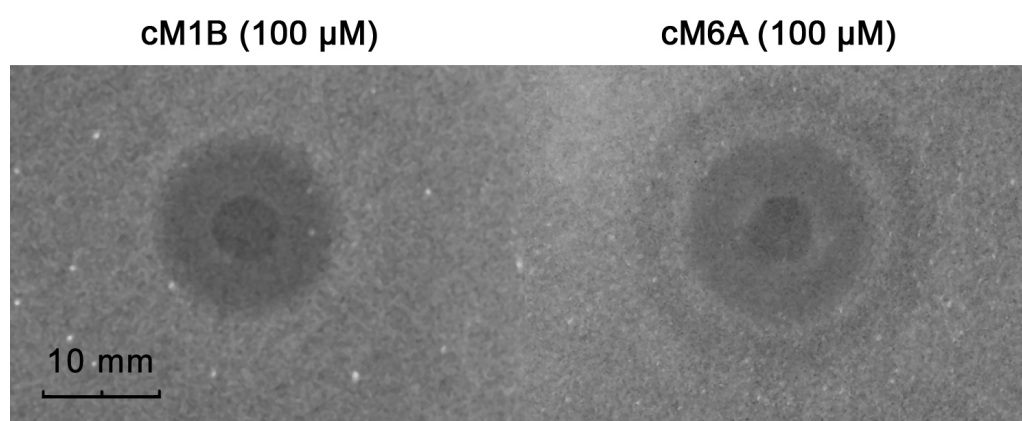
Figure 6-8. **Bi-model antimicrobial activity of cM6A in the radial diffusion assay against *E. coli*.** With the same peptide concentration of 100 µM, cM1B resulted in a normal clear zone (diameter 11.4 mm) as shown in the left panel. In contrast, cM6A resulted in a partial-clear ring outside of the clean zone (diameter 11.8 mm) as shown in the right panel.

5. Membranolytic selectivity

A common characteristic of AMPs is the membranolytic selectivity against microbial and host cell membranes. This selectivity indicates the therapeutic index of an antimicrobial compound and it can be measured the ratio of HD_{50}/MIC. The HD_{50} refers to compound concentration that gives 50% hemolysis of human erythrocytes. Using fresh human erythrocytes isolated from donor's blood, the hemolytic levels caused by different concentrations of synthetic conotoxins were determined by the amount of hemoglobin released into medium by measuring the absorbance at 540 nm. The HD_{50} of MVIIA was determined to be 4.2 mM, and the HD_{50} of 2*SS* cyclic analogs cM1B, cM2B and cM3B were 2.8, 1.3 and 1.9 mM, respectively (**Table 6-3**). The HD_{50} of six 1*SS* cyclic analogs ranged from 1.4 to 3.4 mM. All ten cyclic MVIIA peptides were relatively low hemolytic ($HD_{50} > 1$ mM) but removal of disulfide bonds led to decreased HD_{50} values. The resultant therapeutic indexes HD_{50}/MIC against three microbes were ranged from 36 to 1016.

Collectively, these results indicated that backbone cyclization changed the surface morphology and thus created a neo-epitope with a broad-spectrum of antimicrobial activities on ten cyclic ω-CTXs. The conformational constraints by disulfide linkages were relevant to the non-hemolytic nature of MVIIA and its analogs, but they did not play a substantial role in modulating the antimicrobial effect of the new epitope in the cyclic ω-CTXs.

Table 6-3. The membranolytic selective index (HD_{50}/MIC) of the synthetic conotoxins against microbes or human erythrocytes.

Peptide	*SS*	Backbone	HD_{50} (μM)	HD_{50}/MIC (*E. coli*)	HD_{50}/MIC (*S. aureus*)	HD_{50}/MIC (*C. tropicalis*)
MVIIA	3	Linear	4229	-	-	105.8
cM1B	2	Cyclic	2827	317.6	357.8	252.4
cM2B	2	Cyclic	1316	156.7	164.5	658.0
cM3B	2	Cyclic	1608	187.0	382.9	699.1
cM1B(Acm8,20)	1	Cyclic	1527	121.2	50.6	226.6
CM1B(Acm15,25)	1	Cyclic	3374	1016.3	43.1	80.0
cM2B(Acm1,16)	1	Cyclic	2547	223.4	120.1	163.3
cM2B(Acm15,25)	1	Cyclic	1423	36.1	75.7	291.6
cM3B(Acm1,16)	1	Cyclic	3067	386.3	168.5	387.7
cM3B(Acm8,20)	1	Cyclic	1445	350.7	194.7	208.8

MIC: minimal inhibitory concentration.

HD_{50}: median hemolytic dose that resulted in hemolysis of 50% erythrocytes.

6. Chemotactic activity

Human defensins are known to have chemokine-like chemotactic effects to attract immune cells through binding with G-protect coupled receptors [293-295], which enhances anti-pathogenic responses of host defensive system. We envisioned that the AMP-like cyclic ω-CTXs might also be chemotactic. Chemotaxis assay was performed with human pro-monocytic THP-1 cells using a 96-well Boyden microchambers. Peptide solutions with concentration ranging from 1 nM to 1 mM (7-log scale) were added to the bottom chamber wells. 1×10^6 cells were added into each well of the upper chamber. The chamber plate was incubated at 37°C for 6 h. The THP-1 cells that migrated through the 5 μm polycarbonate filter were lysed and determined by a nucleic acid-interacting CyQuant® fluorescent dye with UV plate reader at 480nm/520 nm. The number of THP-1 cells was quantified by the correlated values of relative fluorescent units (RFU) (**Figure 6-9A**). In the negative control that only RPMI medium was given in the lower chamber well, THP-1 cells migrated randomly with a average migration of 4.3%. In the wells containing cyclic ω-CTXs, THP-1 cells migrated in a concentration-dependent manner (**Figure 6-9B**). The synthetic MVIIA and cyclic ω-CTXs cM(1-3)B started to be chemoattractive at nM concentration. At μM concentration, the migration ratio ranged from 10-14%.

A

B
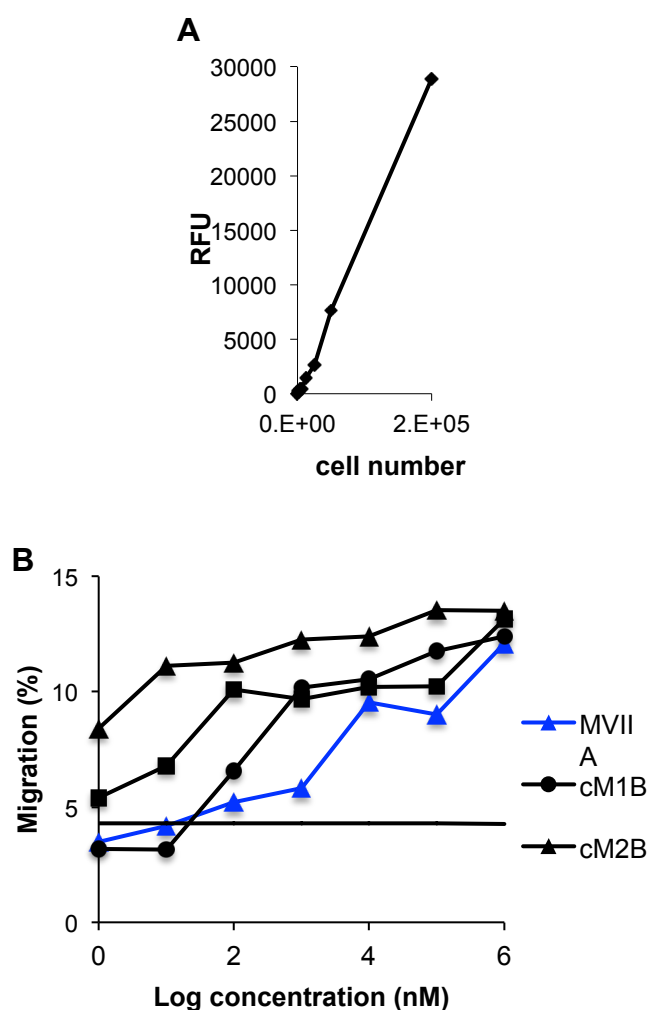
Figure 6-9. **Chemotactic activities of MVIIA and 2*SS* cyclic ω-CTXs**. (A) Quantitation test of THP-1 cells. 2×10^5 cells gave 28907 RFU readout averaged from three assays. (B) Plot of migration (%) against peptide concentration. Peptides solutions were prepared using RMPI medium (1% penicillin/streptomycin) with the concentration ranged from 1 nM to 1 mM (7 log scales). Control assay was conducted with RPMI medium alone without FBS or chemoattractants. 2×10^5 cells in 0.1 ml PBS were used for each assay. Migrated cells were lysed after 6 h and the amount of DNA in the lysate was quantified by CyQuant® fluorescent Dye (480/520 nm). The average RFU readouts from the duplicated assays were used for calculating the percentage of migration.

7. Cell-penetrating activity

A representative biotinylated 2*SS* cyclic conotoxin cM1B-K7biotin **63** (calc. 2956.0 Da, found 2957.7 Da) containing Lys(Biotin) at position K7 was prepared using TEBA-mediated cyclization and organic folding. The purified peptide **63** was incubated with H1299 carcinoma cells at a concentration of 15 μM at 37°C, 5% CO_2 for 30 min. After fixation and permeabilization, the fluorescein-conjugated tags were loaded separately. The biotinylated peptides were labeled with avidin-FITC (Neutravidin-488, green). Actin was labeled with phalloidin-TRITIC (red) to show the cell shape and edge of cellular membrane. Nucleus was stained by DAPI (blue). The internalization of cyclic conotoxin cM1B-K7biotin was observed under confocal microscope (**Figure 6-10**). Interestingly, the distribution of cM1B-K7biotin in the cytosol was concentrated at one side of the nucleus. Small amount of green signal was observed in the nuclei but much than the signal shown in the cytosol, which may be the artificial effect due to formaldehyde fixation [296]. The actin distribution in the cytosol was different from cells without peptides, as actin polymerization near the nuclei was observed. I speculated that internalization of cyclic conotoxin might result in cellular responses related to change of actin morphology, which still needs further study. I also attempted to determine the destination of cM1B-K7biotin. However, I did not observe any overlapping of Neutravidin with fluorescent dyes that label Golgi apparatus or endoplasmic reticulum. In addition, prolonged incubation of cells with peptides (at 15 μM for 24 h) did not result in cell death.
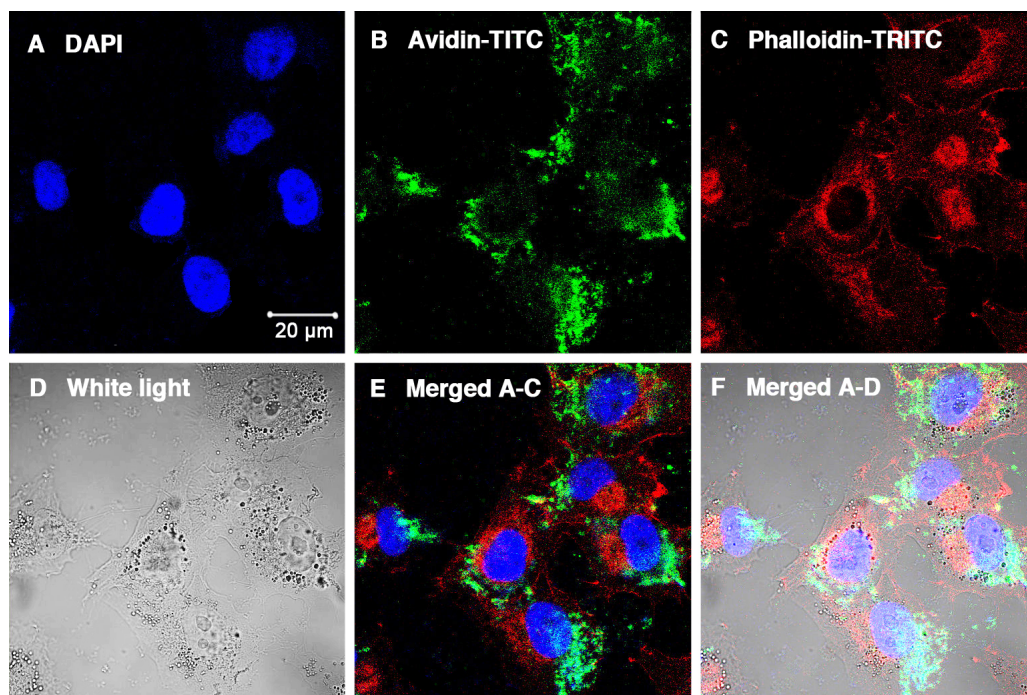
Figure 6-10. **Confocal microscopic views of internalization of cM1B-K7biotin into H1299 cells**. (A) Nucleus stained with DAPI (blue, 405 nm). (B) cM1B-K7biotin stained with avidin-FITC (green, 488 nm). (C) Actin stained with phalloidin-TRITC (red, 633 nm). (D) Cells under white light. (E) Overlay image of nucleus, peptide and actin. (F) Overlay image of field A-D.

8. Discussion

8.1 Stability of cyclic ω-conotoxins

The role of cyclic backbone and disulfide bonds to the molecular stability has been investigated on MVIIA and its cyclic analogs with 0-2 disulfide bonds. 2*SS* cyclic ω-CTXs cM(1-3)B exhibited similar level of stability as the 3*SS* linear MVIIA against heating and acid hydrolysis, which indicated that the reduced conformational rigidity due to deletion of one disulfide bond could be partially restored by the cyclized backbone. Removing all the disulfide bonds (i.e. 0*SS* cM6A) resulted in drastic decrease of molecular stability. Thus cyclic backbone alone was not sufficient to provide enough constraints to protect a 27-residue peptide in harsh conditions such as boiling or acid hydrolysis.

The resistance to trypsin digestion of the 3*SS* linear MVIIA was slightly higher than all three 2*SS* cyclic analogs, which indicated that the cystine-knot motif played an important role in protecting molecules from endopeptidase degradation by decreasing the flexibility of peptidyl loops and thus reducing the interactions with the digestive enzymes. The trypsin-susceptible MVIIA sequence was not an ideal model to demonstrate the development of orally active peptides, although the 2*SS* cyclic analogs displayed good resistance against acid treatment that resembled the environment of stomach. Alternatively, the enzyme-susceptible loops could be substituted by more stable sequences or other bioactive peptides for drug development.

8.2 Cyclic conotoxins as novel antimicrobial peptides

The antimicrobial peptides actively and widely inhibit microbes by their membrane-associated activity, which was generally recognized as the effect of two interactions: the charge-charge interactions between the basic residues of AMPs and anionic lipids and phosphorylated proteins on the microbial membrane; and the hydrophobic interactions between the hydrophobic residues of AMPs and the interior fatty acid chains of microbial membrane. The AMPs usually adopt amphipathic surface by forming secondary structures that mediate microbial membrane disruptions and lead to cellular content leakage,

interruption of membrane-related signaling or synthesis process, and finally growth inhibition and death. Based on the inhibition mechanism of AMPs, we hypothesized that the cationic ω-CTX MVIIA had potential to interact with microbial membrane. In the experiment, MVIIA exhibited a marginal anti-fungal activity due to the scattered basic residues and a limited number of hydrophobic residues, while it was not antibacterial. To enhance the membrane-associated activity, we built our model as shown in **Figure 5-1**. In the simplified illustration of MVIIA, five out of six basic residues were clusters at N- and C-termini located apart. Joining them into one contiguous segment with a dipeptide linker resulted in a more reactive basic epitope in response to microbial membrane binding. In addition, the replacement of one disulfide bond with aminobutyric acids, alanine, or Cys-S-Acm allowed their hydrophobic side chains to flip out of the disulfide core, which further enhanced the surface hydrophobicity. The consequence of backbone cyclization of ω-CTXs was the creation of antimicrobial activity that was as potent as the naturally occurring AMPs (MIC < 10 μM) against both gram-negative and gram-positive bacteria as well as fungal strains.

The concept of backbone cyclization has been previously applied on engineering of AMPs including cyclic protegrin PG-1, tachyplasin TP-1 and defensins. These cyclic AMPs showed enhanced stability, membrane selectivity or salt-insensitivity upon backbone cyclization [118-120]. One report on human defensin HBD-3 indicated that the connectivity and number of disulfide bonds did not affect the antimicrobial activity or cytotoxicity of HBD-3 analogs [297]. Taking together, these findings were coincident with my study as the cyclic ω-CTXs with different disulfide frameworks resulted in similar antimicrobial properties. These results showed that antimicrobial activity of cyclic ω-CTXs was mainly due to backbone cyclization that led to the formation of a microbial membrane-active neo-epitope.

The cyclic ω-CTXs with reduced number of disulfide bonds were found to be 2-3 fold more hemolytic than MVIIA with HD_{50} at 4.2 mM. Among three disulfide bonds, the C8-C20 linkage was found to be more important for maintaining the low hemolytic conformation, as the HD_{50} values of ΔC8-C20

analogs were about 2-3 fold less than MVIIA ranged from 1.3 to 2.5 mM (**Table 6-3**). Even though, the difference between antimicrobial concentration and hemolytic concentration of cyclic ω-CTXs resulted in 30-1000 folds difference as indicated by the therapeutic index (HD_{50}/MIC). These data suggested that the cyclic ω-CTXs had potentials for developing novel antimicrobial therapeutics.

The insight of membranolytic selectivity of cyclic ω-CTXs helped us to understand their antimicrobial mechanism. First, the broad-spectra of antimicrobial activity proved that they inhibited microbes through membrane-associated activity rather than targeting membrane-bound receptors or intracellular proteins. Second, the interaction between the cationic neo-epitope and negatively charged membrane surface would be the major action of the cyclic conotoxins, which led to differential reactivity against microbial membrane and mammalian membrane. I also observed that 2*SS* cyclic conotoxins intended to aggregate in water when we tried to determine their actual 3D structures by NMR. In the presence of 20% structure-enhancing solvent TFE, peptide aggregation dissociated. This results revealed that membrane-association involved conformational changes, while the fact of limited hydrophobic surface suggested that these peptides were unlikely to form toroidal pores by oligomerization across the lipid bilayer (For review see [298]). The carpet model was described as accumulation of cationic peptides lying on the membrane by electrostatic interactions in a "carpet-like" manner. When the peptide concentration reached a critical threshold, peptides induced membrane curvature disruption followed by the formation of micelles (For review see [299]). Both pore-formation model and carpet model were observed in amphipathic β- and α-helical peptides, which may not explain the antimicrobial activity of cyclic ω-CTXs. Electroporation was a proved mechanism of highly basic AMPs such as annexin V [300] and NK-lysin [301]. When binding of the cationic peptides to the membrane surface resulted in 0.2 mV potential across the lipid bilayer and could last for more than 0.1 ms, pores were formed due to this electrical field. Therefore, I speculate that the cationic epitope of cyclic ω-CTXs could accomplish the requirements for maintaining a high enough electrical field that last for enough long to induce pore formation.

Another intrinsic property of MVIIA, the chemotactic activity has been determined and the 2*SS* cyclic ω-CTXs also displayed this activity. Attraction of immune cells to the microbial invasion sites was another important role of natural occurring AMPs in animals. Therefore, the effective chemotactic activity at sub-micromolar level conferred one more advantage of cyclic conotoxins as novel defensive peptidyl therapeutics.

8.3 Cyclic conotoxins as novel cell-penetrating peptides

The cell-penetrating property of 2*SS* cyclic conotoxins was confirmed by immunofluorescence technology using fluorescent confocal microscopy. This property has not been reported in conotoxins as they were ion channel inhibitors that known to act on the outer surface of cellular membrane. The known cell-penetrating peptides were characterized by Arg/Lys-rich and/or aromatic/hydrophobic-rich sequences. Based on the sequence and lipid binding properties, CPPs have been generally classified into primary amphipathic, secondary amphipathic and non-amphipathic CPPs, where the primary amphipathic CPPs were more cytotoxic than the other two types. Based on the different models of cell entry, the known mechanisms were either energy-independent pathways (i.e. direct penetration) or energy-dependent pathways (i.e. endocytosis or pinocytosis) (For recent review see [302]). Incubation with peptides and cells at 4°C could inhibit most energy-dependent pathways [296], thus our results showed that cyclic conotoxins were uptake by cells via energy-dependent mechanisms. The trypsin-inhibitory cyclotide MCoTI-II was the only known CPP in cyclotide databases so far and it enters cells through macropinocytosis. Since cyclic conotoxins were highly soluble peptides, they might enter cell by pinocytosis.

Cell-penetrating peptides possess medicinal values as drug delivery tools. The human antibacterial peptide cathelicidin (a.k.a. LL-37) was an example of native CPPs with membrane-selectivity between prokaryotic and eukaryotic membranes [303]. More importantly, LL-37 could form complex with DNA and enter cells at the sites of lipid rafts by binding with proteoglycan to induce endocytosis and to carry DNA plasmids to the nucleus. In the concern of prompt cellular uptake and low cytotoxicity, cyclic conotoxins could carry

bioactive peptides into cells by grafting the target peptide into the backbone of cyclic conotoxins by replacing one loop or the GS linker. Although we have observed clustering of peptides near the nucleus and actin aggregation at the other side of the nucleus, the intracellular roles and fates of cyclic ω-CTXs were still unrevealed yet and further studies were needed. Collectively, the consequence of engineering a linear peptide into cyclic form has been demonstrated by the cyclic ω-CTXs that were converted into multifunctional membrane active peptides.

Chapter 7. Conclusions

My thesis focuses on development of novel methods for preparing cyclic cysteine-rich peptides. The cyclic CRPs provide stable scaffolds for peptidyl drug design. An efficient synthesis platform would facilitate the applications of cyclic CRPs. In chapter 3, I describe a recombinant synthetic strategy to prepare macrocyclic backbone by intein-splicing using an engineered intein *Mxe* GyrA. The bracelet cyclotide hedyotide B1 was used as a representative of naturally occurring cyclic CRP. The synthesis commenced with co-expression of a linear precursor of hedyotide B1 with *Mxe* and an affinity tag chitin-binding domain (CBD) as a fusion protein B1-*Mxe*-CBD. Intein mediated peptide bond breaking and reforming through catalyzing a series of chemoselective N-S, S-S, and S-N acyl shift reactions to afford the cyclic backbone of hedyotide B1. Oxidative folding was performed using GSH/GSSG under 70% isopropanol denaturing condition and resulted in 50% native-fold hedyotide B1.

Chapter 3 also explores the steric effect at cyclization site as an important factor for the cyclization efficiency. I designed six B1x-*Mxe*-CBD fusion proteins with a different C-terminal residue on each B1x precursor. The results showed that B1G with C-terminal Gly afforded the highest cyclization ratio (>90%) followed by B1R, B1Y, and B1F (50%-80% yield). B1P resulted in the lowest yield (<5%). These data suggest that the efficiency of intein-mediated cyclization was highly affected by the side chain steric hindrance at the splicing site. Therefore, the choice of the ligation site is important to afford high yield in the preparation of cyclic CRPs.

Recombinant synthesis using intein-splicing provides a promising and operationally safe approach for cyclic CRP production. However, this approach takes at least one week from plasmid construction to isolation of cyclic products, and it gives limited productivity in preparing cyclic CRPs with mass below 4 kDa. The formation of insoluble inclusion bodies wasted half of the expressed fusion proteins, even when the codon usage, incubation temperature and inducer concentration were optimized. The extensive washing and

purification steps further reduced the amount of products. Taking together, the average yield of hedyotide B1 from B1G was 1-2 mg per litre of bacteria culture. A scale-up production of cyclic CRPs through recombinant synthesis strategy would be laborious and required large facilities. Therefore, a more efficient and practical synthetic strategy is necessary for preparing cyclic CRPs.

Chapter 4 introduces a successful development and application of a novel cyclization strategy using Fmoc-compatible thioethylamido-based thioester surrogates. Two TEA-based thioester surrogates MeCys and TEBA were synthesized via simple preparation procedures using commercial available compounds, Fmoc-MeCys(Trt) and thioethylbutylamine. The MeCys-resin and TEBA-resin were ready for amino acid coupling using Fmoc chemistry. In the acidic condition, the TEA-based thioester surrogates mediated "safety-switch" thioester formation via a N-S acyl shift. This reaction mimicked intein splicing as the tertiary amide enhanced the *cisoid*-conformation that facilitated acyl shift reaction. Cyclization occurred at neutral to basic conditions, and was accelerated by the thia zip mechanism. Cyclic ω-CTXs were prepared using both TEA-mediated cyclization strategy. It took less than 3 days from microwave-assisted peptide synthesis to purification of the cyclic products. About 30 mg cyclic products were obtained in a 0.1 μmol synthesis scale. Collectively, the TEA-based synthetic approaches for preparing cyclic CRPs was simple and efficient.

Chapter 5 describes the development of a novel oxidative folding strategy using organic systems. This folding approach conferred a rapid preparation of hedyotide B1 and 2*SS* cyclic ω-CTXs cM(1-3)B, which were difficult to fold in aqueous conditions. By optimizing the pH, redox reagents and co-solvents, the sequence-specific organic system afforded folded hedyotide B1 and cM(1-3)B in 27-52% yield within 1 h. Compared with chemoselective disulfide formation and conventional oxidative folding in aqueous conditions, this organic folding process was remarkably faster and could tolerant higher peptide concentration at 0.1 mM. The combination of the novel organic folding strategy and the newly developed cyclization strategy in

one-pot efficiently afford hedyotide B1 and cyclic ω-CTXs in a one-pot manner, which is a promising platform for high-throughput cyclic CRP synthesis.

Chapter 6 reports on the application of the newly developed synthetic strategies for preparing cyclic CRPs with therapeutic potentials. A panel of cyclic ω-CTXs with zero to two disulfide bonds were synthesized by end-to-end cyclizing the linear ω-conotoxin MVIIA. MVIIA was found to be moderately fungicidal with MIC of 39.8 μM. In contrast, the 2SS and 1SS cyclic ω-CTXs became 3 to 10-fold more anti-fungal against *C. tropicalis*, and anti-bacterial at MIC < 10 μM against both gram-negative *E. coli* and gram-positive *S. aureus* bacteria strains. The broad range of antimicrobial activity has been found on 10 synthetic cyclic ω-CTXs with 0-2 native disulfide bonds but not in MVIIA or the 3SS linear analog M-GS. Cyclic ω-CTXs retained the non-hemolytic properties of MVIIA with HD_{50} > 1 μM in the hemolytic assay against human erythrocytes. The membranolytic selectivity of cyclic conotoxins provides enhanced activity and a large therapeutic index (HD_{50}/MIC) that may promote their development as novel antimicrobial drugs. Similar as human defensins, cyclic ω-CTXs were found to be chemotactic against monocytes THP-1 at concentration of 10 nM. The biotinylated cyclic ω-CTX was cell penetrating on carcinoma lung cells (H1299) and monocytes. Collectively, cyclic ω-CTXs are stable defensin-like AMPs with high membranolytic selectivity, chemotactic activity and cell-penetrating property. The antimicrobial cyclic ω-CTX provides stable and low-toxic scaffold to develop novel peptidyl drugs and carry bioactive peptides into cells.

In summary, I have developed a novel chemical synthetic strategy for preparing a macrocyclic peptide by two thioethylamido-based thioester surrogates, MeCys and TEBA. I also established a novel oxidative folding approach using organic system for rapid disulfide formation. A one-pot reaction involving the newly developed cyclization and organic folding approaches was developed as a high-throughput synthetic platform of cyclic CRPs. I applied the newly developed synthetic strategy successfully to prepare naturally occurring cyclotide hedyotide B1 and cyclic CRPs derived from animal *ω*-conotoxin MVIIA. In addition, backbone cyclization could confer new biological

functions to a naturally occurring linear CRP such as the cyclic ω-CTXs that exhibited new biological functions including antimicrobial, chemotactic and cell-penetrating properties. Collectively, my thesis works provide a new synthetic strategy for preparing and engineering cysteine-rich peptide-based biologics through backbone cyclization.

List of Publications

Hemu X., Cai L., Wong T. T., and Tam J. P. (2010) Intein-mediated Biosynthesis of Bracelet Cyclotide. *Proceeding of 11*th *Chinese Peptide Symposium.*

Hemu X. and Tam J. P. (2012) Cyclic ω-conotoxin MVIIA: Antimicrobial Activity Generated by Cyclization. *Proceeding of 12*th *Chinese Peptide Symposium.*

Taichi M., Hemu X., Qiu Y., and Tam J. P. (2013) A Thioethylalkylamido (TEA) Thioester Surrogate in the Synthesis of a Cyclic Peptide via a Tandem Acyl Shift. *Org Lett 15* (11), 2620–2623.

Hemu X., Taichi M., Qiu Y., Liu D. -X., and Tam J. P. (2013) Biomimetic Synthesis of Cyclic Peptides Using Novel Thioester Surrogates. *Biopolymers Peptide Science* 100, 492-501.

Qiu Y., Hemu X., and Tam J. P. (2013) Bidirectional Peptide Bond Cleavage Mediated by *N*-Methyl Cysteine to Thioester and Thiolactones. (In preparation)

Hemu X. and Tam J. P. (2013) End-to-End Cyclization of ω-conotoxin MVIIA Enhance Antimicrobial Activity. (In preparation)

List of Conference Presentations

11th Chinese International Peptide Symposium (2010, Lanzhou, China)

    Oral presentation

    Young Peptide Scientist Award

12th Chinese International Peptide Symposium (2012, Shenyang, China)

    Poster presentation

    Excellent Poster Award

References

1. Olivera, B. M., Rivier, J., Clark, C., Ramilo, C. A., Corpuz, G. P., Abogadie, F. C., Mena, E. E., Woodward, S. R., Hillyard, D. R., and Cruz, L. J. (1990) Diversity of conus neuropeptides, *Science 249*, 257-263.

2. Rao, C., and Tam, J. (1996) Three highly constrained tricyclic peptide libraries containing three disulfide bonds, *PEPTIDES-AMERICAN SYMPOSIUM- 14*, 299-300.

3. Corpuz, G. P., Jacobsen, R. B., Jimenez, E. C., Watkins, M., Walker, C., Colledge, C., Garrett, J. E., McDougal, O., Li, W., Gray, W. R., Hillyard, D. R., Rivier, J., McIntosh, J. M., Cruz, L. J., and Olivera, B. M. (2005) Definition of the M-Conotoxin Superfamily: Characterization of Novel Peptides from Molluscivorous Conus Venoms, *Biochemistry 44*, 8176-8186.

4. Andersson, M., Gunne, H., Agerberth, B., Boman, A., Bergman, T., Sillard, R., Jörnvall, H., Mutt, V., Olsson, B., and Wigzell, H. (1995) NK-lysin, a novel effector peptide of cytotoxic T and NK cells. Structure and cDNA cloning of the porcine form, induction by interleukin 2, antibacterial and antitumour activity, *The EMBO Journal 14*, 1615-1625.

5. Schneider, T., Kruse, T., Wimmer, R., Wiedemann, I., Sass, V., Pag, U., Jansen, A., Nielsen, A. K., Mygind, P. H., Raventós, D. S., Neve, S., Birthe, R., Bonvin, A. M. J. J., Maria, L. D., Andersen, A. S., Gammelgaard, L., Sahl, H.-G., and Kristensen, H.-H. (2010) Plectasin, a Fungal Defensin, Targets the Bacterial Cell Wall Precursor Lipid II, *Science 328*, 1168-1172.

6. Oeemig, J. S., Lynggaard, C., Knudsen, D. H., Hansen, F. T., Nørgaard, K. D., Schneider, T., Vad, B. S., Sandvang, D. H., Nielsen, L. A., Neve, S., Kristensen, H.-H., Sahl, H.-G., Otzen, D. E., and Wimmer, R. (2012) Eurocin, a New Fungal Defensin: STRUCTURE, LIPID BINDING, AND ITS MODE OF ACTION, *Journal of Biological Chemistry 287*, 42361-42372.

7. Zhu, S. (2008) Discovery of six families of fungal defensin-like peptides provides insights into origin and evolution of the CSαβ defensins, *Molecular Immunology 45*, 828-838.

8. Gao, B., Rodriguez, M. d. C., Lanz-Mendoza, H., and Zhu, S. (2009) AdDLP, a bacterial defensin-like peptide, exhibits anti-Plasmodium activity, *Biochemical and Biophysical Research Communications 387*, 393-398.

9. Wang, Z., and Wang, G. (2004) APD: the Antimicrobial Peptide Database, *Nucleic acids research 32*, D590-D592.

10. Nguyen, L. T., Haney, E. F., and Vogel, H. J. (2011) The expanding scope of antimicrobial peptide structures and their modes of action, *Trends Biotechnol 29*, 464-472.

11. Schneider, J., Unholzer, A., Schaller, M., Schäfer-Korting, M., and Korting, H. (2005) Human defensins, *J Mol Med 83*, 587-595.

12. Trabi, M., Schirra, H. J., and Craik, D. J. (2001) Three-dimensional structure of RTD-1, a cyclic antimicrobial defensin from Rhesus macaque leukocytes, *Biochemistry 40*, 4211-4221.

13. Tang, Y.-Q., Yuan, J., Osapay, G., Osapay, K., Tran, D., Miller, C. J., Ouellette, A. J., and Selsted, M. E. (1999) A Cyclic Antimicrobial Peptide Produced in Primate Leukocytes by the Ligation of Two Truncated alpha-Defensins, *Science 286*, 498-502.

14. Tran, D., Tran, P. A., Tang, Y.-Q., Yuan, J., Cole, T., and Selsted, M. E. (2002) Homodimeric theta-Defensins from Rhesus macaqueLeukocytes: ISOLATION, SYNTHESIS, ANTIMICROBIAL ACTIVITIES, AND BACTERIAL BINDING PROPERTIES OF THE CYCLIC PEPTIDES, *Journal of Biological Chemistry 277*, 3079-3084.

15. Garcia, A. E., Ösapay, G., Tran, P. A., Yuan, J., and Selsted, M. E. (2008) Isolation, Synthesis, and Antimicrobial Activities of Naturally Occurring θ-Defensin Isoforms from Baboon Leukocytes, *Infect Immun. 76*, 5883-5891.

16. Nguyen, T. X., Cole, A. M., and Lehrer, R. I. (2003) Evolution of primate alpha-defensins: a serpentine path to a sweet tooth, *Peptides 24*, 1647-1654.

17. Cole, A. M., Hong, T., Boo, L. M., Nguyen, T., Zhao, C., Bristol, G., Zack, J. A., Waring, A. J., Yang, O. O., and Lehrer, R. I. (2002) Retrocyclin: A primate peptide that protects cells from infection by T- and M-tropic strains of HIV-1, *Proceedings of the National Academy of Sciences 99*, 1813-1818.

18. Yasin, B., Wang, W., Pang, M., Cheshenko, N., Hong, T., Waring, A. J., Herold, B. C., Wagar, E. A., and Lehrer, R. I. (2004) Theta-Defensins Protect Cells from Infection by Herpes Simplex Virus by Inhibiting Viral Adhesion and Entry, *Journal of Virology 78*, 5147-5156.

19. Doss, M., White, M. R., Tecle, T., Gantz, D., Crouch, E. C., Jung, G., Ruchala, P., Waring, A. J., Lehrer, R. I., and Hartshorn, K. L. (2009) Interactions of alpha-, beta-, and theta-Defensins with Influenza A Virus and Surfactant Protein D, *The Journal of Immunology 182*, 7878-7887.

20. Liang, Q.-L., Zhou, K., and He, H.-X. (2010) Retrocyclin 2: a new therapy against avian influenza H5N1 virus in vivo and vitro, *Biotechnol Lett 32*, 387-392.

21. Terlau, H., and Olivera, B. M. (2003) Conus Venoms: A rich source of novel ion channel-tageted peptides, *Physiologics Review 84*, 41-68.

22. Adams, M. E. (2004) Agatoxins: ion channel specific toxins from the american funnel web spider, Agelenopsis aperta, *Toxicon 43*, 509-525.

23. Swartz, K. J., and MacKinnon, R. (1995) An inhibitor of the Kv2.1 potassium channel isolated from the venom of a Chilean tarantula, *Neuron 15*, 941-949.

24. Zeng, X.-Z., Xiao, Q.-B., and Liang, S.-P. (2003) Purification and characterization of raventoxin-I and raventoxin-III, two neurotoxic peptides from the venom of the spider Macrothele raveni, *Toxicon 41*, 651-656.

25. Nicholson, G. M., and Graudins, A. (2002) Spiders of medical importance in the Asia–Pacific: Atracotoxin, latrotoxin and related spider neurotoxins, *Clin Exp Pharmacol P 29*, 785-794.

26. Garcia, M. L., Gao, Y.-D., McManus, O. B., and Kaczorowski, G. J. (2001) Potassium channels: from scorpion venoms to high-resolution structure, *Toxicon 39*, 739-748.

27. Bohlen, C. J., Chesler, A. T., Sharif-Naeini, R., Medzihradszky, K. F., Zhou, S., King, D., Sanchez, E. E., Burlingame, A. L., Basbaum, A. I., and Julius, D. (2011) A heteromeric Texas coral snake toxin targets acid-sensing ion channels to produce pain, *Nature 479*, 410-414.

28. Spedding, M., and Paoletti, R. (1992) Classification of calcium channels and calcium antagonists: Progress report, *Cardiovasc Drug Ther 6*, 35-39.

29. Spedding, M., and Paoletti, R. (1992) Classification of calcium channels and the sites of action of drugs modifying channel function, *Pharmacological Reviews 44*, 363-376.

30. Broekaert, I., Lee, H. I., Kush, A., Chua, N. H., and Raikhel, N. (1990) Wound-induced accumulation of mRNA containing a hevein sequence in laticifers of rubber tree (Hevea brasiliensis), *Proceedings of the National Academy of Sciences 87*, 7633-7637.

31. Thomma, B., Cammue, B., and Thevissen, K. (2002) Plant defensins, *Planta 216*, 193-202.

32. Ryan, C. A. (1990) Protease Inhibitors in Plants: Genes for Improving Defenses Against Insects and Pathogens, *Annual Review of Phytopathology 28*, 425-449.

33. Lu, S., Deng, P., Liu, X., Luo, J., Han, R., Gu, X., Liang, S., Wang, X., Li, F., Lozanov, V., Patthy, A. s., and Pongor, S. n. (1999) Solution Structure of the Major Œ±-Amylase Inhibitor of the Crop Plant Amaranth, *Journal of Biological Chemistry 274*, 20473-20478.

34. Carugo, O., Lu, S., Luo, J., Gu, X., Liang, S., Strobl, S., and Pongor, S. n. (2001) Structural analysis of free and enzyme-bound amaranth alpha-amylase inhibitor: classification within the knottin fold superfamily and analysis of its functional flexibility, *Protein engineering 14*, 639-646.

35. Bloch Jr, C., and Richardson, M. (1991) A new family of small (5 kDa) protein inhibitors of insect α-amylases from seeds or sorghum (Sorghum bicolor (L) Moench) have sequence homologies with wheat γ-purothionins, *FEBS letters 279*, 101-104.

36. Franco, O. L., Rigden, D. J., Melo, F. R., and Grossi-de-Sá, M. F. (2002) Plant α-amylase inhibitors and their interaction with insect α-amylases, *European Journal of Biochemistry 269*, 397-412.

37. Witherup, K. M., Bogusky, M. J., Anderson, P. S., Ramjit, H., Ransom, R. W., Wood, T., and Sardana, M. (1994) Cyclopsychotride A, a biologically active, 31-

residue cyclic peptide isolated from Psychotria longipes, *J Nat Prod 57*, 1619-1625.

38. Saether, O., Craik, D. J., Campbell, I. D., Sletten, K., Juul, J., and Norman, D. G. (1995) Elucidation of the primary and three-dimensional structure of the uterotonic polypeptide kalata B1, *Biochemistry 34*, 4147-4158.

39. Gran, L., Sandberg, F., and Sletten, K. (2000) Oldenlandia affinis (R&S) DC. A plant containing uteroactive peptides used in African traditional medicine, *J Ethnopharmacol 70*, 197-203.

40. Goransson, U., and Craik, D. J. (2003) Disulfide mapping of the cyclotide kalata B1. Chemical proof of the cystic cystine knot motif, *J Biol Chem 278*, 48188-48196.

41. Pallaghy, P. K., Nielsen, K. J., Craik, D. J., and Norton, R. S. (1994) A common structural motif incorporating a cystine knot and a triple-stranded beta-sheet in toxic and inhibitory polypeptides, *Protein Sci 3*, 1833-1839.

42. Mer, G., Hietter, H., Kellenberger, C., Renatus, M., Luu, B., and Lefevre, J. F. (1996) Solution structure of PMP-C: a new fold in the group of small serine proteinase inhibitors, *J Mol Biol 258*, 158-171.

43. Scott, R. H., Gorton, V. J., Harding, L., Patel, D., Pacey, S., Kellenberger, C., Hietter, H., and Bermudez, I. (1997) Inhibition of neuronal high voltage-activated calcium channels by insect peptides: a comparison with the actions of omega-conotoxin GVIA, *Neuropharmacology 36*, 195-208.

44. Lehrer, R. I., Rosenman, M., Harwig, S. S., Jackson, R., and Eisenhauer, P. (1991) Ultrasensitive assays for endogenous antimicrobial polypeptides, *J Immunol Methods 137*, 167-173.

45. Cruz, L. J., Gray, W. R., and Olivera, B. M. (1978) Purification and properties of a myotoxin from Conus geographus venom., *Archives of biochemistry and biophysics 190*, 539-548.

46. Kaas, Q., Westermann, J.-C., and Craik, D. J. (2010) Conopeptide characterization and classifications: An analysis using ConoServer, *Toxicon 55*, 1491-1509.

47. Bulaj, G., and Olivera, B. M. (2008) Folding of Conotoxins: Formation of the Native Disulfide Bridges During Chemical Synthesis and Biosynthesis of ConusPeptides, *Antioxidants & redox signaling 10*, 141-156.

48. McIntosh, J. M., Yoshikami, D., Mahe, E., Nielsen, D. B., Rivier, J. E., Gray, W. R., and Olivera, B. M. (1994) A nicotinic acetylcholine receptor ligand of unique specificity, alpha-conotoxin ImI, *Journal of Biological Chemistry 269*, 16733-16739.

49. Fainzilber, M., Nakamura, T., Lodder, J. C., Zlotkin, E., Kits, K. S., and Burlingame, A. L. (1998) gamma-Conotoxin-PnVIIA, A gamma-Carboxyglutamate-Containing Peptide Agonist of Neuronal Pacemaker Cation Currents, *Biochemistry 37*, 1470-1477.

50. Fainzilber, M., Gordon, D., Hasson, A., Spira, M. E., and Zlotkin, E. (1991) Mollusc-specific toxins from the venom of Conus textile neovicarius, *European Journal of Biochemistry 202*, 589-595.

51. Rigby, A. C., Lucas-Meunier, E., Kalume, D. r. E., Czerwiec, E., Hambe, B. r., Dahlqvist, I., Fossier, P., Baux, G. r., Roepstorff, P., Baleja, J. D., Furie, B. C., Furie, B., and Stenflo, J. (1999) A conotoxin from Conus textile with unusual posttranslational modifications reduces presynaptic Ca2+ influx, *Proceedings of the National Academy of Sciences 96*, 5758-5763.

52. Jimenez, E. C., Shetty, R. P., Lirazan, M., Rivier, J., Walker, C., Abogadie, F. C., Yoshikami, D., Cruz, L. J., and Olivera, B. M. (2003) Novel excitatory Conus peptides define a new conotoxin superfamily, *J Neurochem 85*, 610-621.

53. Terlau, H., Shon, K.-J., Grilley, M., Stocker, M., Stuhmer, W., and Olivera, B. M. (1996) Strategy for rapid immobilization of prey by a fish-hunting marine snail, *Nature 381*, 148-151.

54. Cruz, L. J., Gray, W. R., Olivera, B. M., Zeikus, R. D., Kerr, L., Yoshikami, D., and Moczydlowski, E. (1985) Conus geographus toxins that discriminate between neuronal and muscle sodium channels, *Journal of Biological Chemistry 260*, 9280-9288.

55. Sharpe, I. A., Gehrmann, J., Loughnan, M. L., Thomas, L., Adams, D. A., Atkins, A., Palant, E., Craik, D. J., Adams, D. J., Alewood, P. F., and Lewis, R. J. (2001) Two new classes of conopeptides inhibit the [alpha]1-adrenoceptor and noradrenaline transporter, *Nat Neurosci 4*, 902-907.

56. England, L. J., Imperial, J., Jacobsen, R., Craig, A. G., Gulyas, J., Akhtar, M., Rivier, J., Julius, D., and Olivera, B. M. (1998) Inactivation of a Serotonin-Gated Ion Channel by a Polypeptide Toxin from Marine Snails, *Science 281*, 575-578.

57. Buczek, O., Wei, D., Babon, J. J., Yang, X., Fiedler, B., Chen, P., Yoshikami, D., Olivera, B. M., Bulaj, G., and Norton, R. S. (2007) Structure and Sodium Channel Activity of an Excitatory I1-Superfamily Conotoxin, *Biochemistry 46*, 9929-9940.

58. Petrel, C., Hocking, H. G., Reynaud, M., Upert, G., Favreau, P., Biass, D., Paolini-Bertrand, M., Peigneur, S., Tytgat, J., Gilles, N., Hartley, O., Boelens, R., Stocklin, R., and Servent, D. (2013) Identification, structural and pharmacological characterization of τ-CnVA, a conopeptide that selectively interacts with somatostatin sst3 receptor, *Biochem Pharmacol 85*, 1663-1671.

59. Olivera, B., Gray, W., Zeikus, R., and McIntosh, J. (1985) Peptide neurotoxins from fish-hunting cone snails, *Science*.

60. Cruz, L. J., and Olivera, B. M. (1986) Calcium channel antagonists. Omega-conotoxin defines a new high affinity site., *The Journal of biological chemistry 261*, 6230-6233.

61. Feldman, D., Cruz, L., and Olivera, B. (1987) Omega-conotoxin: direct and persistent blockade of specific types of calcium channels in neurons but not muscle, *Proc Natl Acad Sci U S A. 84*, 4327–4331.

62. Cruz, L. J., Johnson, D. S., and Olivera, B. M. (1987) Characterization of the .omega.-conotoxin target. Evidence for tissue-specific heterogeneity in calcium channel types, *Biochemistry 26*, 820-824.

63. Nowycky, M. C., Fox, A. P., and Tsien, R. W. (1985) Three types of neuronal calcium channel with different calcium agonist sensitivity, *Nature 316*, 440-443.

64. Haack, J. A., Kinser, P., Yoshikami, D., and Olivera, B. M. (1993) Biotinylated derivatives of ω-conotoxins GVIA and MVIID: Probes for neuronal calcium channels, *Neuropharmacology 32*, 1151-1159.

65. Miljanich, G. P., and Ramachandran, J. (1995) Antagonists of Neuronal Calcium Channels: Structure, Function, and Therapeutic Implications, *Annual Review of Pharmacology and Toxicology 35*, 707-734.

66. Pringle, A. K., Benham, C. D., Sim, L., Kennedy, J., Iannotti, F., and Sundstrom, L. E. (1996) Selective N-Type Calcium Channel Antagonist Omega Conotoxin MVIIA Is Neuroprotective Against Hypoxic Neurodegeneration in Organotypic Hippocampal-Slice Cultures, *Stroke 27*, 2124-2130.

67. Woppmann, A., Ramachandran, J., and Miljanich, G. P. (1994) Calcium channel subtypes in rat brain: biochemical characterization of the high-affinity receptors for omega-conopeptides SNX-230 (synthetic MVIIC), SNX-183 (SVIB), and SNX-111 (MVIIA). *Molecular and cellular neurosciences 5*, 350-357.

68. Bowersox, S., and Luther, R. (1998) Pharmacotherapeutic potential of omega-conotoxin MVIIA (SNX-111), an N-type neuronal calcium channel blocker found in the venom of Conus magus, *Toxicon 36*, 1651-1658.

69. Schroeder, C. (2006) ω-conotoxins GVIA, MVIIA and CVID: SAR and clinical potential, *Marine Drugs*.

70. Gran, L. (1973) On the effect of a polypeptide isolated from "Kalata-Kalata" (Oldenlandia affinis DC) on the oestrogen dominated uterus, *Acta Pharmacologica et Toxicologica 33*, 400-408.

71. Gran, L. (1970) An oxytocic principle found in Oldenlandia affinis DC., *Medd Nor Farm Selsk 12*, 173-180.

72. Craik, D. J., Daly, N. L., Bond, T., and Waine, C. (1999) Plant cyclotides: A unique family of cyclic and knotted proteins that defines the cyclic cystine knot structural motif, *Journal of Molecular Biology 294*, 1327-1336.

73. Gustafson, K. R., Sowder, R. C., Henderson, L. E., Parsons, I. C., Kashman, Y., Cardellina, J. H., McMahon, J. B., Buckheit, R. W., Pannell, L. K., and Boyd, M. R. (1994) Circulins A and B. Novel human immunodeficiency virus (HIV)-inhibitory macrocyclic peptides from the tropical tree Chassalia parvifolia, *Journal of the American Chemical Society 116*, 9337-9338.

74. Gran, L., Sandberg, F., and Sletten, K. (2000) Oldenlandia affinis (R&S) DC: A plant containing uteroactive peptides used in African traditional medicine, *Journal of Ethnopharmacology 70*, 197-203.

75. Simonsen, S. M., Sando, L., Ireland, D. C., Colgrave, M. L., Bharathi, R., Goransson, U., and Craik, D. J. (2005) A continent of plant defense peptide diversity: Cyclotides in Australian Hybanthus (Violaceae), *Plant Cell 17*, 3176-3189.

76. Heitz, A., Hernandez, J.-F., Gagnon, J., Hong, T. T., Pham, T. T. C., Nguyen, T. M., Le-Nguyen, D., and Chiche, L. (2001) Solution Structure of the Squash Trypsin Inhibitor MCoTI-II. A New Family for Cyclic Knottins, *Biochemistry 40*, 7973-7983.

77. Gruber, C. W., Elliott, A. G., Ireland, D. C., Delprete, P. G., Dessein, S., Goransson, U., Trabi, M., Wang, C. K., Kinghorn, A. B., Robbrecht, E., and Craik, D. J. (2008) Distribution and evolution of circular miniproteins in flowering plants, *Plant Cell 20*, 2471-2483.

78. Poth, A. G., Colgrave, M. L., Philip, R., Kerenga, B., Daly, N. L., Anderson, M. A., and Craik, D. J. (2010) Discovery of Cyclotides in the Fabaceae Plant Family Provides New Insights into the Cyclization, Evolution, and Distribution of Circular Proteins, *ACS chemical biology 6*, 345-355.

79. Nguyen, G. K. T., Zhang, S., Nguyen, N. T. K., Nguyen, P. Q. T., Chiu, M. S., Hardjojo, A., and Tam, J. P. (2011) Discovery and Characterization of Novel Cyclotides Originated from Chimeric Precursors Consisting of Albumin-1 Chain a and Cyclotide Domains in the Fabaceae Family, *Journal of Biological Chemistry 286*, 24275-24287.

80. Nguyen, G. K. T., Lian, Y., Pang, E. W. H., Nguyen, P. Q. T., Tran, T. D., and Tam, J. P. (2013) Discovery of Linear Cyclotides in Monocot Plant Panicum laxum of Poaceae Family Provides New Insights into Evolution and Distribution of Cyclotides in Plants, *Journal of Biological Chemistry 288*, 3370-3380.

81. Jennings, C. V., Rosengren, K. J., Daly, N. L., Plan, M., Stevens, J., Scanlon, M. J., Waine, C., Norman, D. G., Anderson, M. A., and Craik, D. J. (2005) Isolation, solution structure, and insecticidal activity of kalata B2, a circular protein with a twist: do Mobius strips exist in nature?, *Biochemistry 44*, 851-860.

82. Daly, N. L., Clark, R. J., Plan, M. R., and Craik, D. J. (2006) Kalata B8, a novel antiviral circular protein, exhibits conformational flexibility in the cystine knot motif, *Biochem J 393*, 619-626.

83. Heitz, A., Hernandez, J. F., Gagnon, J., Hong, T. T., Pham, T. T., Nguyen, T. M., Le-Nguyen, D., and Chiche, L. (2001) Solution structure of the squash trypsin inhibitor MCoTI-II. A new family for cyclic knottins, *Biochemistry 40*, 7973-7983.

84. Jennings, C., West, J., Waine, C., Craik, D., and Anderson, M. (2001) Biosynthesis and insecticidal properties of plant cyclotides: the cyclic knotted proteins from Oldenlandia affinis, *Proceedings of the National Academy of Sciences of the United States of America 98*, 10614-10619.

85. Gruber, C. W., Cemazar, M., Clark, R. J., Horibe, T., Renda, R. F., Anderson, M. A., and Craik, D. J. (2007) A novel plant protein-disulfide isomerase involved in the oxidative folding of cystine knot defense proteins, *J Biol Chem 282*, 20435-20446.

86. Gillon, A. D., Saska, I., Jennings, C. V., Guarino, R. F., Craik, D. J., and Anderson, M. A. (2008) Biosynthesis of circular proteins in plants, *The Plant Journal 53*, 505-515.

87. Saska, I., Gillon, A. D., Hatsugai, N., Dietzgen, R. G., Hara-Nishimura, I., Anderson, M. A., and Craik, D. J. (2007) An asparaginyl endopeptidase mediates in vivo protein backbone cyclization, *J Biol Chem 282*, 29721-29728.

88. Ireland, D. C., Colgrave, M. L., Nguyencong, P., Daly, N. L., and Craik, D. J. (2006) Discovery and characterization of a linear cyclotide from Viola odorata: implications for the processing of circular proteins, *Journal of Molecular Biology 357*, 1522-1535.

89. Plan, M. R. R., Göransson, U., Clark, R. J., Daly, N. L., Colgrave, M. L., and Craik, D. J. (2007) The Cyclotide Fingerprint in Oldenlandia affinis: Elucidation of Chemically Modified, Linear and Novel Macrocyclic Peptides, *Chembiochem 8*, 1001-1011.

90. Gerlach, S. L., Burman, R., Bohlin, L., Mondal, D., and GoÃàransson, U. (2010) Isolation, Characterization, and Bioactivity of Cyclotides from the Micronesian Plant Psychotria leptothyrsa, *Journal of Natural Products 73*, 1207-1213.

91. Mulvenna, J. P., Mylne, J. S., Bharathi, R., Burton, R. A., Shirley, N. J., Fincher, G. B., Anderson, M. A., and Craik, D. J. (2006) Discovery of cyclotide-like protein sequences in graminaceous crop plants: ancestral precursors of circular proteins?, *Plant Cell 18*, 2134-2144.

92. Nguyen, G. K., Lim, W. H., Nguyen, P. Q., and Tam, J. P. (2012) Novel cyclotides and uncyclotides with highly shortened precursors from Chassalia chartacea and effects of methionine oxidation on bioactivities, *The Journal of biological chemistry 287*, 17598-17607.

93. Conlan, B. F., Gillon, A. D., Craik, D. J., and Anderson, M. A. (2010) Circular proteins and mechanisms of cyclization, *Biopolymers 94*, 573-583.

94. Marx, U. C., Korsinczky, M. L. J., Schirra, H. J., Jones, A., Condie, B., Otvos ., L., Jr, and Craik, D. J. (2003) Enzymatic cyclisation of the potent Bowman-Birk protease inhibitor SFTI-1 and solution structure of an acyclic precursor peptide, *Journal of Biological Chemistry*, M212996200.

95. Tam, J., Lu, Y., Yang, J., and Chiu, K. (1999) An unusual structural motif of antimicrobial peptides containing end-to-end macrocycle and cystine-knot disulfides, *Proceedings of the National Academy of Sciences of the United States of America 96*, 8913.

96. Huang, Y.-H., Colgrave, M. L., Daly, N. L., Keleshian, A., Martinac, B., and Craik, D. J. (2009) The Biological Activity of the Prototypic Cyclotide Kalata B1 Is Modulated by the Formation of Multimeric Pores, *Journal of Biological Chemistry 284*, 20699-20707.

97. Wang, C. K., Colgrave, M. L., Ireland, D. C., Kaas, Q., and Craik, D. J. (2009) Despite a Conserved Cystine Knot Motif, Different Cyclotides Have Different Membrane Binding Modes, *Biophysical Journal 97*, 1471-1481.

98. Gran, L. (1973) On the effect of a polypeptide isolated from Kalata-Kalata(Oldenlandia affinis DC) on the oestrogen dominated uterus, *Acta Pharmacologica et Toxicologica 33*, 400-408.

99. Gustafson, K. R., Walton, L. K., Sowder, R. C., Jr., Johnson, D. G., Pannell, L. K., Cardellina, J. H., Jr., and Boyd, M. R. (2000) New circulin macrocyclic polypeptides from Chassalia parvifolia, *Journal of natural products 63*, 176-178.

100. Hallock, Y. F., Sowder, R. C., 2nd, Pannell, L. K., Hughes, C. B., Johnson, D. G., Gulakowski, R., Cardellina, J. H., 2nd, and Boyd, M. R. (2000) Cycloviolins A-D, anti-HIV macrocyclic peptides from Leonia cymosa, *The Journal of organic chemistry 65*, 124-128.

101. Daly, N. L., Gustafson, K. R., and Craik, D. J. (2004) The role of the cyclic peptide backbone in the anti-HIV activity of the cyclotide kalata B1, *FEBS letters 574*, 69-72.

102. Daly, N. L., Clark, R. J., Plan, M. R., and Craik, D. J. (2006) Kalata B8, a novel antiviral circular protein, exhibits conformational flexibility in the cystine knot motif, *Biochem J 393*, 619-626.

103. Witherup, K. M., Bogusky, M. J., Anderson, P. S., Ramjit, H., Ransom, R. W., Wood, T., and Sardana, M. (1994) Cyclopsychotride A, a biologically active, 31-residue cyclic peptide isolated from Psychotria longipes, *Journal of natural products 57*, 1619-1625.

104. Daly, N. L., Love, S., Paul F Alewood, a., and Craik, D. J. (1999) Chemical Synthesis and Folding Pathways of Large Cyclic Polypeptides: Studies of the Cystine Knot Polypeptide Kalata B1†, *38*, 10606-10614.

105. Gran, L., Sletten, K., and Skjeldal, L. (2008) Cyclic peptides from Oldenlandia affinis DC. Molecular and biological properties, *Chem Biodivers 5*, 2014-2022.

106. Wong, C. T., Taichi, M., Nishio, H., Nishiuchi, Y., and Tam, J. P. (2011) Optimal Oxidative Folding of the Novel Antimicrobial Cyclotide from Hedyotis biflora Requires High Alcohol Concentrations, *Biochemistry 50*, 7275-7283.

107. Hernandez, J. F., Gagnon, J., Chiche, L., Nguyen, T. M., Andrieu, J. P., Heitz, A., Trinh Hong, T., Pham, T. T., and Le Nguyen, D. (2000) Squash trypsin inhibitors from Momordica cochinchinensis exhibit an atypical macrocyclic structure, *Biochemistry 39*, 5722-5730.

108. Lindholm, P., Goransson, U., Johansson, S., Claeson, P., Gullbo, J., Larsson, R., Bohlin, L., and Backlund, A. (2002) Cyclotides: a novel type of cytotoxic agents, *Mol Cancer Ther 1*, 365-369.

109. Svangard, E., Goransson, U., Hocaoglu, Z., Gullbo, J., Larsson, R., Claeson, P., and Bohlin, L. (2004) Cytotoxic cyclotides from Viola tricolor, *Journal of natural products 67*, 144-147.

110. Herrmann, A., Burman, R., Mylne, J. S., Karlsson, G., Gullbo, J., Craik, D. J., Clark, R. J., and Göransson, U. (2008) The alpine violet, Viola biflora, is a rich source of cyclotides with potent cytotoxicity, *Phytochemistry 69*, 939-952.

111. Goransson, U., Svangard, E., Claeson, P., and Bohlin, L. (2004) Novel strategies for isolation and characterization of cyclotides: the discovery of bioactive macrocyclic plant polypeptides in the Violaceae, *Curr Protein Pept Sci 5*, 317-329.

112. Greenwood, K. P., Daly, N. L., Brown, D. L., Stow, J. L., and Craik, D. J. (2007) The cyclic cystine knot miniprotein MCoTI-II is internalized into cells by macropinocytosis, *The International Journal of Biochemistry & Cell Biology 39*, 2252-2264.

113. Plan, M. R. R., Saska, I., Cagauan, A. G., and Craik, D. J. (2008) Backbone Cyclised Peptides from Plants Show Molluscicidal Activity against the Rice Pest Pomacea canaliculata (Golden Apple Snail), *J Agric Food Chem 56*, 5237-5241.

114. U. S. Food and Drug Administration (2012) FY 2012 Innovative Drug Approvals.

115. Hruby, V. J. (1982) Conformational restrictions of biologically active peptides via amino acid side chain groups, *Life Sci 31*, 189-199.

116. Clark, R. J., Fischer, H., Dempster, L., Daly, N. L., Rosengren, K. J., Nevin, S. T., Meunier, F. A., Adams, D. J., and Craik, D. J. (2005) Engineering stable peptide toxins by means of backbone cyclization: Stabilization of the alpha-conotoxin MII, *Proceedings of the National Academy of Sciences of the United States of America 102*, 13767-13772.

117. Clark, R. J., Jensen, J., Nevin, S. T., Callaghan, B. P., Adams, D. J., and Craik, D. J. (2010) The Engineering of an Orally Active Conotoxin for the Treatment of Neuropathic Pain, *Angewandte Chemie International Edition 49*, 6545-6548.

118. Tam, J. P., Lu, Y. A., and Yang, J. L. (2000) Marked increase in membranolytic selectivity of novel cyclic tachyplesins constrained with an antiparallel two-beta strand cystine knot framework, *Biochemical and biophysical research communications 267*, 783-790.

119. Tam, J. P., Wu, C., and Yang, J. L. (2000) Membranolytic selectivity of cystine-stabilized cyclic protegrins, *Eur J Biochem 267*, 3289-3300.

120. Yu, Q., Lehrer, R. I., and Tam, J. P. (2000) Engineered salt-insensitive alpha-defensins with end-to-end circularized structures, *J Biol Chem 275*, 3943-3949.

121. Wong, C. T. T., Rowlands, D. K., Wong, C.-H., Lo, T. W. C., Nguyen, G. K. T., Li, H.-Y., and Tam, J. P. (2012) Orally Active Peptidic Bradykinin B1 Receptor Antagonists Engineered from a Cyclotide Scaffold for Inflammatory Pain Treatment, *Angewandte Chemie International Edition 51*, 5620-5624.

122. Sandall, D. W., Satkunanathan, N., Keays, D. A., Polidano, M. A., Liping, X., Pham, V., Down, J. G., Khalil, Z., Livett, B. G., and Gayler, K. R. (2003) A Novel alpha-Conotoxin Identified by Gene Sequencing Is Active in Suppressing the Vascular Response to Selective Stimulation of Sensory Nerves in Vivo, *Biochemistry 42*, 6904-6911.

123. Vincler, M., Wittenauer, S., Parker, R., Ellison, M., Olivera, B. M., and McIntosh, J. M. (2006) Molecular mechanism for analgesia involving specific antagonism of

α9α10 nicotinic acetylcholine receptors, *Proceedings of the National Academy of Sciences 103*, 17880-17884.

124. Vincler, M., and McIntosh, J. M. (2007) Targeting the α9α10 nicotinic acetylcholine receptor to treat severe pain, *Expert Opinion on Therapeutic Targets 11*, 891-897.

125. Callaghan, B., Haythornthwaite, A., Berecki, G., Clark, R. J., Craik, D. J., and Adams, D. J. (2008) Analgesic alpha-conotoxins Vc1.1 and Rg1A inhibit N-type calcium channels in rat sensory neurons via GABAB receptor activation, *J Neurosci 28*, 10943-10951.

126. Colgrave, M. L., and Craik, D. J. (2004) Thermal, chemical, and enzymatic stability of the cyclotide kalata B1: the importance of the cyclic cystine knot, *Biochemistry 43*, 5965-5975.

127. Antos, J. M., Popp, M. W. L., Ernst, R., Chew, G. L., Spooner, E., and Ploegh, H. L. (2009) A Straight Path to Circular Proteins, *Journal of Biological Chemistry 284*, 16028-16036.

128. Abrahmsen, L., Tom, J., Burnier, J., Butcher, K. A., Kossiakoff, A., and Wells, J. A. (1991) Engineering subtilisin and its substrates for efficient ligation of peptide bonds in aqueous solution, *Biochemistry 30*, 4151-4159.

129. Chang, T. K., Jackson, D. Y., Burnier, J. P., and Wells, J. A. (1994) Subtiligase: a tool for semisynthesis of proteins, *Proceedings of the National Academy of Sciences 91*, 12544-12548.

130. Jackson, D. Y., Burnier, J. P., and Wells, J. A. (1995) Enzymic Cyclization of Linear Peptide Esters Using Subtiligase, *Journal of the American Chemical Society 117*, 819-820.

131. Muir, T., Sondhi, D., and Cole, P. (1998) Expressed protein ligation: a general method for protein engineering, *Proceedings of the National Academy of Sciences 95*, 6705.

132. Shih, C. K., Wagner, R., Feinstein, S., Kanikennulat, C., and Neff, N. (1988) A Dominant Trifluoperazine Resistance Gene from Saccharomyces-Cerevisiae Has Homology with F0f1 Atp Synthase and Confers Calcium-Sensitive Growth, *Mol Cell Biol 8*, 3094-3103.

133. Bowman, E. J., Tenney, K., and Bowman, B. J. (1988) Isolation of genes encoding the Neurospora vacuolar ATPase. Analysis of vma-1 encoding the 67-kDa subunit reveals homology to other ATPases, *Journal of Biological Chemistry 263*, 13994-14001.

134. Zimniak, L., Dittrich, P., Gogarten, J. P., Kibak, H., and Taiz, L. (1988) The cDNA sequence of the 69-kDa subunit of the carrot vacuolar H+-ATPase. Homology to the beta-chain of F0F1-ATPases, *Journal of Biological Chemistry 263*, 9102-9112.

135. Hirata, R., Ohsumk, Y., Nakano, A., Kawasaki, H., Suzuki, K., and Anraku, Y. (1990) Molecular structure of a gene, VMA1, encoding the catalytic subunit of H

(+)-translocating adenosine triphosphatase from vacuolar membranes of Saccharomyces cerevisiae., *Journal of Biological Chemistry 265*, 6726.

136. Kane, P., Yamashiro, C., Wolczyk, D., Neff, N., Goebl, M., and Stevens, T. (1990) Protein splicing converts the yeast TFP1 gene product to the 69-kD subunit of the vacuolar H (+)-adenosine triphosphatase, *Science 250*, 651.

137. Davis, E. O., Sedgwick, S. G., and Colston, M. J. (1991) Novel structure of the recA locus of Mycobacterium tuberculosis implies processing of the gene product, *Journal of Bacteriology 173*, 5653-5662.

138. Hodges, R. A., Perler, F. B., Noren, C. J., and Jack, W. E. (1992) Protein splicing removes intervening sequences in an archaea DNA polymerase, *Nucleic acids research 20*, 6153-6157.

139. Davis, E. O., Jenner, P. J., Brooks, P. C., Colston, M. J., and Sedgwick, S. G. (1992) Protein splicing in the maturation of M. tuberculosis recA protein: a mechanism for tolerating a novel class of intervening sequence, *Cell 71*, 201-210.

140. Gu, H. H., Xu, J., Gallagher, M., and Dean, G. E. (1993) Peptide splicing in the vacuolar ATPase subunit A from Candida tropicalis, *The Journal of biological chemistry 268*, 7372-7381.

141. Shub, D. A., and Goodrich-Blair, H. (1992) Protein introns: a new home for endonucleases, *Cell 71*, 183-186.

142. Doolittle, R. F. (1993) The comings and goings of homing endonucleases and mobile introns, *Proceedings of the National Academy of Sciences of the United States of America 90*, 5379-5381.

143. Colston, M. J., and Davis, E. O. (1994) The Ins and Outs of Protein Splicing Elements, *Mol Microbiol 12*, 359-363.

144. Perler, F. B., Davis, E. O., Dean, G. E., Gimble, F. S., Jack, W. E., Neff, N., Noren, C. J., Thorner, J., and Belfort, M. (1994) Protein splicing elements: inteins and exteins--a definition of terms and recommended nomenclature, *Nucleic acids research 22*, 1125-1127.

145. Perler, F. B. (1999) InBase, the New England Biolabs Intein Database, *Nucleic acids research 27*, 346-347.

146. Perler, F. B., Comb, D. G., Jack, W. E., Moran, L. S., Qiang, B. Q., Kucera, R. B., Benner, J., Slatko, B. E., Nwankwo, D. O., Hempstead, S. K., Carlow, C. K. S., and Jannasch, H. (1992) Intervening Sequences in an Archaea DNA-Polymerase Gene, *Proceedings of the National Academy of Sciences of the United States of America 89*, 5577-5581.

147. Cooper, A. A., Chen, Y. J., Lindorfer, M. A., and Stevens, T. H. (1993) Protein splicing of the yeast TFP1 intervening protein sequence: a model for self-excision, *The EMBO Journal 12*, 2575-2583.

148. Xu, M., Southworth, M., Mersha, F., and Hornstra, L. (1993) In vitro protein splicing of purified precursor and the identification of a branched intermediate, *Cell 75*, 1371-1377.

149. Xu, M. Q., Comb, D. G., Paulus, H., Noren, C. J., Shao, Y., and Perler, F. B. (1994) Protein Splicing - an Analysis of the Branched Intermediate and Its Resolution by Succinimide Formation, *Embo J 13*, 5517-5522.

150. Clarke, N. D. (1994) A proposed mechanism for the self-splicing of proteins, *Proceedings of the National Academy of Sciences of the United States of America 91*, 11084-11088.

151. Cooper, A. A., and Stevens, T. H. (1995) Protein Splicing - Self-Splicing of Genetically Mobile Elements at the Protein Level, *Trends in biochemical sciences 20*, 351-356.

152. Shao, Y., Xu, M. Q., and Paulus, H. (1995) Protein Splicing - Characterization of the Aminosuccinimide Residue at the Carboxyl-Terminus of the Excised Intervening Sequence, *Biochemistry 34*, 10844-10850.

153. Davis, E. O., and Jenner, P. J. (1995) Protein Splicing - the Lengths Some Proteins Will Go To, *Anton Leeuw Int J G 67*, 131-137.

154. Shao, Y., Xu, M. Q., and Paulus, H. (1996) Protein splicing: Evidence for an N-O acyl rearrangement as the initial step in the splicing process, *Biochemistry 35*, 3810-3815.

155. Xu, M., and Perler, F. (1996) The mechanism of protein splicing and its modulation by mutation., *The EMBO Journal 15*, 5146.

156. Klabunde, T., Sharma, S., Telenti, A., Jacobs, W. R., Jr., and Sacchettini, J. C. (1998) Crystal structure of GyrA intein from Mycobacterium xenopi reveals structural basis of protein splicing, *Nat Struct Biol 5*, 31-36.

157. Kimura, R., and Camarero, J. A. (2005) Expressed protein ligation: A new tool for the biosynthesis of cyclic polypeptides, *Protein Pept Lett 12*, 789-794.

158. Camarero, J. A., Kimura, R. H., Woo, Y.-H., Shekhtman, A., and Cantor, J. (2007) Biosynthesis of a Fully Functional Cyclotide inside Living Bacterial Cells, *Chembiochem 8*, 1363-1366.

159. Camarero, J. A., and Muir, T. W. (1999) Biosynthesis of a Head-to-Tail Cyclized Protein with Improved Biological Activity, *Journal of the American Chemical Society 121*, 5597-5598.

160. Sheehan, J. C., and Hess, G. P. (1955) A New Method of Forming Peptide Bonds, *Journal of the American Chemical Society 77*, 1067-1068.

161. König, W., and Geiger, R. (1970) Eine neue Methode zur Synthese von Peptiden: Aktivierung der Carboxylgruppe mit Dicyclohexylcarbodiimid unter Zusatz von 1-Hydroxy-benzotriazolen, *Chem Ber 103*, 788-798.

162. Carpino, L. A. (1993) 1-Hydroxy-7-azabenzotriazole. An efficient peptide coupling additive, *Journal of the American Chemical Society 115*, 4397-4398.

163. Valeur, E., and Bradley, M. (2009) Amide bond formation: beyond the myth of coupling reagents, *Chem Soc Rev 38*, 606-631.

164. Coste, J., Le-Nguyen, D., and Castro, B. (1990) PyBOP: A new peptide coupling reagent devoid of toxic by-product, *Tetrahedron Letters 31*, 205-208.

165. Albericio, F., Bofill, J. M., El-Faham, A., and Kates, S. A. (1998) Use of Onium Salt-Based Coupling Reagents in Peptide Synthesis1, *The Journal of Organic Chemistry 63*, 9678-9683.

166. Bergmann, M., and Zervas, L. (1932) Über ein allgemeines Verfahren der Peptid-Synthese, *Berichte der deutschen chemischen Gesellschaft (A and B Series) 65*, 1192-1201.

167. Meienhofer, J. (1973) Peptide Synthesis: A Review of the Solid-Phase Method, In *Hormonal Proteins and Peptides* (Li, C. H., Ed.), p 45.

168. Carpino, L. A., and Han, G. Y. (1972) 9-Fluorenylmethoxycarbonyl amino-protecting group, *The Journal of Organic Chemistry 37*, 3404-3409.

169. Atherton, E., Logan, C. J., and Sheppard, R. C. (1981) Peptide synthesis. Part 2. Procedures for solid-phase synthesis using Nα-fluorenylmethoxycarbonylamino-acids on polyamide supports. Synthesis of substance P and of acyl carrier protein 65-74 decapeptide, *J Chem Soc Perk T 1*.

170. Kemp, D. S. (1981) The amine capture strategy for peptide bond formation—an outline of progress, *Biopolymers 20*, 1793-1804.

171. Kemp, D. S., and Galakatos, N. G. (1986) Peptide synthesis by prior thiol capture. 1. A convenient synthesis of 4-hydroxy-6-mercaptodibenzofuran and novel solid-phase synthesis of peptide-derived 4-(acyloxy)-6-mercaptodibenzofurans, *The Journal of Organic Chemistry 51*, 1821-1829.

172. Kemp, D. S., Galakatos, N. G., Bowen, B., and Tan, K. (1986) Peptide synthesis by prior thiol capture. 2. Design of templates for intramolecular O,N-acyl transfer. 4,6-Disubstituted dibenzofurans as optimal spacing elements, *The Journal of Organic Chemistry 51*, 1829-1838.

173. Liu, C. F., and Tam, J. P. (1994) Peptide segment ligation strategy without use of protecting groups., *Proceedings of the National Academy of Sciences of the United States of America 91*, 6584-6588.

174. Liu, C. F., and Tam, J. P. (1994) Chemical Ligation Approach to Form a Peptide-Bond between Unprotected Peptide Segments - Concept and Model Study, *Journal of the American Chemical Society 116*, 4149-4153.

175. Schnölzer, M., and Kent, S. B. H. (1992) Constructing Proteins by Dovetailing Unprotected Synthetic Peptides: Backbone-Engineered HIV Protease, *Science 256*, 221-225.

176. Dawson, P. E., Muir, T. W., Clark-Lewis, I., and Kent, S. B. (1994) Synthesis of proteins by native chemical ligation, *Science 266*, 776-779.

177. Wieland, T., Bokelmann, E., Bauer, L., Lang, H. U., and Lau, H. (1953) Über Peptidsynthesen. 8. Mitteilung Bildung von S-haltigen Peptiden durch intramolekulare Wanderung von Aminoacylresten, *Justus Liebigs Annalen der Chemie 583*, 129-149.

178. Tam, J. P., Lu, Y. A., Liu, C. F., and Shao, J. (1995) Peptide synthesis using unprotected peptides through orthogonal coupling methods., *Proceedings of the National Academy of Sciences of the United States of America 92*, 12485-12489.

179. Tam, J. P., Lu, Y. A., and Eom, K. D. (1997) Synthesis of large cyclic cystine-knot peptide by orthogonal coupling strategy using unprotected peptide precursor, *Tetrahedron Lett 38*, 5599-5602.

180. Johnson, E. C. B., and Kent, S. B. H. (2006) Insights into the Mechanism and Catalysis of the Native Chemical Ligation Reaction, *Journal of the American Chemical Society 128*, 6640-6646.

181. Zhang, L., and Tam, J. P. (1997) Orthogonal coupling of unprotected peptide segments through histidyl amino terminus, *Tetrahedron Letters 38*, 3-6.

182. Tam, J. P., and Yu, Q. (1998) Methionine ligation strategy in the biomimetic synthesis of parathyroid hormones, *Biopolymers 46*, 319-327.

183. Yan, L. Z., and Dawson, P. E. (2001) Synthesis of peptides and proteins without cysteine residues by native chemical ligation combined with desulfurization, *Journal of the American Chemical Society 123*, 526-533.

184. Crich, D., and Banerjee, A. (2007) Native Chemical Ligation at Phenylalanine, *Journal of the American Chemical Society 129*, 10064-10065.

185. Yang, R., Pasunooti, K. K., Li, F., Liu, X.-W., and Liu, C.-F. (2009) Dual Native Chemical Ligation at Lysine, *Journal of the American Chemical Society 131*, 13592-13593.

186. Montalban-Lopez, M., Spolaore, B., Pinato, O., Martinez-Bueno, M., Valdivia, E., Maqueda, M., and Fontana, A. (2008) Characterization of linear forms of the circular enterocin AS-48 obtained by limited proteolysis, *FEBS Lett 582*, 3237-3242.

187. Zhang, L., and Tam, J. (1999) Lactone and Lactam Library Synthesis by Silver Ion-Assisted Orthogonal Cyclization of Unprotected Peptides†, *J. Am. Chem. Soc 121*, 3311-3320.

188. Nilsson, B. L., Kiessling, L. L., and Raines, R. T. (2000) Staudinger Ligation: A Peptide from a Thioester and Azide, *Organic Letters 2*, 1939-1941.

189. Saxon, E., Armstrong, J. I., and Bertozzi, C. R. (2000) A "traceless" Staudinger ligation for the chemoselective synthesis of amide bonds, *Organic Letters 2*, 2141-2143.

190. Brik, A., Yang, Y.-Y., Ficht, S., and Wong, C.-H. (2006) Sugar-Assisted Glycopeptide Ligation, *Journal of the American Chemical Society 128*, 5626-5627.

191. Haase, C., Rohde, H., and Seitz, O. (2008) Native chemical ligation at valine, *Angew Chem Int Edit 47*, 6807-6810.

192. Chen, C. L., Pan, T. Y., Kan, S. C., Kuan, Y. C., Hong, L. Y., Chiu, K. R., Sheu, C. S., Yang, J. S., Hsu, W. H., and Hu, H. Y. (2008) Genome sequence of the lytic bacteriophage P1201 from Corynebacterium glutamicum NCHU 87078: evolutionary relationships to phages from Corynebacterineae, *Virology 378*, 226-232.

193. Johnson, E. C. B., Malito, E., Shen, Y., Pentelute, B., Rich, D., Florián, J., Tang, W.-J., and Kent, S. B. H. (2007) Insights from Atomic-Resolution X-Ray Structures of Chemically Synthesized HIV-1 Protease in Complex with Inhibitors, *Journal of Molecular Biology 373*, 573-586.

194. Nakamura, K., Kanao, T., Uesugi, T., Hara, T., Sato, T., Kawakami, T., and Aimoto, S. (2009) Synthesis of peptide thioesters via an N-S acyl shift reaction under mild acidic conditions on an N-4,5-dimethoxy-2-mercaptobenzyl auxiliary group, *J Pept Sci 15*, 731-737.

195. Yang, J. Y., and Yang, W. Y. (2009) Site-specific two-color protein labeling for FRET studies using split inteins, *Journal of the American Chemical Society 131*, 11644-11645.

196. Li, X., Lam, H. Y., Zhang, Y., and Chan, C. K. (2010) Salicylaldehyde Ester-Induced Chemoselective Peptide Ligations: Enabling Generation of Natural Peptidic Linkages at the Serine/Threonine Sites, *Organic Letters 12*, 1724-1727.

197. Zhang, L., and Tam, J. P. (1997) Metal Ion-Assisted Peptide Cyclization, *Tetrahedron Letters 38*, 4.

198. Saxon, E., and Bertozzi, C. R. (2000) Cell Surface Engineering by a Modified Staudinger Reaction, *Science 287*, 2007-2010.

199. Hemu, X., Taichi, M., Qiu, Y., Liu, D.-X., and Tam, J. P. (2013) Biomimetic synthesis of cyclic peptides using novel thioester surrogates, *Pept. Sci. 100*, 492-501.

200. Tam, J., and Xu, J. (2001) Methods and strategies of peptide ligation*, *Peptide Science*.

201. Mende, F., and Seitz, O. (2011) 9-Fluorenylmethoxycarbonyl-Based Solid-Phase Synthesis of Peptide α-Thioesters, *Angewandte Chemie International Edition 50*, 1232-1240.

202. Li, X. Q., Kawakami, T., and Aimoto, S. (1998) Direct preparation of peptide thioesters using an Fmoc solid-phase method, *Tetrahedron Letters 39*, 8669-8672.

203. Futaki, S., Sogawa, K., Maruyama, J., Asahara, T., Niwa, M., and Hojo, H. (1997) Preparation of Peptide Thioesters using Fmoc-Solid-Phase Peptide

Synthesis and its Application to the Construction of a Template-Assembled Synthetic Protein (TASP), *Tetrahedron Letters 38*, 6237-6240.

204. Raz, R., and Rademann, J. (2011) Fmoc-Based Synthesis of Peptide Thioesters for Native Chemical Ligation Employing a tert-Butyl Thiol Linker, *Organic Letters 13*, 1606-1609.

205. Ingenito, R., Bianchi, E., Fattori, D., and Pessi, A. (1999) Solid Phase Synthesis of Peptide C-Terminal Thioesters by Fmoc/t-Bu Chemistry, *Journal of the American Chemical Society 121*, 11369-11374.

206. Miteva, M., Andersson, M., Karshikoff, A., and Otting, G. (1999) Molecular electroporation: a unifying concept for the description of membrane pore formation by antibacterial peptides, exemplified with NK-lysin, *FEBS Lett 462*, 155-158.

207. Blanco-Canosa, J. B., and Dawson, P. E. (2008) An efficient Fmoc-SPPS approach for the generation of thioester peptide precursors for use in native chemical ligation, *Angew Chem Int Edit 47*, 6851-6855.

208. Jacobs, T., Bruhn, H., Gaworski, I., Fleischer, B., and Leippe, M. (2003) NK-lysin and its shortened analog NK-2 exhibit potent activities against Trypanosoma cruzi, *Antimicrob Agents Chemother 47*, 607-613.

209. Fang, G.-M., Li, Y.-M., Shen, F., Huang, Y.-C., Li, J.-B., Lin, Y., Cui, H.-K., and Liu, L. (2011) Protein Chemical Synthesis by Ligation of Peptide Hydrazides, *Angewandte Chemie International Edition 50*, 7645-7649.

210. Kenner, G. W., McDermott, J. R., and Sheppard, R. C. (1971) The safety catch principle in solid phase peptide synthesis, *Journal of the Chemical Society D: Chemical Communications 0*, 636-637.

211. Camarero, J. A., Hackel, B. J., de Yoreo, J. J., and Mitchell, A. R. (2004) Fmoc-Based Synthesis of Peptide α-Thioesters Using an Aryl Hydrazine Support †, *The Journal of Organic Chemistry 69*, 4145-4151.

212. Pellegrini, A., Thomas, U., Bramaz, N., Hunziker, P., and von Fellenberg, R. (1999) Isolation and identification of three bactericidal domains in the bovine α-lactalbumin molecule, *Biochimica et Biophysica Acta (BBA) - General Subjects 1426*, 439-448.

213. Zheng, J.-S., Tang, S., Guo, Y., Chang, H.-N., and Liu, L. (2012) Synthesis of Cyclic Peptides and Cyclic Proteins via Ligation of Peptide Hydrazides, *ChemBioChem 13*, 542-546.

214. Ollivier, N., Behr, J. B., El-Mahdi, O., Blanpain, A., and Melnyk, O. (2005) Fmoc solid-phase synthesis of peptide thioesters using an intramolecular N,S-acyl shift, *Organic Letters 7*, 2647-2650.

215. Kawakami, T., Sumida, M., Nakamura, K., Vorherr, T., and Aimoto, S. (2005) Peptide thioester preparation based on an N-S acyl shift reaction mediated by a thiol ligation auxiliary, *Tetrahedron Letters 46*, 8805-8807.

216. Nagaike, F., Onuma, Y., Kanazawa, C., Hojo, H., Ueki, A., Nakahara, Y., and Nakahara, Y. (2006) Efficient microwave-assisted tandem N- to S-acyl transfer and thioester exchange for the preparation of a glycosylated peptide thioester, *Organic Letters 8*, 4465-4468.

217. Kawakami, T., and Aimoto, S. (2007) Sequential peptide ligation by using a controlled cysteinyl prolyl ester (CPE) autoactivating unit, *Tetrahedron Letters 48*, 1903-1905.

218. Hojo, H., Onuma, Y., Akimoto, Y., Nakahara, Y., and Nakahara, Y. (2007) N-alkyl cysteine-assisted thioesterification of peptides, *Tetrahedron Letters 48*, 25-28.

219. Ollivier, N., Dheur, J., Mhidia, R., Blanpain, A., and Melnyk, O. (2010) Bis(2-sulfanylethyl)amino Native Peptide Ligation, *Organic Letters 12*, 5238-5241.

220. Hou, W., Zhang, X., Li, F., and Liu, C.-F. (2010) Peptidyl N,N-Bis(2-mercaptoethyl)-amides as Thioester Precursors for Native Chemical Ligation†, *Organic Letters 13*, 386-389.

221. Sharma, R. K., and Tam, J. P. (2011) Tandem Thiol Switch Synthesis of Peptide Thioesters via N-S Acyl Shift on Thiazolidine, *Organic Letters 13*, 5176-5179.

222. Kawakami, T., Akaji, K., and Aimoto, S. (2001) Peptide bond formation mediated by 4,5-dimethoxy-2-mercaptobenzylamine after periodate oxidation of the N-terminal serine residue, *Organic Letters 3*, 1403-1405.

223. Dheur, J., Ollivier, N., and Melnyk, O. (2011) Synthesis of Thiazolidine Thioester Peptides and Acceleration of Native Chemical Ligation, *Organic Letters 13*, 1560-1563.

224. Dheur, J., Ollivier, N., Vallin, A., and Melnyk, O. (2011) Synthesis of Peptide Alkylthioesters Using the Intramolecular N,S-Acyl Shift Properties of Bis(2-sulfanylethyl)amido Peptides, *J Org Chem 76*, 3194-3202.

225. Tsuda, S., Shigenaga, A., Bando, K., and Otaka, A. (2009) N -> S Acyl-Transfer-Mediated Synthesis of Peptide Thioesters Using Anilide Derivatives, *Organic Letters 11*, 823-826.

226. Tam, J. P., and Lu, Y. A. (1998) A biomimetic strategy in the synthesis and fragmentation of cyclic protein., *Protein science : a publication of the Protein Society 7*, 1583-1592.

227. Tam, J., Lu, Y., and Yu, Q. (1999) Thia zip reaction for synthesis of large cyclic peptides: Mechanisms and applications, *Journal of the American Chemical Society 121*, 4316-4324.

228. Sela, M., and Lifson, S. (1959) On the reformation of disulfide bridges in proteins, *Biochim Biophys Acta 36*, 471-478.

229. Volkmer-Engert, R., Landgraf, C., and Schneider-Mergener, J. (1998) Charcoal surface-assisted catalysis of intramolecular disulfide bond formation in peptides, *The Journal of Peptide Research 51*, 365-369.

230. Manning, M., and du Vigneaud, V. (1965) 4-beta-Alanine-oxytocin: An Oxytocin Analog Containing a Twenty-one-membered Disulfide Ring, *Biochemistry 4*, 1884-1888.

231. Pelton, J. T., Gulya, K., Hruby, V. J., Duckles, S. P., and Yamamura, H. I. (1985) Conformationally restricted analogs of somatostatin with high mu-opiate receptor specificity, *Proceedings of the National Academy of Sciences 82*, 236-239.

232. Tam, J. P., Wu, C. R., Liu, W., and Zhang, J. W. (1991) Disulfide bond formation in peptides by dimethyl sulfoxide. Scope and applications, *Journal of the American Chemical Society 113*, 6657-6662.

233. Annis, I., Chen, L., and Barany, G. (1998) Novel Solid-Phase Reagents for Facile Formation of Intramolecular Disulfide Bridges in Peptides under Mild Conditions1,2, *Journal of the American Chemical Society 120*, 7226-7238.

234. Camacho, C. J., and Thirumalai, D. (1995) Modeling the role of disulfide bonds in protein folding: Entropic barriers and pathways, *Proteins: Structure, Function, and Bioinformatics 22*, 27-40.

235. Veber, D., Milkowski, J., Varga, S., Denkewalter, R., and Hirschmann, R. (1972) Acetamidomethyl. A Novel Thiol Protecting Group for Cysteine, *Journal of the American Chemical Society 94*, 5456-5461.

236. Tam, J. (1997) Synthesis of large cyclic cystine-knot peptide by orthogonal coupling strategy using unprotected peptide precursor, *Tetrahedron Letters*.

237. Cuthbertson, A., and Indrevoll, B. (2000) A method for the one-pot regioselective formation of the two disulfide bonds of [alpha]-conotoxin SI, *Tetrahedron Letters 41*, 3661-3663.

238. Muttenthaler, M., Nevin, S. T., Grishin, A. A., Ngo, S. T., Choy, P. T., Daly, N. L., Hu, S.-H., Armishaw, C. J., Wang, C.-I. A., Lewis, R. J., Martin, J. L., Noakes, P. G., Craik, D. J., Adams, D. J., and Alewood, P. F. (2010) Solving the alpha-conotoxin folding problem: efficient selenium-directed on-resin generation of more potent and stable nicotinic acetylcholine receptor antagonists., *Journal of the American Chemical Society 132*, 3514-3522.

239. Hwang, C., Sinskey, A. J., and Lodish, H. F. (1992) Oxidized Redox State of Glutathione in the Endoplasmic Reticulum, *Science 257*, 1496-1502.

240. Arolas, J. L., Aviles, F. X., Chang, J.-Y., and Ventura, S. (2006) Folding of small disulfide-rich proteins: clarifying the puzzle, *Trends in biochemical sciences 31*, 292-301.

241. Kubo, S., Tanimura, K., Nishio, H., Chino, N., Teshima, T., Kimura, T., and Nishiuchi, Y. (2008) Optimization of the Oxidative Folding Reaction and Disulfide Structure Determination of Human α-Defensin 1, 2, 3 and 5, *Int J Pept Res Ther 14*, 341-349.

242. Göransson, U., and Craik, D. J. (2003) Disulfide Mapping of the Cyclotide Kalata B1: Chemical Proof of the Cyclic Cystine Knot motif *Journal of Biological Chemistry 278*, 48188-48196.

243. Kubo, S., Chino, N., Kimura, T., and Sakakibara, S. (1996) Oxidative folding of ω-conotoxin MVIIC: Effects of temperature and salt, *Biopolymers 38*, 733-744.

244. DeLa, C., Whitby, F., Buczek, O., and Bulaj, G. (2003) Detergent-assisted oxidative folding of delta-conotoxins, *J. Peptide Res 61*, 202-212.

245. Price-Carter, M., Gray, W., and Goldenberg, D. (1996) Folding of [omega]-Conotoxins. 1. Efficient Disulfide-Coupled Folding of Mature Sequences in Vitro, *Biochemistry 35*, 15537-15546.

246. Leta Aboye, T., Clark, R. J., Craik, D. J., and Göransson, U. (2008) Ultra-stable peptide scaffolds for protein engineering-synthesis and folding of the circular cystine knotted cyclotide cycloviolacin O2, *Chembiochem 9*, 103-113.

247. Gunasekera, S., Daly, N. L., Clark, R. J., and Craik, D. J. (2009) Dissecting the oxidative folding of circular cystine knot miniproteins, *Antioxid. Redox Signal 11*, 971-980.

248. Nielsen, J. S., Buczek, P., and Bulaj, G. (2004) Cosolvent-assisted oxidative folding of a bicyclicα-conotoxin ImI, *J Pept Sci 10*, 249-256.

249. Sharp, P. M., and Li, W.-H. (1987) The codon adaptation index-a measure of directional synonymous codon usage bias, and its potential applications, *Nucleic Acids Research 15*, 1281-1295.

250. Schagger, H. (2006) Tricine-SDS-PAGE, *Nat. Protocols 1*, 16-22.

251. Lehrer, R. I., Rosenman, M., Harwig, S. S. S. L., Jackson, R., and Eisenhauer, P. (1991) Ultrasensitive assays for endogenous antimicrobial polypeptides, *J Immunol Methods 137*, 167-173.

252. Tam, J. P., Yu, Q., and Yang, J.-L. (2001) Tandem Ligation of Unprotected Peptides through Thiaprolyl and Cysteinyl Bonds in Water, *Journal of the American Chemical Society 123*, 2487-2494.

253. Klabunde, T., Sharma, S., Telenti, A., and Jacobs, W. (1998) Crystal structure of GyrA intein from Mycobacterium xenopi reveals structural basis of protein splicing, *Nature Structural Biology 5,* 31-36.

254. Nguyen, G. K. T., Zhang, S., Wang, W., Wong, C. T. T., Nguyen, N. T. K., and Tam, J. P. (2011) Discovery of a linear cyclotide from the bracelet subfamily and its disulfide mapping by top-down mass spectrometry, *Journal of Biological Chemistry 286*, 44833-44

255. Daly, N. L., Love, S., Alewood, P. F., and Craik, D. J. (1999) Chemical Synthesis and Folding Pathways of Large Cyclic Polypeptides: Studies of the Cystine Knot Polypeptide Kalata B1, *Biochemistry 38*, 10606-10614.

256. Leta Aboye, T., Clark, R. J., Craik, D. J., and Göransson, U. (2008) Ultra-Stable Peptide Scaffolds for Protein Engineering—Synthesis and Folding of the Circular Cystine Knotted Cyclotide Cycloviolacin O2, *Chembiochem 9*, 103-113.

257. Gisin, B. F., and Merrifield, R. B. (1972) Carboxyl-catalyzed intramolecular aminolysis. Side reaction in solid-phase peptide synthesis, *Journal of the American Chemical Society 94*, 3102-3106.

258. Khosla, M. C., Smeby, R. R., and Bumpus, F. M. (1972) Failure sequence in solid-phase peptide synthesis due to the presence of an N-alkylamino acid, *Journal of the American Chemical Society 94*, 4721-4724.

259. Lukszo, J., Patterson, D., Albericio, F., and Kates, S. A. (1996) 3-(1-Piperidinyl)alanine formation during the preparation ofC-terminal cysteine peptides with the Fmoc/t-Bu strategy, *Letters in Peptide Science 3*, 157-166.

260. Chatzi, K. B. O., Gatos, D., and Stavropoulos, G. (1991) 2-Chlorotrityl chloride resin, *Int J Pept Prot Res 37*, 513-520.

261. Curtius, T. (1902) Synthetische Versuche mit Hippurazid, *Berichte der deutschen chemischen Gesellschaft 35*, 3226-3228.

262. Curtius, T. (1904) Verkettung von Amidosäuren I. Abhandlung, *Journal für Praktische Chemie 70*, 57-72.

263. Fischer, E. (1903) Synthese von Derivaten der Polypeptide, *Berichte der deutschen chemischen Gesellschaft 36*, 2094-2106.

264. Fischer, E., and Otto, E. (1903) Synthese von Derivaten einiger Dipeptide, *Berichte der deutschen chemischen Gesellschaft 36*, 2106-2116.

265. Determann, H., and Wieland, T. (1963) Über Peptidsynthesen, XXIX. Untersuchungen zur Racemisierung bei Peptid-Synthesen, *Justus Liebigs Annalen der Chemie 670*, 136-140.

266. Gillessen, D., Schnabel, E., and Meienhofer, J. (1963) Synthese der Insulinsequenz B 13–20, *Justus Liebigs Annalen der Chemie 667*, 164-171.

267. Wang, S.-S., and Merrifield, R. B. (1969) Preparation of a tert-alkyloxycarbonylhydrazide resin and its application to solid phase peptide synthesis, *Journal of the American Chemical Society 91*, 6488-6491.

268. Wang, S.-S. (1973) p-Alkoxybenzyl alcohol resin and p-alkoxybenzyloxycarbonylhydrazide resin for solid phase synthesis of protected peptide fragments, *Journal of the American Chemical Society 95*, 1328-1333.

269. Wang, S.-S. (1975) Solid-phase synthesis of protected peptide hydrazides. Preparation and application of hydroxymethyl resin and 3-(p-benzyloxyphenyl)-1,1-dimethylpropyloxycarbonylhydrazide resin, *The Journal of Organic Chemistry 40*, 1235-1239.

270. Curtius, T. (1890) Ueber Stickstoffwasserstoffsäure (Azoimid) N3H, *Berichte der deutschen chemischen Gesellschaft 23*, 3023-3033.

271. Honzl, J., and Rudinger, J. (1961) Amino-acidsandpeptides. XXXIII. Nitrosyl chloride and butyl nitrite as reagents in peptide synthesis by the azide method; suppression of amide formation, *Collect. Czech. Chem. Commun. 26*, 2333-2344.

272. Sakakibara, S., Shimonishi, Y., kishida, Y., okada, M., and Sugihara, H. (1967) Use of anhydrous hydrogen fluoride in peptide synthesis. I. Behavior of various protective groups in anhydrous hydrogen fluoride, *Bulletin of the Chemical Society of Japan 40*, 2164-2167.

273. Nakamura, K., Kawakami, T., and Aimoto, S. (2006) N-S acyl shift reaction on peptide backbone, *J Pept Sci 12*, 114-114.

274. Nakamura, K., Sumida, M., Kawakami, T., Vorherr, T., and Aimoto, S. (2006) Generation of an S-peptide via an N-S acyl shift reaction in a TFA solution, *Bulletin of the Chemical Society of Japan 79*, 1773-1780.

275. Kang, J., Richardson, J. P., and Macmillan, D. (2009) 3-Mercaptopropionic acid-mediated synthesis of peptide and protein thioesters, *Chemical Communications*, 407-409.

276. Nakahara, Y., Matsuo, I., Ito, Y., Ubagai, R., Hojo, H., and Nakahara, Y. (2010) High-pressure-promoted Fmoc-aminoacylation of N-ethylcysteine: preparation of key devices for the solid-phase synthesis of peptide thioesters, *Tetrahedron Letters 51*, 407-410.

277. Chino, N., Kubo, S., Miyazato, M., Nakazato, M., Kangawa, K., and Sakakibara, S. (1996) Generation of two isomers with the same disulfide connectivity during disulfide bond formation of human uroguanylin, *Letters in Peptide Science 3*, 45-52.

278. Erlich, L. A., Kumar, K. S. A., Haj-Yahya, M., Dawson, P. E., and Brik, A. (2010) N-Methylcysteine-mediated total chemical synthesis of ubiquitin thioester, *Org Biomol Chem 8*, 2392-2396.

279. Urban, J. A. N., Vaisar, T., Shen, R., and Lee, M. S. (1996) Lability of N-alkylated peptides towards TFA cleavage, *Int J Pept Prot Res 47*, 182-189.

280. Kim, J., Takahashi, M., Ohtake, A., and Wakamiya, A. (1995) Tyr13 is essential for the activity of ω-conotoxin MVIIA and GVIA, specific N-type calcium channel blockers, *... and biophysical research ...*.

281. Flinn, J. P., Murphy, R., Boubliek, J. H., Lew, M. J., Writh, C. E., and Angus, J. A. (1995) Synthesis and biological characterization of a series of analogues of ω-conotoxin gvia, *J Pept Sci 1*, 379-384.

282. Price-Carter, M., Bulaj, G., and Goldenberg, D. P. (2002) Initial Disulfide Formation Steps in the Folding of an ω-Conotoxin †, *Biochemistry 41*, 3507-3519.

283. Singh, R., and Whitesides, G. M. (2010) Thiol—disulfide interchange, In *Sulphur-Containing Functional Groups (1993)*, pp 633-658, John Wiley & Sons, Inc.

284. Freter, R., Pohl, E. R., Wilson, J. M., and Hupe, D. J. (1979) Role of the central thiol in determining rates of the thiol-disulfide interchange reaction, *The Journal of Organic Chemistry 44*, 1771-1774.

285. Nadasdi, L., Yamashiro, D., and CHUNG, D. (1995) Structure-activity analysis of a Conus peptide blocker of N-type neuronal calcium channels, *Biochemistry*.

286. Kubo, S., Chino, N., Kimura, T., and Sakakibara, S. (1996) Oxidative folding of omega-conotoxin MVIIC: effects of temperature and salt., *Biopolymers 38*, 733-744.

287. Sato, K., Raymond, C., Martin-Moutot, N., Sasaki, T., Omori, A., Ohtake, A., Kim, J., Kohno, T., Takahashi, M., and Seagar, M. (1997) Binding of chimeric analogs of [omega]-conotoxin MVIIA and MVIIC to the N-and P/Q-type calcium channels, *FEBS letters 414*, 480-484.

288. Craik, D., and Daly, N. (2006) Cyclized conotoxin peptides (Patent 7001883).

289. Price-Carter, M., Hull, M. S., and Goldenberg, D. P. (1998) Roles of individual disulfide bonds in the stability and folding of an omega-conotoxin., *Biochemistry 37*, 9851-9861.

290. Wan, Q., and Danishefsky, S. J. (2007) Free-radical-based, specific desulfurization of cysteine: A powerful advance in the synthesis of polypeptides and glycopolypeptides, *Angew Chem Int Edit 46*, 9248-9252.

291. Steinberg, D., and Lehrer, R. (1997) Designer Assays for Antimicrobial Peptides, In *Antibacterial Peptide Protocols* (Shafer, W., Ed.), pp 169-186, Humana Press.

292. Wu, Z. B., Hoover, D. M., Yang, D., Boulegue, C., Santamaria, F., Oppenheim, J. J., Lubkowski, J., and Lu, W. Y. (2003) Engineering disulfide bridges to dissect antimicrobial and chemotactic activities of human beta-defensin 3, *Proceedings of the National Academy of Sciences of the United States of America 100*, 8880-8885.

293. Zhu, Q., and Solomon, S. (1992) Isolation and mode of action of rabbit corticostatic (antiadrenocorticotropin) peptides, *Endocrinology 130*, 1413-1423.

294. Chertov, O., Michiel, D. F., Xu, L., Wang, J. M., Tani, K., Murphy, W. J., Longo, D. L., Taub, D. D., and Oppenheim, J. J. (1996) Identification of Defensin-1, Defensin-2, and CAP37/Azurocidin as T-cell Chemoattractant Proteins Released from Interleukin-8-stimulated Neutrophils, *Journal of Biological Chemistry 271*, 2935-2940.

295. Yang, D., Chertov, O., Bykovskaia, S. N., Chen, Q., Buffo, M. J., Shogan, J., Anderson, M., Schröder, J. M., Wang, J. M., Howard, O. M. Z., and Oppenheim, J. J. (1999) Beta-Defensins: Linking Innate and Adaptive Immunity Through Dendritic and T Cell CCR6, *Science 286*, 525-528.

296. Richard, J. P., Melikov, K., Vives, E., Ramos, C., Verbeure, B., Gait, M. J., Chernomordik, L. V., and Lebleu, B. (2003) Cell-penetrating Peptides: A reevalution of the mechanism of cellular uptake, *Journal of Biological Chemistry 278*, 585-590.

297. Klüver, E., Schulz-Maronde, S., Scheid, S., Meyer, B., Forssmann, W.-G., and Adermann, K. (2005) Structure-Activity Relation of Human β-Defensin 3:

Influence of Disulfide Bonds and Cysteine Substitution on Antimicrobial Activity and Cytotoxicity, *Biochemistry 44*, 9804-9816.

298. Brogden, K. A. (2005) Antimicrobial peptides: pore formers or metabolic inhibitors in bacteria?, *Nat Rev Micro 3*, 238-250.

299. Bechinger, B. (1999) The structure, dynamics and orientation of antimicrobial peptides in membranes by multidimensional solid-state NMR spectroscopy, *Biochimica et Biophysica Acta (BBA) - Biomembranes 1462*, 157-183.

300. Karshikov, A., Berendes, R., Burger, A., Cavalié, A., Lux, H.-D., and Huber, R. (1992) Annexin V membrane interaction: an electrostatic potential study, *European Biophysics Journal 20*, 337-344.

301. Miteva, M., Andersson, M., Karshikoff, A., and Otting, G. (1999) Molecular electroporation: a unifying concept for the description of membrane pore formation by antibacterial peptides, exemplified with NK-lysin, *FEBS letters 462*, 155-158.

302. Madani, F., Lindberg, S., Langel, Ü., Futaki, S., and Gräslund, A. (2011) Mechanisms of Cellular Uptake of Cell-Penetrating Peptides, *Journal of Biophysics 2011*, 1-10.

303. Sandgren, S., Wittrup, A., Cheng, F., Jönsson, M., Eklund, E., Busch, S., and Belting, M. (2004) The Human Antimicrobial Peptide LL-37 Transfers Extracellular DNA Plasmid to the Nuclear Compartment of Mammalian Cells via Lipid Rafts and Proteoglycan-dependent Endocytosis, *Journal of Biological Chemistry 279*, 17951-17956.